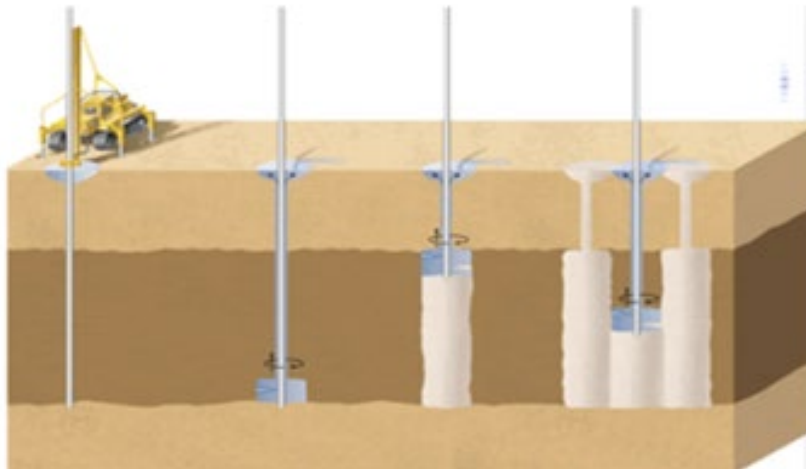




Evaluation and guidance development for Post-Grouted drilled shafts for highways



16 PDH

**Professional Development Hours (PDH) or
Continuing Education Hours (CE)
Online PDH or CE course**

SI* (MODERN METRIC) CONVERSION FACTORS

APPROXIMATE CONVERSIONS TO SI UNITS

Symbol	When You Know	Multiply By	To Find	Symbol
LENGTH				
in	inches	25.4	millimeters	mm
ft	feet	0.305	meters	m
yd	yards	0.914	meters	m
mi	miles	1.61	kilometers	km
AREA				
in ²	square inches	645.2	square millimeters	mm ²
ft ²	square feet	0.093	square meters	m ²
yd ²	square yard	0.836	square meters	m ²
ac	acres	0.405	hectares	ha
mi ²	square miles	2.59	square kilometers	km ²
VOLUME				
fl oz	fluid ounces	29.57	milliliters	mL
gal	gallons	3.785	liters	L
ft ³	cubic feet	0.028	cubic meters	m ³
yd ³	cubic yards		0.765	m ³
cubic meters NOTE: volumes				
MASS				
oz	ounces	28.35	grams	g
lb	pounds	0.454	kilograms	kg
T	short tons (2000 lb)	0.907	megagrams (or "metric ton")	Mg (or "t")
TEMPERATURE (exact degrees)				
°F	Fahrenheit		5 (F- Celsius	°C
32)/9				
ILLUMINATION				
fc	foot-candles	10.76	lux	lx
fl	foot-Lamberts	3.426	candela/m ²	cd/m ²
FORCE and PRESSURE or STRESS				
lbf	poundforce	4.45	newtons	N
lbf/in ²	poundforce per square inch	6.89	kilopascals	kPa
APPROXIMATE CONVERSIONS FROM SI UNITS				
Symbol	When You Know	Multiply By	To Find	Symbol
LENGTH				
mm	millimeters	0.039	inches	in
m	meters	3.28	feet	ft
m	meters	1.09	yards	yd
km	kilometers	0.621	miles	mi
AREA				
mm ²	square millimeters	0.0016	square inches	in ²
m ²	square meters	10.764	square feet	ft ²
m ²	square meters	1.195	square yards	yd ²
ha	hectares	2.47	acres	ac
km ²	square kilometers	0.386	square miles	mi ²
VOLUME				
mL	milliliters	0.034	fluid ounces	fl oz
L	liters	0.264	gallons	gal
m ³	cubic meters	35.314	cubic feet	ft ³
m ³	cubic meters	1.307	cubic yards	yd ³
MASS				
g	grams	0.035	ounces	oz
kg	kilograms	2.202	pounds	lb
Mg (or "t")	megagrams (or "metric ton")	1.103	short tons (2000 lb)	T
TEMPERATURE (exact degrees)				
°C	Celsius	1.8C+32	Fahrenheit	°F
ILLUMINATION				
lx	lux	0.0929	foot-candles	fc
cd/m ²	candela/m ²	0.2919	foot-Lamberts	fl
FORCE and PRESSURE or STRESS				
N	newtons	0.225	poundforce	lbf
kPa	kilopascals	0.145	poundforce per square inch	lbf/in ²

* SI is the symbol for the International System of Units. Appropriate rounding should be made to comply with Section 4 of ASTM E380. (Revised March 2003)

Table of Contents

List Figures.....	vi
List of Tables.....	xii
CHAPTER 1: INTRODUCTION	1
1.1 Overview	1
1.2 Historical Use.....	2
1.3 Existing Technical Guidance for Post-Grouted Drilled Shafts.....	7
1.4 Objectives.....	8
CHAPTER 2: IMPROVEMENT MECHANISMS FOR POST-GROUTED DRILLED SHAFTS.....	9
2.1 Introduction	9
2.2 Performance Improvement Mechanisms	9
2.3 Pre-mobilization.....	9
2.4 Ground Improvement.....	12
2.5 Tip Enlargement.....	13
2.6 Improvement in Side Resistance.....	13
2.7 Summary	14
CHAPTER 3: GROUTING PRINCIPLES FOR PGDS APPLICATIONS.....	17
3.1 Grout Defined	17
3.2 Particulate Grout Components.....	17
3.2.1 Cement and Particle Size.....	18
3.2.2 Grout Admixtures.....	20
3.3 Properties of Fluid Particulate Grouts for PGDS.....	20
3.3.1 Grout Rheology	20
3.3.2 Bleed.....	21
3.3.3 Pressure Filtration.....	21
3.4 Commonly Measured Grout Properties	21
3.5 Grouting Techniques.....	22
3.5.1 Permeation Grouting	22
3.5.2 Compaction or Limited Mobility Grouting.....	23
3.5.3 Jet Grouting	24
3.5.4 Hydrofracture Grouting.....	25

3.6	Stage Grouting	26
3.7	Grouting Equipment.....	26
3.7.1	Grout Mixers	27
3.7.2	Grout Pumps.....	29
3.8	Summary	29
CHAPTER 4: CURRENT POST-GROUTING PRACTICES		31
4.1	Introduction.....	31
4.2	Contracting Practices in the United States.....	31
4.2.1	Typical Grouting Procedure	32
4.3	Common Requirements and Specifications for PGDS in the United States.....	33
4.3.1	Materials.....	33
4.3.2	Equipment	33
4.3.3	Record Keeping and Submittals.....	34
4.3.4	Qualifications of On-site Personnel.....	35
4.3.5	Load Testing and Demonstration Shafts	35
4.4	Chinese Post-Grouting Practice	36
4.4.1	General Requirements	36
4.4.2	Post-Grouting Parameters.....	36
4.4.3	Post-Grouting Provisions.....	37
CHAPTER 5: GROUT DISTRIBUTION SYSTEMS FOR PGDS APPLICATIONS		39
5.1	Introduction.....	39
5.2	Open-Type Grout Distribution System: Stem (Orifice).....	39
5.3	Open-Type Grout Distribution System: Sleeve-Port (Tube-À-Manchette).....	39
5.4	Open-Type Grout Distribution System: Low Mobility Grouting (LMG) Device	44
5.5	Closed-Type Grout Distribution System: Flat-Jack.....	45
5.6	Gravel Bedding	47
5.7	Summary	48
CHAPTER 6: MEASUREMENTS AND CONTROL DURING GROUTING.....		49
6.1	Introduction	49
6.2	Measurement of Grout Pressure and Pressure Termination Criterion	49
6.3	Measurement of Grout Volume and Volume Termination Criteria.....	51
6.4	Measurement of Shaft Uplift and Uplift Termination Criterion	52

6.5	Control of Grouting Operations Based on Measurements	54
6.6	Use of Strain Gauge Measurements	57
6.7	Measurements for Grout Quality Control	58
6.8	Summary	59
CHAPTER 7: CURRENT DESIGN METHODS		61
7.1	Introduction	61
7.2	Tip Capacity Multiplier Approach.....	61
7.2.1	Mullins, Winters, and Dapp (2006).....	62
7.2.2	Dapp and Brown (2010).....	63
7.2.3	Design Procedure for TCM Approach	66
7.3	Axial Capacity Multiplier Approach	67
7.4	Component Multiplier Approach.....	71
7.4.1	Hu, Li, and Wu (2001)	72
7.4.2	Chinese <i>Technical Code for Building Pile Foundations</i>	72
7.4.3	Xiao, Wu, and Wu (2009)	73
7.4.4	Dai, Gong, Zhao, and Zhou (2012)	73
7.4.5	Liu and Zhang (2011).....	74
7.4.6	Discussion on the Component Multiplier Approach.....	75
7.5	Simplified Approach.....	76
7.6	Summary on Applicability and Limitations of Design Methods	77
CHAPTER 8: COMPREHENSIVE EVALUATION OF RESULTS FROM SELECTED LOAD TEST PROGRAMS		79
8.1	Introduction	79
8.2	Methodology	79
8.3	Illustration of Methodology	80
8.3.1	Response of UngROUTED Shaft.....	81
8.3.2	Adaptation of Load-transfer Models to Account for Pre- mobilization	83
8.3.3	Response of Grouted Shaft to Subsequent Top-down Loading	86
8.3.4	Response of Grouted Shaft to Subsequent Bi-directional Loading.....	88
8.3.5	Quantification of Ground Improvement at the Shaft Tip	89
8.4	Analyses for Selected Load Test Cases	90
8.4.1	Analysis Procedure.....	91

8.4.2	Example Results from Analysis of Selected Cases	92
8.5	Collective Results from Comprehensive Analyses	94
8.6	Summary	98
CHAPTER 9: EVALUATION OF PGDS RESISTANCE FROM LOAD TESTS.....		99
9.1	Introduction & Methodology	99
9.2	Improvement in Sand from Load Test Results	99
9.3	Improvement in Clay from Load Test Results.....	103
9.4	Improvement in Rock from Load Test Results	107
9.5	Comparison of Measured and Predicted Tip Resistance	107
9.6	Comparison of Predictions for Shafts in Sand.....	108
9.7	Comparison of Predictions for Shafts in Clay	111
9.8	Summary and Implications	114
CHAPTER 10: LOAD TESTS TO EVALUATE IMPROVEMENT DUE TO PRE-MOBILIZATION.....		117
10.1	Introduction	117
10.2	Field Load Test Program	117
10.2.1	Site Conditions and Test Shafts.....	117
10.2.2	Pre-mobilization Loading.....	118
10.2.3	Top-Down Loading	122
10.3	Interpretation of Load Test Measurements	125
10.4	Comparison of Measured and Predicted Response.....	130
10.4.1	Test Shaft TS-2.....	130
10.4.2	Test Shaft TS-4.....	130
10.4.3	Test Shaft TS-5.....	134
10.5	Summary and Implications	136
CHAPTER 11: SIGNIFICANT FINDINGS AND RECOMMENDATIONS FOR DESIGN AND CONSTRUCTION.....		137
11.1	Introduction	137
11.2	Improvement Mechanisms from Post-Grouting	138
11.3	Magnitude of Improvement due to Post-grouting.....	139
11.4	Design of PGDS.....	140
11.5	Grouting Practices.....	142
11.6	Quality Control/Quality Assurance for Post-Grouting Operations.....	142

11.7	Use of Post-grouting as a QC/QA Method	144
CHAPTER 12: RECOMMENDATIONS FOR FUTURE WORK		145
12.1	Introduction	145
12.2	Evaluation of Relaxation Following Grouting.....	145
12.3	Evaluation and Development of Improved Design Methods.....	145
12.4	Evaluation of Ground Improvement	145
12.5	Evaluation of Reliability	146
12.6	Shaft Performance: Stiffness vs. Nominal Resistance vs. Ultimate Resistance.....	146
12.7	Evaluation of Potential for Degradation in Side Resistance	147
12.8	Evaluation of Post-Grouting as a QC/QA Tool	147
12.9	Recommendations for Load Testing of PGDS	148
REFERENCES.....		149

List of Figures

Figure 1.1:	Diagram of grouting apparatus used at the Paraná River bridge project (Bolognesi and Moretto, 1973).....	3
Figure 1.2:	Diagram of grout distribution device or “pre-loading cell” described by Lizzi (1983).....	4
Figure 1.3:	Diagram of the “U-Shaped Grouting Cell” described by Sliwinski and Fleming (1984).....	5
Figure 1.4:	Diagram of the “U-Shaped” grout distribution apparatus utilized in Taipei, Taiwan (Lin et al., 2000).....	5
Figure 1.5:	Schematic of the remedial stem grouting system used in Jeddah, Saudi Arabia (Littlejohn et al., 1983).	6
Figure 2.1:	Schematic illustrating mobilization of resistance for PGDS: (a) constructed drilled shaft prior to post-grouting; (b) grouting at the shaft tip mobilizes negative side resistance and positive tip resistance; (c) mobilized resistance following post-grouting, including any relaxation of mobilized load that may occur following grouting; and (d) top-down loading reverses side resistance and mobilizes remaining tip resistance (adapted from Brown et al., 2010).....	10
Figure 2.2:	Schematic illustrating effect of pre-mobilization: (a) load-displacement response of ungrouted shaft, (b) pre-mobilization of resistance during post-grouting, (c) pre-mobilization prior to subsequent top-down loading, and (d) load-displacement behavior for ungrouted and post-grouted shafts (adapted from Fleming, 1993). ..	11
Figure 2.3:	Photo of exhumed PGDS showing unintentional flow of grout up the side of the shaft (Brown et al., 2010).....	14
Figure 3.1:	Effect of water content on grout properties (from Littlejohn and Bruce, 1977)....	18
Figure 3.2:	Particle size distribution for various cements (from Karol, 2003).....	19
Figure 3.3:	Limited mobility grout extruding from an injection pipe (Cadden et al., 2000)....	24
Figure 3.4:	Schematic depicting the jet grouting process (courtesy of Hayward Baker, Inc.)..	25
Figure 3.5:	Diagram for estimating effective grout pressure (USACE, 2009).....	27
Figure 3.6:	Schematic of a high speed, high shear grout mixer	28
Figure 3.7:	Schematic of a grout agitator and holding tanks with paddle blades	28
Figure 3.8:	Grout plant with two tanks to maintain a continuous supply (courtesy of Applied Foundation Testing).....	28

Figure 3.9:	Single-stage piston pump (courtesy of Applied Foundation Testing).....	29
Figure 5.1:	Diagram of typical components used for a sleeve-port device (from Mullins et al., 2001).	40
Figure 5.2:	Photograph of components and connections at the bottom of a sleeve-port device (Mullins et al., 2001).....	41
Figure 5.3:	Sleeve-port devices: (a) single circuit sleeve-port device for small diameter shafts (Mullins et al., 2003), (b) four circuit sleeve-port device for a 12-ft diameter shaft (photo courtesy of Applied Foundation Testing), and (c) four circuit sleeve-port device used in conjunction with O-cell testing (Brown et al., 2010).....	42
Figure 5.4:	Radial circuit arrangements for sleeve-port grout distribution systems at the (a) Sutong Bridge (Safaqah et al., 2007), and (b) Paksey Bridge (Castelli, 2012).....	43
Figure 5.5:	Square arrangement of a sleeve-port grout distribution system (Bruce, 1986).....	44
Figure 5.6:	Photograph of a sleeve-port system constructed using flexible hoses (courtesy of Dr. H.H. Hsieh).....	44
Figure 5.7:	Low mobility grouting device: (a) schematic, and (b) photograph of device used for laboratory-scale tests (Pooranampillai, 2010).....	45
Figure 5.8:	Diagram of typical components used for a flat-jack device for a 48-inch diameter shaft (Mullins et al., 2001).	46
Figure 5.9:	Flat-jack post-grouting device on a 4-ft diameter shaft (photo courtesy of Applied Foundation Testing).	47
Figure 6.1:	Photograph of a Bourdon-type pressure gauge and a pressure transducer (courtesy of Applied Foundation Testing).	49
Figure 6.2:	Photograph of an LVDT between the reference beam and the top of the shaft during grouting (courtesy of Applied Foundation Testing).....	53
Figure 6.3:	Photograph of the survey level readings (automatic and manual) during grouting (courtesy of Applied Foundation Testing)	53
Figure 6.4:	Proposed graphing method from Mullins (2015) to guide control of post-grouting operations.	55
Figure 6.5:	Plot of measured grout pressure and strain versus time during post-grouting (courtesy of Applied Foundation Testing).....	58
Figure 7.1:	Normalized load-transfer curve for tip resistance of drilled shafts in cohesionless soil (Reese and O'Neill, 1988) used as backbone curve by Mullins et al. (2006).	63

Figure 7.2:	Graph of TCM from Equation 7.3 for normalized displacements between 0 and 5 percent, and GPI between 0 and 5 percent (after Mullins et al., 2006).....	64
Figure 7.3:	Measured load-settlement response from bi-directional load tests performed at the Audubon Bridge site (Dapp and Brown, 2010).	64
Figure 7.4:	Graph of TCM from Equation 7.5 for normalized displacements between 0 and 5 percent, and GPI between 2 and 3 percent.	65
Figure 7.5:	Design chart for determining ACM as a function of shaft head displacement and SGPI (from Pando and Ruiz, 2005).....	68
Figure 7.6:	Schematic illustrating effect of three improvement mechanisms considered for development of ACM method on load transfer models (from Fernandez et al., 2007): (a) compression of soil beneath shaft tip, (b) stress reversal along shaft due to upward movement during grouting, and (c) increase of shaft tip area from formation of grout bulb.	69
Figure 7.7:	Schematic illustrating enlarged shaft tip according to the truncated cone approach (after Liu and Zhang, 2011).	75
Figure 8.1:	Simple load-transfer models used for predicting performance of PGDS considering pre-mobilization alone: (a) bi-linear load-transfer model for tip resistance, and (b) tri-linear load-transfer model for tip resistance.	80
Figure 8.2	Load-transfer (t-z) model for side resistance.....	81
Figure 8.3:	Load-transfer (q-w) model for tip resistance.	82
Figure 8.4:	Simulated load-displacement response for a conventional ungrouted shaft subject to top-down loading for the simple example.....	82
Figure 8.5:	Pre-mobilization of side resistance from application of 200 psi grout pressure	84
Figure 8.6:	Comparison of load-transfer models for side resistance prior to, and after post-grouting.	84
Figure 8.7:	Pre-mobilization of tip resistance from application of 200 psi grout pressure.	85
Figure 8.8:	Comparison of load-transfer models for tip resistance prior to, and after post-grouting.	85
Figure 8.9:	Load-transfer model in side resistance after application of 200 psi grout pressure.	86
Figure 8.10:	Load-transfer model in tip resistance after application of 200 psi grout pressure.	87

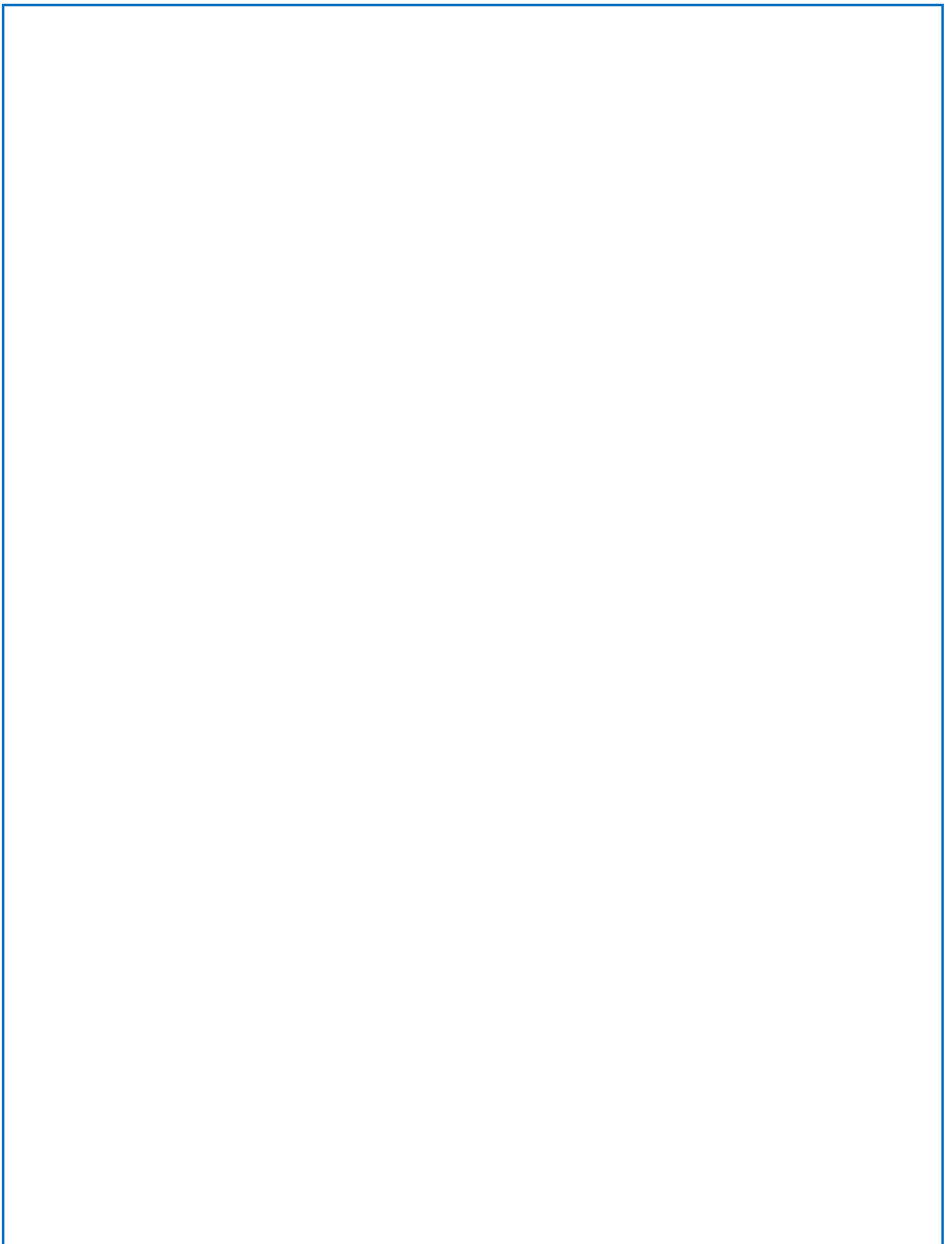
Figure 8.11:	Comparison of load-displacement response of the ungrouted and PGDS considering the effect of pre-mobilization alone.	87
Figure 8.12:	Modified load-transfer model for side resistance to account for pre-mobilized resistance showing remaining side resistance for a grouted shaft if subsequently loaded in an upward or downward direction.....	88
Figure 8.13:	Predicted and measured load-displacement response for ungrouted and post-grouted test shafts from the University of Houston Sand site. Predicted response for grouted shaft considers pre-mobilization only with no ground improvement.	92
Figure 8.14:	Predicted and measured load-displacement response for ungrouted and post-grouted test shafts from the University of Houston Sand site. Predicted response for grouted shaft includes both pre-mobilization and ground improvement	93
Figure 8.15:	Predicted and measured load-displacement response for ungrouted and post-grouted test shafts from the PGA Blvd. site. Predicted response for grouted shaft considers pre-mobilization only with no ground improvement.....	93
Figure 8.16:	Predicted and measured load-displacement response for ungrouted and post-grouted test shafts from the PGA Blvd. site. Predicted response for grouted shaft includes both pre-mobilization and ground improvement.	94
Figure 8.17:	GIR derived from simulations considering pre-mobilization for all analyzed cases with top-down load tests. Sites with bars indicate the range of GIR calculated using different plausible interpretations.....	95
Figure 8.18:	TIR derived from simulations considering pre-mobilization and ground improvement collectively for all analyzed cases.	96
Figure 8.19:	Calculated GIR and TIR for the respective cases plotted as a function of shaft diameter.	97
Figure 8.20:	Calculated GIR and TIR for the respective cases plotted as a function of the maximum sustained grout pressure for the respective shafts.....	97
Figure 9.1:	TIR vs. diameter for shafts tipped in sand, plotted according to: (a) grouting apparatus, and (b) load test type	101
Figure 9.2:	TIR vs. grout pressure for shafts tipped in sand, plotted according to: (a) grouting apparatus, and (b) load test type.	102
Figure 9.3:	TIR vs. diameter for shaft tipped in clay, including two points with exceptionally high values for the grout pressure index (GPI).	104
Figure 9.4:	TIR vs. diameter for shafts tipped in clay, plotted according to: (a) grouting apparatus, and (b) load test type.	105

Figure 9.5:	TIR vs. grout pressure for shafts tipped in clay, plotted according to: (a) grouting apparatus, and (b) load test type.....	106
Figure 9.6:	Ratio of predicted TCM to observed TIR for: (a) TCM using GPI from N60 , (b) TCM using GPI from load test measurements, and (c) component multiplier methods vs. diameter for shafts tipped in sand.	109
Figure 9.7:	Ratio of predicted TCM to observed TIR for: (a) TCM using GPI from N60 , (b) TCM using GPI from load test measurements, and (c) component multiplier methods vs. grout pressure for shafts tipped in sand.	110
Figure 9.8:	Ratio of predicted TCM to observed TIR for: (a) TCM using GPI from load test measurements, and (b) component multiplier methods vs. shaft diameter for shafts tipped in clay.	112
Figure 9.9:	Ratio of predicted TCM to observed TIR for: (a) TCM using GPI from load test measurements, and (b) component multiplier methods vs. maximum reported grout pressure for shafts tipped in clay.	113
Figure 10.1:	Test site stratigraphy: (a) test shafts, and (b) instrumentation.....	118
Figure 10.2:	Layout of test and reaction shafts.....	119
Figure 10.3:	Bi-directional loading devices: (a) flat jack, (b) RIM Cell, and (c) O-Cell.	120
Figure 10.4:	Bi-directional loading for TS-4.....	121
Figure 10.5:	RIM Cell pressure versus displacement for TS-4.	121
Figure 10.6:	QA/QC graphs for post-grouting of Test Shaft TS-5.....	122
Figure 10.7:	Load test setup for top-down loading.....	123
Figure 10.8:	Load-settlement response for all test shafts.	124
Figure 10.9:	Representative load-settlement response.	124
Figure 10.10:	Interpreted load transfer for Test Shaft TS-2.	126
Figure 10.11:	Interpreted load transfer for Test Shaft TS-4.	126
Figure 10.12:	Interpreted load transfer for Test Shaft TS-5.	127
Figure 10.13:	Strain gauge measurement interpretation.	127
Figure 10.14:	Mobilization of unit side resistance.....	129
Figure 10.15:	Mobilization of tip resistance.	129

Figure 10.16: Load-settlement response for Test Shaft TS-2.....	131
Figure 10.17: <i>t-z</i> response for Test Shaft TS-2.....	131
Figure 10.18: <i>q-w</i> response for Test Shaft TS-2.....	132
Figure 10.19: Load-settlement response for Test Shaft TS-4.....	132
Figure 10.20: <i>t-z</i> response for Test Shaft TS-4.....	133
Figure 10.21: <i>q-w</i> response for Test Shaft TS-4.....	133
Figure 10.22: Load-settlement response for Test Shaft TS-5.....	134
Figure 10.23: <i>t-z</i> response for Test Shaft TS-5.....	135
Figure 10.24: <i>q-w</i> response for Test Shaft TS-5.....	135

List of Tables

Table 3.1:	Approximate guidelines for the feasibility of permeation grouting in granular soils and rock when using particulate grouts (Adapted from Karol, 2003).....	23
Table 7.1:	Recommended improvement coefficients from Hu et al. (2001).....	72
Table 7.2:	Improvement coefficients provided in the Chinese <i>Technical Code for Building Pile Foundations</i> (China Academy of Building Research, 2008).....	73
Table 7.3:	Recommended improvement coefficients from Xiao et al. (2009).....	73
Table 7.4:	Recommended improvement coefficients from Dai et al. (2011).....	73
Table 8.1:	Summary of cases analyzed to separate contributions from pre-mobilization and ground improvement.	90
Table 9.1:	Summary of TIR for drilled shafts tipped and post-grouted in sand.	100
Table 9.2:	Summary of TIR analysis of drilled shafts tipped and post-grouted in clay and sand.	104
Table 9.3:	Comparison of predictions and measurements for shafts tipped in sand.	108
Table 9.4:	Comparison of predictions and measurements for shafts tipped in clay.....	111
Table 10.1:	Nominal resistance according to failure criteria.	125



CHAPTER 1: INTRODUCTION

1.1 Overview

The term post-grouting, or tip or base grouting, refers to a variety of practices related to injection of grout under pressure below the tip of a drilled shaft foundation to improve performance when subjected to compressive axial load. Although post-grouting of drilled shafts has been performed for nearly four decades in Europe, there has been limited application of post-grouting in the United States (U.S.). Variations of post-grouting have received increased interest within the United States private and public sectors following research supported by the Florida Department of Transportation (FDOT) in the early 2000s. Additional research has also recently been conducted for other state Departments of Transportation (DOTs) to evaluate the effectiveness of post-grouting for improving the performance of drilled shafts as structural foundations.

Post-grouting is typically accomplished using a grout delivery system that is incorporated into a drilled shaft during construction. The grout delivery system generally includes one or more tubes or pipes that pass from the top of the shaft to a grout distribution apparatus located at the tip of the shaft. Grout distribution devices can generally be classified as either open-type systems or closed-type systems. Open-type systems are ones in which grout directly contacts the ground upon injection at the tip of the shaft. In closed-type systems, the grout is contained within a variable-volume chamber and does not contact the ground directly. The vast majority of post-grouting applications involve injecting neat cement grout (i.e., Portland cement and water) under pressure beneath the tip of a drilled shaft to improve the stiffness and nominal resistance of the shaft to top-down loading. Side grouting of drilled shafts has been used to improve the side resistance along the length of the shaft in some cases (e.g., Sliwinski and Fleming, 1984; McVay et al., 2009; McVay et al., 2010), but such a technique is beyond the scope of this report.

In the U.S., the drilled shaft is constructed using the appropriate technique for the ground conditions, and grout is injected under pressure beneath the tip of the drilled shaft after the concrete has set. In instances where the grout pressure does not reach a “target grout pressure” during the initial grouting, repeated attempts may be made using a “staged grouting” approach. Post-grouting has also been used for remediation of drilled shafts found to contain construction defects. In such cases, specific grouting devices are not available, and common practice generally includes coring the shaft to flush and grout the unacceptable portion of the shaft or to inject grout at the tip of the shaft. Remediation of drilled shaft defects through post-grouting is beyond the scope of this report.

Post-grouting at the tip of drilled shafts has been purported to:

- Increase the tip resistance of drilled shafts, thereby allowing design lengths of drilled shafts to be shortened.
- “Stiffen” the load-deformation response of a shaft by pre-mobilizing side and tip resistance.
- Verify a “lower-bound” load carrying resistance of a drilled shaft as a function of the maximum sustained grout pressure.
- Reduce the effects of, and risk associated with, bottom cleanliness and potential “soft-bottom” conditions.

When adequately instrumented and properly monitored, the post-grouting process is believed to provide increased reliability compared to conventional (ungROUTED) drilled shafts, since the process provides a measurable indication of performance.

Despite the potential benefits from post-grouting, concerns remain regarding the reliance on improved performance for post-grouted drilled shafts (PGDS). These concerns arise from a variety of reasons that include:

- Lack of consensus regarding the magnitude and variability of improvement that may be expected from post-grouting.
- Lack of consensus about the specific mechanisms that contribute to improved performance.
- Questions regarding the geotechnical conditions that are suitable for post-grouting.
- Lack of well-vented quality control and quality assurance requirements that are established or endorsed by authoritative organizations such as the Federal Highway Administration (FHWA) or the American Association of State Highway and Transportation Officials (AASHTO).
- Need for better means to predict achievable grout pressures during the design phase, including consideration of the potential for grouting-induced hydrofracture.
- Concerns regarding potentially detrimental effects of upward displacement of drilled shafts during post-grouting, and the lack of established criteria for acceptable magnitudes of upward displacements.
- Concern about post-grouting becoming a routine item in specifications as a substitute for proper quality control, even in projects where it is not needed.
- Potential for designers to specify post-grouting as a substitute for proper geotechnical design.

The work described in this report was undertaken to address these questions and develop recommendations for design and construction of PGDS. The work included thorough review of available literature, review and evaluation of available load test results and case histories, conduct of field load tests, and consultation with practicing designers and constructors with extensive experience with both conventional and post-grouted drilled shafts.

1.2 Historical Use

Post-grouting has been used extensively to improve the performance of drilled shafts throughout Europe and Asia since the 1970s, and the practice has been widely documented in the technical literature (e.g., Bruce, 1986a; Bruce, 1986b; Sherwood and Mitchell, 1989; Troughton and Thompson, 1996; Castelli and Wilkins, 2004; and Bittner et al., 2007). Bruce (1986a; 1986b) provides a comprehensive summary of practices for pressure grouting the base of large-diameter drilled shafts, and traces the use and evolution of post-grouting technology to the mid-1980s.

Bolognesi and Moretto (1973) documented one of the first uses of post-grouting for drilled shafts. For this case, post-grouting was performed in multiple stages using the device shown in Figure 1.1 to improve the performance of foundations for two bridges crossing the Paraná River in South America. The shafts were founded in sand, ranged from 40 inches to 78 inches in diameter, and were about 250 ft in length. The grouting apparatus was composed of a basket of

uniform, coarse gravel sandwiched between two steel plates. The basket was attached to the end of the steel reinforcing cage and encapsulated by a rubber sheet. Both the steel plates and rubber sheet were perforated with 40 holes that were located in different positions to prevent backflow of the grout. The basket was “intended to serve both as a grouting and pressure distribution chamber.” As the void space in the basket was filled with grout, the pressure that developed within the basket pushed on the steel plates. The upward movement of the upper plate was resisted by the buoyant self-weight of the drilled shaft and downward side resistance, while the downward movement of the lower plate was resisted by the soil below the basket.

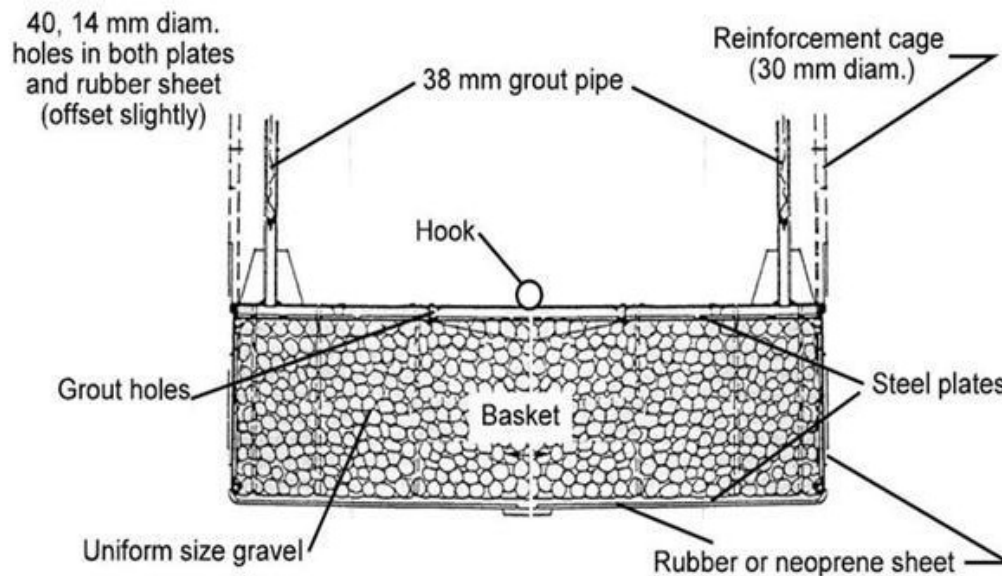


Figure 1.1: Diagram of grouting apparatus used at the Paraná River bridge project (Bolognesi and Moretto, 1973).

Bolognesi and Moretto (1973) postulated that there are two beneficial effects to post-grouting. The first effect is attributed to filling of voids created during shaft construction and strengthening of the soil at the shaft tip by “grout penetration.” The second effect is attributed to “pre-compression of the soil below the pile tip, which considerably decreases the settlement necessary to develop a certain amount of point load.”

Lizzi et al. (1983) described a similar grout distribution device, referred to as a “pre-loading cell,” composed of two steel plates but separated by steel mechanical spacers instead of uniform gravel (Figure 1.2). The device was attached to the bottom of the rebar cage and wrapped with “an outer impermeable PVC membrane and an inner canvas envelope.” Lizzi et al. (1983) stated that the device acted as a “flat-jack with unlimited travel” that uniformly compressed the soil beneath the shaft tip and pushed the shaft upward when pressurized grout was introduced. Because grout could flow freely across the base of the shaft, Lizzi et al. contended that the grout pressure served as “a very reliable estimate of the upward force exerted upon the pile bottom.” Based on evaluation of several case histories, Lizzi et al. concluded that use of “pre-loading cells” improves both the load-settlement response and the ultimate capacity of drilled shafts.

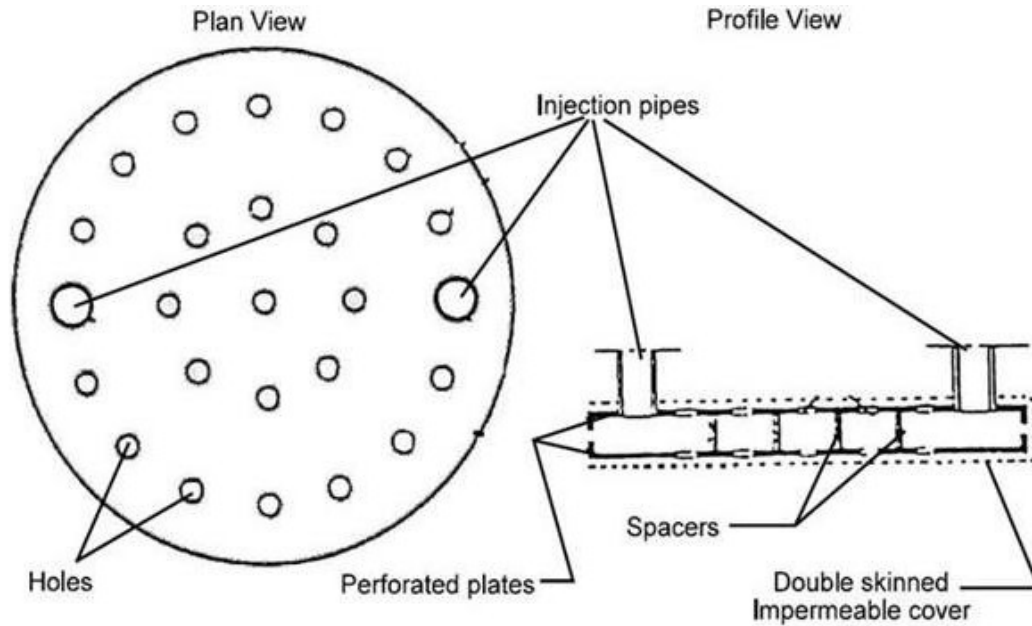


Figure 1.2: Diagram of grout distribution device or “pre-loading cell” described by Lizzi (1983).

Numerous variations of “flat-jack” devices similar to those described by Bolognesi and Moretto (1973) and Lizzi et al. (1983) have also been proposed and used. The devices have slightly different components and geometrical arrangements but typically include some form of membrane to contain the grout and/or to distribute the grout across the tip of the shaft. Such membranes are frequently made of rubber, but geotextiles have also been used to provide separation between the concrete in the drilled shaft and the grout injected during post-grouting.

In contrast to the “flat-jack” grouting systems, Sliwinski and Fleming (1984) describe a “U-Shaped” grout distribution system whereby grout is injected through perforations in pipes at the bottom of the shaft and into the ground beneath the shaft (Figure 1.3). Such systems are substantially different from “flat-jack” systems and are typically referred to as tube-à-manchette systems throughout Europe and Asia or as sleeve-port systems in the U.S. With sleeve-port systems, grout is pushed through the perforations in the pipes and into the ground when the injection pressure exceeds the confining stress provided by the rubber sleeve(s) and the surrounding ground or concrete. Like “flat-jack” distribution systems, upward movement of the drilled shaft is resisted by the buoyant self-weight of the drilled shaft and downward side resistance, while downward and radial movement of the grout is resisted by the soil below and surrounding the grouting device. However, unlike flat-jack systems, sleeve port systems are universally “open” systems that allow direct contact between the grout and the surrounding soil. As the grout is pressurized, the state of stress in the ground is presumed to increase; consequently, the soil is compressed and possibly cemented.

Numerous variations of sleeve-port grout distribution systems have been proposed and used. Lin et al. (2000) described two such systems that have been used for post-grouting (referred to as “base mud treatment”) in Taipei; one of these grout distribution systems is illustrated in Figure 1.4. Lin et al. also described utilizing a high-pressure flushing system to create a cavity below

the tip of drilled shafts prior to and in conjunction with pressure grouting in some cases. Similar sleeve-port systems and configurations were used for foundations of the Sutong Bridge across the lower Yangtze River in China (Bittner et al., 2007), and for the Paksey Bridge over the Padma (Ganges) River in Bangladesh (Castelli and Wilkins, 2004). Various sleeve-port systems have also been successfully used for numerous projects in and around the London area (Troughton and Platis, 1989; Yeats and O’Riordan, 1989; and Sherwood and Mitchell, 1989).

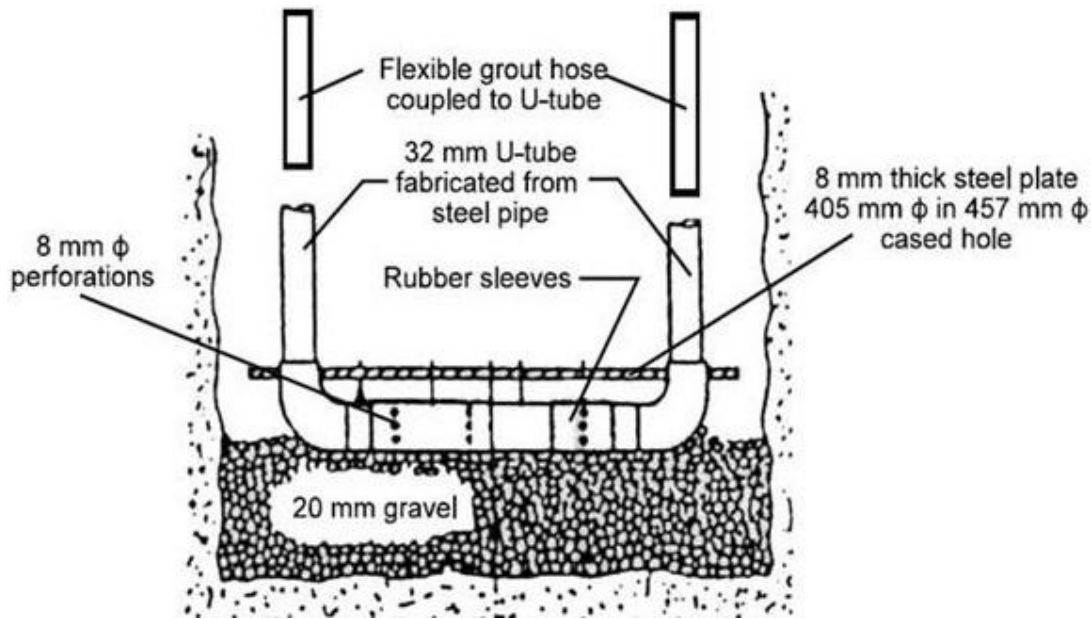


Figure 1.3: Diagram of the “U-Shaped Grouting Cell” described by Sliwinski and Fleming (1984).

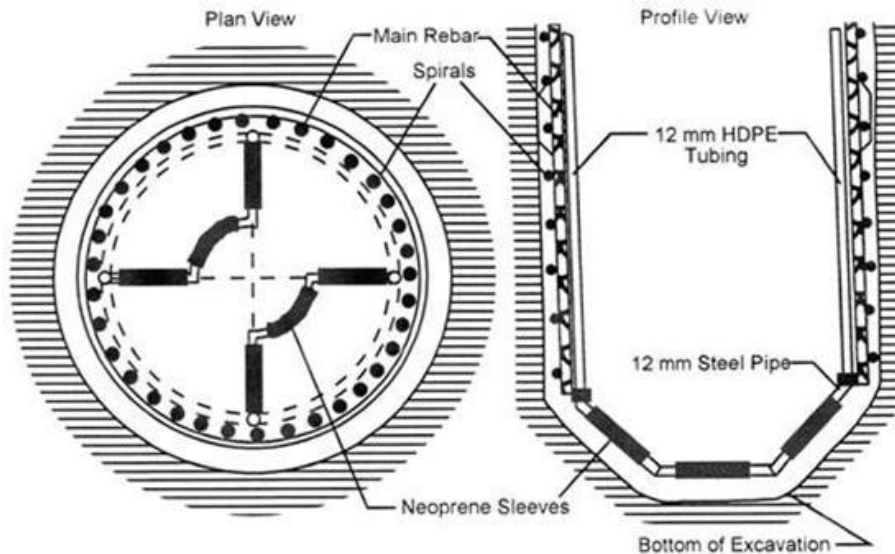


Figure 1.4: Diagram of the “U-Shaped” grout distribution apparatus utilized in Taipei, Taiwan (Lin et al., 2000).

Alternatives to the “flat-jack” and sleeve-port systems can also be found in the literature. One such example is described by Littlejohn et al. (1983) and shown in Figure 1.5. In this system, a vertical, “linear” tube-à-manchette system (i.e., not a “U-tube”) was used to remediate a soft or loose toe condition and to limit settlement of drilled shafts in sand in Jeddah, Saudi Arabia. In this particular case, resorcinol formaldehyde grout was injected through the tube-à-manchette system instead of cement grout, with the intent of permeating the resorcinol formaldehyde into the soil beneath the shaft tip.

Although post-grouting of drilled shaft foundations has been used worldwide for more than 40 years, there was little use of the technology in U.S. practice until the late 1990s. The increased use of PGDS in the U.S. during the last 20 years can be traced to FDOT sponsored research described in Mullins et al. (2000, 2001), and Mullins and Winters (2004), and to FDOT’s use of post-grouting in the sandy soils of Florida. The FDOT research was expanded by Mullins et al. (2006) and Dapp and Brown (2010).

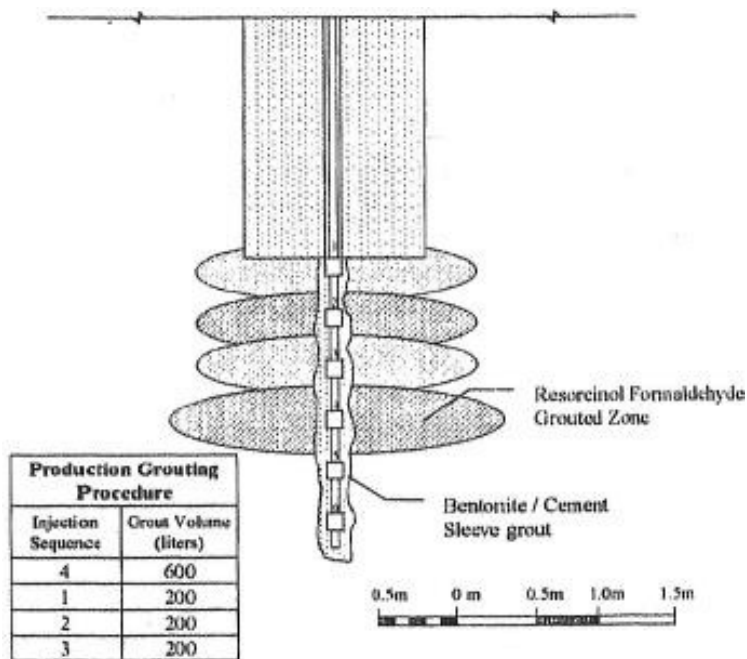


Figure 1.5: Schematic of the remedial stem grouting system used in Jeddah, Saudi Arabia (Littlejohn et al., 1983).

One of the earlier experiences with post-grouting in U.S. practice is described by Brusey (2000) for a project at JFK International Airport in New York. In this case, drilled shafts were installed through sands and organic deposits using an oscillator, and subsequently subjected to side grouting followed by tip post-grouting. Ported grout tubes were attached to the rebar cage and cast into the shaft, without a designated grouting device. Water was then pumped through the grout pipes 24 hours after the concrete was placed to fracture the concrete and provide paths for grout delivery. Brusey also references another project performed in 1989 in which the New York State Department of Transportation (NYSDOT) had used PGDS to support a bridge structure. Other historical references exist in the literature, and selected citations have been

included in the reference section of this report. A more comprehensive description of grouting systems commonly employed in current practice is provided in Chapter 5.

The majority of PGDS work in the U.S. during the last 15 years has been performed by specialty geotechnical service firms, whose practices for quality control and quality assurance of the grouting operations have evolved and established the current state of U.S. practice (Muchard, 2003, 2004, 2005, 2009, 2011). A partial summary of post-grouting experiences in the U.S., and the associated impact on quality control and quality assurance (QC/QA) for post-grouting operations in the U.S., is presented in Dapp et al. (2006). In recent years, foundation-drilling subcontractors have also begun to self-perform post-grouting work.

1.3 Existing Technical Guidance for Post-Grouted Drilled Shafts

Neither FHWA nor AASHTO has established recommended design and construction procedures for PGDS, and current practice for highway applications has generally evolved from work funded by FDOT and experience gained since that work. However, some recognition of PGDS can be found in more general guidance documents. In an FHWA technical guidance document on the design and construction of drilled shaft foundations, O'Neill and Reese (1999) briefly described post-grouting as a method of offsetting construction techniques that led to loosening of granular bearing soils, which resulted in a "soft" load-settlement response. O'Neill and Reese also describe remedial applications utilizing post-grouting, which could be used to address suspected problems with the tip of the shaft due to various construction issues. However, use of post-grouting was seen as too expensive for routine practice in the U.S. at the time, and was recommended only for critical situations. O'Neill and Reese (1999) also emphasize that post-grouting requires considerable expertise on the part of the contractor and that post-grouting may not be successful in all cases.

Mullins et al. (2006) introduced a design procedure to predict the ultimate tip resistance for post-grouted drilled shafts founded in cohesionless soils. This procedure has generally been the basis for design of PGDS on highway projects where the improved tip resistance is related to the maximum sustained grout pressure. Using this method, the tip resistance for a conventional (i.e., ungrouted) drilled shaft is multiplied by a Tip Capacity Multiplier (*TCM*) established for a desired level of displacement and sustained grout pressure.

In the most recent FHWA technical guidance on drilled shafts (Geotechnical Engineering Circular 10), Brown et al. (2010) described the limited use of post-grouting for drilled shafts founded in cohesionless (i.e., sandy) soils where there is sufficient side resistance available to develop the necessary grout pressure at the tip of the shaft. Brown et al. also stated that post-grouting seems unlikely to produce much improvement in tip resistance for drilled shafts bearing in clay, assuming that good construction practice and quality control are utilized for conventional shafts. Brown et al. also concluded that post-grouting is unlikely to produce significant benefit for drilled shafts bearing in rock, since sufficient tip resistance is likely available without the need for post-grouting.

1.4 Objectives

The primary objective of the work described in this report was to develop recommendations for design and construction of PGDS that can be disseminated to state DOTs and transportation partners to provide for cost effective, appropriate use of post-grouting techniques. The work included review of available technical literature; consultation with those currently involved with post-grouting, collection, and interpretation of results from full-scale load tests on post-grouted and conventional drilled shafts; investigation and evaluation of load transfer and improvement mechanisms for PGDS using numerical models, conduct of field load tests intended to evaluate improvement due to pre-mobilization alone; and development of recommendations for design and construction of PGDS based on the collective work. This report summarizes the current state of practice for post-grouting of drilled shafts in the U.S., documents the analyses and evaluations performed to evaluate alternative improvement mechanisms for PGDS, and describes the findings and recommendations developed based on the work performed. The report concludes with recommendations for future work needed to improve post-grouting practice for transportation infrastructure.

CHAPTER 2: IMPROVEMENT MECHANISMS FOR POST-GROUTED DRILLED SHAFTS

2.1 Introduction

Several different mechanisms have been suggested to explain the improved performance that is observed for PGDS. Knowledge of these mechanisms, and understanding how each mechanism contributes to actual performance, is important for establishing appropriate and reliable design and construction methods. Knowledge of the mechanisms for improvement also provides a technical basis for conceptual evaluation of post-grouting for different conditions and applications (e.g., different soil types, different loading, different post-grouting apparatus, etc.). This chapter contains a discussion of the potential improvement mechanisms and their practical implications.

2.2 Performance Improvement Mechanisms

The primary objective of post-grouting is to improve the overall performance of a drilled shaft either by increasing the ultimate axial resistance, improving mobilization of shaft resistance, or both. Four general mechanisms have been suggested for improving the performance of drilled shafts by post-grouting:

1. Improved mobilization of shaft resistance due to “pre-mobilization” of load in the shaft.
2. Improved tip resistance due to improvement of the ground beneath the tip of the shaft.
3. Improved tip resistance due to the formation of an enlarged shaft tip.
4. Improved side resistance due to the upward flow of grout around the perimeter of the shaft during grouting.

Additional descriptions of each of these mechanisms are provided in subsequent sections of this chapter. Each of these mechanisms can individually produce improved performance of a PGDS over that of a conventional shaft; however, it is likely that multiple mechanisms contribute to improved performance in many cases. Unfortunately, isolating contributions from the different mechanisms based on common measurements from field load tests is challenging. Nevertheless, consideration of these improvement mechanisms provides a reasonable framework from which to judge the effects of post-grouting, to predict the performance of PGDS, and/or to consider ways to improve the consistency and reliability of the performance of PGDS.

2.3 Pre-mobilization

The conceptual basis for improving the mobilization of resistance for a drilled shaft due to “pre-mobilization” is described by Fleming (1993) and illustrated in Figures 2.1 and 2.2. Figure 2.1 shows the general sequence of loading for PGDS, including loading induced during post-grouting, while Figure 2.2 compares the load-deflection response for similar ungrouted and post-grouted shafts.

Figures 2.1(a) and 2.2(a) reflect the performance of a conventional, ungrouted drilled shaft. In this case, the “total” load-deflection response to top-down loading is established from summation

of the mobilized side and tip resistance at a given displacement. Figure 2.2(a) also shows that both “positive” (i.e., upward) and “negative” (i.e., downward) side resistance can be mobilized depending on the direction of loading; whereas tip resistance is mobilized only if loading in the downward direction.

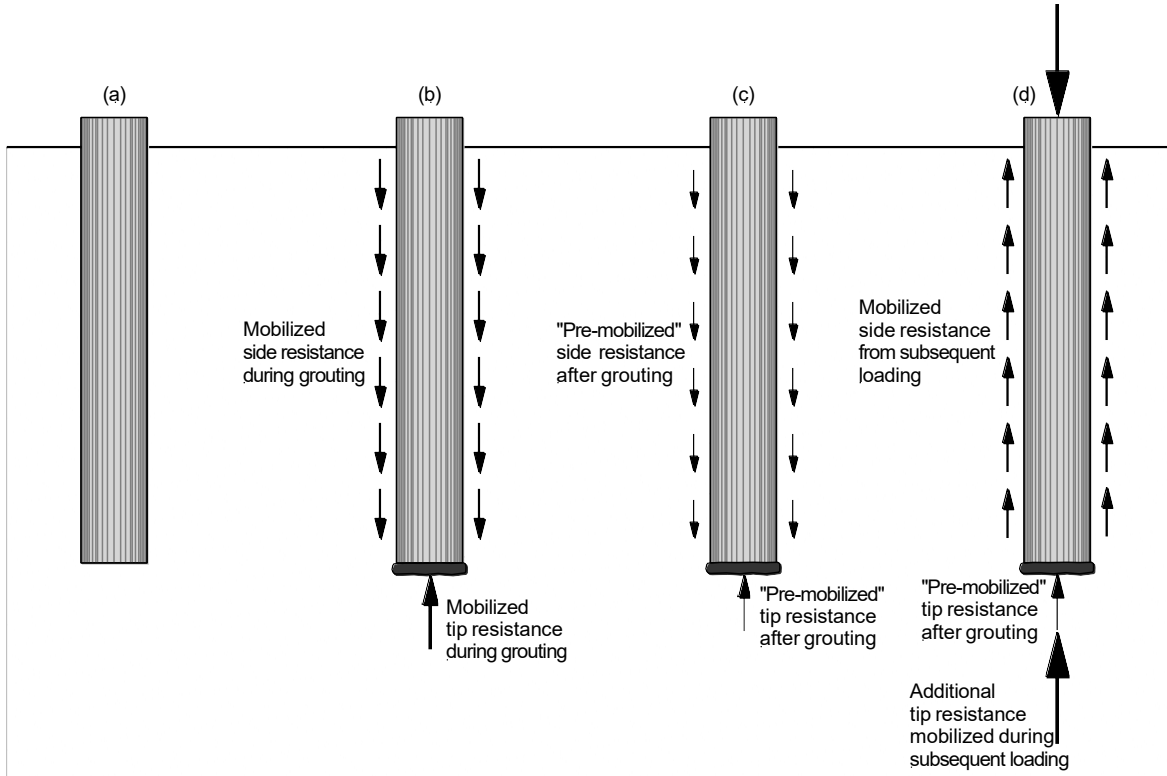


Figure 2.1: Schematic illustrating mobilization of resistance for PGDS: (a) constructed drilled shaft prior to post-grouting; (b) grouting at the shaft tip mobilizes negative side resistance and positive tip resistance; (c) mobilized resistance following post-grouting, including any relaxation of mobilized load that may occur following grouting; and (d) top-down loading reverses side resistance and mobilizes remaining tip resistance (adapted from Brown et al., 2010).

Figures 2.1(b) and 2.2(b) reflect loading induced during grouting at the shaft tip. Application of pressurized grout induces a bi-directional load at the shaft tip, which simultaneously mobilizes “negative” side resistance to resist the upward loading, and “positive” tip resistance to resist the downward loading. In Figure 2.2(b), the bi-directional load induced by post-grouting is indicated to have magnitude, P , which mobilizes negative side resistance to Point X and positive tip resistance to Point Y in the figure.

Following post-grouting, some relaxation of the resistance mobilized during grouting may occur as indicated in Figure 2.1(c), in which case the mobilized side and tip resistance will be reduced along some unloading curves as illustrated in Figure 2.2(c). The relaxation is indicated in Figure 2.2(c) as the unloading paths between Points X and X' for side resistance and Points Y and Y' for tip resistance, and the net pre-mobilized load following relaxation is indicated as P' . Points X'

and Y' reflect the net mobilized resistance developed due to post-grouting, and these points serve as the starting point for subsequent loading on the shaft. The net result of the pre-mobilized resistance due to post-grouting is therefore to increase the amount of side resistance that can be subsequently mobilized while simultaneously decreasing the amount of tip resistance by an equal amount.

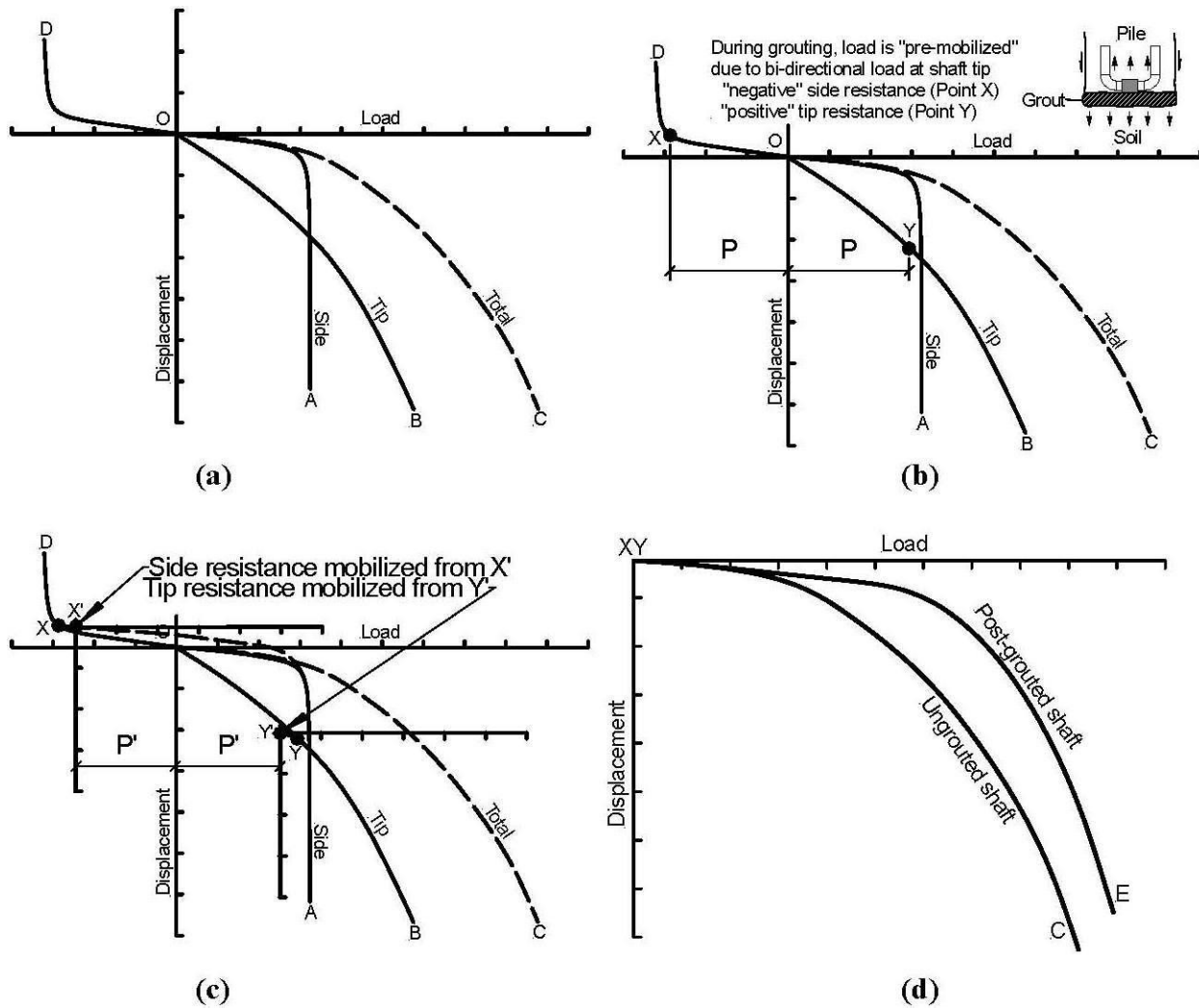


Figure 2.2: Schematic illustrating effect of pre-mobilization: (a) load-displacement response of ungrouted shaft, (b) pre-mobilization of resistance during post-grouting, (c) pre-mobilization prior to subsequent top-down loading, and (d) load-displacement behavior for ungrouted and post-grouted shafts (adapted from Fleming, 1993).

Since side resistance is generally mobilized at substantially smaller displacements than tip resistance (as shown in Figure 2.2(a)), the increase in side resistance that can be mobilized following pre-mobilization produces a “stiffer” shaft response to subsequent top-down loading, as illustrated in Figure 2.2(d). It should be noted that pre-mobilization alone produces no increase in the ultimate axial resistance of the shaft, but may substantially increase the resistance that can be mobilized at a given post-construction shaft displacement. Or, conversely, pre-

mobilization may reduce the magnitude of displacement that will occur for a given applied load. It should also be noted that subsequent bi-directional loading (e.g., from a bi-directional load test) will simply continue loading in the same directions as loading during post-grouting. As such, the effect of pre-mobilization will not be captured in measurements from a bi-directional load test, and would require further interpretation to assess its influence on the performance of the shaft under top-down loading from the superstructure.

The magnitude of improvement from pre-mobilization is directly related to the magnitude of the load, P' , induced during post-grouting. The load P' is related to the grout pressure achieved during post-grouting. Since pre-mobilization is dependent on the magnitude of P' , improvement from pre-mobilization can occur in any type of soil/rock. However, the magnitude of P' is generally constrained by the magnitude of available side resistance and the magnitude of the grout pressure that can be achieved in the field, both of which generally depend on the geometry of the shaft and the subsurface conditions present at a particular site. The magnitude of P' may also be influenced by the specific grout delivery system used for a PGDS and the specific procedure followed for post-grouting.

2.4 Ground Improvement

Post-grouting can improve the performance of drilled shafts through improvement of the ground beneath the tip of the shaft. Such improvement may result from densification of the soil or rock near the shaft tip, or from permeation of grout into the formation at the tip of the shaft. Unlike the pre-mobilization mechanism, ground improvement at the shaft tip may lead to an increase in the ultimate axial resistance of a PGDS over that of an ungrouted shaft. Such ground improvement may also “stiffen” the response of the shaft tip to loading, which would result in a stiffer overall response of PGDS.

There is some debate about whether ground improvement following post-grouting is due to “densification” of the ground or due to permeation of grout into the ground near the tip, or perhaps some of both. In a closed-type grout delivery system that does not rupture, grout should be contained within the system and should not permeate into the ground at the shaft tip. Therefore, it is reasonable to expect that any ground improvement that occurs for closed-type systems will be a consequence of densification under the applied grout pressure. In highly permeable soils (e.g., clean sand), densification should occur rapidly. In other soils, however, densification will take some time depending on the degree of saturation of the soil, the hydraulic conductivity of the soil, and the duration of grout pressure application.

Densification tends to increase the stiffness and strength of the ground, both of which will improve the performance of PGDS depending on the degree and volume of densification. The degree of densification is likely dependent on the initial density of the soil beneath the shaft tip as well as the magnitude of the grout pressure and the duration of its application. The improved volume should theoretically be larger for larger shafts and greater grout pressures. In reality, however, the volume of ground improvement is likely to be limited by the details of the grout delivery system, the initial properties of the ground, and by existing in situ stresses.

Open-type post-grouting systems may allow permeation of some types of grout into the ground in addition to, or instead of, densification. Like closed-type systems, open-type post-grouting

systems may also promote densification of the soil beneath the shaft tip through cake formation and dewatering of the grout. Whether a filter cake forms or permeation occurs will depend on the type of grout and the grain size distribution of the soil beneath the shaft tip. It is also notable that some closed-type post-grouting systems have been known to rupture during grouting, which may allow permeation of the grout near the shaft tip similar to open-type systems.

Like densification, permeation of grout into the soil beneath the shaft tip will increase both the strength and stiffness of the soil and, thus, improve the performance of a PGDS. Because the effects of densification and permeation are at least qualitatively similar, it is generally difficult to distinguish between the two based on load test measurements alone; therefore, improvement due to both sources is generally considered collectively as “ground improvement.” Regardless of the specific form of ground improvement or the specific delivery system used, the degree of ground improvement is likely to be most significant in loose, clean, granular materials and less significant in cohesive materials or intact rock.

2.5 Tip Enlargement

In addition to pre-mobilization and ground improvement, the performance of PGDS may be enhanced due to enlargement of the shaft tip. As is the case for the ground improvement mechanism described previously, enlargement of the shaft tip due to post-grouting will generally increase the ultimate tip resistance, and in turn the ultimate axial resistance for a PGDS. However, an enlarged tip may not produce the stiffer response that may be observed with the ground improvement mechanism because the larger tip area will generally impose stresses over a greater depth of ground below the shaft tip. The degree of tip enlargement is likely to be influenced by in situ stress conditions, the relative density of the soil/rock at the shaft tip, the applied grout pressure, and perhaps grout properties. Enlargement of the shaft tip is likely to be greatest for loose, clean, granular materials and least for cohesive soils/rock.

Tip enlargement can only occur in conjunction with densification of the ground or permeation of the grout into the ground beneath the shaft tip. Since few PGDS are actually exhumed, it is generally difficult to establish confidently whether observed improvements for PGDS are a result of ground improvement or tip enlargement, or some combination of both mechanisms. As a result, the ground improvement and tip enlargement improvement mechanisms are often considered collectively, despite the fact that the improved performance introduced by the alternative mechanisms may differ somewhat.

2.6 Improvement in Side Resistance

The performance of PGDS may also be improved from increased side resistance attributed to upward migration of grout during tip grouting. The practice of “side grouting” is a technique that specifically targets improvement in side resistance by injecting grout at discrete locations along the length and around the perimeter of a shaft (e.g., Sliwinski and Fleming, 1984; Brusey, 2000; McVay et al., 2010). Such practice is uncommon in the U.S. and is beyond the scope of this report. However, unintended upward flow of grout around the shaft perimeter has been documented in some cases (e.g. Mullins and Winters, 2004; Muchard and Farouz, 2009) for PGDS that are subject to “tip grouting” using devices similar to those described in Chapter 1, as shown in Figure 2.3. While such occurrences are unintentional, they may nevertheless increase

the ultimate side resistance over a portion of the shaft and contribute to the improvement observed for some PGDS. Predicting such improvement is challenging due to the difficulty of predicting the upward distance over which grout will flow, which likely depends on the specific grouting apparatus and grouting process used, characteristics of the fluid grout, ground conditions, in situ stresses, and the method of shaft excavation and concrete placement. It is therefore generally prudent to neglect such improvements in side resistance for design. However, potential improvements in side resistance should be considered for interpretation of load tests on PGDS to avoid incorrectly attributing improved performance to alternative mechanisms.

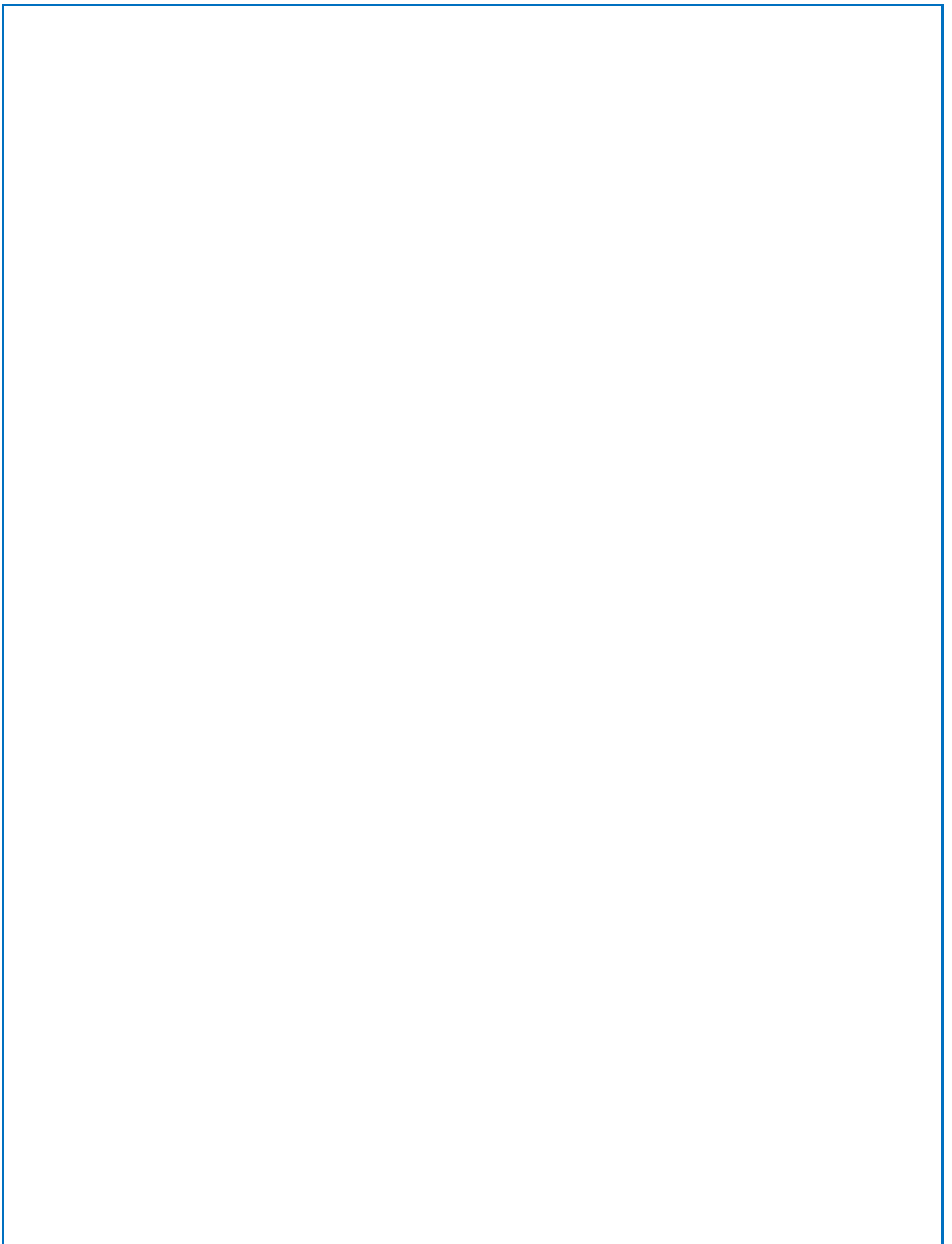


Figure 2.3: Photo of exhumed PGDS showing unintentional flow of grout up the side of the shaft (Brown et al., 2010).

2.7 Summary

Four possible mechanisms that may contribute to improved performance for PGDS as compared to conventional, ungrouted drilled shafts were described in this chapter. The possible improvement mechanisms include pre-mobilization, ground improvement, tip enlargement, and improvement in side resistance. Pre-mobilization is a result of mobilizing negative side resistance and positive tip resistance during grouting at the shaft tip. Pre-mobilization will occur in any type of ground and is dependent only on the magnitude of the load induced during grouting. Pre-mobilization does not increase the ultimate axial resistance of a PGDS compared to a similar ungrouted shaft. However, pre-mobilization does lead to improved shaft performance in that pre-mobilization produces a “stiffer” shaft response with less deformation

occurring at a given load or greater resistance being mobilized at a given settlement. In contrast, both the ground improvement and tip enlargement improvement mechanisms will increase the ultimate axial resistance of a PGDS compared to a similar ungrouted shaft. Both the ground improvement and tip enlargement mechanisms are likely “ground dependent,” with much greater improvement expected for PGDS tipped in clean, loose granular materials and lesser improvement expected in cohesive soils or intact rock. Finally, improvement in side resistance may result from unintentional upward flow of grout around the shaft perimeter. Improvement in side resistance is generally neglected for design because of the challenge associated with predicting the upward flow, but should be considered for interpretation of load tests on PGDS to avoid erroneously attributing improved performance to other improvement mechanisms.



CHAPTER 3: GROUTING PRINCIPLES FOR PGDS APPLICATIONS

3.1 Grout Defined

Grout is a broad term that describes a construction material used for a variety of functions that includes permeating the ground to fix soil/rock in place, densifying loose soils, displacing soft soils, and filling voids. Grout also has important applications in ground anchors, soil nails, micropile systems, and for ground improvement. For geotechnical applications, grout is generally classified as either chemical or particulate grout based on its composition.

Chemical grout is typically used in cohesionless soils and rock for creating water barriers, sealing leaks, and filling small voids and fissures. In addition, chemical grouts may be used as an improvement mechanism for bearing capacity and excavation support. Chemical grouts are soluble in water and may consist of one or more components, including sodium silicate or acrylamide. The penetrability of a chemical grout in a given particulate medium is a function of its viscosity (Karol, 2003).

Particulate or cementitious grouts are used to fill void space in the soil or rock and are composed of varying proportions of solid particles suspended in water. These types of grouts are commonly used to improve the strength and stiffness of soil or rock to enhance bearing capacity and reduce settlement, to control water seepage in fractured rock or coarse grained soils, and as the bonding medium between the ground and structural reinforcement (e.g., micropiles, soil nails, or ground anchors). The most common solid in most particulate grout is Portland cement, which is readily available commercially. Aggregates such as sand, fly ash, bentonite, and/or clay may also be used in a grout mix and admixtures may be introduced to increase grout workability, delay set time, resist sulfate attack, and increase pumpability in some applications.

In U.S. practice, cement-based grouts are typically used for PGDS. While there have been instances where chemical grouts were utilized for improvement of tip resistance beneath drilled shafts (e.g., Littlejohn et al., 1983), such uses are rare. This report, therefore, focuses on the use of particulate (cement) grouts for PGDS.

3.2 Particulate Grout Components

Cement-based particulate grouts are most commonly used because of their cost effectiveness, and because the methods used to prepare and place the grout are widely known and readily available throughout the construction industry. Characteristics of particulate grout are largely determined by the water-to-solids (e.g., water-to-cement) ratio of the grout mixture, which is frequently controlled to produce acceptable grout stability, rheology, strength, and permeability for a particular application (Littlejohn, 1982). The water-to-solids ratio is defined as the ratio of the weight of water to the weight of dry solids (e.g., cement, sand, etc.) within a mix. “Neat” cement grout mixtures composed exclusively of Portland cement and water are commonly used for PGDS. For such grouts, a lower water-to-cement ratio (w/c) results in higher grout strength but lower pumpability and fluidity as shown in Figure 3.1.

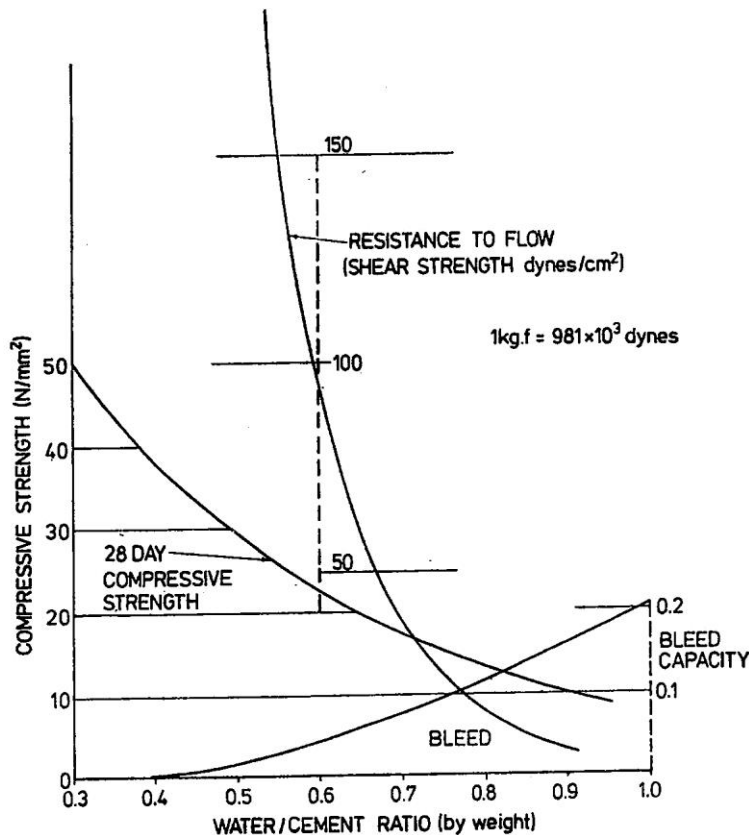


Figure 3.1: Effect of water content on grout properties (from Littlejohn and Bruce, 1977).

For PGDS applications, relatively high water-to-cement ratios are commonly used at the beginning of post-grouting to: (a) prime/lubricate the grout pump and access lines; (b) distribute grout more readily across the tip of the shaft; and (c) fill the voids in a gravel-bedding layer when one is used. Initial water-to-cement ratios are typically 0.7 to 0.9. Following this initial phase, the water-to-cement ratio is typically decreased systematically in increments of approximately 0.02 to 0.05 to: (a) provide a mix that is less mobile, less susceptible to hydrofracture, and more capable of achieving the desired grout pressure, and (b) prevent blockages that could be induced by a sudden introduction of a more dense mix into the system. Final water-to-cement ratios for PGDS typically range from 0.4 to 0.6. Although water-to-cement ratios of 0.22 to 0.24 provide for full hydration of the cement particles (Weaver and Bruce, 2007), a water-to-cement ratio of about 0.4 is the practical lower limit to maintain pumpability of the grout.

3.2.1 Cement and Particle Size

Cement-based particulate grouts have different classifications depending on the particle size and composition of the cement. There are five types of Portland cement (ASTM Standard C150, 2012). Type I cement is most common and represents most of the cement production in the U.S. Type II cement provides protection against moderate sulfate exposure and is suitable for use when the concrete is placed in direct contact with sulfate-containing soil or in regions where

aggregates susceptible to alkali-silica reactivity are employed. For PGDS applications, neat grouts comprised of water and Type I/Type II Portland cement (often found as a combination Type I/II) are common. Type III cement is known for having “high early strength.” Type IV cement has a “low heat of hydration,” and has been utilized for grouting in and beneath dams, and/or when careful control of hydration is needed. Type V cement is used where high sulfate resistance is required.

The particle size distribution of the cement plays a major role in determining whether a grout can penetrate a specific soil formation. The size of cement particles also has an important effect on the rate at which the particles will hydrate when mixed with water. Type III Portland cement is ground finer than other cements, resulting in shorter hydration and setting times compared to other types of cement. The fineness of cement is measured using a Blaine Permeameter (ASTM Standard C204, 2011), which indirectly measures the specific surface area of cement expressed as the total surface area per unit mass. For typical Portland cement, the Blaine fineness ranges from 3,000 to 5,000 cm^2/g , with the higher values corresponding to Type III Portland cement.

Microfine cements (MC) were developed in Japan and were first used in the U.S. in the 1970s. MCs are used to grout smaller voids than is possible with ordinary Portland cement, and are approximately ten times more expensive than ordinary Portland cement due to the additional mechanical grinding and blending of raw materials required for their production. Grain size distributions of various cements are shown in Figure 3.2. MC-500 is composed of 75 percent Portland cement and 25 percent blast furnace slag. MC-300 is composed of 100 percent finely ground Portland cement. MC-100 is composed of 100 percent blast furnace slag and is relatively inexpensive, but admixtures are typically required due to the long set time. MCs are frequently used for permeation grouting, but seldom for PGDS applications.

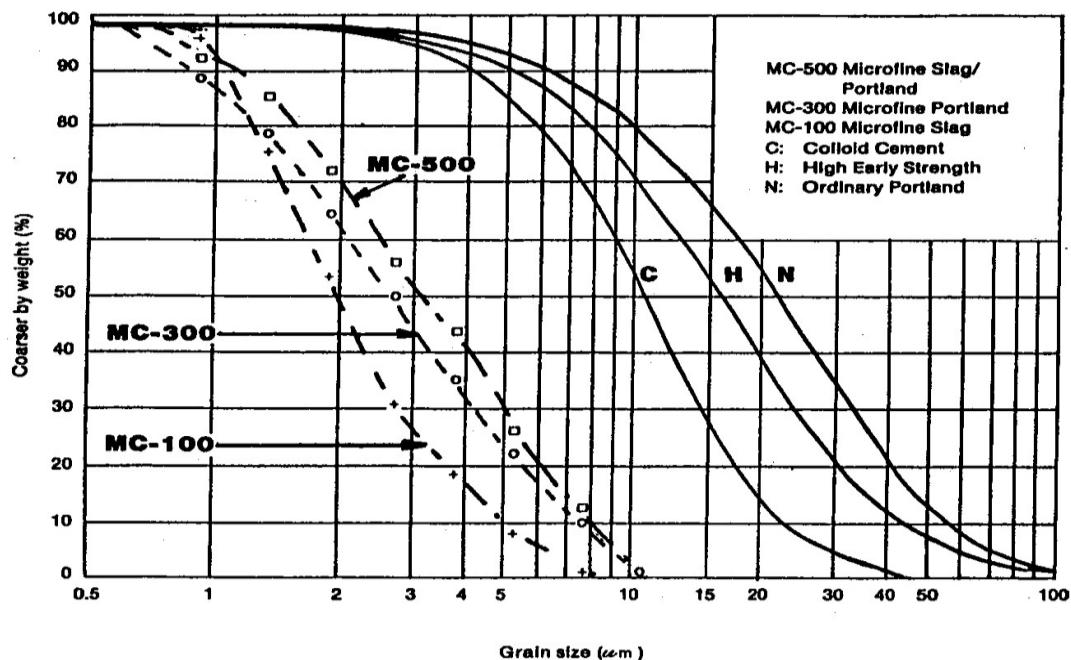


Figure 3.2: Particle size distribution for various cements (from Karol, 2003).

3.2.2 Grout Admixtures

Admixtures can be used to modify the properties of cement grout. Admixtures are primarily used to: reduce the cost of concrete construction; modify the properties of hardened concrete; ensure the quality of concrete during mixing, transportation, placement, and curing; and overcome unexpected situations during concrete operations. There are five main classes of admixtures: (1) air-entraining, (2) water-reducing, (3) retarding, (4) accelerating, and (5) plasticizing. In addition, specialty admixtures are available to inhibit corrosion, reduce shrinkage, reduce alkali-silica reactivity, increase anti-washout and integrity, enhance workability, increase bonding, enhance damp proofing, and add coloring.

Admixtures have rarely been used in PGDS applications. Potential reasons include a desire to keep grouting operations simple and because admixtures have not been perceived to produce sufficient benefit to justify the additional expense in PGDS applications.

3.3 Properties of Fluid Particulate Grouts for PGDS

Several characteristics of fluid particulate grout affect construction and performance for PGDS applications including rheology, bleed, and pressure filtration, which are discussed in subsequent sections.

3.3.1 Grout Rheology

Rheology is the study of the flow of materials and is characterized by three parameters: viscosity, cohesion, and internal friction. Of these three, viscosity is the most influential for PGDS operations. Viscosity is defined as the ratio of shear stress to the shear strain rate. Newtonian fluids exhibit a linear relationship between shear stress and shear strain rate, and do not require a minimum amount of shear stress to initiate strain or flow. Thus, viscosity for Newtonian fluids can be expressed as:

$$\mu = \frac{\tau}{\gamma} \quad (3.1)$$

where: μ = viscosity
 τ = shear stress
 γ = shear strain rate

Particulate grouts, however, are non-Newtonian fluids and are generally considered to be Binghamian fluids, which require a certain amount of shear stress to initiate flow. As such, Equation 3.1 is not generally applicable to particulate grouts and the following expression is used instead:

$$\tau = YP + PV(\gamma) \quad (3.2)$$

where: YP = yield point
 PV = plastic velocity

The value YP in Equation 3.2 is the shear stress required to initiate fluid movement of the grout. Once flow is established, the shear stress, τ , necessary to maintain flow is directly proportional to the rate of shear strain, $\dot{\gamma}$, within the grout. The value PV reflects the slope of the shear stress (τ) versus shear strain rate ($\dot{\gamma}$) curve. Therefore, the viscosity (μ) of the grout decreases with increasing shear strain rate. The viscosity of a grout is generally governed by the water-to-cement ratio and influenced by the addition of admixtures or fillers (Weaver and Bruce, 2007).

3.3.2 Bleed

Bleed is the separation of water from the grout solution. Bleed can be reduced by thorough mixing and use of a lower water-to-cement ratio. Bleed development for neat cement grouts is related primarily to the fineness of the cement and the water-to-cement ratio. In PGDS operations, controlling bleed is important to ensure complete filling of cracks and voids. Water that has exited the solution may create pockets of bleed water in the grout and cause the hardened grout to be porous, permeable, and susceptible to erosion (Weaver and Bruce, 2007).

Bleed capacity is defined as the total settlement per unit of original paste height. As shown in Figure 3.1, the bleed capacity for a grout with a water-to-cement ratio of 0.4 to 0.5 is less than 2 percent, which is suitable for PGDS operations. However, grout with a water-to-cement ratio of 1 or more will have substantially greater bleed, greater than 20 percent, causing the negative impacts described above.

3.3.3 Pressure Filtration

Pressure filtration occurs when grout is forced into small cracks and spaces, and water is expelled from the grout in motion. This leaves behind a cementitious “filter cake,” which clogs small cracks and interfaces, and prevents additional grout from passing. A coefficient of pressure filtration and a coefficient of filter cake growth can be calculated for cementitious grouts to quantify these two parameters. In general, a low coefficient of pressure filtration is desired to maximize the penetrability of a grout, whereas a high coefficient of pressure filtration will enhance formation of a filter cake and a grout “bulb” within the ground (Weaver and Bruce, 2007).

3.4 Commonly Measured Grout Properties

Several grout properties are commonly measured for quality control/quality assurance (QC/QA) of grouting operations. Commonly measured properties for neat cement grouts include specific gravity, Marsh funnel viscosity, and compressive strength. Specific gravity and viscosity are measured for the fluid grout mix during placement, whereas compressive strength is measured from grout cubes or cylinders that are cast during grout placement and allowed to cure prior to testing. All three properties are commonly measured for PGDS applications.

The specific gravity (G_s) of the grout mix is the ratio of the density of the grout mix to the density of water at a reference temperature. Specific gravity is measured following ASTM Standard D4380 (2012) or API Recommended Practice 13B-1 (2009) using a “mud balance,” where grout is placed in a cup of known volume, capped, and then weighed. Specific gravity is

possibly the most important measured property of the fluid grout because it can be correlated to compressive strength and viscosity, as well as other properties.

Viscosity (μ) of a grout mix is an indirect measurement of flowability and fluidity, which affect flow of grout through and potentially out of the grout distribution system. Viscosity is generally measured using a Marsh funnel following ASTM Standard D6910 (2009) and is reported as the time (in seconds) required for one quart of grout to flow from the Marsh funnel. Viscosity is seldom measured for PGDS applications, likely because few viscosity problems have been encountered due to the relatively high water-to-cement ratios that are specified for the neat cement grouts used for PGDS. Such high water-to-cement ratios lead to grouts with relatively low viscosity.

The compressive strength of grout is generally measured using grout cubes or grout cylinders prepared during grout placement and tested in a laboratory following ASTM Standard C109 (2013). The minimum compressive strength of the grout is generally specified in advance of construction based on the anticipated stress to be transmitted to and through the grout. For most PGDS applications, a high slump, neat cement grout with a 28-day minimum compressive strength of 2,000 to 4,000 psi is typically specified in accordance with ASTM Standard C476 (2010). Figure 3.1 shows the direct relationship between water/cement ratio and grout compressive strength.

3.5 Grouting Techniques

In general, grouting methods can be categorized into four basic techniques: permeation grouting, compaction or limited mobility grouting, jet grouting, and hydrofracture grouting. Each of these four basic techniques and their respective improvement mechanisms is described in the following subsections.

3.5.1 Permeation Grouting

Permeation grouting refers to the process of injecting chemical- or cement-based grouts into a soil or rock formation to improve the strength and reduce the permeability of the formation by introducing grout into the formation void space. Permeation grouting is generally applicable for cohesionless soil containing little to no fines, or rock with open fractures or fissures. Soils having appreciable fines content are generally considered too impermeable to accept grout (Karol, 2003). The primary mechanism of improvement from permeation grouting is to replace void spaces and to cement soil particles together, thereby increasing the strength and reducing the permeability of the improved soils. It is possible to improve a relatively large volume of soil using a fluid grout with high mobility, if the injection pressure can be maintained for the duration of grouting, if a properly designed grout mix is utilized, and if the soils are conducive to being permeated with the specific grout used.

For particulate grouts, the penetrability of a grout is generally controlled by the particle size distribution of the grout and the particle size distribution of the soil, or the aperture of fractures or fissures in rock. Table 3.1 summarizes the general feasibility of permeation grouting using common neat cement grout based on three parameters, N , N_c , and N_R , that reflect relative gradation characteristics of the soil/rock and the grout. The rheological properties of the grout

can often be controlled to obtain a desired penetrability into the pore space and a specific set time for the grout.

Table 3.1: Approximate guidelines for the feasibility of permeation grouting in granular soils and rock when using particulate grouts (Adapted from Karol, 2003).

	Soils		Rock
	$N = \frac{(D_{15})_{soil}}{(D_{65})_{grout}}$	$N_c = \frac{(D_{10})_{soil}}{(D_{95})_{grout}}$	$N_R = \frac{\text{Width of Fissure}}{(D_{95})_{grout}}$
Feasible	$N > 24$	$N_c > 11$	$N_R > 5$
Not feasible	$N < 11$	$N_c < 6$	$N_R < 2$

Grout permeation is generally not considered to contribute substantially to the improved performance that has been observed for PGDS compared to conventional drilled shafts. Rather, the grout is commonly believed to form a filter cake of cement that precludes permeation into the formation and subsequently leads to formation of a “grout bulb” that compresses and densifies the soil/rock below the shaft tip. However, in cohesionless soils with little fines content, some grout permeation may nevertheless occur.

3.5.2 Compaction or Limited Mobility Grouting

Compaction or limited (or low) mobility grouting is used primarily to “increase the density of soft, loose or disturbed soil, typically for settlement control, structural re-leveling [and] increasing the soil’s bearing capacity” (Schaefer et al., 1997). Limited mobility grouts (LMG) are typically particulate grouts with lower water-to-cement ratios than grouts used for permeation grouting. LMG are also more viscous, having a mortar-like consistency, and are designed to remain as an intact mass during injection without flowing into fractures or pore spaces within the formation as is presumed to occur in permeation grouting.

LMG contains coarse grained and silt-sized particles to limit mobility within the formation. The sand- and fine gravel-sized components in the mix develop internal friction, allowing the grout to expand as a growing homogeneous mass during injection. The fine-grained (silt) component facilitates pumpability while allowing the water in the mix to bleed slowly from the grout into the surrounding soil during injection. Ideally, the injection of LMG under pressure produces a controlled displacement and/or densification of soils, and becomes immobile when the injection pressure ceases. A photograph depicting the consistency of LMG is shown in Figure 3.3.

In general, LMG has broader applications than traditionally associated with permeation grouting. Numerous examples have been published describing the use of LMG in various applications. LMG is frequently used to densify loose materials beneath foundations to limit settlement, reduce liquefaction potential, and improve the strength properties of the in situ soil (e.g., Byle and Border, 1995; Schaefer et al., 1997; Siegel and Belgeri, 1999; Scherer and Gray, 2000). LMG is also widely used for treatment of karst conditions in both commercial and highway applications (e.g., Cadden and Traylor, 1998; Cadden et al., 2000; Bruce and Cadden, 2002; Gómez and Cadden, 2003; Englert et al., 2005; Wilder et al., 2005; Gómez et al., 2006).



Figure 3.3: Limited mobility grout extruding from an injection pipe (Cadden et al., 2000).

The neat cement grout typically used for PGDS would not normally be considered suitable for compaction grouting because it lacks coarse aggregate and because the water-to-cement ratio is generally much greater than typically used for LMG. However, it has been postulated that a filter cake of cement may form during grouting to create an interface between the grout and the surrounding soil and, further, that this filter cake allows the fluid within the grout to pass while retaining the cement particles at a greatly reduced water-to-cement ratio. Through this “dewatering” process, the neat cement grout may achieve results similar to what would occur with traditional LMG. To date, there has been limited investigation on the use of more traditional LMG for PGDS (Pooranampillai and Norris, 2010; Pooranampillai et al., 2009, 2010), and it has not been incorporated into typical practice.

3.5.3 Jet Grouting

Jet grouting is a technique that is “based on the introduction of hydraulic (sometimes combined with pneumatic) energy in order to erode soil and mix/replace the eroded material with an engineered grout to form a solidified mixture of the parent soil formation and cement grout” (Schaefer et al., 1997). Jet grouting has been utilized in conjunction with excavation support systems, underpinning, and ground improvement.

The jet grouting process consists of inserting a nozzle/bit to the desired depth and eroding and grouting the in situ soil using a pressurized fluid of grout, air, and/or water as the nozzle/bit and drill string are extracted (Figure 3.4). The diameter of the grouted column and the relative proportions of soil and cement components in the column vary depending on the characteristics of the surrounding geologic material and the jet grouting system used. Some adapted forms of jet grouting have been used to repair anomalies in drilled shafts. However, jet grouting has not been used for post-grouting at the tip of drilled shafts.

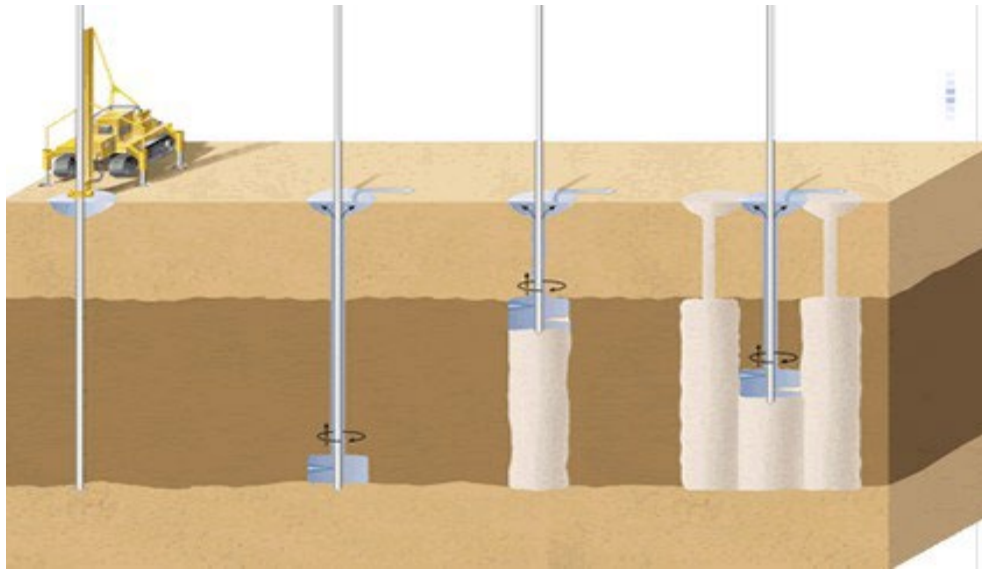


Figure 3.4: Schematic depicting the jet grouting process (courtesy of Hayward Baker, Inc.).

3.5.4 Hydrofracture Grouting

Hydraulic fracture, or hydrofracture, occurs when a fluid injected into the ground generates tensile or shear failure of the ground, and separation within the surrounding soil or rock. In grouting applications, hydrofracture can be induced by injecting pressurized grout into the ground. Continued injection of grout causes the grout to flow into the separations, which causes further separation of the soil and advance of the grout with desirable improvement to the ground. The occurrence of hydrofracture is generally accompanied by an observable increase in the rate of grout injected (i.e., grout “take”) with little or no increase in the measured grout pressure as grout flows into the space created by hydrofracture. In some cases, the grout pressure may be observed to drop as a result of hydrofracture. In planned geo-construction applications, hydrofracture grouting has been used to re-level structures that have been subjected to differential settlement and to reduce future settlement.

While hydrofracture is considered desirable for many grouting applications, it has generally been considered undesirable for post-grouting. The principal concern with hydrofracture in post-grouting operations is that it may limit the magnitude of the grout pressure that can be applied, and thus, the improvement that can be achieved for PGDS. The occurrence of hydrofracture also represents a loss of control of where the grout is traveling. Thus, the area over which the grout pressure acts becomes uncertain, which compromises the potential to use grout pressure as a quality control measure. Standard protocol for post-grouting operations has been to halt grout injection when hydrofracture occurs (based on observation of grout pressure and grout take) and allow the grout to set before continuing with grouting in a staged grouting approach as described in the following section. Uncontrolled injection of grout may also potentially lead to heave of surrounding ground and possible damage to nearby structures, although the likelihood of such damage seems remote since grouting is generally performed at relatively large depths in PGDS applications.

The grout pressure that causes hydrofracture is generally related to the in situ stress, and to the tensile or shear strength of the ground. Marchi et al. (2013) provide a good summary of methods for predicting the occurrence of hydrofracture. In general, the grout pressure that causes hydrofracture has been observed to be linearly related to the minor principal total stress in the ground, with a slope ranging between 1 and 2 depending upon whether hydrofracture occurs as a result of tensile or shear failure of the ground.

As illustrated in Figure 3.5, determination of the grout pressure at the point of injection must account for several factors, including head losses in both the supply line and the vertical grout tube, the pressure increase from the self-weight of the grout, and the water pressure at the bottom of the vertical grout tube. Head losses are a function of the flow rate, tube length, and the viscosity of the grout mix among other factors. The effective grout pressure (P_{eff}) can be calculated using Equation 3.3.

$$P_{eff} = P_g + (H_g + H_s - H_L)\gamma_{grout} - H_{gw}\gamma_w \quad (3.3)$$

where:

P_g	=	gauge pressure
H_g	=	gauge head
H_s	=	static head
H_{gw}	=	groundwater head
H_L	=	line losses
γ_w	=	unit weight of water
γ_{grout}	=	unit weight of grout

3.6 Stage Grouting

In some cases, a “stage grouting” approach may be adopted for grouting of PGDS. In stage grouting, grouting is halted following initial grout injection, and the grout is allowed to set for a period of hours to acquire some strength and seal off potential escape paths for the grout. Subsequent grouting attempts are then made with the hope that greater grout pressures can be sustained than was possible in previous grouting attempts. This procedure can be repeated multiple times in order to maximize the sustained grout pressure that can be achieved, although practical considerations generally limit stage grouting to three or potentially four grouting attempts. While stage grouting may be planned during design, it is generally adopted in cases where the anticipated grout pressure established during design cannot be achieved during the initial grouting attempt, either because of unexpected hydrofracture, because of excessive upward movement of the shaft during grouting, or other unknown reasons. An undesirable consequence of stage grouting is that cured grout from previous grouting phases may limit the mobility of the grout in subsequent phases. Thus, it may become difficult, if not impossible, to establish the area over which the applied grout pressure acts, which limits the potential to use the sustained grout pressure as a quality control measure.

3.7 Grouting Equipment

The following subsections present information on grout mixers and grout pumps commonly used in PGDS applications.

3.7.1 Grout Mixers

High speed, high shear mixers capable of effectively hydrating cement particles are typically used for the preparation of neat cement grout for PGDS applications. When thoroughly mixed, the cement and water are sometimes referred to as a semi-colloidal mix where the suspension of individual cement particles has a high resistance to settling or segregation as compared to a poorly mixed grout. A well-mixed, homogeneous grout mix is less susceptible to segregation or bleeding of the fluid grout during delivery and is less likely to clog the grout delivery system. Thus, the quality of the mixer directly affects the quality and consistency of the grout.

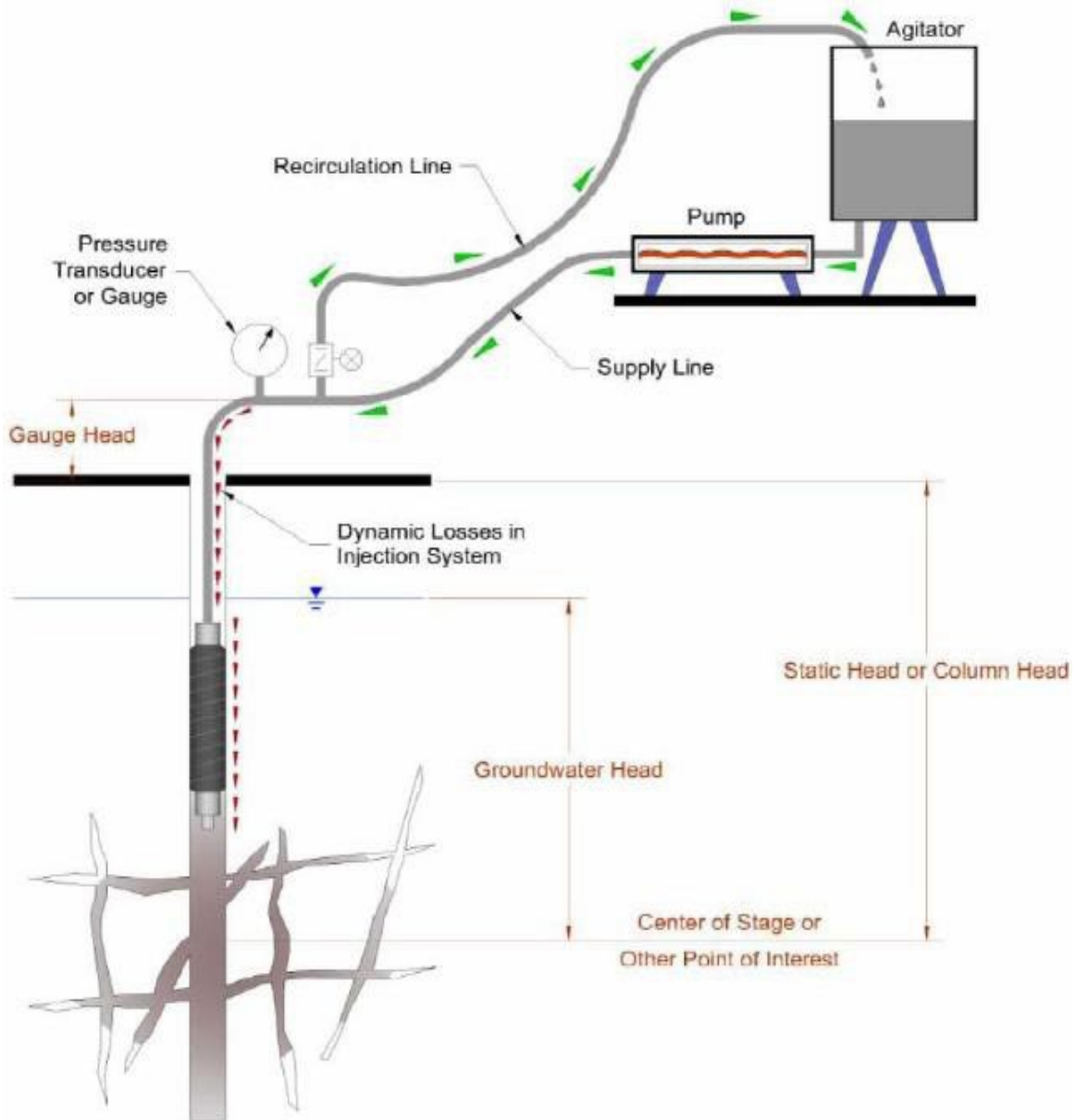


Figure 3.5: Diagram for estimating effective grout pressure (USACE, 2009).

As depicted schematically in Figure 3.6, an effective high speed, high shear mixer is able to quickly produce a thoroughly suspended mix, which limits the potential increase in temperature (paddle mixers require far greater time to achieve a suitable suspension) that could lead to premature setting of the grout. After the grout has been initially prepared using a high shear mixer, paddle mixers or agitators are suitable to keep the grout mixed prior to pumping (Figure 3.7). For typical post-grouting operations, grout plants with two tanks are commonly utilized (Figure 3.8). One tank is used to mix a batch of grout while the second tank serves as a holding or storage tank from which the grout is withdrawn and pumped to the tip of the shaft.

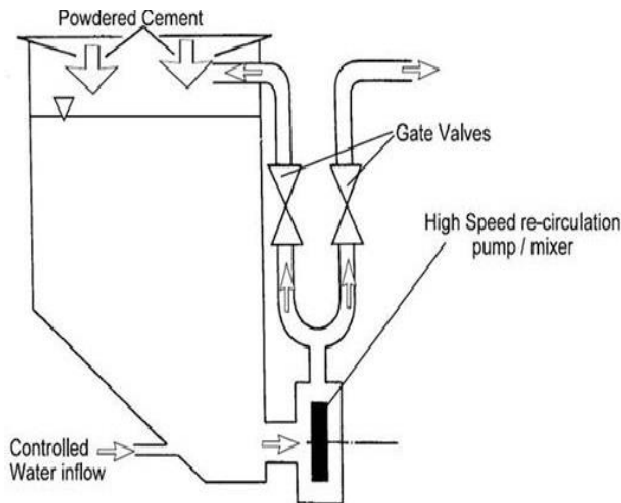


Figure 3.6: Schematic of a high speed, high shear grout mixer.

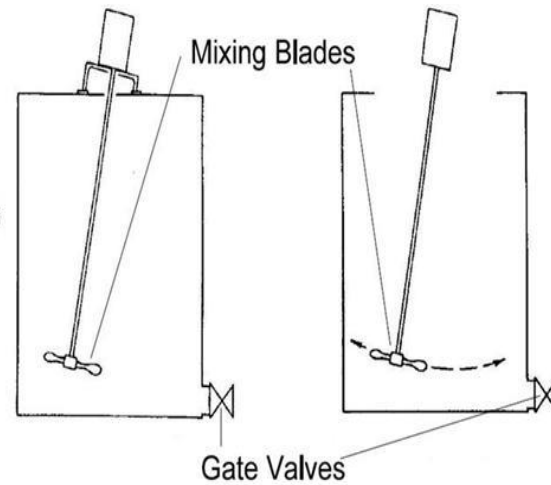


Figure 3.7: Schematic of a grout agitator and holding tanks with paddle blades.



Figure 3.8: Grout plant with two tanks to maintain a continuous supply (courtesy of Applied Foundation Testing).

3.7.2 Grout Pumps

Positive displacement piston pumps are typically utilized for post-grouting applications, as these pumps are capable of developing the high pressures (300 to 700 psi) commonly required for post-grouting applications. Multi-staged progressive cavity pumps or diaphragm pumps could conceivably be used to grout shafts where lower pressures are required. Piston pumps produce a pulsing type of pressure, similar to a systolic and diastolic action. A single-stage piston pump is shown in Figure 3.9.



Figure 3.9: Single-stage piston pump (courtesy of Applied Foundation Testing).

3.8 Summary

Common principles and practices for grouting of soil and rock that are relevant to post-grouting of drilled shafts were summarized in this chapter. “Neat” cement grouts, particulate grouts composed of Portland cement and water, are almost exclusively used for PGDS applications. Important characteristics of grout were also described including grout rheology, bleed, and pressure filtration characteristics. Several grout properties are commonly measured during or after grouting including specific gravity, viscosity, and compressive strength. Specific gravity and viscosity are measurements taken of the fluid grout, while compressive strength is obtained by testing cured samples of the grout.

Several different grouting techniques that are commonly utilized for ground improvement were described including permeation grouting, compaction or limited mobility grouting, jet grouting, and hydrofracture grouting. Post-grouting for drilled shafts is generally considered to most closely mimic compaction grouting; however, the grout commonly used for PGDS is substantially different from the grout conventionally used for compaction grouting. This apparent conflict is generally resolved by considering that the high mobility grouts used for post-grouting will form a cement filter cake, which in turn will lead to dewatering of the grout and formation of a “grout bulb” much like occurs with compaction grouting. Some permeation of

grout into the surrounding soil may also occur depending on the relative size of both the cement and the soil particles. Techniques similar to jet grouting have been used to remediate drilled shafts with construction defects, but are fundamentally different from typical post-grouting techniques. Hydrofracture grouting is also fundamentally different from typical post-grouting techniques. However, the occurrence of hydrofracture due to the grout pressure imposed during post-grouting may affect the degree of improvement observed due to post-grouting since it may limit the grout pressures that may be achieved and produce some loss of grout control.

Finally, common grouting equipment used for PGDS was described. High speed, high shear mixers capable of effectively hydrating the cement particles are typically used for the preparation of neat cement grout for PGDS applications. Positive displacement piston pumps are typically utilized for post-grouting applications, as these pumps are capable of developing the high pressures (300 psi to 700 psi) that are often required or desired for post-grouting applications.

CHAPTER 4: CURRENT POST-GROUTING PRACTICES

4.1 Introduction

Use of PGDS has expanded in states where drilled shaft construction is common. The most prevalent use of PGDS has been for projects with large axial loads that require relatively large diameter shafts with lengths exceeding 50 ft or more. Use of PGDS has been more prevalent in granular soils, but they have also been used in cohesive soil and rock on a more limited basis. This chapter summarizes current U.S. practices for PGDS, including common contracting methods, typical grouting procedures, and common requirements and specifications for PGDS. The information provided was derived from documented case histories and interviews with contractors experienced with constructing PGDS for the public and private sectors.

4.2 Contracting Practices in the U.S.

Contracting practices for PGDS in the U.S. differ from state to state and between the public and private sectors. In the private sector, incorporation of PGDS into a project depends on the project location and the owner or design engineer. PGDS have been designed and specified by the Geotechnical Engineer of Record on various projects throughout the southeast, south central, and western U.S. (Kitchens, 2013; Richards, 2013). PGDS have also been incorporated into design-bid-build projects through value engineering mechanisms.

Contracting for post-grouting work on public sector projects depends on the agency sponsoring the work as well as the selected contracting method implemented for a given project. On traditional design-bid-build transportation projects, design of PGDS is performed prior to bid letting, and construction specifications are generally established and enforced by the contracting agency or their design consultants. PGDS have also been used as part of value engineering programs for public sector design-bid-build projects; in such cases, contractors often have a more significant role in establishing construction methods and specifications, but these requirements are still largely controlled and enforced by the contracting agency. The situation is different for design-build contracts that are increasingly being used for large transportation projects. For design-build projects, responsibility is placed on the contractor to deliver a product that satisfies performance requirements for the project and the contractor is responsible for developing and enforcing construction specifications and requirements. The contractor also consequently carries the risk of performance, however, so the contracted price for PGDS on design-build projects reflects the relative balance of risk with potential cost savings associated with fewer and/or shorter drilled shafts. PGDS have been used on several design-build projects as a means to both control risk of potential foundation problems and to improve foundation efficiency.

Payment provisions for PGDS also vary from agency to agency. For example, payment for post-grouting work for projects sponsored by the Washington State Department of Transportation (WSDOT) is made on a “per each” basis for the first grouting stage, and by force account for subsequent grouting stages. In contrast, post-grouting work performed for the Florida Department of Transportation (FDOT) is paid “at the contract unit price per each accepted shaft,” but re-grouting below the tip of the shaft is paid at “a percentage of the contract unit price per each accepted shaft in addition to the payment for the original grouting.”

For both public and private sector projects in the U.S., post-grouting has most commonly been performed by a specialty geotechnical firm that develops and executes the post-grouting program, working under subcontract to the foundation subcontractor. More recently, there have been projects where post-grouting was “self-performed” by foundation subcontractors who were responsible for developing and executing the post-grouting program.

4.2.1 Typical Grouting Procedure

Grouting for PGDS is performed following construction of the drilled shaft once the shaft concrete has attained an established minimum compressive strength. Common steps in performing post-grouting include the following:

1. The elevation and spatial location of the top of the drilled shaft is surveyed and recorded to establish a reference for subsequent measurements.
2. The pump hoses and grout access tubes are flushed with clean water until the return flow is observed to be clean; grouting valves are then closed.
3. Neat cement grout is mixed using a high shear mixer until the mix is in a semi-colloidal suspension.
4. The grout pump is connected sequentially to each “circuit” and grout is initially pumped with the return side access line open until competent grout (i.e., specific gravity matches grout from pump) is returned to indicate that the circuit has been filled with grout. The return line is then closed and pumping is continued until one of the following termination criteria is met:
 - a. Pressure – the design grout pressure is sustained for a specified minimum period (e.g., two minutes), and the minimum volume of grout has been delivered.
 - b. Displacement – the upward displacement of the drilled shaft exceeds the established upward displacement threshold.
 - c. Volume – the volume of grout delivered exceeds a specified maximum grout volume threshold.
5. Once one of the termination criteria is met, the grouting valves are closed and the process is repeated for each circuit in the grout distribution system; the grout pressure is commonly released prior to closing the valves, but may be maintained until the valves are closed. Grouting of all circuits is completed as a continuous operation for each shaft.
6. If the design grout pressure and minimum grout volume are not achieved, additional stages of grouting may be required. Therefore, the grout tubes are commonly flushed with water prior to the grout setting to allow for subsequent grouting phases.
7. Measurements of grout pressure, grout volume, and upward displacement of the top of the shaft are recorded as a function of time throughout the grouting process (using two redundant methods). Upon completion of grouting, the elevation and spatial location of the top of the drilled shaft are measured and recorded along with the maximum upward displacement, net grout volume, and maximum sustained grout pressure.
8. Documentation of grouting operations and measurements is submitted in accordance with the specifications.

For typical PGDS applications, a pumping or flow rate of about 1 to 3 gallons/minute (gpm) may be used at the beginning of grouting, but the rate is then reduced incrementally as the grout pressure increases. Fleming (1993) recommends that the “lowest practicable grout injection rate

should be used,” and reported that grout injection rates are generally in the range of 1 to 3 liters/minute (0.3 to 0.8 gpm). Mullins and Winters (2004) report pumping rates for nine different post-grouting projects in the U.S. in terms of a flow rate per unit area of the shaft tip; the reported rates range from just under 0.04 gpm/ft² to just over 0.8 gpm/ft², with an average of approximately 0.3 gpm/ft².

4.3 Common Requirements and Specifications for PGDS in the U.S.

Contractual requirements and specifications for PGDS vary somewhat depending on the specific owner/agency and geographic location of a project. However, requirements and specifications for PGDS in the U.S. share many common elements related to the materials, equipment, record keeping and submittals, qualifications of on-site personnel, and construction and load testing of demonstration shafts. Common provisions for PGDS derived from review of various public and private sector project specifications for post-grouting work are described in this section.

4.3.1 Materials

Material specifications and requirements for PGDS focus primarily on grout characteristics, but also address other materials necessary for grouting. Requirements for the grout generally include specification of the cement, water, admixtures, and compressive strength. The cement is most commonly specified to be Type I/II Portland cement, but alternative cements may be specified depending on sulfate resistance and strength requirements. The water used for the grout is required to be potable water and to be available in sufficient quantity to maintain acceptable grout production. The final water-to-cement ratio is also generally specified, most commonly to be between 0.4 and 0.6 at the end of grouting. Although uncommon, required admixtures are also included in specifications. Compressive strength requirements are typically specified as a minimum grout strength after some duration of curing (e.g., 28-day minimum strength of 4,000 psi as tested by ASTM C109/C109M-98 Standard Test Method for Compressive Strength of Hydraulic Cement Mortars). This corresponds to a specific gravity between 1.8 and 1.9.

Additional relevant specifications may include requirements for gravel if it is used as part of the grout distribution system, and for grout tubes, pipes, fittings, and supply lines. In general, specifications for the gravel, derived most often from standard agency aggregate specifications, will include gradation and durability requirements. Requirements for the grout delivery system are focused primarily on ensuring that the delivery system is capable of withstanding the anticipated maximum grout pressure. In some cases, tubes used for integrity testing may be utilized for post-grouting; in such cases, the tubes must satisfy requirements for both integrity testing and grouting.

4.3.2 Equipment

Contract documents and specifications generally address requirements for equipment necessary for post-grouting including grout and water pumps, grout mixer and plant, the grout distribution system, and instrumentation necessary for control of grouting operations. Grout pumps are commonly required to be single- or double-stage hydraulic piston pumps capable of supplying the anticipated design grout pressure to the tip of the shafts, while water pumps must be sufficient to adequately flush and clear the grout delivery system if staged grouting becomes

necessary. The grout mixer and plant are generally required to be high efficiency, high shear mixers capable of producing a homogeneous grout mix in a semi-colloidal suspension. The grout plant is generally required to include a holding tank with an agitator and sufficient capacity to provide suitable quantities of grout for uninterrupted grouting of a shaft. Contracts and specifications generally require that PGDS are constructed with redundant grout circuits in case one of the circuits becomes clogged or obstructed.

Instrumentation and control equipment requirements vary substantially from project to project but generally include requirements for equipment to monitor and document the grout pressure, grout volume, and displacement of the top of the shaft as a function of time for the duration of grouting operations. Analog or digital pressure transducers and flow meters attached directly to the grout plant are generally specified to monitor grout pressure and volume. Dial gages or displacement transducers are commonly specified along with a reference beam for monitoring the movement of the top of the shaft. In some cases, additional or alternative requirements may be specified including additional transducers to measure pressure and volume nearer to the shafts, alternative means for monitoring the top of shaft movement, or requirements for automated data acquisition equipment. Strain gages and/or tell-tale rods within the shafts are also specified in some cases to assist in evaluating load transfer during post-grouting or for subsequent load testing of PGDS. Additional detailed descriptions and discussions of the instrumentation and monitoring systems used for PGDS are provided in Chapter 6.

4.3.3 Record Keeping and Submittals

Prior to construction of PGDS, the grouting subcontractor is generally required to submit a comprehensive grouting plan for review and approval. The grouting plan generally includes the following items:

- Details and drawings for the grout distribution device and appurtenances
- Anticipated sequence of grouting operations
- Plans and equipment for grout mixing
- Procedures for grouting individual shafts
- Procedures and equipment for measurement and monitoring of grout pressure, grout volume, and shaft movement
- Contingency plans for use in cases where the design grout pressure is not achieved, or other problems are encountered during grouting
- Planned record keeping and forms to be used for QC/QA during grouting

During grouting operations, records are kept to document grouting and QC/QA activities performed for each PGDS. Records generally include documentation of the following:

- Drilled shaft designation
- Specific grouting equipment used
- Grout mix proportions and changes to proportions
- Fluid grout characteristics such as specific gravity and viscosity (if measured)
- Termination and acceptance criteria and the specific criterion that was met
- Grout volume used in each circuit and stage of grouting

- Records of grout pressure, grout volume, and shaft movement measured at specified time intervals (e.g., 2 to 5 minutes) throughout grouting
- Graphs of grout pressure, grout volume, and shaft displacement versus time
- Grout cubes or cylinders cast and measured compressive strengths

In addition, records should include documentation of any unusual or unanticipated conditions or events that occur during grouting. Most specifications require that a minimum of four sets of grout pressure, grout volume, and shaft uplift measurements be made for each shaft, although greater numbers of measurements are common and desirable. Records of post-grouting operations are generally submitted daily and may subsequently be used to prepare a comprehensive report of grouting operations following completion of all PGDS.

4.3.4 Qualifications of On-site Personnel

Specifications and contract documents used in both the private and public sectors commonly require that qualified personnel with relevant experience be utilized to perform and to inspect post-grouting operations. Personnel requirements in contract documents and specifications commonly share similarities, but have variations in required experience and expertise. These documents most commonly require that both the grouting contractor and on-site inspectors have completed a minimum number of successful projects during a specified time (e.g., three successful projects in a five-year period). Such project experience is commonly required to have been performed in similar ground conditions, for similar shaft dimensions, and similar grouting devices as planned for the project to be undertaken.

4.3.5 Load Testing and Demonstration Shafts

It is relatively common for agencies to require pre-construction “demonstration” shafts (also known as “method” shafts, or “technique” shafts) for projects where PGDS are planned, and to require that PGDS demonstration shafts be load tested. Demonstration shafts for PGDS are generally intended to provide means to evaluate and refine procedures and practices prior to construction. Construction of demonstration shafts also allows agency and contractor personnel to become familiar with the practices and techniques that will be used for production shafts during construction.

Much like pre-construction load testing performed for conventional drilled shafts, load testing for PGDS demonstration shafts serves as a direct means to verify that the required performance of the PGDS can be realized for the specific materials, equipment, and procedures that are anticipated for production shafts. However, the need for and value of pre-construction load tests for PGDS is generally greater than for conventional drilled shafts because of the uncertainties involved with quantifying how alternative grout characteristics, grout distribution systems, grouting procedures, ground conditions, and other factors described throughout this report will affect the performance of PGDS. As knowledge and recognition of how such factors influence the performance of PGDS improves, the need for pre-construction load testing will naturally diminish. The primary purpose of the work performed to prepare this report has been to progress towards this end. However, many sources of uncertainty remain and it is likely that pre-construction load tests will remain necessary for PGDS for the foreseeable future.

Requirements for pre-construction load tests for PGDS seldom include testing of a companion, ungrouted shaft because such tests are not necessary for establishing whether a PGDS can fulfill the performance requirements for a particular project. However, lack of companion test results does preclude the ability to directly quantify the improved performance that results from post-grouting. The relative scarcity of companion tests has impeded development of knowledge of the improvement that can be realized from post-grouting and the effects of different grouting methods and procedures.

Pre-construction load tests are frequently performed using bi-directional load tests (commonly referred to as “Osterberg Cell,” or “O-Cell” tests) or Statnamic tests. Conventional top-down load tests are seldom performed because of the large loads that are required and challenges with providing suitable reaction for conventional static tests. While the prevalent use of bi-directional tests for PGDS is certainly understandable, the typical interpretation of bi-directional test measurements for ungrouted shafts is not directly applicable to post grouted shafts. Therefore, use of bi-directional tests in PGDS applications requires proper interpretation of the test measurements that accountS for reversal of loading that will occur from top-down loading.

4.4 Chinese Post-Grouting Practice

Post-grouting of drilled shafts is also prevalent in China (Xiao et al., 2009; Hu et al., 2001; Dai et al., 2011; Liu and Zhang, 2011). The *Chinese Technical Code for Building Pile Foundations* (China Academy of Building Research, 2008) describes specifications and practices for design and construction, which are outlined in the following sections. Note that this technical code has been translated into English and some sections are somewhat difficult to interpret.

4.4.1 General Requirements

The Chinese building code specifies the use of steel grout delivery pipes welded to the rebar cage of the shaft. It also prescribes using two grouting circuits for shaft diameters of 1200 mm (47 in) and smaller, and three circuits spaced evenly for shafts measuring between 1200 and 2500 mm (47 and 98 inch).

Interestingly, Chinese practice uses targeted side grouting when the shaft length is greater than 15 m (49 ft) and “higher bearing capacity amplification is needed.” In these cases, the code states that the quantity of skin post-grouting circuits must be determined based on the stratigraphy, shaft length, and the required improvement in bearing capacity of the shaft. “Skin grouting “valves” (ports) may be arranged every 6 to 12 m (20 to 39 ft) along the shaft, 5 to 15 m (16 to 49 ft) above the pile toe, and 8 m (26 ft) below the pile top.” The Chinese code also prescribes physical parameters of the grout, as described in the following sections.

4.4.2 Post-Grouting Parameters

For saturated soil, the Chinese building code prescribes a water-to-cement ratio of 0.45 to 0.65. For unsaturated soil, the water-to-cement ratio should be 0.7 to 0.9, while for “loose soil aggregate and grit,” the water-to-cement ratio should be 0.5 to 0.6.

The code also defines maximum pressures to be used depending on the classification of the stratum to be post-grouted. For disintegrated rock, unsaturated “cohesive soil and silty soil,” the

code prescribes a grouting pressure of 3 to 10 MPa (435 to 1450 psi); while for saturated soils, the pressure should be 1.2 to 4 MPa (174 to 580 psi), with the lower range of values adopted for “soft soils” and the higher range for “dense soils.” The code also dictates that the maximum grout flow is 75 L/min (20 gpm) and that the target grout volume must be calculated using shaft length, diameter, soil properties, and desired bearing capacity with empirical coefficients for drilled shaft tip and shaft side grouting volumes, as discussed further in Chapter 7. There is also a distinction made between individual shafts and those clustered in groups, with the calculated volume multiplied by a value of 1.2 for individual drilled shafts, and for shafts in groups where the shaft spacing is larger than 6 times the shaft diameter.

4.4.3 Post-Grouting Provisions

The Chinese code dictates that post-grouting should take place within two to 30 days after shaft installation, and provides instructions for sequencing post-grouting operations. The translated instructions are somewhat difficult to interpret; they read: “Compound grouting for saturated soil should be taken out from pile side to pile tip; for unsaturated soil, the compound grouting should start from pile tip to pile side; the grouting for multisection pile-side shall start from the upper to the lower; the grouting spacing interval of pile-side and pile-tip grouting should not be less than 2h.” When grouting groups of shafts, the grouting should begin at the peripheral shafts and progress to the inner shafts where applicable.

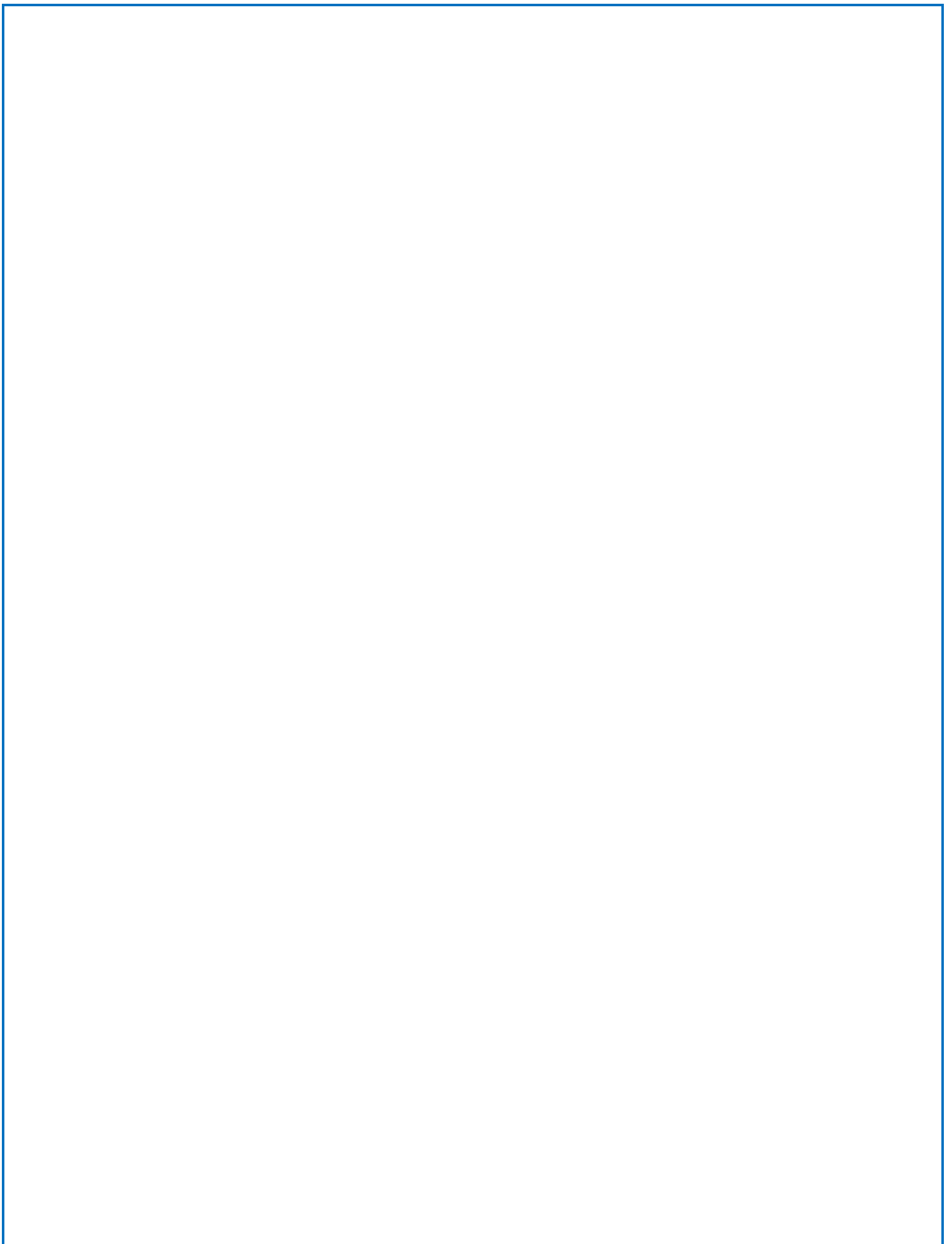
The code establishes the following grouting termination criteria:

1. Total grout volume and grout pressure reach the design requirements.
2. The total grout volume has reached 75% of the design value, and the grouting pressure exceeds the design value.

The code indicates that “interval” grouting should be performed in instances where it is not possible to reach the target grout pressure, where there is communication between shafts, or when there is grout flow to the ground surface. Consecutive grouting events should take place after 30 to 60 minute intervals. It also provides the alternative option of decreasing the water-to-cement ratio of the grout.

The code requires development of complete records of the post-grouting process for each PGDS. It also requires load testing of the PGDS 20 days after post-grouting and after the concrete is proven to meet the strength requirements. It is not clear, however, if proof testing is required for a significant number of PGDS at each site.

Although there is still much to learn about Chinese PGDS practices, it is apparent that the main differences with U.S. practice are deliberate side grouting, a much higher maximum grout flow rate (20 gpm compared to U.S. average values of 0.3 to 1 gpm), and distinguishing between single and group shafts when computing grout volume and grouting sequencing.



CHAPTER 5: GROUT DISTRIBUTION SYSTEMS FOR PGDS APPLICATIONS

5.1 Introduction

Several different devices have been used for post-grouting of drilled shafts. These devices can be classified as open-type systems or closed-type systems. An open-type system is an apparatus for delivering grout at the shaft tip without any means to contain the grout or provide separation between the grout and the surrounding ground. In an open-type system, the grout is directly injected into the surrounding ground and is free to flow along the path of least resistance. Conversely, a closed-type system is an apparatus with a barrier (e.g., flexible rubber membrane) that is intended to contain the grout and provide separation between the grout and the surrounding ground. Barring rupture of the separation barrier, grout will be contained within the apparatus. Both open- and closed-type systems have been used extensively for PGDS applications. The following subsections describe alternative open- and closed-type grouting devices that have been used for PGDS.

5.2 Open-Type Grout Distribution System: Stem (Orifice)

The simplest open-type grout distribution system is the stem or orifice grouting system. Stem grouting can be accomplished by grouting through one or several cored hole(s) extending through an existing drilled shaft, or through the bottom of an integrity testing tube if one or more are available (e.g., Figure 1.5). Grout distribution at the shaft tip can be improved by utilizing multiple stem grouting tubes distributed at various locations across the base of the shaft, particularly for large diameter shafts. In current U.S. practice, this relatively simple method is commonly utilized as a technique for remediating shafts with inadequate axial resistance or tip anomalies identified via shaft integrity tests (e.g., crosshole sonic logging tests, thermal integrity tests, etc.), but is not generally utilized for PGDS that are intentionally constructed.

Stem grouting devices do not appear to be efficient compared to more robust distribution devices that are intentionally incorporated into the shaft prior to concrete placement. Stem grouting devices are also not well suited to a staged grouting sequence because of challenges with flushing and cleaning of pipes that “dead end” rather than forming a complete pipe “circuit.” Further discussion of remediation grouting techniques is beyond the scope of this report; however, additional discussion can be found in Bruce and Traylor (2000).

5.3 Open-Type Grout Distribution System: Sleeve-Port (Tube-à-Manchette)

The most common open-type grout distribution system is the tube-à-manchette or sleeve-port system, which has been used in various geometric configurations. Sleeve-port systems are typically composed of one or more grouting “circuits” created by two vertical tubes and a horizontal tube forming a “U” shape, commonly referred to as a “U-Tube.” The vertical tubes in a circuit are typically attached to longitudinal reinforcing bars and cast into the drilled shaft while the horizontal tube is typically located at or near the bottom of the shaft, below the rebar cage. The horizontal tube is usually separated or protected from the concrete of the drilled shaft

by a steel plate. A diagram of a typical sleeve-port device and its various components is shown in Figure 5.1.

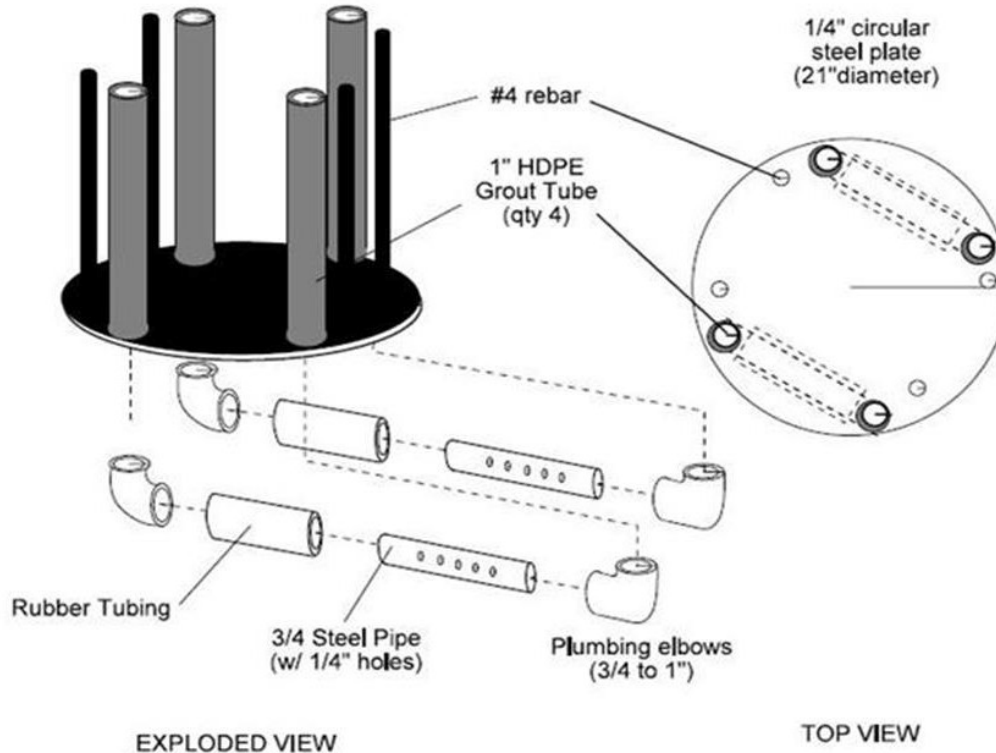


Figure 5.1: Diagram of typical components used for a sleeve-port device (from Mullins et al., 2001).

Pipe with a nominal one-inch inside diameter is commonly used in the U.S. for dedicated grout tubes in sleeve-port distribution systems. The tubes are typically composed of Schedule 80 PVC for the length cast within the concrete, although steel pipe is also used. Steel pipe is used for segments that extend below the concreted shaft. Crosshole sonic logging (CSL) tubes have also been used for post-grouting to avoid introducing excessive elements within the rebar cage. In such cases, a pair of CSL tubes (typically 2-inch nominal inside diameter) is connected to a sleeve-port pipe below the shaft to form a U-Tube circuit. Tubes installed for alternative types of integrity testing (e.g., gamma-gamma logging, thermal integrity testing, etc.) could also conceivably be used in a similar manner. When CSL tubes are used for post-grouting, grouting operations are generally performed after CSL testing is completed to avoid the potential for blocking the tubes with grout.

The horizontal segment of pipe at the shaft tip is perforated with multiple small holes (or ports) along a portion of its length and wrapped in a rubber sleeve (Figure 5.1) to allow injection of grout at the tip of the shaft. The tight-fitting sleeve completely covers the holes and provides a seal against the pipe to prevent infiltration or plugging by concrete or soil during placement of the rebar cage and concreting of the shaft. The rubber sleeve essentially acts as a one-way valve during subsequent grouting that allows grout or water to flow out of the tube, but restricts flow back into the tube when pumping is ceased. The rubber sleeve is commonly left unrestrained at

its ends (Figure 5.2) when dedicated grout tubes are used, but is usually restrained using pipe clamps or other similar banding (Figure 5.3) when CSL tubes are used for post-grouting to provide an active seal to keep water within the tubes during CSL testing.



Figure 5.2: Photograph of components and connections at the bottom of a sleeve-port device (Mullins et al., 2001).

Within 24 to 48 hours after placing the shaft concrete, sleeve-port systems are generally flushed with water while the concrete is still green (i.e., not fully cured) to ensure that the ports are not blocked. When CSL tubes are used for post-grouting, the rubber sleeve must be burst (typically with water) following CSL testing to allow for subsequent injection of grout because of the restraining bands used at the ends of the rubber sleeve. In cases where a steel separation plate is not used and the horizontal grout tubes are embedded within the concrete at the bottom of the shaft (Figure 5.4), the green concrete must be ruptured during flushing of the grout tubes to create passageways for subsequent injection of grout through the concrete.

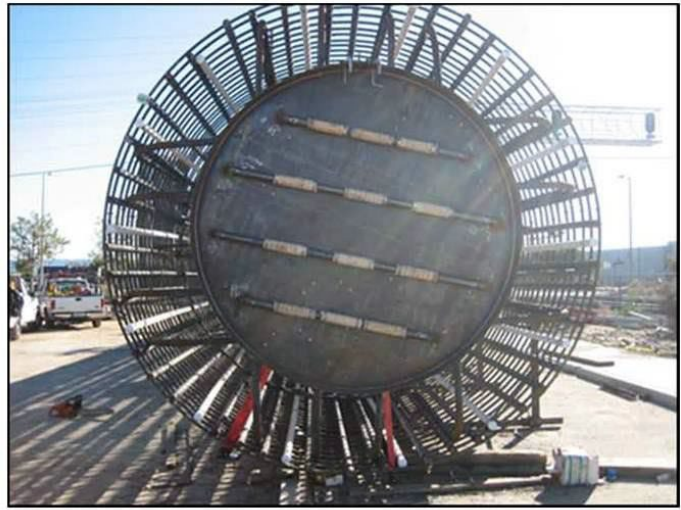
Multiple grouting circuits are typically used to provide redundancy and to ensure better coverage across the base of a shaft, especially for large diameter drilled shafts. Sleeve-port circuits are most often installed in a parallel arrangement across the bottom of the shaft as illustrated in Figure 5.3, although alternative arrangements are sometimes used as shown in Figure 5.4. As few as one or two grouting circuits have been used for small diameter shafts, whereas three to five grouting circuits are typically used for larger diameter shafts. Within the past decade, a perimeter “scuff ring” has been used more frequently around the edge of the steel separation plate to improve separation between the shaft concrete and the sleeve-port system, and to facilitate opening of the sleeve ports during grouting (Dapp et al., 2006). Steel sections (e.g., angles and flat plate) have sometimes been welded to the steel separation plate for large diameter shafts to increase its stiffness and safeguard against crushing of the sleeve-port tubes under the weight of the cage and concrete. In addition, sleeve-port systems have been used in conjunction with and below bi-directional load-testing devices (commonly known as the “Osterberg Cell,” or “O-Cell”), as shown in Figure 5.3(c).

Sleeve-port grouting systems have proven conducive for use when multiple grouting attempts are made because the tubes and ports can be easily flushed with water and cleaned between grouting

stages without disturbing the freshly injected grout. Sleeve-port systems may also act to hold grout pressure at the tip of the shaft following grouting, regardless of whether the grout pressure is released at the surface, because they act as a “one-way valve.”



(a)



(b)



(c)

Figure 5.3: Sleeve-port devices: (a) single circuit sleeve-port device for small diameter shafts (Mullins et al., 2003), (b) four circuit sleeve-port device for a 12-ft diameter shaft (photo courtesy of Applied Foundation Testing), and (c) four circuit sleeve-port device used in conjunction with O-cell testing (Brown et al., 2010).



(a)



(b)

Figure 5.4: Radial circuit arrangements for sleeve-port grout distribution systems at the (a) Sutong Bridge (Safaqah et al., 2007), and (b) Paksey Bridge (Castelli, 2012).

Drilled shaft boreholes commonly have minor deviations in alignment and, at times, may not be precisely terminated at the planned tip elevation because of variable ground conditions, imperfect depth measurement, and/or unintentional depth variations due to shaft tip cleaning operations. Use of down-hole grabs or reverse circulation drilling methods for shaft excavation also tend to produce a conical or dish shape at the base of the borehole, rather than a flat base that is often assumed. Such conditions pose challenges for post-grouting, especially if the rebar cage and the grouting apparatus are fabricated in advance of excavation. Several alternative adaptations have been utilized to address these challenges including using alternative arrangements for the sleeve ports (Figures 1.5 and 5.5), using flexible grout tubes (Figure 5.6), or using slip joints on the grout tubes to laterally restrain the tubes while allowing them to “float” vertically so that the depth of the grouting device can be adjusted (Mullins et al., 2001). Although not used in current U.S. practice, the grout tubes can also simply be embedded in the shaft concrete at the planned elevation. This approach requires that the green concrete be fractured with high pressure water to create conduits for subsequent grouting operations. Figure 5.4 is an example of such a system. In yet other cases, clean gravel bedding has been used to produce a flat surface upon which to place the grouting apparatus at the appropriate elevation, to facilitate distribution of grout across the shaft tip, and to provide a conduit and void space for grout delivery.

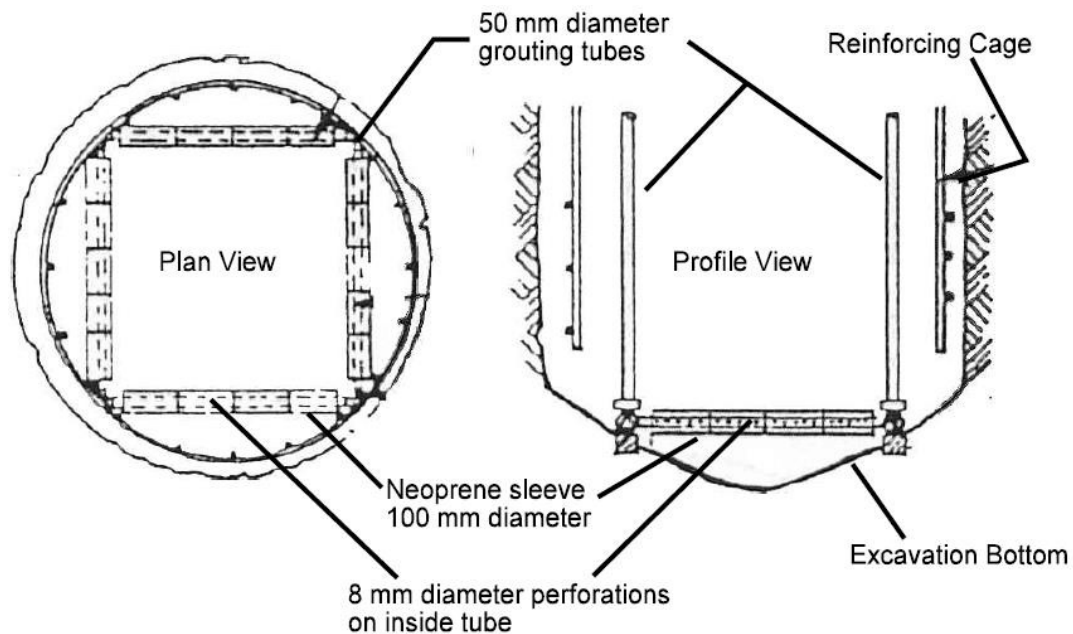


Figure 5.5: Square arrangement of a sleeve-port grout distribution system (Bruce, 1986).



Figure 5.6: Photograph of a sleeve-port system constructed using flexible hoses (courtesy of Dr. H.H. Hsieh).

5.4 Open-Type Grout Distribution System: Low Mobility Grouting (LMG) Device

An alternative open-type grout distribution system that has recently been developed is the low mobility grouting (LMG) device (Pooranampillai et al., 2009, 2010; Pooranampillai, 2010). Key features of this device include a single internal pipe with a 2-in. nominal inside diameter and a “starter void” beneath the shaft to facilitate delivery of low mobility grout across the tip of the shaft (Figure 5.7). The device is conceptually similar to a stem-type grouting device, since it utilizes a single grout delivery tube. However, the technique differs from the more common neat cement grouting in that a low slump grout is used to fill the void space, compact the soil beneath

the drilled shaft, and develop a “bulb” of some geometry beneath the LMG device. Because low mobility grout is used, permeation of grout into the ground is unlikely. While substantial testing and evaluation of the LMG device have been performed, there are no available published references citing its use for production shafts to date. However, there are reported cases of use of LMG for remediation of existing drilled shafts where the grout is delivered via a grout pipe inserted adjacent to the installed shaft to target the formation at the tip of the shaft or along the length of the shaft (Englert et al., 2005). This type of application of LMG for shaft remediation is not considered base grouting within the context of this report and is not discussed further.

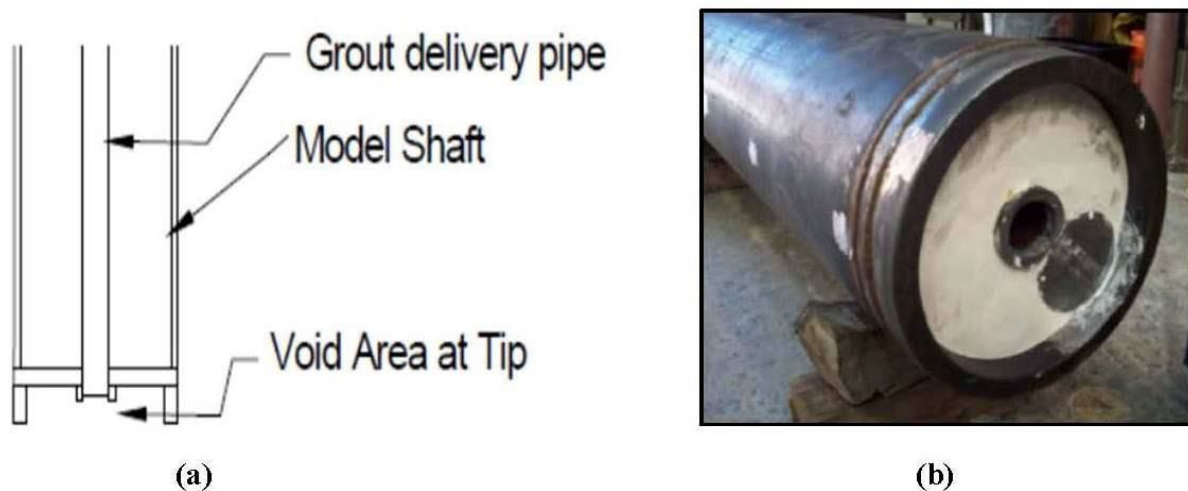


Figure 5.7: Low mobility grouting device: (a) schematic, and (b) photograph of device used for laboratory-scale tests (Pooranampillai, 2010).

5.5 Closed-Type Grout Distribution System: Flat-Jack

“Flat-jack” post-grouting devices are also commonly used in U.S. practice for PGDS. Modern flat-jack devices are closed-type systems that represent adaptations to earlier devices described in Chapter 1. Typical flat-jack devices include two or more vertical grout distribution tubes that are connected to a steel plate that is covered with an impermeable membrane. The vertical grout tubes are typically one-inch nominal diameter steel or PVC pipes that are attached to the longitudinal bars in the rebar cage and cast into the drilled shaft to deliver grout to the device. Recent variants of the flat-jack distribution system typically use a rubber membrane in lieu of a lower steel plate. The impermeable membrane is wrapped around the edges of and secured to the upper steel plate as shown in Figures 5.8 and 5.9. In some cases, corrugated material (similar to the backing on prefabricated strip-drains) or perforated pipe is included between the steel plate and membrane to facilitate grout flow across the tip of the shaft. A scuff ring is also generally included around the perimeter of the plate to prevent damage to the membrane while placing the device in the bottom of the shaft.

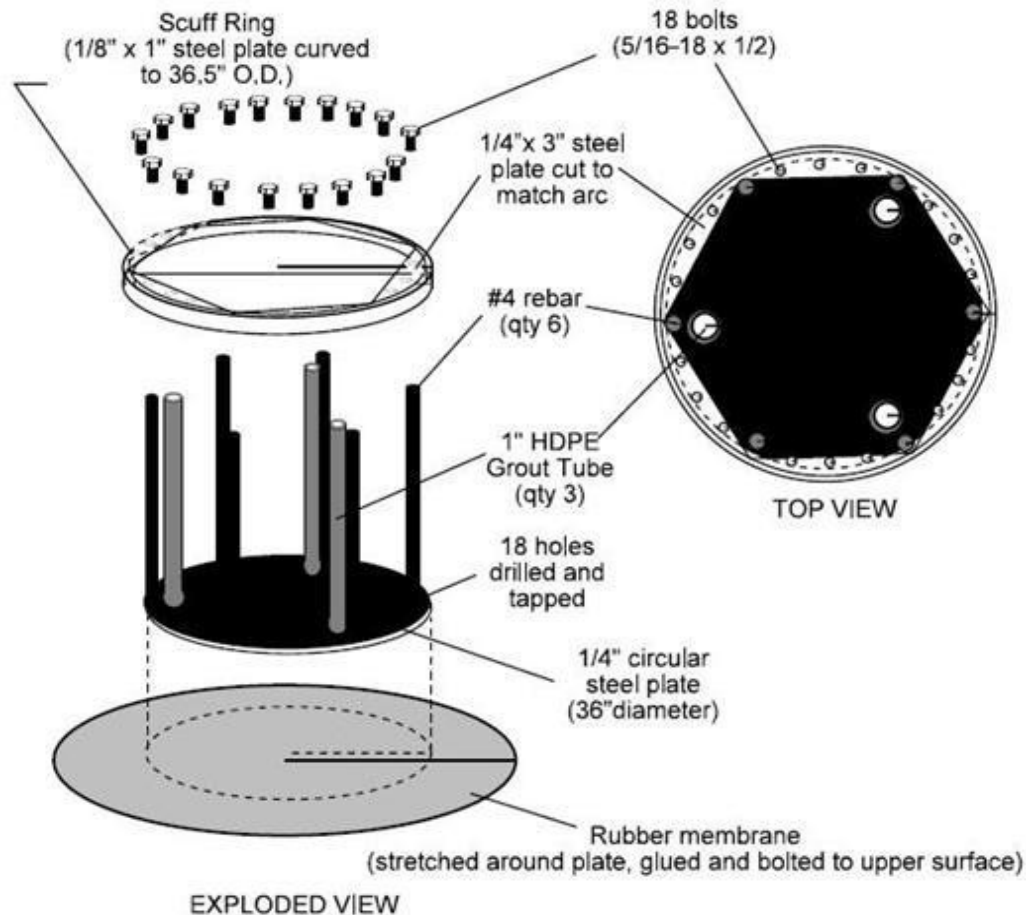


Figure 5.8: Diagram of typical components used for a flat-jack device for a 48-inch diameter shaft (Mullins et al., 2001).

Unlike open-type grout distribution systems, grout injected into a flat-jack device fills the space between the steel plate and rubber membrane, expanding the membrane as grouting progresses. The grout is therefore contained within the apparatus and is not injected into the ground unless the membrane ruptures during grouting. A notable advantage of this feature is that the area over which the grout pressure acts at the shaft tip is known with greater certainty than for sleeve-port systems.

As with other post-grouting devices, flat-jack devices must be located at or very near the bottom of the shaft. In cases where the shaft excavation is not terminated at the planned depth or elevation, the location of the flat-jack system must be adjusted so that the device is in close proximity to the bottom of the as-constructed shaft. When the rebar cage and grouting device have been assembled prior to completion of the borehole excavation, slip joints and/or flexible grout hoses can be used to extend the device to the desired location (Mullins et al., 2001).



Figure 5.9: Flat-jack post-grouting device on a 4-ft diameter shaft (photo courtesy of Applied Foundation Testing).

While common flat-jack devices are considered to be closed-type systems, the impermeable membranes are susceptible to rupture for various reasons including damage incurred during installation and over-pressurizing of the grout during injection. Concerns about membrane rupture due to large hydrostatic pressure differentials have prompted the use of overlapping thin metal plates beneath the membrane for protection when used for extreme shaft depths (in excess of 200 ft).

Flat-jack devices are not as amenable to repeated grouting as sleeve-port systems. In instances where staged grouting is desired with flat-jack systems, the fluid grout within the vertical grout tubes can be flushed by inserting a smaller tube into the grouting tube as water is injected to permit subsequent stages of grouting to be performed. However, such flushing does not seem to be as reliable as flushing of sleeve-port systems.

5.6 Gravel Bedding

A gravel bedding layer has sometimes been used with both open-type and closed-type grout distribution systems, most frequently for PGDS larger than 6 ft in diameter. Reasons for utilizing gravel bedding include facilitating distribution of grout across the tip area of the shaft, producing a flat level surface on which to place the grouting apparatus, and providing a conduit and void space through which the grout can travel. The flat gravel bedding surface is needed if the bottom of the grout distribution device is flat and intended to be in direct contact with the base of the excavation. A steel plate is generally placed between the bottom of the rebar cage and the grout distribution device when gravel bedding is used (e.g., Figures 1.3 and 5.3) to separate the grout delivery system from the drilled shaft concrete and minimize the potential for intrusion of concrete into the gravel during placement.

Gravel bedding is typically composed of clean, coarse gravel with particle sizes between $\frac{5}{8}$ inch and $1\frac{1}{4}$ inch. A minimum thickness of 12 inches of gravel is often required, but the primary requirement is that the gravel must be continuous across the base of the shaft to facilitate grout distribution across the entire tip area. The gravel bedding layer is not intended to eliminate the

need for high quality workmanship and for proper cleaning of the bottom of the shaft because excessive soft sediment in the base of the shaft is likely to result in clogging of some or all of the void space, which will compromise the potential benefit of the gravel bedding.

5.7 Summary

Several alternative grout distribution systems used for PGDS were described in this chapter. The most common systems in current use are “sleeve-port” distribution systems and “flat-jack” distribution systems. Sleeve-port systems are open-type grout delivery systems commonly composed of a series of U-Tube pipe circuits with ports located at the bottom of the device for delivering grout at the tip of a PGDS. Sleeve-port systems deliver the grout in direct contact with the ground. Flat-jack distribution systems are closed-type grout delivery systems composed of a steel plate with an impermeable membrane that is intended to contain the grout within the delivery system. Both types of systems have occasionally been used with gravel bedding that is intended to provide a level surface upon which to place the grout distribution device and to facilitate distribution of grout across the shaft tip. Stem or orifice grouting systems are seldom used except in remedial applications. An alternative “low mobility grout” or LMG system that is currently being developed was also described.

CHAPTER 6: MEASUREMENTS AND CONTROL DURING GROUTING

6.1 Introduction

Reliable and standardized procedures for control of post-grouting operations and quality are essential to expanded use and acceptance of PGDS. Several parameters are commonly monitored and recorded during post-grouting operations to assist with control of grouting operations as well as to provide quality control over grout characteristics and grouting methods. Grout pressure, grout volume, and shaft uplift are measured and typically plotted in real time as grout is delivered to provide a rational basis for process control of post-grouting operations. Some PGDS are also instrumented with strain gauge to capture the load-transfer response of the shaft during or after grouting. In addition, specific gravity and viscosity are measured for the fluid grout mix, and compressive strength is measured for cured samples of the grout to provide quality control over the grout. Collectively, these measurements are used, along with appropriate limit or threshold values for each parameter, as termination and acceptance criteria for grouting operations as described in more detail in this chapter.

6.2 Measurement of Grout Pressure and Pressure Termination Criterion

Grout pressure is typically monitored using a Bourdon-type (analog) pressure gauge located near the grout pump. Pressure measurements from these gages are monitored and manually recorded at frequent time intervals throughout the grouting process. These analog measurements are often supplemented with automated readings from a digital pressure transducer also located near the grout pump. Figure 6.1 shows a typical combination of a Bourdon gauge and a pressure transducer attached at the grout pump. Automated transducers are convenient for recording measurements at frequent time intervals, but analog gages are often more useful for on-site monitoring of grouting operations. Resistance-based pressure transducers are generally more desirable than vibrating wire transducers for post-grouting applications because resistance-based transducers allow for faster sampling rates, which allow the dynamic nature of the grouting pressures to be more closely captured.



Figure 6.1: Photograph of a Bourdon-type pressure gauge and a pressure transducer (courtesy of Applied Foundation Testing).

A simple “field check” of the Bourdon gauge and pressure transducer is generally performed prior to grouting by filling the grout line with water, capping or “dead-heading” the line, and applying a nominal pressure. Readings from the Bourdon gauge and pressure transducer are compared to establish that both measurements are practically consistent. As is often the case when making similar measurements using different devices, it is common to have small discrepancies between pressures measured using the Bourdon gauge and pressure transducer. The alternative readings can generally be considered consistent if the readings fall within a few percent of the range of the gages. Pressures measured at various positions across the system (e.g., at pump, top of shaft, etc.) should also be expected to differ because of variance in elevation and/or pressure losses along the grout tubes and hoses. However, pressures measured at different positions should be consistent considering relative elevation and expected pressure losses in the hoses/lines. Trends in pressure measured at different positions should also be consistent.

One component of grouting termination criteria that guides and controls grouting operations in the field is a grout pressure threshold established as part of PGDS design. The magnitude of the grout pressure threshold varies substantially from project to project, but typically ranges between 100 and 700 psi. The grout pressure threshold is generally established based on consideration of the grout pressure needed to achieve the desired drilled shaft performance as well as consideration of the grout pressure that can likely be achieved in the field. The maximum grout pressure that can be achieved is limited by the least of the following constraints:

1. *Practical limits of the grouting equipment.* The practical upper limit for grout pressure is typically around 700 psi because of limitations of typical pumps and pipes used for post-grouting. Specified target pressures should therefore not exceed 700 psi unless measures are taken to ensure that grouting equipment can produce and sustain greater pressures.
2. *Available reaction to upward movement of the shaft.* The upward force induced by the grout pressure at the shaft tip cannot exceed the available reaction force. The available reaction is commonly provided by the shaft side resistance and buoyant self-weight of the shaft unless additional reaction is provided at the top of the shaft. Presuming that the grout pressure acts over the entire area of the shaft tip and neglecting the buoyant self-weight, the maximum achievable grout pressure is often estimated as the side resistance divided by the tip area of the shaft.
3. *Hydrofracture pressure for soil/rock at shaft tip.* The grout pressure threshold should not exceed the pressure that will cause hydrofracture of the ground at the shaft tip. Accurate prediction of the hydrofracture pressure is challenging, but it can be crudely estimated to be approximately three times the effective overburden stress in cohesionless soils and one to two times the total confining pressure in cohesive soils. In cases where hydrofracture may control PGDS design, more rigorous consideration of the hydrofracture pressure using available theoretical and empirical methods is likely warranted.

In some cases, two different threshold pressures have been specified: a lower, “design” value established as a minimum value that must be achieved to produce the required nominal shaft resistance; and a greater, “target” value reflecting the maximum grout pressure that can likely be achieved based on the expected reaction and hydrofracture pressure. In such cases, the intent is to attempt to achieve the greater target threshold pressure but to consider the lower “design” threshold as being acceptable if the target pressure cannot be achieved.

For post-grouting operations, the grout pressure threshold is universally accompanied by the requirement that a minimum net volume of grout also be injected for the criterion to be satisfied. The additional requirement is included to confirm that the measured grout pressure is being transmitted to the shaft tip, and is not an artifact of a blocked grout line (which would produce a buildup of pressure with little or no grout delivery).

6.3 Measurement of Grout Volume and Volume Termination Criteria

Measurements of the cumulative volume of grout delivered are taken at regular intervals throughout the grouting process to inform grouting personnel about grouting progress and to identify potential problem conditions. Grout volume measurements can be used in conjunction with pressure measurements to identify blocked or leaking grout lines, potential occurrence of hydrofracture, potential rupture of flat-jack or sleeve-port membranes, and other grouting issues.

For post-grouting applications, grout volume has been most commonly measured by monitoring and recording the grout level in the holding tank that supplies grout to the pump at periodic time intervals. Automated flow meters are also used, although they appear to be much less common. Holding tank measurements are generally taken as back-up measurements even when automated meters are used. For neat cement grouts with relatively high water-to-cement ratios like those commonly used for PGDS, electromagnetic flow meters are generally most appropriate (Taylor and Choquet, 2012). For additional verification, a running tally of empty cement bags is often tracked to estimate volume from the theoretical yield of each grout batch.

While the total volume of grout delivered is generally measured and plotted, decisions about grouting progress and termination are made based on the “net” volume of grout. The net volume of grout is computed as the total volume of grout delivered minus the volume required to fill all void space in the grout delivery system, including all grout lines and gravel-bedding (if used), and any wasted grout. The volume of void space is commonly established from theoretical calculation of the void space in the grout delivery system. However, the void space can also be established by measuring the grout volume required to flush grout through the delivery system, prior to closing the return line and building grout pressure. These two alternative methods will produce different estimates of net grout volume. Theoretical estimates are likely to underestimate the volume of void space, and thus overestimate the net volume, because the theoretical calculations neglect potential expansion of grout lines under pressure and any “lost” grout. Conversely, measurements of void space during initial flushing of the grout delivery system are likely to overestimate the volume of void space and underestimate the net grout volume because some of the grout may flow out of the device prior to building pressure, especially when hydrostatic grout pressures at the shaft tip are substantial.

Two grout volume thresholds are typically specified as part of grouting termination criteria. The first threshold is referred to as the minimum net volume. As described in the previous section, the minimum net volume threshold is used in combination with the grout pressure threshold to confirm that a nominal amount of grout is being delivered to the post-grouting device and that the measured grout pressure is being transmitted to the shaft tip. Selection of a minimum net volume threshold has typically been based on judgment with the intent of ensuring that “some” grout is delivered to the post-grouting device beyond what would be required to simply fill the device. Values of 2 ft³ or 3 ft³ are commonly selected, although values as great as 5 ft³ have

been used. Selected values have generally been independent of shaft diameter, although there is logic to having the minimum net volume threshold be dependent on the shaft diameter, the method used for establishing the volume of void space, and perhaps the specific grouting device.

The second grout volume threshold is the maximum net volume. In practice, the maximum net volume threshold has really been used as a grouting control limit to identify when changes to grouting operations should be considered, rather than as a strict criterion to be used for establishing whether post-grouting can be considered acceptable. In fact, a maximum net volume is not always specified in grouting procedures and construction specifications, and it is common for the total net volume delivered for a particular shaft to exceed the specified maximum net volume. Specified values for the maximum net volume vary substantially from project to project, but are generally in the range of 5 ft³ to 30 ft³, or between 2 and 10 times the minimum net volume established for the shafts. Such values have typically been selected based on judgment with consideration given to the grout volume that is expected if grouting proceeds as desired. Such judgment is often informed and improved based on experience obtained from grouting site-specific demonstration shafts.

6.4 Measurement of Shaft Uplift and Uplift Termination Criterion

Upward movement of PGDS is generally monitored during grouting to provide an indication that side resistance is being mobilized and to provide means to avoid excessive upward displacement that might degrade side resistance. Excessive upward movement of the shaft can also provide an indication that side resistance may be less than considered in design if the movement occurs at relatively low grout pressures.

Shaft uplift is commonly measured using a reference beam and displacement gages or transducers (Figure 6.2) or using manual or automated optical survey equipment (Figure 6.3) similar to what is done for axial load tests on deep foundations (ASTM Standard D1143, 2013). Uplift measurements for test shafts and initial production shafts are commonly made using automated systems and electronic devices like those shown in Figures 6.2 and 6.3 to allow uplift criteria to be refined. Subsequent measurements made for production shafts are commonly performed using instruments with less precision such as conventional optical survey techniques, laser levels, or analog displacement gages.



Figure 6.2: Photograph of an LVDT between the reference beam and the top of the shaft during grouting (courtesy of Applied Foundation Testing).

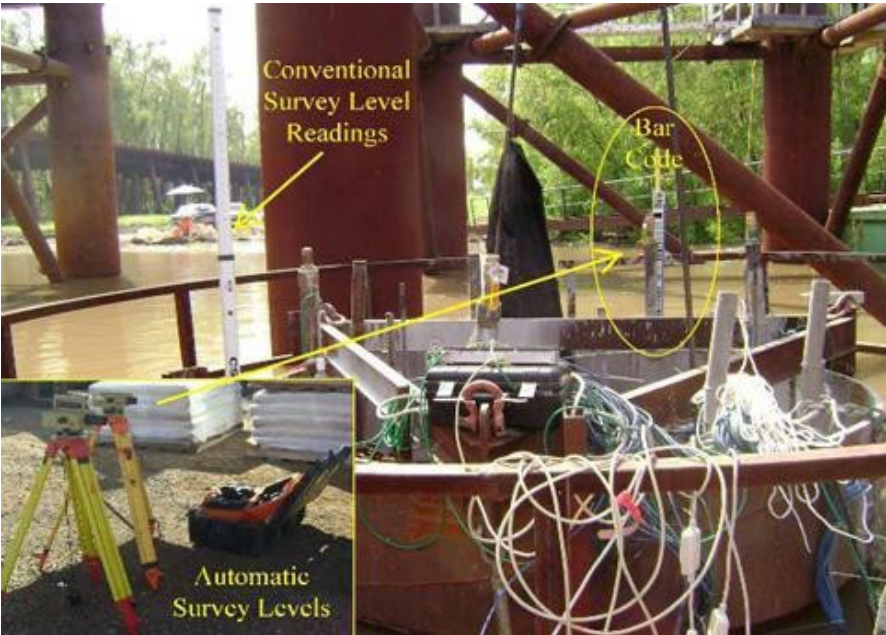


Figure 6.3: Photograph of the survey level readings (automatic and manual) during grouting (courtesy of Applied Foundation Testing).

A shaft uplift threshold is typically specified as part of the grout termination criteria for PGDS. Common threshold values used in recent U.S. practice range between $\frac{1}{4}$ inch and $\frac{3}{4}$ inch for an individual grouting stage. For repeated grouting stages, uplift displacements are generally “re-zeroed” for each stage, meaning that the cumulative shaft displacement is not explicitly considered as part of the grout termination criteria. The basis and justification for these practices are not completely clear. Shaft displacements of $\frac{1}{4}$ to $\frac{3}{4}$ inch are certainly consistent with generally accepted displacements required to fully mobilize side resistance. It seems likely that the values commonly used may have been derived from such considerations given that potential

displacement-softening should not occur at displacements less than those required to mobilize the peak resistance. However, it is important to note that displacement at depth will be greater than that measured at the top of the shaft because of elastic compression of the shaft. Also, the cumulative displacement of the shaft will govern whether displacement-softening will occur rather than the incremental displacement experienced during individual grouting stages.

As a practical matter, however, it is rare for more than two grouting stages to be performed for PGDS, so the cumulative displacement is unlikely to be greater than twice the shaft uplift threshold. Nevertheless, it seems logical that application of the shaft uplift threshold should consider the cumulative displacement of the shaft in addition to the displacement during an individual grouting stage. Finally, it is noteworthy that similar shaft uplift threshold values have typically been used for all types of ground conditions, regardless of whether the ground is considered to be displacement-softening (e.g., stiff, fissured clays, dense sands, etc.). Such practice may impose unnecessary constraint in ground conditions where displacement-softening is unlikely.

6.5 Control of Grouting Operations Based on Measurements

During post-grouting, grout pressure, grout volume, and shaft uplift measurements are monitored and recorded as a function of time while grout is steadily delivered to provide indication of grouting progress and to guide grouting operations. The desired response to grouting is that the grout pressure will rise steadily in rough proportion to the grout volume delivered, with a simultaneously proportional upward shaft displacement. Such a response indicates that grouting is proceeding as anticipated and should be continued.

In many cases, however, the measured volume of grout delivered, uplift of the shaft, and grout pressure may deviate from the desired “proportional response,” especially as the grout pressure becomes large. Such deviations serve as indication that a limit condition is being approached, and that changes to grouting operations may be required. For example, observation of rapidly increasing grout pressure with little increase in volume delivered and little shaft uplift serves as an indication that the grout supply line(s) have become blocked.

A more common occurrence is to observe an increase in the volume delivered without a proportionate increase in grout pressure. Such observations provide indication of several potential conditions:

- The mobilized side resistance that is providing reaction to the upward force on the shaft due to the measured grout pressure is approaching the ultimate side resistance, which results in non-linear upward displacement of the shaft and increasing volume at the shaft tip with little or no increase in the grout pressure.
- The mobilized tip resistance at the tip of the shaft is approaching the ultimate tip resistance, which results in non-linear downward displacement of the soil/rock beneath the shaft tip and increasing volume at the shaft tip with little or no increase in pressure.
- The grout pressure imposed at the shaft tip has resulted in hydrofracture of the ground around the shaft tip, which provides additional space for grout to flow with little or no increase in pressure.

The first condition can be distinguished from the others by observing whether a simultaneous increase in upward displacement of the shaft is occurring. At times, hydrofracture may result in a slight decrease in the grout pressure while the volume delivered continues to increase so observation of such a response can be used as an indication of hydrofracture. Hydrofracture and bearing failure can also sometimes be distinguished by comparing the measured grout pressure to theoretical estimates of the ultimate unit tip resistance and the hydrofracture pressure if the estimates are substantially different. However, it can be difficult to distinguish between the hydrofracture and bearing failure conditions based on observation of grout pressure, volume, and shaft uplift alone. Fortunately, it is seldom critical to distinguish between the two conditions in a production environment because the necessary responses by the grouting personnel are often similar.

Mullins (2015) formalized these concepts and recommended graphing measurements of grout pressure, grout volume, and shaft uplift as shown in Figure 6.4. In the figure, the desired grouting response is represented by the green arrows that radiate diagonally from the center of the figure. Conditions that deviate from the diagonal path towards a vertical or horizontal path indicate that post-grouting has become ineffective for one of the reasons described in this section and noted in the figure. Graphing of such measurements in real time can improve the effectiveness of post-grouting operations.

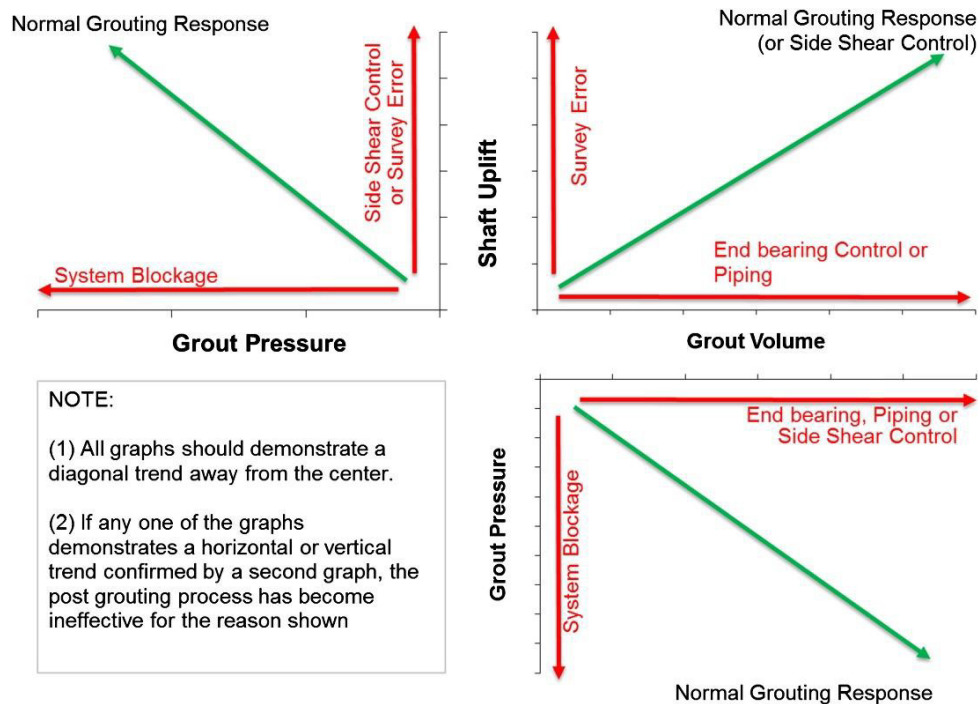


Figure 6.4: Proposed graphing method from Mullins (2015) to guide control of post-grouting operations.

Three grouting termination criteria are generally specified to guide control of grout delivery in response to conditions that may develop during grouting. For most projects, grout delivery is continued until one of the following termination criteria is met:

1. The target grout pressure is sustained for a specified period and the net volume delivered exceeds the specified minimum net volume.
2. The upward displacement of the shaft exceeds the specified upward displacement threshold.
3. The net volume delivered exceeds the specified maximum net volume threshold.

Satisfying the sustained grout pressure criterion, including the requirement that a minimum net volume of grout has been delivered, is generally most desirable because it substantiates that the intended pressure has been applied at the shaft tip and provides a degree of verification of the tip resistance for the PGDS (Mullins et al., 2006). Most specifications generally require that the grout pressure be maintained for a period of 1 to 2 minutes in order to be considered “sustained.” The other grout termination criteria are intended to address conditions that may necessitate changes to grouting operations.

When grouting is terminated because the net volume delivered has exceeded the specified maximum net volume threshold, but the other criteria have not been met, the following actions are typically considered:

1. Grouting can be continued “as-is” until one of the other termination criteria is achieved.
2. The water-to-cement ratio of the grout can be systematically reduced in decrements of about 0.05 to 0.10 to reduce the mobility of the grout followed by repeated attempts to continue grouting.
3. Grouting can be delayed for a short period (e.g., 15 to 30 minutes) to allow the grout that has been delivered to the shaft tip to become more viscous and to allow induced excess pore pressures to dissipate. This is generally accomplished by depressurizing the system, opening the return line, and slowly pumping grout through the access lines to keep them open (wasting the return).
4. Grouting can be halted for an extended period (typically 4 hours or more) to allow the grout to set, followed by a subsequent stage of grouting. When grouting is halted in this manner, the access lines must be flushed with water to allow for subsequent grouting stages and enough time must pass for the delivered grout to set.

The first option is generally given preference if the measured grout pressure is near to the target grout pressure and if the measured shaft uplift is substantially less than the specified uplift threshold. The second option is given preference if the grout has a relatively high water-to-cement ratio, with consideration given to the fact that the practical lower limit for the water-to-cement ratio is approximately 0.4. The third and fourth options are generally less desirable because they slow production, but both are commonly implemented if the more desirable alternatives are ineffective or impractical. In the event that the target grout pressure criterion is not initially satisfied during a second stage of grouting, the maximum net volume threshold may be increased to allow more grout to be delivered in an attempt to satisfy the target grout pressure criterion. Three stages of grouting are rarely performed as a practical consideration.

The situation is more problematic when grouting is terminated because the shaft uplift threshold is exceeded and represents one of the greatest risks associated with post-grouting: that the established design grout pressure cannot be achieved. In such cases, an additional grouting phase may be attempted after allowing the delivered grout to set, as in the fourth option listed

above, and after considering the likelihood of displacement-softening of the shaft interface. Alternatively, the design of the PGDS may be re-evaluated and grouting for the specific shaft may be stopped entirely. In such cases, the foundation(s) may have to be re-designed or remedial measures may have to be undertaken to improve the reaction to uplift or to increase the hydrofracture pressure, any of which will increase the overall cost of construction. Examples of remedial measures that might be undertaken include compaction grouting along the sides of the shafts to improve the reaction to uplift, addition of reaction force at the top of the shafts, or ground improvement measures to increase the hydrofracture pressure for the ground at the shaft tip. It should be noted that careful selection of target grout pressures and construction of site-specific demonstration shafts are perhaps the most effective means to alleviate and control risks associated with failure to achieve target grout pressures for PGDS.

6.6 Use of Strain Gauge Measurements

Strain gages provide a valuable means to help determine the effectiveness of post-grouting, to evaluate the upward load induced during post-grouting, and to establish the load-deformation response for PGDS along different segments of the shaft, both during and following grouting. The effect and uniformity of the applied grout pressure can be evaluated from observation of strain gauge measurements for several strain gages installed in close proximity to the shaft tip, as illustrated in Figure 6.5. Such measurements can be used to confirm that the applied grout pressure is producing an upward force on the tip of the shaft by observing similar trends in the grout pressure versus time and strain versus time records. Consistent measurements from multiple strain gages installed in close proximity to the shaft tip suggest that the grout pressure is being uniformly applied, whereas inconsistent measurements suggest non-uniform grout pressure and induced bending within the shaft.

Strain gages can also be used to estimate the axial load in the shaft at the location of the strain gages. The axial load at a given elevation (Q_i) can be estimated as:

$$Q_i = \sigma_i A_i = \varepsilon_{i,avg} \cdot E_{composite} \cdot \left(\frac{\pi}{4} D_i^2 \right) \quad (6.1)$$

where:

- σ_i = axial stress
- A_i = cross-sectional area of the shaft
- $\varepsilon_{i,avg}$ = average of the strain gauge readings

- $E_{composite}$ = appropriate composite value of the modulus of elasticity
- D_i = shaft diameter

all taken at the given elevation. If gages are placed at several elevations along the shaft, the axial load estimates can be used to establish the load transferred along each shaft segment, and the load transfer (or “t-z”) response for each segment.

Several alternative types of strain gages can be used for PGDS, including resistance-type gages, vibrating wire gages, and fiber optic gages. Each of these gauge types is commonly available as “sister-bar” gages and concrete embedment gages. Each type and form of strain gauge has advantages and disadvantages in terms of cost, sampling rate, drift, and other factors that should be considered in selecting the most appropriate type of gauge for a particular project. For axially-

loaded deep foundations of all types, it is generally desirable to install multiple levels of strain gages along the length of the shaft to allow for evaluation of load transfer, and to install multiple strain gages at each level to allow for evaluation of potential bending strains. The same is true for PGDS, although having gages installed near to the tip of the shaft is most important for evaluation of grouting operations.

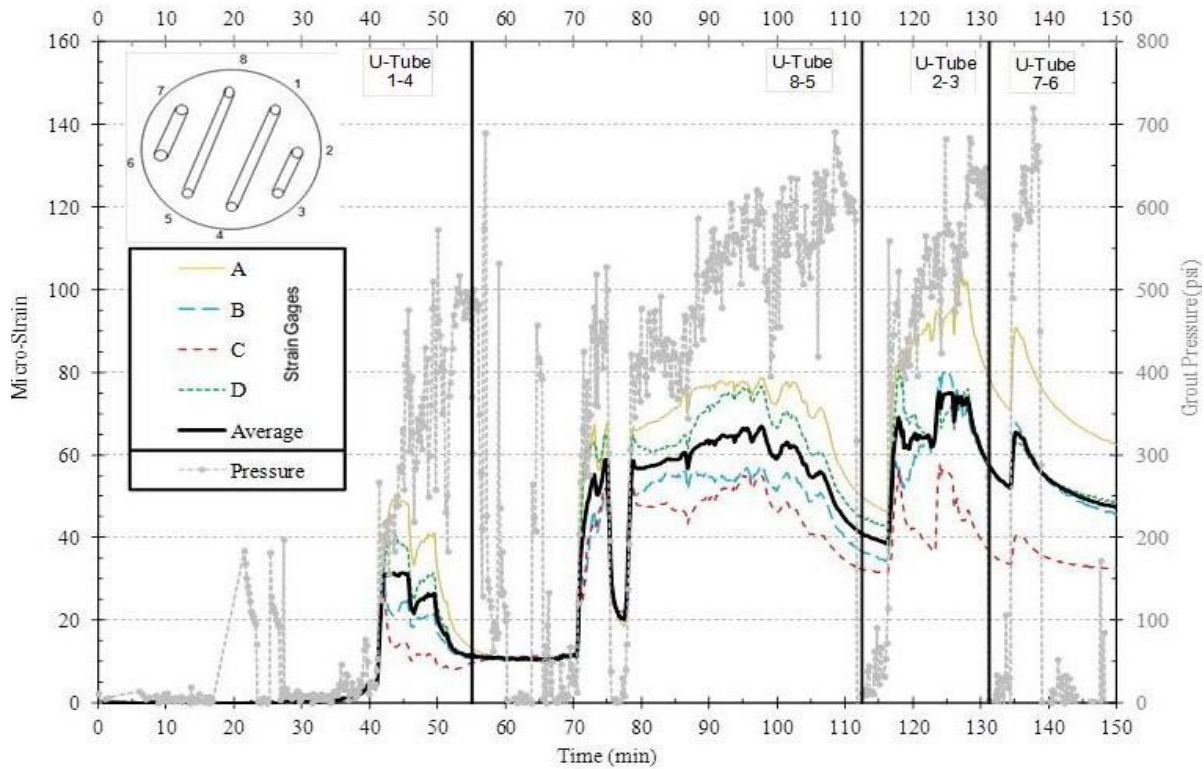


Figure 6.5: Plot of measured grout pressure and strain versus time during post-grouting (courtesy of Applied Foundation Testing).

Various types of extensometers, or “telltales” can also be used as an alternative to strain gages. Telltales come in different forms, but generally utilize a sleeved rod or wire to measure the change in distance between two locations (Dunncliff, 1988). Dapp and Mullins (2002) describe use of a stainless steel braided cable through the center of a ½-inch Schedule 40 PVC pipe for PGDS. While telltales strictly measure the displacement of a given point on the shaft relative to a reference location (typically the top of the shaft), multiple telltales anchored at different elevations can be used to establish the average strain between two anchor elevations, and these strains can then be used to establish load and load transfer in the shaft.

6.7 Measurements for Grout Quality Control

Reliable and standardized quality control procedures are essential to expanded use and acceptance of PGDS. Common quality control measurements described in Chapter 3 for general grouting applications include specific gravity, viscosity, and compressive strength. These same techniques are generally appropriate for QC/QA in post-grouting applications and such measurements are relatively common for PGDS projects. However, common specifications for construction of PGDS generally provide few explicit requirements to control and assure grout

quality. Common PGDS specifications do frequently require that the grout be mixed at a specified water-to-cement ratio (commonly 0.5) and that the grout cube strength exceed some specified minimum value (commonly 2,000 to 4,000 psi). However, these specifications seldom include explicit requirements for how the water-to-cement ratio should be measured or verified, or how frequently it should be verified. Grout strengths are generally required to be measured in accordance with ASTM Standard C109 (2013) or prior versions of this standard, but no provisions are included to stipulate requirements for the number or frequency of grout strength tests. Requirements for measurement of fluid grout properties like viscosity or specific gravity are also lacking in common PGDS specifications.

The result is that grout strength has served as the sole verification of grout quality for PGDS applications in the U.S. There is some logic to this practice given that strength and water-to-cement ratio are directly related for neat cement grouts; thus, grout strength can serve as an index to verify that the grout was adequately prepared, regardless of whether grout strength is a significant concern in terms of the performance of the PGDS. However, given the importance of the fluid grout characteristics for PGDS applications and that grouting complications are commonly attributed to using grout with high water-to-cement ratios (Mullins and Winters, 2004), the lack of requirements for verification of fluid grout characteristics is difficult to justify.

To improve QC/QA for PGDS, future specifications and special provisions for PGDS should include means to verify the characteristics of the fluid grout mix. Measurements of both specific gravity and viscosity are generally simple, robust, and efficient, and unlikely to place undue burden on field inspectors or grouting personnel. Specific gravity is directly related to the water-to-cement ratio for neat cement grouts so such measurements seem like the most appropriate means to verify that the water-to-cement ratio is as intended. Specific gravity is also directly related to the compressive strength of the grout, and thus serves as immediate verification of strength as opposed to grout cubes (Figure 3.1). Viscosity is less directly related to the water-to-cement ratio because it will vary with time. However, viscosity may be more closely correlated with grouting complications, and thus serves as a better indicator of the likelihood of grouting problems. It therefore seems logical to require both types of measurements for PGDS applications, at least until it can be shown that one measurement is preferable and sufficient.

Future specifications for PGDS should also include explicit requirements for the frequency and number of tests to be performed. A logical starting point would be to require strength and specific gravity tests for each post-grouted shaft, with additional tests required depending on the number of grout batches used in each shaft and on whether changes are made to the grout mix. Viscosity tests should also be performed for each shaft, but additional tests should be considered if the duration of grouting is long enough to produce significant changes in viscosity. For example, a specification might require a minimum of one viscosity test for each shaft, with an additional test being required for each 30-minute period following initial mixing of each batch.

6.8 Summary

Reliable and standardized procedures for control of post-grouting operations and PGDS quality are paramount to expanded use and acceptance of PGDS. Grout pressure, grout volume, and shaft uplift are commonly measured during grouting of PGDS. These measurements are used in combination with threshold values for each measurement to guide and control grouting

operations and as an indicator of the expected performance of the PGDS. The grout pressure threshold varies substantially from project to project depending upon the grout pressure required to produce the desired nominal shaft resistance as well as constraints that may limit the pressure that can be developed. Minimum and maximum net volume thresholds are generally more consistent from project to project, with the minimum net volume threshold commonly ranging from 2 to 5 ft³ and the maximum net volume threshold commonly ranging from 5 to 30 ft³. The shaft uplift threshold is commonly taken to be between ¼ and ¾ inch. Strain gages and telltales may also be installed in PGDS to facilitate interpretation of loading and load transfer during and after post-grouting.

The primary requirement for verification of grout quality in most PGDS specifications is that the grout achieves a specified 28-day compressive strength that typically ranges between 2,000 and 4,000 psi. Regardless of whether grout strength is likely to affect the performance of PGDS, grout strength serves as a general index for grout quality since it is directly related to the water-to-cement ratio for neat cement grout. PGDS specifications have seldom included requirements for specific gravity or viscosity tests, despite the fact that specific gravity and viscosity can be readily measured in the field using a mud balance and Marsh funnel, respectively. Such measurements are strongly recommended to improve QA/QC for future PGDS projects.

CHAPTER 7: CURRENT DESIGN METHODS

7.1 Introduction

Design of PGDS is conceptually similar to design of conventional drilled shafts in the sense that the shafts must be sized to provide sufficient resistance to support anticipated loads. Sizing of shafts is performed by predicting the nominal resistance for different shaft dimensions (length and diameter), and then selecting the smallest shaft size that will support the nominal loads with some appropriate margin of safety. However, design of post-grouted shafts also involves the additional requirement of specifying a target grout pressure that should be achieved in order to develop the resistance established in the design. One of the risks associated with PGDS is that the design, or target grout pressure, may not be achieved during grouting, in which case corrective measures must be taken to provide the required nominal resistance. This risk is conceptually similar to the practice of driving piles to achieve a specific driving resistance; if the specified blow count is not achieved using the anticipated pile length, corrective actions must be undertaken to provide the required resistance.

Several different approaches have been proposed and are used for predicting the nominal capacity of PGDS. Most methods involve multiplying the nominal resistance for a conventional shaft, or some component of nominal resistance, by an empirical multiplier to predict the nominal resistance for a similarly sized PGDS. Three specific approaches have been proposed including: the Tip Capacity Multiplier (*TCM*) approach, the Axial Capacity Multiplier (*ACM*) approach, and the “Component Multiplier” approach. Each of these approaches is presented in this chapter, including specific equations for predicting the nominal resistance for PGDS, and discussion of the strengths and limitations of each approach. Predictions of nominal resistance from several of the methods presented in this chapter are subsequently compared to measured values of resistance from full-scale load tests in Chapter 9.

7.2 Tip Capacity Multiplier Approach

The most commonly adopted approach for predicting the nominal resistance of PGDS in the U.S. is the so-called “Tip Capacity Multiplier” approach originally proposed by Mullins et al. (2006). In this approach, the nominal unit tip resistance for a PGDS is predicted as:

$$\bar{q}_{p,gr} = TCM \cdot q_p \quad (7.1)$$

where:

- $q_{(p,gr)}$ = nominal unit tip resistance for a PGDS
- TCM = “tip capacity multiplier” reflecting improvement in the unit tip resistance for a PGDS compared to the unit tip resistance for a conventional drilled shaft
- q_p = nominal unit tip resistance for a conventional drilled shaft

The nominal unit side resistance for PGDS is taken to be identical to that for conventional shafts. Thus, the nominal total resistance for a PGDS is taken to be:

$$R_n = R_s + R_{p,gr} = \sum_{i=1}^n (q_{s_i} A_{s_i}) + q_{p,gr} A_p \quad (7.2)$$

where:

- R_n = nominal resistance for PGDS
- R_s = nominal side resistance for conventional drilled shaft and PGDS
- $R_{p,gr}$ = nominal tip resistance for PGDS
- q_{s_i} = nominal unit side resistance for soil layer i
- A_{s_i} = nominal area of the soil-shaft interface for soil layer i
- n = number of soil layers
- $q_{p,gr}$ = nominal unit tip resistance for PGDS (from Eq. 7.1)
- A_p = nominal area of the shaft tip

The area A_p in Equation 7.2 is calculated from the design shaft diameter, and does not reflect potential enlargement of the tip due to post-grouting. The value of the TCM in Equation 7.1 is taken to be a function of the maximum sustained grout pressure imposed during grouting and the displacement of the post-grouted shaft. Two specific methods have been proposed for computing the TCM . Each of these methods is described in the following subsections.

7.2.1 Mullins, Winters, and Dapp (2006)

Mullins et al. (2006) proposed an empirical method for establishing the value of TCM for PGDS tipped in cohesionless soil. The method was derived from analysis of load test measurements performed at five different test sites where PGDS were tipped in sand, silty sand, shelly sand, or slightly cemented sand. Nine load tests were performed on PGDS employing either sleeve-port or flat-jack grouting devices. Six additional load tests were performed on conventional drilled shafts. The test shafts had diameters ranging from 2 ft to 4 ft, and lengths ranging from 15 ft to 115 ft. Based on empirical analysis of these load test measurements, Mullins et al. (2006) proposed that TCM be computed as:

$$TCM = [0.713 \cdot GPI \cdot (\%D)^{0.364}] + \frac{(\%D)}{0.4(\%D) + 3} \quad (7.3)$$

where:

- GPI = grout pressure index
- $\%D$ = normalized shaft displacement, expressed as a percentage of the nominal shaft diameter, D

GPI is a normalized measure of the maximum sustained grout pressure that is computed as:

$$GPI = \frac{p_{g-max}}{q_p} \quad (7.4)$$

where:

- p_{g-max} = maximum sustained grout pressure
- q_p = nominal unit tip resistance for a conventional shaft, using the method recommended by Reese and O'Neill (1988) for cohesionless soils

The second term in Equation 7.3 reflects the normalized mobilization of tip resistance for a conventional shaft (i.e., with no improvement due to post-grouting), termed the “backbone

curve.” The backbone curve used in Equation 7.3 was established from a fit to the normalized load transfer curve recommended by Reese and O’Neill (1988) for tip resistance in cohesionless soil (Figure 7.1). The first term in Equation 7.3 reflects the empirically observed improvement in the mobilized tip resistance for PGDS, relative to the Reese and O’Neill backbone curve. The improvement due to post-grouting was taken to be a function of the normalized shaft displacement, $%D$, and the dimensionless grout pressure index, GPI . Figure 7.2 shows a plot of TCM from Equation 7.3 as a function of $%D$ and GPI .

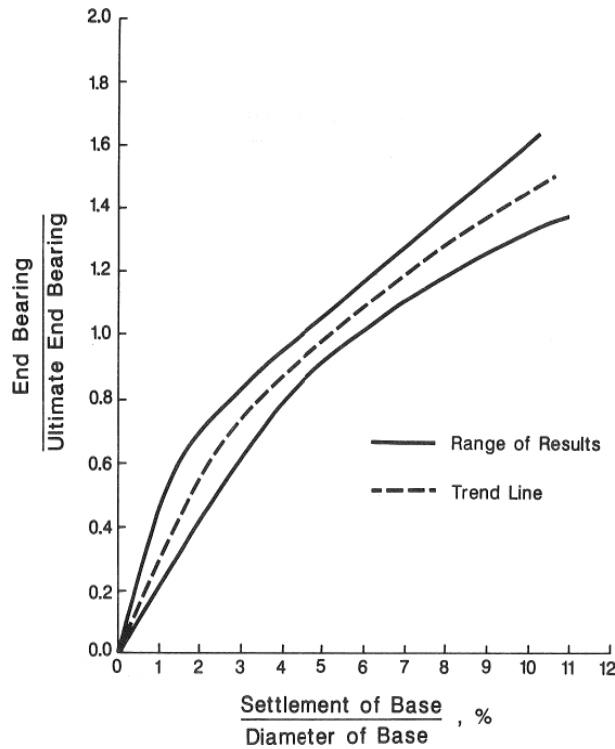


Figure 7.1: Normalized load-transfer curve for tip resistance of drilled shafts in cohesionless soil (Reese and O’Neill, 1988) used as backbone curve by Mullins et al. (2006).

It is important to emphasize that Mullins et al. (2006) used the normalized load-transfer curve for ungrouted shafts (Figure 7.1) and the nominal unit tip resistance, q_p , recommended by Reese and O’Neill (1988) for cohesionless soils to empirically establish Equation 7.3. As such, Equation 7.3 is strictly restricted to be used with the Reese and O’Neill methods, although alternative methods that adopt different backbone curves and/or different predictions of the nominal unit tip resistance can be developed following a similar rationale.

7.2.2 Dapp and Brown (2010)

Dapp and Brown (2010) developed an alternative expression for TCM based on measurements from multiple bi-directional load tests performed for the Audubon Bridge project in Louisiana. The test shafts were approximately 200 ft long, tipped in alluvial sand deposits that contain some gravel and clay, and grouted using sleeve-port devices. Uncased segments of the tested shafts were 7.5 ft in diameter. A gravel bedding layer was used in combination with a sleeve-port

device for one of the test shafts (Castelli, 2012). The maximum sustained grout pressures ranged from approximately 750 psi to 1000 psi, which leads to *GPI* values ranging from approximately 2 to 3. The measured load-settlement responses from bi-directional load tests performed on the one ungrouted shaft and nine post-grouted shafts are plotted in Figure 7.3.

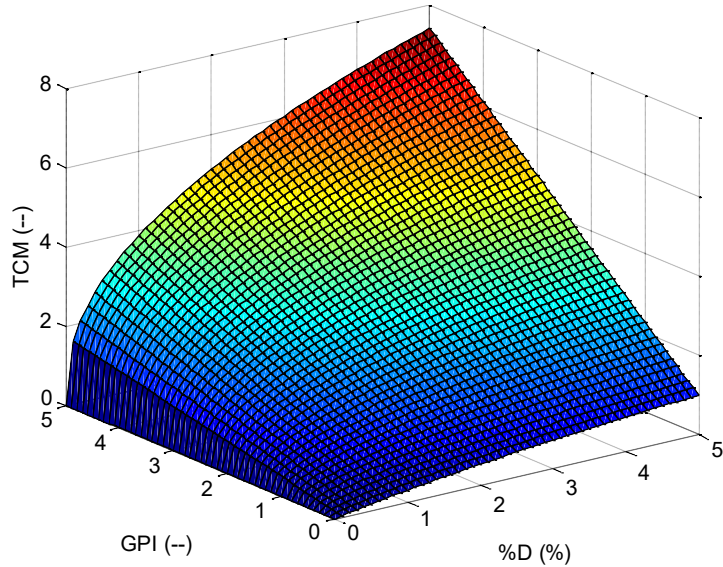


Figure 7.2: Graph of *TCM* from Equation 7.3 for normalized displacements between 0 and 5 percent, and *GPI* between 0 and 5 percent (after Mullins et al., 2006).

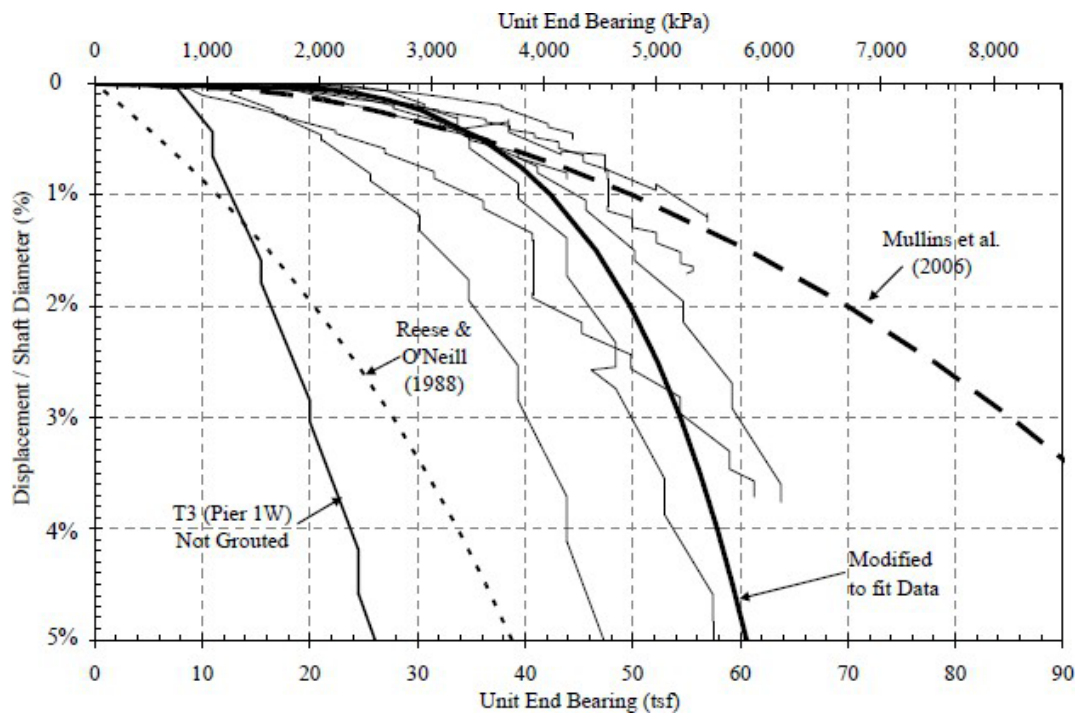


Figure 7.3: Measured load-settlement response from bi-directional load tests performed at the Audubon Bridge site (Dapp and Brown, 2010).

Comparison of the measured load-settlement response for the post-grouted test shafts to the response predicted using Equation 7.3 (also shown in Figure 7.3) reveals that the measured response tended to be stiffer than predicted at relatively low loads but had significantly less resistance than predicted at greater loads. A similar comparison can be made between the measured response for the ungrouted test shaft and the response predicted using Reese and O'Neill (1988), which is used as the backbone curve for Equation 7.3. Based on these observations and to better reflect the measured load-settlement response at the Audubon Bridge site, Dapp and Brown (2010) developed the following modified equation for computation of TCM :

$$TCM = [0.713 \cdot GPI \cdot (\%D)^{0.200}] + \frac{(D)}{4.0(\%D) + 6} \quad (7.5)$$

Figure 7.4 shows a graph of TCM calculated from Equation 7.5 for normalized shaft displacements between 0 and 5 percent and for GPI between 2 and 3. Note that Equation 7.5 has a different backbone curve than is used in Equation 7.3, as reflected in the second term, and a different exponent in the first term that represents the improvement in mobilized tip resistance due to post-grouting. As is true for Equation 7.3, Equation 7.5 is strictly predicated on calculation of GPI using the nominal unit tip resistance from Reese and O'Neill (1988).

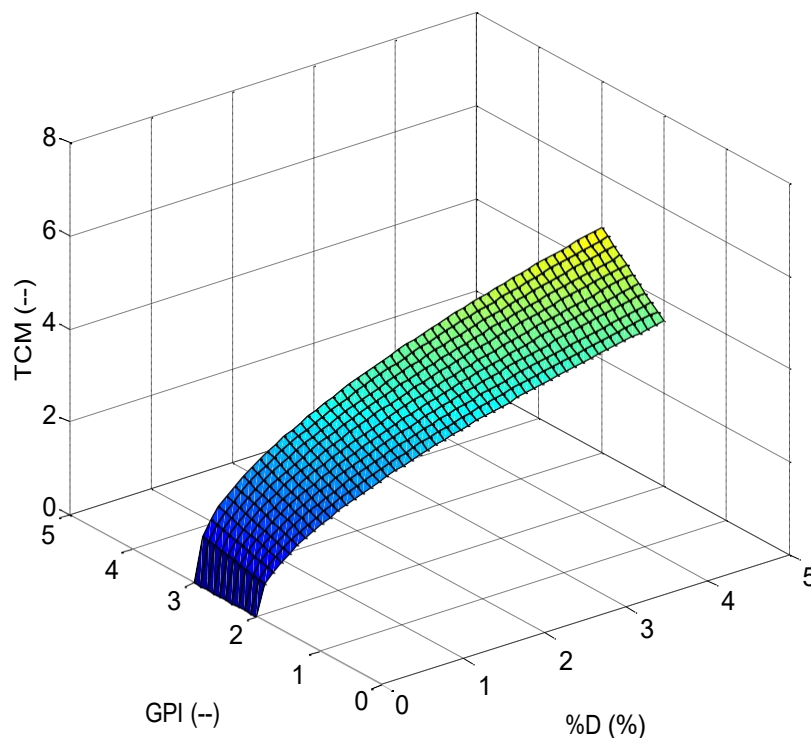


Figure 7.4: Graph of TCM from Equation 7.5 for normalized displacements between 0 and 5 percent, and GPI between 2 and 3 percent.

7.2.3 Design Procedure for TCM Approach

Mullins et al. (2006) proposed the following procedure for predicting the nominal resistance for PGDS tipped in cohesionless soils for a given shaft diameter (D) and embedment length (L).

1. Calculate the nominal unit tip resistance for an ungrouted shaft according to Reese and O'Neill (1988):

$$q_p = 1.2 \cdot N_{60} \leq 90 \text{ ksf} \quad (7.6)$$

where: q_p = nominal unit tip resistance (in ksf)
 N_{60} = corrected standard penetration test (SPT) N -value for soil beneath the shaft tip (in blows/ft) $\leq 75 \text{ bpf}$

Note that both the methods by Mullins et al. (2006) and Dapp and Brown (2010) are predicated on the use of Equation 7.6 for determining q_p .

2. Calculate the nominal side resistance (R_s) for the total embedded length of the shaft:

$$R_s = \sum_{i=1}^n (q_{s_i} A_{s_i}) \quad (7.7)$$

where: q_{s_i} = nominal unit side resistance for soil layer i
 A_{s_i} = nominal area of the soil-shaft interface for soil layer i
 n = total number of soil layers within the embedded length

This step does not require use of specific methods for the prediction of q_s . Therefore, appropriate methods for computing q_s for the soil or rock present, e.g., methods in AASHTO (2012), can be used.

3. Calculate the maximum anticipated grout pressure (p_{g-max}) that can be resisted by the nominal side resistance computed in Step 2:

$$p_{g-max} = \frac{R_s}{A_p} \quad (7.8)$$

where: R_s = nominal side resistance for conventional drilled shaft
 A_p = nominal area of the shaft tip

The buoyant unit weight of the shaft may also be added to the numerator of Equation 7.8, but is commonly neglected.

4. Compute the grout pressure index (GPI) using Equation 7.4 with the maximum anticipated grout pressure from Step 3 and the nominal unit tip resistance from Step 1.
5. Establish the maximum allowable displacement, expressed as a ratio of the shaft diameter (i.e., $\%D$), from consideration of serviceability.

6. Calculate the tip capacity multiplier (TCM) using Equation 7.3 with the GPI from Step 4 and $\%D$ from Step 5.
7. Compute the predicted unit tip resistance for the PGDS ($q_{p,gr}$) using Equation 7.1 with TCM from Step 6 and q_p from Step 1.

This same procedure can be followed using the method proposed by Dapp and Brown (2010), but replacing Equation 7.3 with Equation 7.5 in Step 6.

One practical concern with the proposed design procedure is that it provides no margin for error in establishing the maximum anticipated grout pressure, which can lead to complications during construction. If the maximum anticipated grout pressure cannot be sustained when grouting PGDS, whether due to hydrofracture or unexpected upward movement of the shaft, the predicted resistance established during design is, at least theoretically, not achieved. Such situations may be remedied through stage grouting that may allow the maximum anticipated grout pressure to be sustained. However, stage grouting will not always lead to achieving the maximum anticipated grout pressure, so other remedies must be considered.

The TCM approach represents a practical method for predicting the mobilized resistance for PGDSs in cohesionless soil, whereby the method explicitly accounts for the effect of grout pressure as well as changes to the load-displacement response of the shaft due to post-grouting. However, the methods by Mullins et al. (2006) and Dapp and Brown (2010) are empirically-derived and based on rather limited data sets. Both methods consider improvement due to pre-mobilization, ground improvement beneath the tip of the shaft, and tip enlargement collectively, which makes it difficult to extend the methods to conditions where the contributions from these effects may be different. The proposed methods are also strictly restricted to use in cohesionless soils and to use of Reese and O'Neill (1988) for prediction of the ungrouted unit tip resistance (Equation 7.6).

Differences between the methods by Mullins et al. (2006) and Dapp and Brown (2010) also suggest that there are factors associated with post-grouting that are not fully understood at this time (e.g., diameter, depth, shaft installation procedures, ground conditions, grouting devices, grouting procedures, etc.). Differences between the two methods can be attributed to differences in the load-settlement response for ungrouted shafts (the backbone curves) at different sites, as well as differences in the degree of improvement observed due to post-grouting at different sites. Such differences are currently difficult to predict without the benefit of site-specific load tests, which provide substantial motivation for performing project-specific load tests for PGDS.

7.3 Axial Capacity Multiplier Approach

Pando and Ruiz (2005) proposed a method for predicting the total resistance for PGDS, termed the Axial Capacity Multiplier (ACM) method, that was derived from theoretical consideration of load transfer for PGDS (Ruiz et al., 2005; Fernandez et al., 2007; Ruiz and Pando, 2009). The ACM approach is based on the prediction of total shaft resistance rather than tip resistance and is based on consideration of settlement at the shaft head rather than at the tip of the shaft. Using the ACM approach, the total shaft resistance at a given shaft settlement is computed as:

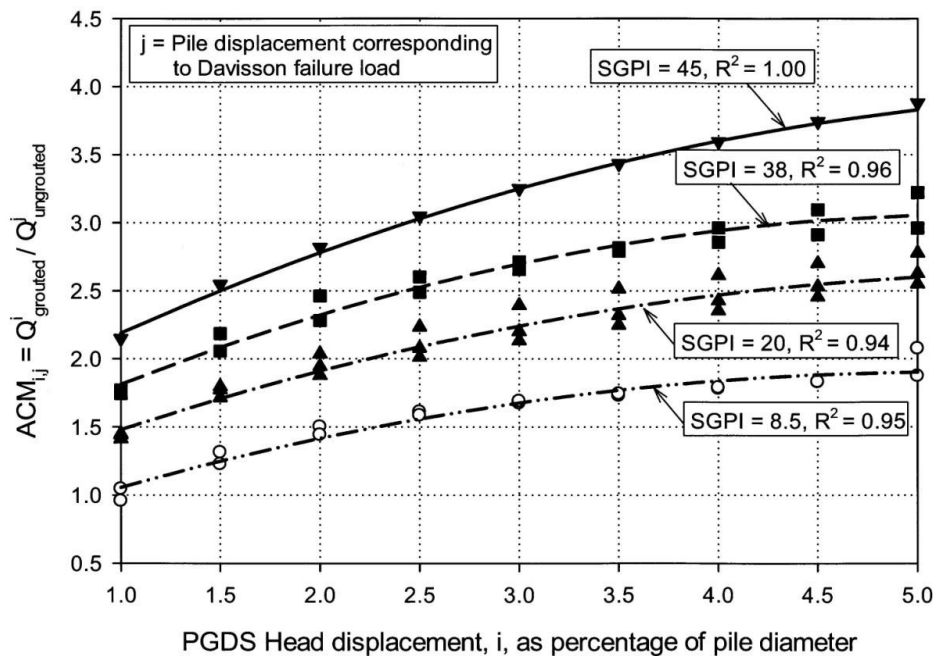
$$R_{n,gr}^i = ACM \cdot R_n^j \quad (7.9)$$

where: $R_{n,gr}^i$ = total axial resistance of PGDS at shaft head displacement i
 ACM = Axial Capacity Multiplier relating mobilized resistance for PGDS at shaft head displacement i to mobilized resistance for conventional shaft at shaft head displacement j
 R_n^j = total axial resistance of conventional drilled shaft at shaft head displacement j

Pando and Ruiz (2005) developed design charts to provide values of ACM as a function of normalized shaft settlement (relative to the shaft diameter) and normalized maximum sustained grout pressure as shown in Figure 7.5. Values of ACM shown in Figure 7.5 were computed from load-transfer analyses described subsequently, based on use of Davisson's failure criterion (Davisson, 1972) for establishing R_n for a conventional shaft. In Figure 7.5, the maximum sustained grout pressure is represented using a grout pressure parameter termed the Shaft Grout Pressure Index (SGPI), defined as:

$$SGPI = \frac{p_{g-max}}{q_s^{Ave}} \quad (7.10)$$

where: p_{g-max} = maximum sustained grout pressure
 q_s^{Ave} = average unit side resistance along the embedded shaft length



Note: Q^i = R^i = total axial resistance of PGDS at shaft head displacement i and

$Q_{ungrouned}^{grouned} = R_n^{n,gr}$ = total axial resistance of conventional drilled shaft at shaft head displacement j .

Figure 7.5: Design chart for determining ACM as a function of shaft head displacement and $SGPI$ (from Pando and Ruiz, 2005).

The design chart in Figure 7.5 was established using load-transfer analyses (i.e., t - z analyses) developed to account for three different mechanisms of improvement (Pando and Ruiz, 2005; Ruiz et al., 2005; Fernandez et al., 2007; Ruiz and Pando, 2009) that include:

1. Ground improvement of the soil beneath the shaft tip
2. Stress reversal along the shaft due to upward movement of the shaft during grouting
3. Increased tip area due to formation of a grout bulb beneath the shaft tip

Figure 7.6 shows qualitative changes to load-transfer functions for side and tip resistance attributed to each of these mechanisms (Fernandez et al., 2007; Ruiz and Pando, 2009). Compression of the soil beneath the shaft tip was considered to increase the stiffness of the q - w response at the shaft tip as shown in Figure 7.6(a). Stress reversal along the shaft was considered to produce an effective translation of the starting point on the t - z curve for subsequent top-down loading (generally following logic presented in Chapter 2), as illustrated in Figure 7.6(b). Finally, the increase in the tip area was considered to increase both the ultimate tip resistance and the stiffness of the q - w response for the ground beneath the shaft tip as shown in Figure 7.6(c).

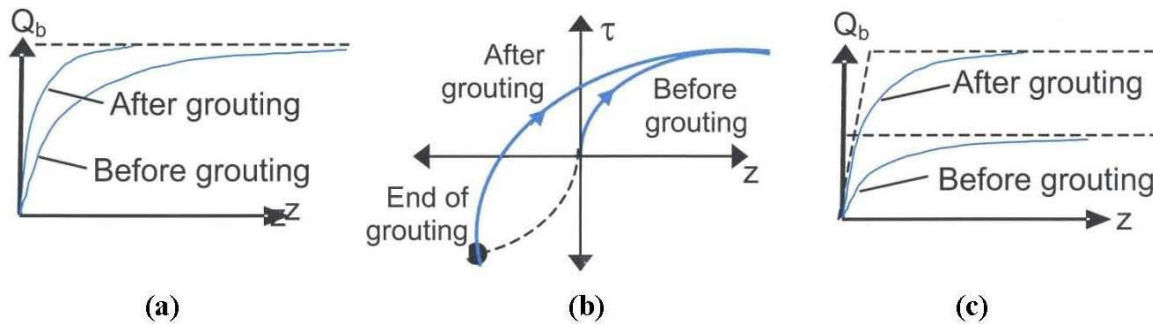


Figure 7.6: Schematic illustrating effect of three improvement mechanisms considered for development of ACM method on load transfer models (from Fernandez et al., 2007): (a) compression of soil beneath shaft tip, (b) stress reversal along shaft due to upward movement during grouting, and (c) increase of shaft tip area from formation of grout bulb.

Based on these considerations and the work of Pando et al. (2004), Ruiz et al. (2005) proposed theoretically derived load-transfer relationships that incorporate the initial shear modulus of the soils (G_0 or G_{max}), soil nonlinearity through use of a modified hyperbolic relation, and asymptotic values derived from CPT-based static methods. The proposed t - z relationship for mobilization of side resistance is:

$$Z = Z_a + \frac{(\tau_o - \tau_a)r_o}{G_o g} \cdot \ln \left(\frac{\left(\frac{r_m}{r_o}\right)^g - f \cdot \left(\frac{\tau_o - \tau_a}{\tau_{max} \cdot n}\right)^g}{1 - f \cdot \left(\frac{\tau_o - \tau_a}{\tau_{max} \cdot n}\right)^g} \right) \quad (7.11)$$

where:

- Z = relative displacement of the shaft section due to top-down loading
- Z_a = relative displacement of the shaft section due to post-grouting
- τ_0 = initial shear stress
- τ_a = residual shear stress in the shaft section following post-grouting
- r_0 = radius of the drilled shaft
- G_0 = initial shear modulus of the soil for shear strains below 10^{-5} (from seismic CPT or SASW)
- g = empirical fitting parameter (typically = 0.3)
- r_m = radius of influence of the drilled shaft
- τ_{max} = max shear stress = $R_f \cdot \tau_{ult}$ (where R_f is the failure ratio ≤ 1)
- n = empirical fitting parameter ranging between 1 and 2
- f = empirical fitting parameter (typically = 0.98)

The proposed $q-w$ relation for mobilization of tip resistance is:

$$Z_{base} = \frac{Q_b \cdot (1 - \nu)}{4G_0 r_0 \cdot \left(\frac{Q_b \cdot (1 - \nu)}{1 - f \cdot \left(\frac{Q_b}{Q_{b-max}} \right)^g} \right)} \quad (7.12)$$

where:

- Z_{base} = displacement of the shaft tip
- Q_b = current load at the shaft tip
- ν = Poisson's ratio of the soil beneath the tip of the shaft
- Q_{b-max} = ultimate tip load

The proposed load transfer functions (Equations 7.11 and 7.12) were used to evaluate the measured response from load tests on nine different PGDS at four different test sites (Pando and Ruiz, 2005; Ruiz et al., 2005; Fernandez et al., 2007; Ruiz and Pando, 2009) in order to characterize the contributions of the different improvement mechanisms considered. Six of the test shafts considered were tipped in sand and three of the shafts were tipped in clay. Both flat-jack and sleeve-port systems were used to grout the test shafts. Empirical parameters (f , g , and n) that produced a match between predicted and measured performance for the respective test shafts were also subsequently used to establish the values for ACM presented in Figure 7.5.

The basic ACM method presented in Equation 7.9 represents a practical method for estimating the total resistance for PGDS following a design procedure similar to that presented in Section 7.2 (Pando and Ruiz, 2005). The ACM method is based on fundamentally sound theoretical concepts and methods, which lend considerable credence to the approach. However, since the recommended values of ACM in Figure 7.5 were established based on analysis of a collection of load test measurements, the ACM method is also empirical despite having a strong theoretical basis. The empirical measurements from which the ACM values in Figure 7.5 were established include measurements for shafts tipped in both sands and clays, so the ACM approach is more broadly applicable than the TCM methods described in Section 7.2. However, both of these methods are based on relatively limited data sets, so it is reasonable to question how well either method will reflect performance in a wide range of ground conditions.

One can also debate the approach of applying a multiplier to total shaft resistance, as is done in the *ACM* method, compared to applying a multiplier to tip resistance alone as is done in the *TCM* approach. It is convenient to use the total shaft resistance; however, the *ACM* method essentially considers that both the grout pressure and stress reversal are controlled by skin friction, regardless of end bearing, so the same *ACM* values may not be appropriate for shafts with different proportions of side and tip resistance. A similar limitation as described previously for the *TCM* approach also holds true; while the load-transfer analyses used to develop values of *ACM* are capable of separately considering contributions due to ground improvement at the shaft tip, pre-mobilization, and enlargement of the shaft tip, the resulting values of *ACM* are presented as a combination of these effects. Therefore, the values of *ACM* presented in Figure 7.5 may not be appropriate for cases where the individual mechanisms of improvement may be substantially different from those present in the empirical data (as is also true for the *TCM* approach). The load-transfer functions proposed and used for development of Figure 7.5 rely on soil property values, some of which are often unavailable and require estimation through correlations or experience. This may restrict the potential for use of the functions to model PGDS in ground conditions that are significantly different than those tested.

Despite some limitations, the fundamental approach adopted for the *ACM* load transfer analyses provides a sound basis for modeling of PGDS. Therefore, a similar approach was adopted to evaluate results of load test measurements for the present work, as described in Chapter 8.

7.4 Component Multiplier Approach

Duan and Kulhawy (2009) describe an empirical design approach originally developed by Hu et al. (2001) that has become the basis for design of PGDS in the Chinese *Technical Code for Building Pile Foundations* (China Academy of Building Research, 2008). This approach is referred to as the “component multiplier” approach within this report. In the component multiplier approach, “improvement coefficients” for both the side and tip resistance components of total resistance are applied to account for the improved resistance due to post-grouting. The basic expression for predicting the nominal resistance for PGDS is thus:

$$R_{n,gr} = R_{s,gr} + R_{p,gr} = \pi D \sum \lambda_{si} q_{si} \ell_i + 0.25\pi D^2 \lambda_p q_p \quad (7.13)$$

- where:
- $R_{n,gr}$ = nominal resistance for PGDS
 - $R_{s,gr}$ = nominal side resistance for PGDS
 - $R_{p,gr}$ = nominal tip resistance for PGDS
 - D = shaft diameter
 - λ_{si} = improvement coefficient for side resistance along shaft segment i due to post-grouting
 - q_{si} = nominal unit side resistance for ungrouted shaft along shaft segment i from Chinese Code (China Academy of Building Research, 2008)
 - ℓ_i = length of shaft segment i
 - λ_p = improvement coefficient for tip resistance due to post-grouting
 - q_p = nominal unit tip resistance for ungrouted shaft from Chinese Code (China Academy of Building Research, 2008)

Equation 7.13 follows the general form of conventional static methods used in U.S. design practice, except for the coefficients λ_{si} and λ_p that reflect increases in side and tip resistance attributed to post-grouting. Alternative values for the improvement coefficients have been reported for different soil/rock types based on analysis of load test measurements for PGDS. Several versions of these recommended improvement coefficients are presented in the following subsections. Note that the values of q_{si} and q_p are established using presumptive values provided in the Chinese *Technical Code for Building Pile Foundations*.

7.4.1 Hu, Li, and Wu (2001)

Hu et al. (2001) evaluated results from load tests for 186 PGDS in the Hankou District in Wuhan Province, China, and compared them to test results for conventional shafts (Duan and Kulhawy, 2009). The test shafts had diameters ranging from 28 to 40 inches and lengths ranging from about 80 to 160 ft. All shafts were grouted at the shaft tip with an average of 5,300 lbs of cement. Based on this considerable database, Hu et al. (2001) found that λ_p ranged between 1.3 and 5.1, and that λ_{si} ranged between 1.3 and 2.2. A summary of recommended ranges for the coefficients λ_{si} and λ_p for different soil types is provided in Table 7.1.

Table 7.1: Recommended improvement coefficients from Hu et al. (2001).

Improvement Coefficient	Clay	Silt	Silty & Fine Sand	Medium Sand	Coarse Sand	Gravel & Cobble
λ_{si}	1.2 - 1.5	1.3 - 1.5	1.5 - 1.9	1.6 - 1.9	1.7 - 2.2	1.7 - 2.2
λ_p	1.2 - 1.7	1.4 - 1.8	1.8 - 2.5	2.0 - 2.8	2.2 - 2.8	2.2 - 3.0

Note: $\lambda_{si} = 1$ for soil layers > 65 ft away from tip of the shaft.

One important difference between Chinese design practice, as reflected by Equation 7.13, and current U.S. practice, is that improvement in side resistance due to post-grouting is routinely considered in Chinese practice, even for PGDS that are only grouted at the tip of the shaft. Consideration of improved side resistance may reflect a belief that grout will flow up the interface between the shaft concrete and soil/rock for some distance, or it may reflect some recognition of improvement due to pre-mobilization of load in the shaft during grouting. Regardless of the motivation or justification, improvement in side resistance is considered for PGDS that are grouted exclusively at the shaft tip, although such improvement is generally considered limited to some distance above the tip of the shaft (as indicated in footnote to Table 7.1). Intentional “side grouting” of drilled shafts (e.g., Xiao et al., 2009) is also much more common in China than in the U.S., but does not seem to be required in order to consider the improvement in side resistance suggested in Table 7.1.

7.4.2 Chinese Technical Code for Building Pile Foundations

The current Chinese *Technical Code for Building Pile Foundations* mandates that the ultimate resistance for PGDS be determined using static load tests (China Academy of Building Research, 2008). However, the code provides ranges for λ_{si} and λ_p , shown in Table 7.2, that can be used for estimating the ultimate resistance using the component multiplier approach for different types of ground. These values are intended for use in conjunction with presumptive values for q_{si} and q_p that are specified in the code.

Table 7.2: Improvement coefficients provided in the Chinese *Technical Code for Building Pile Foundations* (China Academy of Building Research, 2008).

Improvement Coefficient	Silt, Mucky Soil	Cohesive Soil, Silty Soil	Mealy Sand, Fine Sand	Medium Sand	Coarse Sand, Gravelly Sand	Gravel & Pebbles	Highly Weathered Rock
λ_{si}	1.2 – 1.3	1.4 – 1.8	1.6 – 2.0	1.7 – 2.1	2.0 – 2.5	2.4 – 3.0	1.4 – 1.8
λ_p	2.2 – 2.5	2.4 – 2.8	2.6 – 3.0	3.0 – 3.5	3.2 – 4.0	2.0 – 2.4	---

7.4.3 Xiao, Wu, and Wu (2009)

Xiao et al. (2009) reported alternative ranges for λ_{si} and λ_p based on model tests and full-scale load tests from more than 100 projects as summarized in Table 7.3. Values for λ_p ranged between 2.0 and 4.0 while values for λ_{si} ranged between 1.2 and 3.0. No indication is provided regarding the distance over which improvement in side resistance should be considered.

Table 7.3: Recommended improvement coefficients from Xiao et al. (2009).

Improvement Coefficient	Peat	Clay & Silt	Fine Sand	Medium Sand	Coarse Sand	Gravel & Pebbles	Highly Weathered Rock
λ_{si}	1.2 – 1.3	1.4 – 1.8	1.6 – 2.0	1.7 – 2.1	2.0 – 2.5	2.4 – 3.0	1.4 – 1.8
λ_p	---	2.2 – 2.5	2.4 – 2.8	2.6 – 3.0	3.0 – 3.5	3.2 – 4.0	2.0 – 2.4

7.4.4 Dai, Gong, Zhao, and Zhou (2012)

Dai et al. (2011) reported recommended ranges for λ_{si} and λ_p based on analysis of a collection of load test results for more than 50 PGDS. The reported ranges, provided in Table 7.4, tend to reflect narrower ranges compared to those reported by both Hu et al. (2001) and Xiao et al. (2009). The improvement coefficients proposed by Dai et al. (2011) ranged between 1.5 and 2.5 for λ_p , and ranged between 1.3 and 2.0 for λ_{si} .

Table 7.4: Recommended improvement coefficients from Dai et al. (2011).

Improvement Coefficient	Clayey Soil or Silt	Silty Sand	Fine Sand	Medium Sand	Coarse Sand	Gravel Sand	Detritus Soil
λ_{si}^*	1.3 - 1.4	1.5 - 1.6	1.5 - 1.7	1.6 - 1.8	1.5 - 1.8	1.6 - 2.0	1.5 - 1.6
λ_p	1.5 - 1.8	1.8 - 2.0	1.8 - 2.1	2.0 - 2.3	2.2 - 2.4	2.2 - 2.4	2.2 - 2.5

* Enhancement of side resistance is limited to a distance of: (a) 30 to 50 ft above the shaft tip when grouting in saturated soil, and (b) 13 to 16 ft above the shaft tip when grouting in unsaturated soil. $\lambda_{si} = 1$ beyond these limits.

Dai et al. (2011) also provide conditions for use of the improvement factors provided in Table 7.4. The conditions include:

1. The grout water-to-cement ratio should be limited to a range of 0.5 to 0.7 for saturated soils, 0.7 to 0.9 for unsaturated soils, and 0.5 to 0.6 for loose gravel and sand.
2. The maximum grout injection pressure should be limited to a range of 725 to 1,450 psi for weathered rock, unsaturated clay, and silt, and to a range of 220 to 875 psi for saturated soil (with the pressure tending toward the lower end for softer soil and the higher end for denser soil).
3. The injection of the grout should occur for at least 5 minutes.
4. The flow rate of the grout should be limited to a maximum of 20 gal/min.

7.4.5 Liu and Zhang (2011)

Liu and Zhang (2011) proposed a variation to the component multiplier approach, referred to in this report as the “truncated cone” approach. In this approach, the capacity of a PGDS is calculated in a manner similar to that presented in Equation 7.13, but considering an enlarged tip area derived from the volume of injected grout assuming that the grout takes the form of a truncated circular cone as illustrated in Figure 7.7.

$$R = \sqrt[3]{\frac{V \tan\theta}{\pi} + (r)^3} \quad (7.14)$$

where: R = radius of the base of the truncated circular cone
 V = volume of grout injected
 θ = angle of truncated circular cone (typically assumed to be 60°)
 r = radius of drilled shaft = $D/2$

Using the truncated cone approach, the nominal resistance for a PGDS is calculated following Equation 7.13, but using a shaft tip area (A_p) calculated from the enlarged radius given by Equation 7.14 and using alternative improvement coefficients. Liu and Zhang (2011) recommended using a tip improvement coefficient (λ_p) between 0.5 and 0.9, and a side improvement coefficient (λ_{si}) between 1.2 and 1.6.

While there is some logic to use of an enlarged tip area for PGDS, the truncated cone approach appears to provide little benefit over alternative component multiplier methods described previously. The fact that recommended values of λ_p for the truncated cone approach are less than unity suggests that the enlarged area predicted using Equation 7.14 is likely greater than the actual area, thus requiring use of λ_p less than 1.0 to compensate for the error. While Liu and Zhang (2011) do present analyses for three load tests, the basis for the recommended improvement coefficients also seems to be severely limited compared with alternative component multiplier methods.

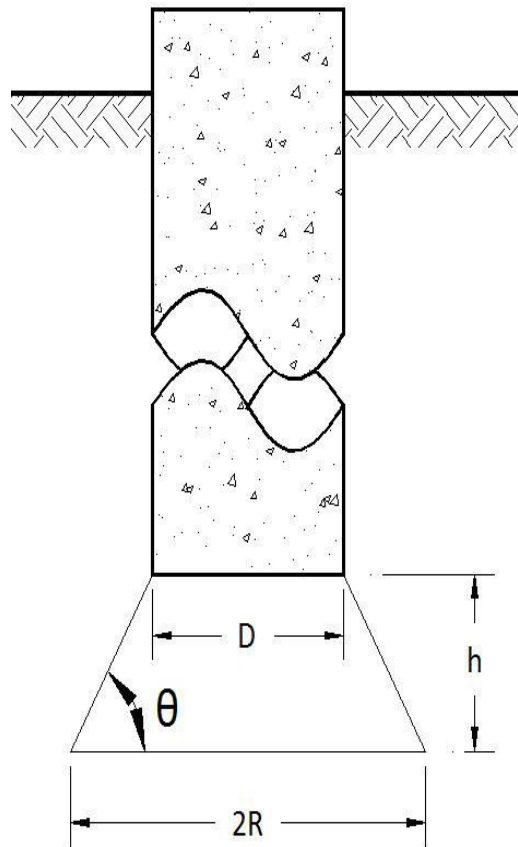


Figure 7.7: Schematic illustrating enlarged shaft tip according to the truncated cone approach (after Liu and Zhang, 2011).

7.4.6 Discussion on the Component Multiplier Approach

The component multiplier approach has practical appeal for design of PGDS. The methods rely on calculations (Equation 7.13) that are familiar to those involved with foundation design, with the addition of relatively simple multipliers to account for the improvement attributed to post-grouting. However, the component multiplier approach also evokes several concerns regarding its use for U.S. practice, as described in more detail in the following paragraphs.

Perhaps the most significant concern that arises when considering the component multiplier methods is the reliance on improvement in side resistance over significant lengths of the shaft, even when grout is only injected at the shaft tip. There is certainly evidence to support that grout may, at times, flow up the sides of PGDS during tip grouting (e.g., Mullins and Winters, 2004; Muchard and Farouz, 2009). It is also reasonable to assume that such grout may increase the available side resistance. However, consideration of upward flow over lengths that may approach 60 ft or more seems highly implausible to most foundation designers in the U.S., which leads to significant concern over reliance on improvement in side resistance. It is possible that differences between U.S. and Chinese construction practices may contribute to more substantial, and more reliable upward flow of grout along the shaft perimeter when following Chinese practices. However, the differences in current practices seem relatively minor and insufficient to justify such an argument. A more likely explanation is that the improvement attributed to side

resistance in component multiplier methods may, in fact, be due to improved tip resistance since the component multiplier approach is a purely empirical approach. Thus, the net result of considering improvement in both side and tip resistance may lead to prediction of overall improvement that is similar to what has been observed in full-scale load tests. As a practical matter, designers could choose to adopt the basic component multiplier approach but to neglect improvement in side resistance by adopting $\lambda_{si} = 1.0$ for the entire length of the shaft. Such a tactic is likely to produce conservative results, since some of the improvement attributed to post-grouting will be neglected, but such practice also negates some of the benefit of using empirical methods. Additional study regarding the potential upward flow of grout, and the potential benefits of such flow is needed before this issue can be acceptably resolved.

As with all empirical methods, the accuracy of the component multiplier approach rests upon how closely actual construction practices match those used to install the test shafts utilized to develop the design approach. Since the component multiplier methods were established entirely from projects constructed following current Chinese practices, and established relative to presumptive values for unit side and tip resistance that may differ from current U.S. practice, use of such methods for projects that follow current U.S. practices may introduce significant errors into the predictions. Additional study of the component multiplier methods, including comparison with measured resistances determined for PGDS constructed following current U.S. practices, is needed to evaluate the potential magnitude and impact of such errors. Some evidence in this regard is provided in Chapter 9.

In addition, component multiplier methods lack explicit consideration of the maximum sustained grout pressure. While it seems reasonable to assume that the magnitude of the sustained grout pressure will affect the nominal resistance of a PGDS, it is possible that Chinese grouting procedures (i.e., grout pressures, grout characteristics, grouting sequence, etc.) have been standardized to the point where some consistency is achieved across different sites and projects. Thus, the component multiplier methods may appropriately reflect the improvement that can be achieved given that grouting is performed according to standardized criteria, and that such improvement may be largely independent of the absolute grout pressure. It is noted that the grout volumes and grout pressures cited by Dai et al. (2011) are generally larger than those typically seen in U.S. practice.

Finally, it is important to emphasize that the Chinese *Technical Code for Building Pile Foundations* (China Academy of Building Research, 2008) mandates that the ultimate resistance for PGDS be determined from static load tests. As such, the component multiplier methods are really used for “preliminary design” in Chinese practice (Liu and Zhang, 2011): to establish reasonable shaft dimensions to achieve a specific resistance rather than as a direct means to demonstrate a specific capacity. Use of the methods in this manner alleviates some of the concerns associated with the component multiplier methods.

7.5 Simplified Approach

McVay et al. (2010) proposed a simple method for estimating the minimum total design resistance for PGDS in cohesionless soil based on observations from small-scale experiments using a rigid wall test chamber (McVay et al., 2010; Thiyyakkandi et al., 2013). Results from the small-scale experiments showed that the increase in axial resistance of model PGDS was

predominantly due to pre-loading of the shaft tip, and, to a lesser degree, an increase in tip area. McVay et al. (2010) therefore suggest that a “minimum ultimate design resistance” can be estimated as:

$$R_n = q_s A_s + q_s A_s + q_p A_p = 2R_s + R_p \quad (7.15)$$

where: R_n = nominal axial resistance of PGDS
 R_s = nominal side resistance for a conventional drilled shaft
 R_p = nominal tip resistance for a conventional drilled shaft

Equation 7.15 neglects potential contributions from an increase in side resistance that may occur due to grouting at the shaft tip and from an enlarged tip area due to the grouting. The method is therefore said to produce conservative estimates for PGDS resistance since it neglects contributions from these mechanisms. While the method is attractive in its simplicity, Equation 7.15 relies on assumptions that may not be routinely satisfied. First, the method relies on the assumption that full (upward) side resistance will be mobilized during post-grouting. While such an assumption may be satisfied in some cases, there will inevitably be instances when the upward side resistance may not be fully mobilized during post-grouting (e.g., due to hydrofracture, limited tip resistance, limitations of grouting equipment, etc.). The method also neglects the fact that some tip resistance will be “consumed” during post-grouting, and thus will not be available to resist subsequent top-down loading. In cases where these assumptions are not satisfied, Equation 7.15 will overestimate the resistance provided by a PGDS unless the improvement provided from the neglected mechanisms (i.e., improved side resistance and enlarged tip) is sufficient to compensate for the errors introduced by the unsatisfied assumptions.

7.6 Summary on Applicability and Limitations of Design Methods

The general design approaches and specific design methods presented in this chapter are all empirical methods for estimating the nominal resistance for PGDS, although some of the approaches have a theoretical basis. Since the methods are empirical, the accuracy of resistance estimates for a given project will depend upon the degree to which site conditions and construction methods are consistent with those used to develop the respective design methods. It is important to note that prediction of post-grouted shaft capacity during design is not necessarily more, or less, reliable than prediction of capacity for conventional drilled shafts, as illustrated and described in more detail in Chapter 9. The uncertainty generally revolves around the magnitude of available side and tip resistance, as well as the degree to which the selected prediction methods reflect performance. The act of post-grouting may serve to demonstrate that capacity, or some portion of capacity, has been achieved but this does not reduce uncertainty in predicting capacity during design.

In general, the *TCM* and *ACM* approaches are based on relatively limited numbers of load test measurements. Grouting procedures followed for the test shafts that were used to develop these methods are generally consistent with current practices for post-grouting in the U.S., and the empirical data sets generally include measurements for PGDS that were grouted using both sleeve-port and flat-jack grouting devices. The post-grouted test shafts used to develop the respective measurements were load tested using a combination of conventional static tests, Statnamic tests, and O-Cell test methods. Load tests used to develop the *TCM* methods were

restricted to shafts in sand and silty/shelly sand; whereas load tests used to develop the *ACM* method included PGDS tipped in both sand and clay. When calculating the nominal resistance for ungrouted shafts (used as input for both approaches), the *TCM* methods by Mullins et al. (2006) and Dapp and Brown (2010) are strictly restricted to use with equations by Reese and O'Neill (1988) for cohesionless soil, while the *ACM* method is restricted to use with predictions from load-transfer analyses using Davisson's failure criterion.

The component multiplier methods are generally based on much larger collections of load test results that include PGDS tipped in relatively wide ranges of ground conditions. Therefore, the methods are likely to better reflect performance that can be expected across the spectrum of ground conditions where PGDS may be used. However, the grouting devices used for the PGDS in these empirical data sets may be substantially different from those commonly used in the U.S. Grouting procedures used for the PGDS to establish component multipliers differ from those currently used in U.S. practice, although the differences may not be significant. The component multiplier methods are generally restricted for use with presumptive unit side and tip resistance values for ungrouted drilled shafts that are specified in the Chinese *Technical Code for Building Pile Foundations* (China Academy of Building Research, 2008), which may differ substantially from measured and predicted resistances for PGDS in the U.S.

The simplified method suggested by McVay et al. (2010) is largely based on purely theoretical considerations that are independent of ground conditions, grout devices, and the method for estimation of the resistance for conventional drilled shafts. However, the method is also based on assumptions that are likely flawed for many sites and, thus, is unlikely to produce reliable estimates of nominal resistance for PGDS.

Given the limitations of existing methods, it is clear that none of the existing methods is completely suitable for establishing the nominal resistance for PGDS across the spectrum of ground conditions, grouting devices, and grouting procedures that are likely to be encountered for PGDS in the U.S. Such limitations should not prevent future use of PGDS, since there is ample evidence to demonstrate that post-grouting may substantially improve the performance of drilled shafts compared to the performance of similarly-sized conventional shafts. However, these limitations do lead to challenges with establishing appropriate values for the nominal resistance for PGDS, especially in clayey soil and rock. For the foreseeable future, it therefore seems prudent to require that PGDS performance be demonstrated through site-specific load testing as is currently required in Chinese practice.

One additional limitation that impacts use of PGDS in the U.S. is the lack of calibrated and/or vetted resistance factors in the current AASHTO design code (AASHTO, 2012). While arguments can be made to support the belief that PGDS may be more or less reliable than similar ungrouted shafts, the fact remains that the issue of appropriate resistance factors is unresolved. Therefore, common practice has been to use resistance factors and/or factors of safety that are similar to those used for conventional drilled shafts.

CHAPTER 8: COMPREHENSIVE EVALUATION OF RESULTS FROM SELECTED LOAD TEST PROGRAMS

8.1 Introduction

There are numerous reported cases where load tests have been performed on comparable ungrouted and post-grouted drilled shafts at the same site. Results of most of these tests consistently demonstrate that post-grouting improves the axial load-deformation response of drilled shafts either by “stiffening” the response of the shafts, by increasing the ultimate axial resistance, or both. However, the scatter present in the load test measurements is substantial, which makes it difficult to develop methods for predicting the improved performance of PGDS. Such scatter is not uncommon in results of load tests of ungrouted drilled shafts and of many other deep foundation element types, but is possibly aggravated by the use of different grouts, grout delivery systems, and grouting procedures across the various reported cases, as well as by different shaft construction and load testing methods.

The challenge in interpreting load test measurements is compounded in the case of PGDS because the degree of improvement from each improvement mechanism – pre-mobilization, ground improvement by densification and/or permeation, improvement due to an enlarged tip, and improvement in side resistance – is likely dependent on the grout and grouting procedure utilized. The analyses presented in this chapter, and analyses presented subsequently in Chapter 9, were conducted to try to reduce or explain a portion of the scatter in load test measurements so that improved predictions can be made. Analyses presented in this chapter were performed to separate effects of pre-mobilization from effects of ground improvement while analyses presented in Chapter 9 were conducted to try to isolate effects of different shaft characteristics and grouting procedures. This chapter focuses on results of “select” load test programs because the analyses are intensive and require comprehensive information that is not available for all of the load tests.

8.2 Methodology

The fundamental objective for the “comprehensive” analyses was to identify and separate improvement attributable to pre-mobilization of resistance during grouting from improvement due to ground improvement at the tip of PGDS. This objective was achieved by using numerical analyses to simulate the axial response of PGDS considering pre-mobilization alone (with no ground improvement) and then comparing the simulated response to the actual measured response of the PGDS. The portion of the improvement not predicted using the pre-mobilization model was attributed to ground improvement at the tip of the shaft. For the purpose of these analyses, improvement due to densification or permeation of grout into the ground at the tip of the shaft and enlargement of the shaft tip was collectively considered to be “ground improvement.” Improvement in side resistance was neglected in these analyses.

The numerical model used for prediction of the axial response of PGDS, considering the effects of pre-mobilization, was adapted from common techniques for modeling axial load transfer for deep foundations, commonly referred to as the “*t-z* method” (Reese et al., 2006). For this report, the load-transfer analyses were implemented using the finite element method with relatively

simple bi-linear or tri-linear t - z models to represent load transfer in side resistance, and similar q - w models to represent load transfer in tip resistance (Figure 8.1).

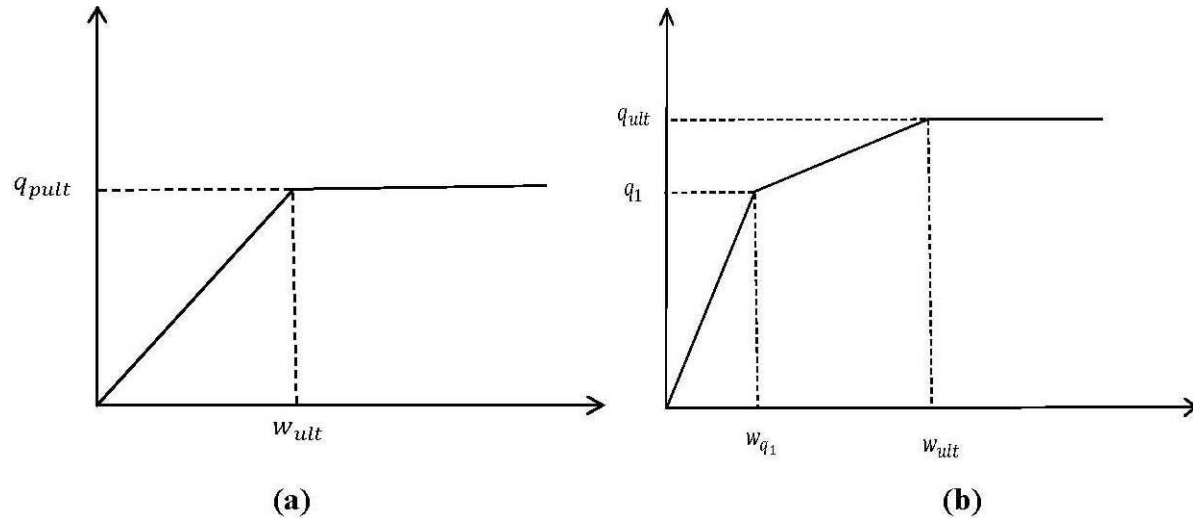


Figure 8.1: Simple load-transfer models used for predicting performance of PGDS considering pre-mobilization alone: (a) bi-linear load-transfer model for tip resistance, and (b) tri-linear load-transfer model for tip resistance.

The adaptations to conventional load-transfer methods include the ability to model load transfer during the post-grouting stage of construction. The post-grouting stage was modeled by applying simultaneous upward and downward loads within a “zero-stiffness” element located at the tip of the shaft to simulate the bi-directional loading induced during grouting. The magnitude of the bi-directional load was considered to be consistent with the grout pressure achieved in the field. Given this loading, the distribution of load and displacement along the shaft due to the post-grouting load was computed, including the downward displacement of the ground at the tip of the shaft. The resulting displacements were then used to modify the load-transfer models to reflect pre-mobilization, in a manner consistent with the concepts described in Chapter 2, and the modified load-transfer models were subsequently used to predict the response of the shaft to further loading.

8.3 Illustration of Methodology

To illustrate use of the load-transfer method for simulating the improvement in performance due to pre-mobilization alone, a simple example problem involving an infinitely rigid, 4-ft diameter shaft is presented herein. Actual analyses performed for the respective load tests presented subsequently also include appropriate modeling of the shaft stiffness. The primary steps in the modeling process are as follows:

1. Simulate the load-displacement response for the conventional, ungrouted shaft to establish calibrated t - z and q - w models that are consistent with the observed performance of the ungrouted test shaft.
2. Model load transfer due to post-grouting using the calibrated load-transfer models from Step 1 to establish the distribution of load and displacement along the test shaft due to post-grouting.

3. Modify the calibrated load-transfer models to account for pre-mobilization by “shifting” the origin of the load-transfer models (as described in Chapter 2) using displacements established in Step 2.
4. Simulate the load-displacement response of the PGDS for subsequent loading using the modified load-transfer models established in Step 3.

The last step, modeling of load-displacement response for the PGDS, differs depending upon whether the loading is top-down (e.g., from a conventional static test or Statnamic test) or bi-directional (e.g., from an O-Cell test) as described subsequently in more detail.

8.3.1 Response of UngROUTed Shaft

Modeling the load-displacement response for an ungrouted shaft follows traditional application of the load-transfer method. For the simple example considered here, the idealized load-transfer models and simulated performance for the ungrouted shaft are shown in Figures 8.2 through 8.4.

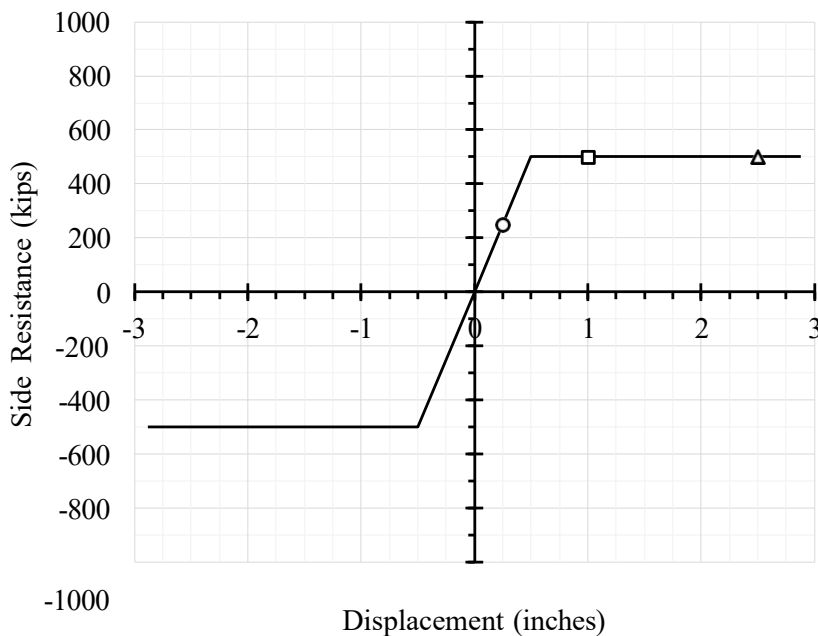


Figure 8.2 Load-transfer ($t-z$) model for side resistance.

The load-transfer model for side resistance shown in Figure 8.2 is a simple, linearly elastic, perfectly plastic model reflecting linear mobilization of resistance up to some limit resistance, which remains constant for larger displacements. Since side resistance can be mobilized for both positive (downward) and negative (upward) displacements, the ultimate resistance and corresponding displacement are modeled as being symmetric about the origin of zero load and displacement. For conventional “top-down” axial loading, the shaft is displaced into the ground (downward), and the load transferred to the soils surrounding the shaft is considered positive. Conversely, for upward loading, like that induced during post-grouting or during bi-directional load testing, the shaft is displaced upward, and displacements and mobilized side resistance are considered negative.

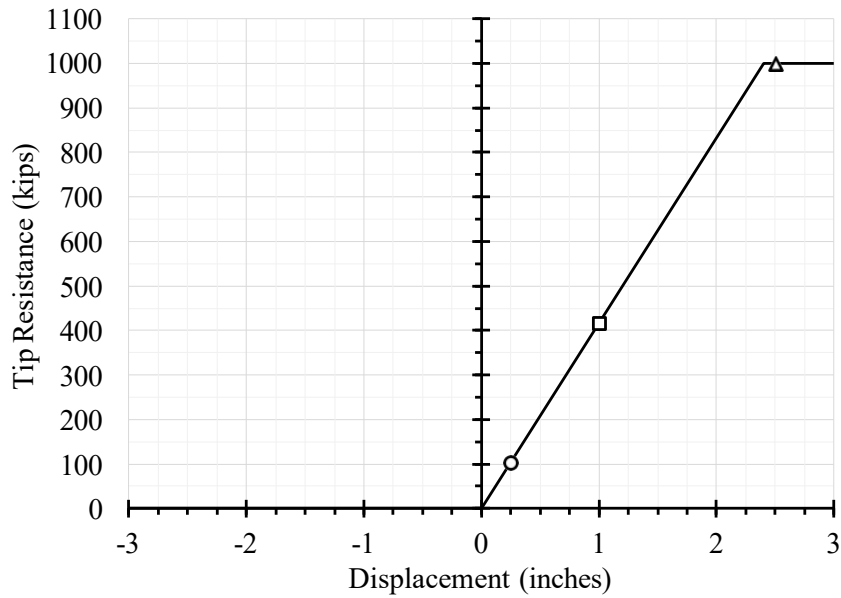


Figure 8.3: Load-transfer ($q-w$) model for tip resistance.

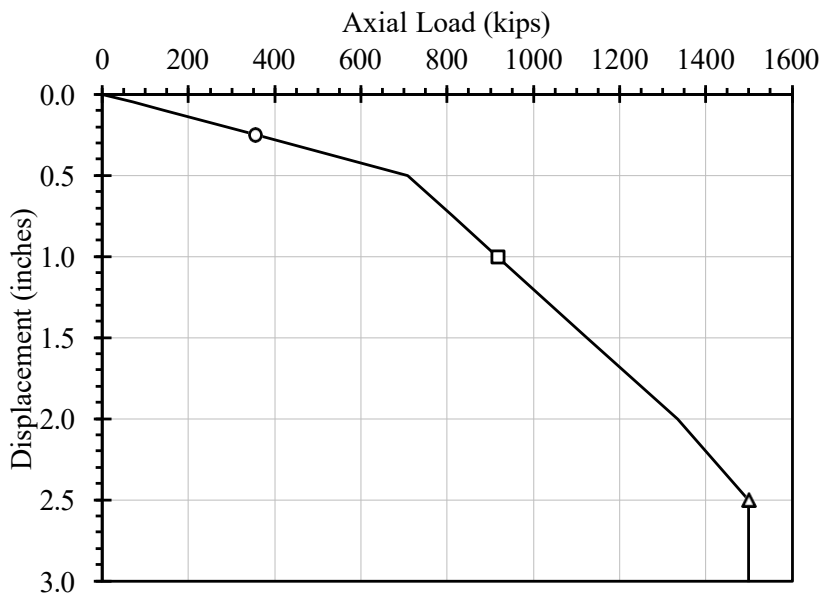


Figure 8.4: Simulated load-displacement response for a conventional ungrouted shaft subject to top-down loading for the simple example.

A similar model was used for load transfer in tip resistance, as shown in Figure 8.3. However, the load-transfer model for tip resistance does not allow for negative (upward) mobilization because upward movement of the shaft tip would result in loss of contact between the shaft tip and the underlying soils. The load-transfer model for tip resistance therefore reflects zero resistance for negative (upward) displacement of the shaft tip.

Figure 8.4 depicts the simulated load-displacement response for the rigid shaft determined using the load-transfer models shown in Figures 8.2 and 8.3. In this figure, the load at a given shaft displacement is taken to be the summation of the mobilized side and tip resistance at the same displacement. Note that the piecewise linear appearance of the load-settlement response results from consideration of a rigid shaft. A finite shaft stiffness value will produce a more realistic, “smooth” load-displacement response.

Points representing three displacements (0.25 inch, 1 inch, and 2.5 inches) are shown in Figures 8.2 to 8.4, respectively, to illustrate the side and tip resistance contributions to the overall load-displacement behavior. The circles correspond to displacements of 0.25 inch, the squares to displacements of 1 inch, and the triangles to displacements of 2.5 inches. The load-displacement curve shown in Figure 8.4 has two inflection points – one at a displacement of 0.5 inch and the other at a displacement of 2.5 inches – that correspond to full mobilization of side and tip resistance, respectively. At displacements less than 0.5 inch, both side and tip resistance are mobilized and contribute to overall resistance, although the resistance is largely dominated by side resistance because of the “stiffer” load transfer in side resistance. For displacements between 0.5 and 2.5 inches, additional resistance is mobilized from continuously increasing tip resistance, while side resistance remains constant because it has been fully mobilized. The plunging behavior at loads greater than 1,500 kips results from mobilization of the entirety of shaft resistance.

8.3.2 Adaptation of Load-transfer Models to Account for Pre-mobilization

The concepts presented in Figures 8.2 to 8.4 apply to analysis of ungrouted shafts and leave room for expansion to accommodate analysis of post-grouting. Application of pressurized grout to the tip of a shaft results in a bi-directional force with a magnitude corresponding to the product of the grout pressure and the area over which the grout pressure acts. Such loading results in upward (negative) displacement of the shaft above the tip and downward (positive) displacement of the soil below the tip. These displacements are responsible for pre-mobilization of side and tip resistance for the PGDS.

Continuing with the example shaft, the magnitude of the bi-directional load under a grout pressure of 200 psi is 362 kips, assuming the grout pressure acts over the entire shaft tip area. Application of the grout load in an upward direction mobilizes 362 kips of side resistance (neglecting the weight of the shaft) with corresponding upward displacement of approximately 0.3 inch in the negative direction as shown in Figure 8.5.

To account for the pre-mobilized side resistance for subsequent loading, the origin of the coordinate system was shifted to reflect the new “zero condition” following post-grouting. The dashed lines in Figure 8.5 indicate the shifted origin for the load-transfer model after grouting. This is the essence of pre-mobilization: that loading imposed subsequent to post-grouting starts from a condition that reflects loading induced during the grouting process. Barring deterioration of the ground-shaft interface as a consequence of the initial shearing, pre-mobilization does not produce an increase in side resistance *per se* because the limit resistance remains as it was prior to grouting. However, the load that must be applied to the shaft to reach this limit does increase because load in the negative direction has been pre-mobilized. Thus, for subsequent top-down loading, it is necessary to overcome the pre-mobilized load before “positive” side resistance can

be mobilized. Pre-mobilization of load due to post-grouting results in a shifting of the load-displacement behavior, allowing more side resistance to be mobilized when loading downward, and less resistance to be mobilized if the shaft is loaded upward after grouting, as illustrated in Figure 8.6.

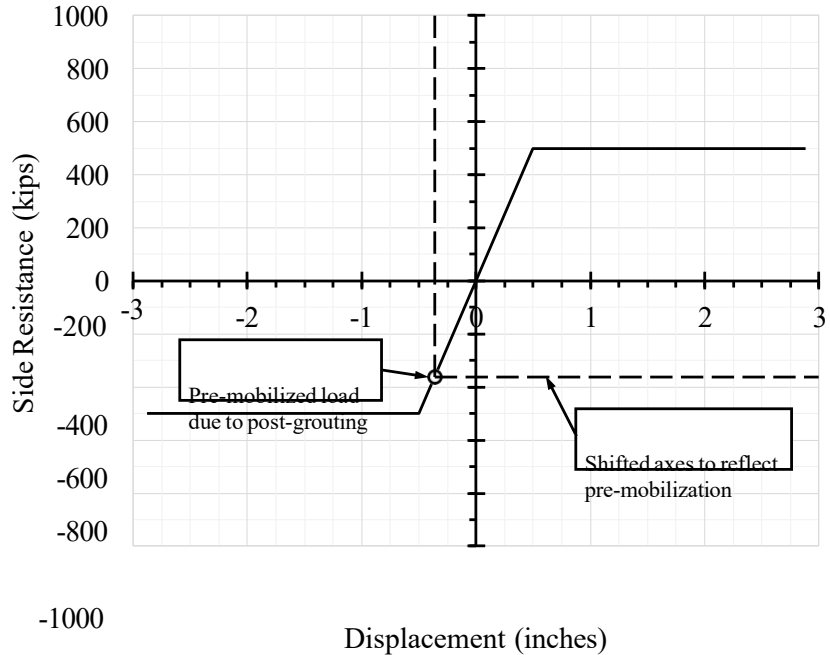


Figure 8.5: Pre-mobilization of side resistance from application of 200 psi grout pressure.

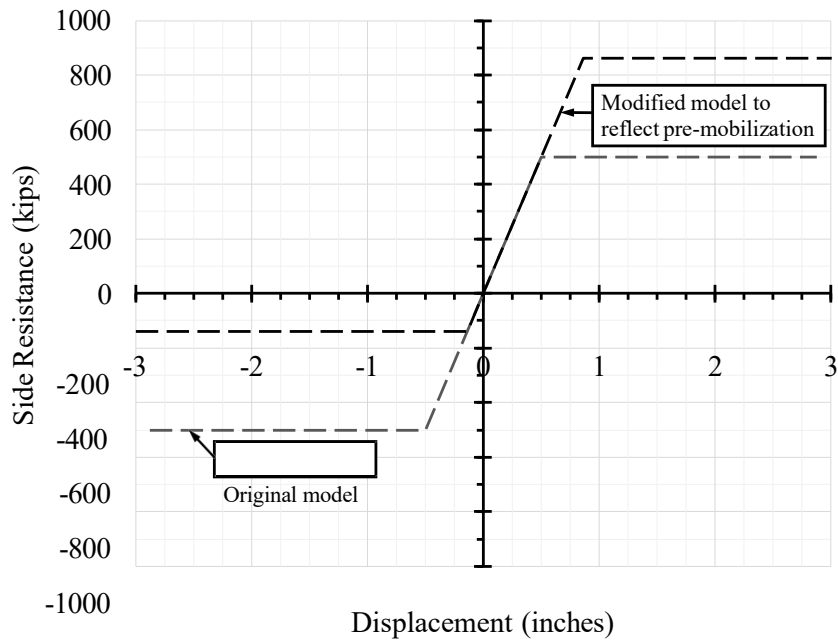


Figure 8.6: Comparison of load-transfer models for side resistance prior to, and after

post-grouting.

When considering pre-mobilization of tip resistance, displacement of the soil/rock at the shaft tip due to application of the same grout pressure is positive (downward), which results in “consumption” of some tip resistance during grouting as shown in Figure 8.7. Since subsequent top-down loading of the shaft continues loading in the same direction at the tip, the amount of additional tip resistance that can be mobilized following post-grouting is reduced from that which existed prior to grouting (Figure 8.8), presuming that no ground improvement or deterioration occurs during grouting.

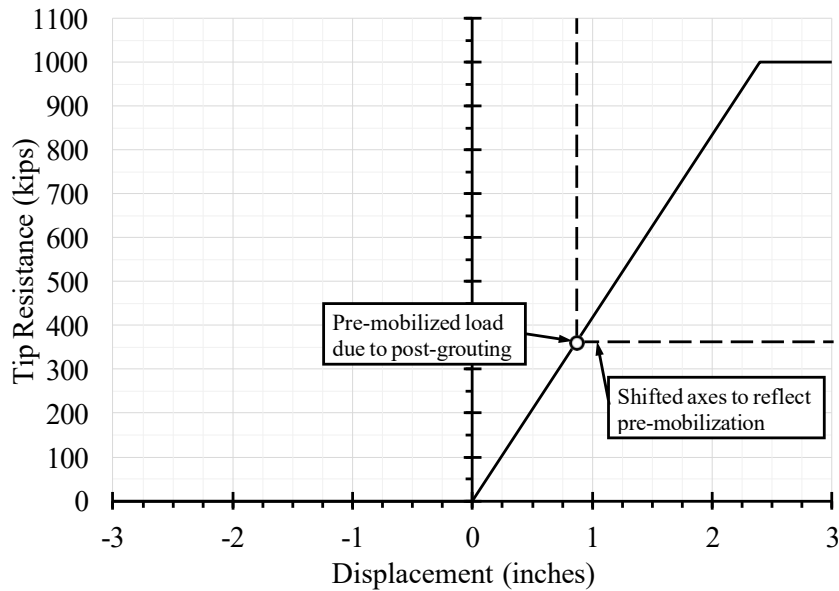


Figure 8.7: Pre-mobilization of tip resistance from application of 200 psi grout pressure.

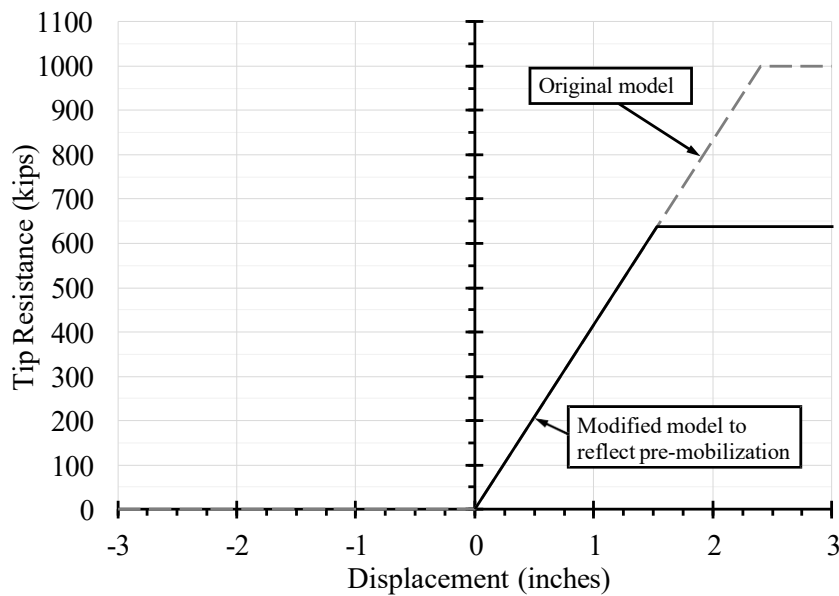


Figure 8.8: Comparison of load-transfer models for tip resistance prior to, and after post-grouting.

The load applied at the shaft tip due to post-grouting is equal in magnitude in both directions so the apparent gain in pre-mobilized side resistance is equal to the apparent loss in pre-mobilized tip resistance. Therefore, the pre-mobilization effect is essentially a redistribution of load-transfer behavior in which greater resistance is mobilized in side resistance, but lesser resistance is available from tip resistance compared to the ungrouted shaft.

8.3.3 Response of Grouted Shaft to Subsequent Top-down Loading

The shaft response to subsequent top-down loading was simulated using the t - z and q - w load-transfer models that were modified to account for pre-mobilization effects (neglecting any ground improvement). The load-transfer models for side and tip resistance of the pre-mobilized shaft are shown in Figures 8.9 and 8.10, considering the same applied grout pressure of 200 psi. The adjusted axes are plotted using dashed lines to indicate that the origin was shifted to the point corresponding to the mobilized condition due to grouting.

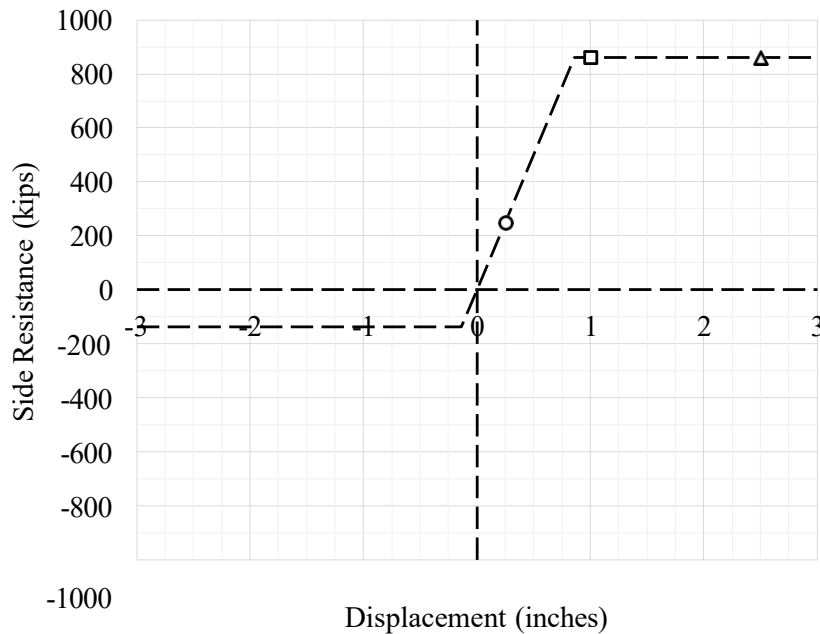


Figure 8.9: Load-transfer model in side resistance after application of 200 psi grout pressure.

Figure 8.11 shows the simulated load-displacement response of the shaft resulting from use of the modified load-transfer models to account for pre-mobilization, along with the load-displacement response for an identical ungrouted shaft (previously presented in Figure 8.4). As shown, pre-mobilization of resistance due to grouting produces a substantially “stiffer” response at intermediate loads. For small loads, where the load-displacement response is dictated by both side and tip resistance, the response is identical for both the grouted and ungrouted shafts. Similarly, the ultimate axial resistance is identical to that for the ungrouted shaft because the apparent increase in side resistance due to pre-mobilization is exactly countered by an equivalent consumption in tip resistance. Thus, pre-mobilization produces an improved load-displacement response but does not increase the ultimate axial resistance for the shaft.

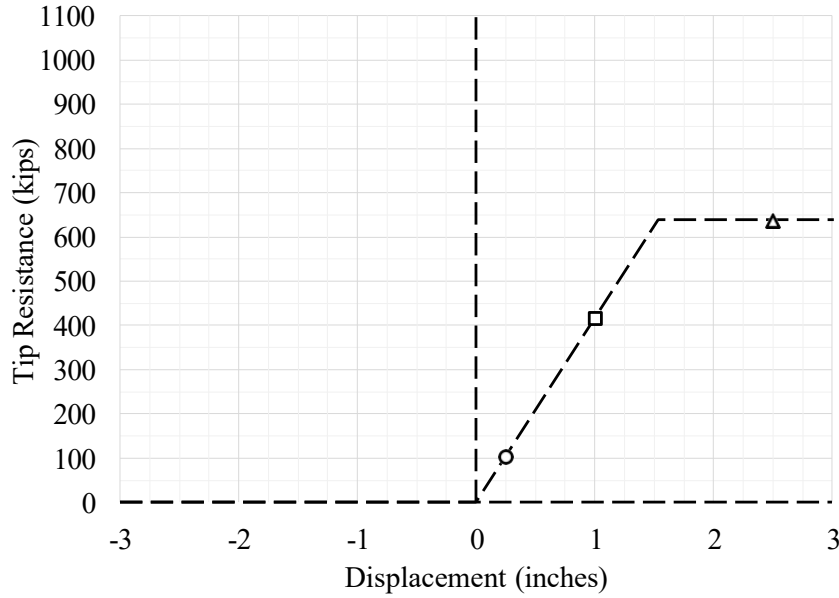


Figure 8.10: Load-transfer model in tip resistance after application of 200 psi grout pressure.

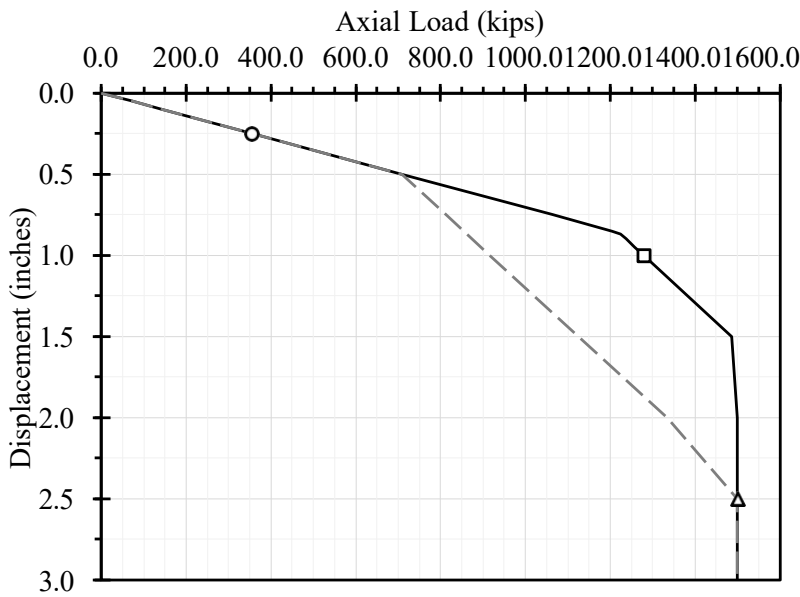


Figure 8.11: Comparison of load-displacement response of the ungrouted and PGDS considering the effect of pre-mobilization alone.

Note that the magnitude of the improvement in the load-displacement response due to pre-mobilization is related to the load induced during grouting, which is in turn related to the grout pressure achieved during grouting. Thus, when considering pre-mobilization alone, shafts subjected to greater post-grouting pressures will have greater improvement than shafts subjected to lesser grout pressures.

It is important to emphasize that the analyses for the idealized example presented in this section have neglected any contributions from ground improvement that may occur due to post-grouting at the shaft tip. The analyses have also neglected the potential for relaxation of the pre-mobilized resistance that may occur following grouting, or factors such as hardening in the load-transfer models. Ground improvement, whether due to densification or permeation of grout, may produce an increase in the limit resistance and the stiffness of the load-transfer model for tip resistance. The increased limit resistance and/or stiffness will produce improvement in excess of that simulated due to pre-mobilization alone. Relaxation of the load induced during grouting introduces an unloading stage that diminishes the improvement observed due to pre-mobilization. Hardening load-transfer behavior for side or tip resistance will change the basic form of the load-transfer models that were assumed for these idealized analyses and may affect the magnitude of pre-mobilization. Such phenomena can be considered and modeled using similar techniques, but have been avoided here in the interest of clarity.

8.3.4 Response of Grouted Shaft to Subsequent Bi-directional Loading

Shafts subjected to bi-directional loading following post-grouting will exhibit a different response than that shown in Figure 8.11. The different response occurs because bi-directional loading continues loading in the same direction as induced during grouting. Bi-directional loading results in the upward (negative) displacement of the shaft, which continues to mobilize resistance in the third quadrant of the load-transfer plot, as shown in Figure 8.12. Continued displacement in the negative direction results in approximately 160 kips of available side resistance compared to the approximately 860 kips of side resistance that would be available if the direction of loading were reversed as is done in a top-down test. Thus, the measured side resistance from a bi-directional load test will theoretically reflect the resistance that remains after post-grouting (assuming that no ground improvement occurs).

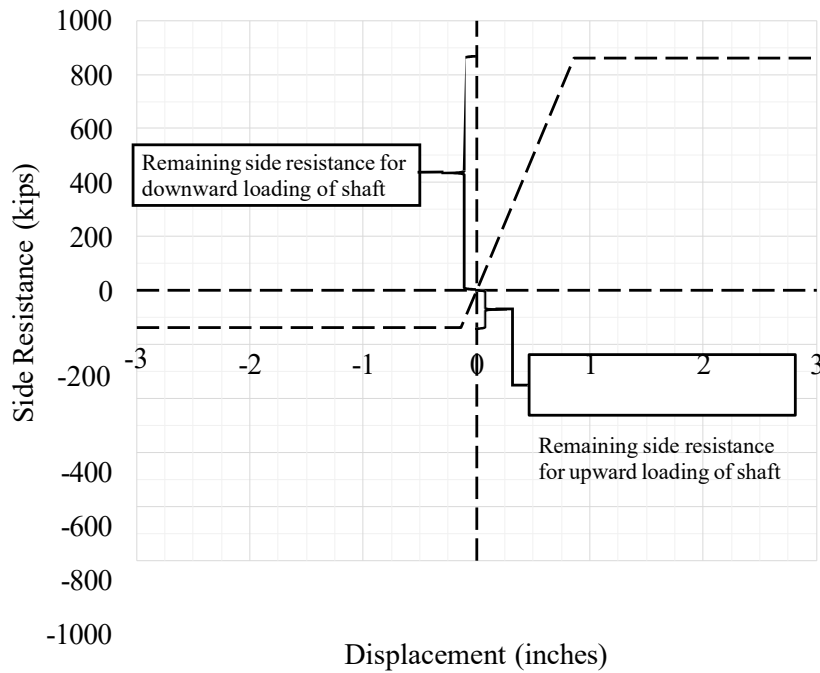


Figure 8.12: Modified load-transfer model for side resistance to account for pre-mobilized resistance showing remaining side resistance for a grouted shaft if

subsequently loaded in an upward or downward direction.

Following similar logic, the remaining tip resistance in a bi-directionally loaded shaft is equivalent to that for top-down loading because both displace soil at the shaft tip in a positive (downward) direction. Thus, the measured tip resistance from a bi-directional load test for a PGDS will theoretically reflect the tip resistance that remains after post-grouting, in addition to any improvement in tip resistance that occurs due to post-grouting.

8.3.5 Quantification of Ground Improvement at the Shaft Tip

When comparing results from simulations that model pre-mobilization alone to actual load test measurements, it is common for the simulated response to underestimate the actual measured response because ground improvement that may occur due to post-grouting is not modeled. In such cases, the improvement in the shaft response attributed to ground improvement at the shaft tip can be quantified by performing additional simulations using ultimate unit tip resistance values, q_{p-ult} , that reflect potential ground improvement at the shaft tip. These simulations, which include modeling of pre-mobilization, are repeated using alternative values for q_{p-ult} until a reasonable comparison between the simulated and measured load-displacement responses is found. The degree of ground improvement is then represented using a “ground improvement ratio,” GIR , defined as:

$$GIR = \frac{q_{p,gr-ult-premob}}{q_{p-ult}} \quad (8.1)$$

where: $q_{p,gr-ult-premob}$ = ultimate unit tip resistance required to produce a reasonable comparison between the simulated and measured load-displacement response for PGDS using simulations that model pre-mobilization

q_{p-ult} = ultimate unit tip resistance required to produce a reasonable comparison between the predicted and measured response for a comparable ungrouted shaft

Since GIR values are established using simulations that model pre-mobilization, these values reflect the improvement in performance that can be attributed to ground improvement alone because improvement due to pre-mobilization is inherently included in the model simulations. Thus, GIR only reflects improvement in performance attributed to improvement of the ground at the tip of the shaft (via densification, permeation, or both).

The GIR is fundamentally different from similar parameters described in Chapter 7 in that these other parameters quantify improved performance due to all mechanisms collectively. In order to provide for more direct comparison with these other parameters, a second parameter, termed the “total” improvement ratio (TIR), is also defined as:

$$TIR = \frac{q_{p,gr-ult}}{q_{p-ult}} \quad (8.2)$$

where: $q_{p,gr-ult}$ = ultimate unit tip resistance required to produce a reasonable comparison between the simulated and measured load-displacement response for PGDS using simulations that do not model pre-mobilization

q_{p-ult} = ultimate unit tip resistance required to produce a reasonable comparison between the predicted and measured response for the comparable ungrouted shaft

The fundamental difference between the *GIR* and *TIR* is that *GIR* is established using simulations that account for pre-mobilization, while *TIR* is established using simulations that do not consider pre-mobilization. Thus, *GIR* reflects improved performance due to ground improvement alone, while *TIR* reflects the improved performance from all improvement mechanisms collectively. The *TIR* is conceptually similar to the *TCM* described in Chapter 7 (Mullins et al., 2006); however, *TIR* is established relative to the ultimate unit tip resistance derived from measurements for an ungrouted test shaft, whereas *TCM* is established relative to the nominal unit tip resistance calculated from Reese and O’Neill (1988) for shafts in cohesionless soil. Values for the *GIR* and *TIR* were determined for the selected cases considered in this chapter.

8.4 Analyses for Selected Load Test Cases

Analyses were performed for a series of comprehensive load test cases to separately quantify the magnitude of contributions due to pre-mobilization and ground improvement. The analyses performed were similar to those described for the simple, rigid shaft example in the previous section, but consider the estimated stiffness of the respective drilled shafts. The specific cases considered are summarized in Table 8.1. These cases were selected because they include load tests on both conventional ungrouted shafts and nearby companion PGDS. The load test sites are well-characterized and the grouting protocols well-defined so that pre-mobilization can be reasonably modeled. As shown in the table, the selected cases include tests performed on PGDS that were tipped in both “sand” and “clay,” post-grouted using both flat-jack and sleeve-port distribution systems, and tested using conventional top-down, Statnamic, and bi-directional load tests.

Table 8.1: Summary of cases analyzed to separate contributions from pre-mobilization and ground improvement.

Case	Soil Type	Grouting Apparatus	Load Test Method
Texas A&M University	Clayey Sand	Flat-jack	Static
Texas A&M University	Clay	Flat-jack	Static
University of Houston	Sand	Flat-jack	Statnamic
University of Houston	Clay	Flat-jack	Statnamic
PGA Blvd	Sand	Sleeve-port	Statnamic
Broadway Viaduct	Sand	Both	Statnamic O-Cell
Zoo Interchange – SW Core	Sand	Sleeve-port	O-Cell
Zoo Interchange – NE Core	Sand	Sleeve-port	O-Cell
Zoo Interchange – West Leg	Clay	Sleeve-port	O-Cell

The load test cases analyzed included nine pairs of shafts constructed as part of research, value engineering, and/or bridge construction projects from the states of Texas, Iowa, Florida, and

Wisconsin. The cases include six top-down load tests (conventional static tests and Statnamic tests) and four bi-directional O-cell tests. Two cases (Texas A&M and University of Houston) had companion grouted and ungrouted shafts tipped in both sand and clay, while one case (Broadway Viaduct) includes shafts tested using both top-down and bi-directional load tests. Each of the cases analyzed also has adequate information required for modeling including:

- Site information such as boring logs, soil properties, and a summary of the construction methods
- Load-displacement curves measured from load tests on similar ungrouted and grouted shafts, in similar soils
- Information on the grouting procedure used including grout pressure and the staging/timeframe of grouting, as well as the top of shaft displacement measured during grouting

8.4.1 Analysis Procedure

Analyses for each case were completed in five general steps:

1. Establish “calibrated” load-transfer models representing mobilization of side and tip resistance for the ungrouted condition by matching the simulated response to the measured load-displacement response for tests on ungrouted shafts.
2. Simulate load-displacement response considering pre-mobilization using the “calibrated” load-transfer models from Step 1, and adjust the ultimate unit side and tip resistance for the post-grouted load-transfer models until the simulated and measured load-displacement responses for the PGDS compare favorably.
3. Compute the *GIR* from Equation 8.1 using the ultimate unit tip resistance that produced the favorable comparison between the simulated and measured responses for the PGDS from Step 2.
4. Simulate load-displacement response without considering pre-mobilization using the “calibrated” load-transfer models from Step 1, and adjust the ultimate unit side and tip resistance for the post-grouted load-transfer models until the simulated and measured load-displacement responses for the PGDS compare favorably.
5. Compute the *TIR* from Equation 8.2 using the ultimate unit tip resistance that produced the favorable comparison between the simulated and measured responses for the PGDS from Step 4.

The “calibrated” load-transfer models for the ungrouted condition (Step 1) were established by adjusting theoretical values for the ultimate unit side and tip resistances, and their associated displacements at the ultimate condition, until the simulated response matched the measured load-displacement response for the ungrouted test shaft. The bi-directional load used to simulate pre-mobilization in Step 2 was established from the reported grout pressure assuming that the pressure was applied across the entire tip area. Calculated displacements along the shaft following application of the bi-directional load due to grouting were then used to adjust the *t-z* and *q-w* models for each element along the shaft to account for pre-mobilization, as described previously in this chapter.

8.4.2 Example Results from Analysis of Selected Cases

Measured and simulated load-displacement curves from two of the cases in Table 8.1 are presented in Figures 8.13 through 8.15 to illustrate application of the analyses performed. Figures 8.13 and 8.14 show the simulated and measured load-displacement responses for the ungrouted and post-grouted test shafts at the University of Houston Sand test site. Figures 8.15 and 8.16 show similar results for grouted and ungrouted test shafts from the PGA Boulevard Project site. Figures 8.13 and 8.15 show results from analyses considering pre-mobilization alone, while Figures 8.14 and 8.16 show results from analyses considering both pre-mobilization and ground improvement at the shaft tip.

The figures include measured load-displacement curves for both grouted and ungrouted test shafts at the respective sites. Each figure also shows the simulated load-displacement response for the ungrouted test shafts, established by calibrating the individual load-transfer models to produce a reasonable comparison with the measured load-displacement response for the ungrouted shafts. These three curves (measured curves for grouted and ungrouted shafts and simulated curve for the ungrouted shaft) are identical in Figures 8.13 and 8.14, and in Figures 8.15 and 8.16. As is the case for the other sites considered, the simulated load-displacement curves for the ungrouted test shafts closely match the measured response.

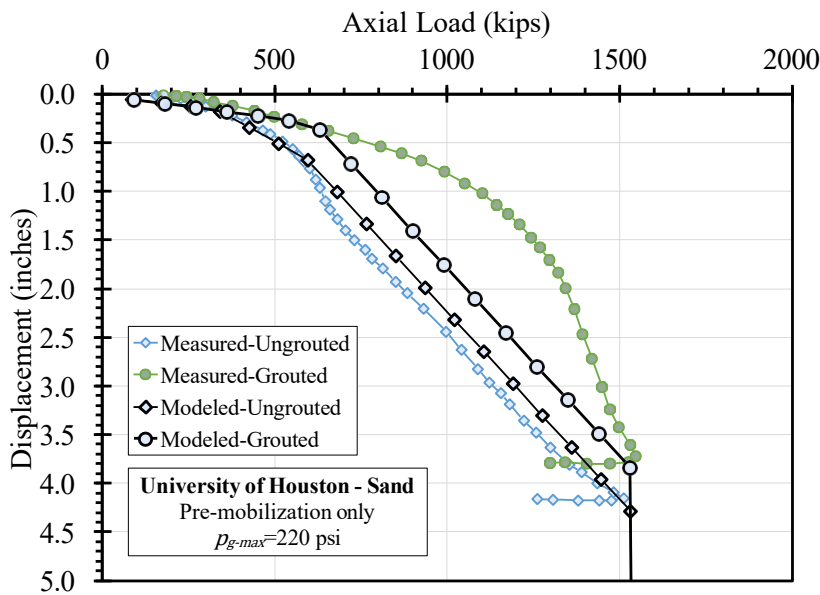


Figure 8.13: Predicted and measured load-displacement response for ungrouted and post-grouted test shafts from the University of Houston Sand site. Predicted response for grouted shaft considers pre-mobilization only with no ground improvement.

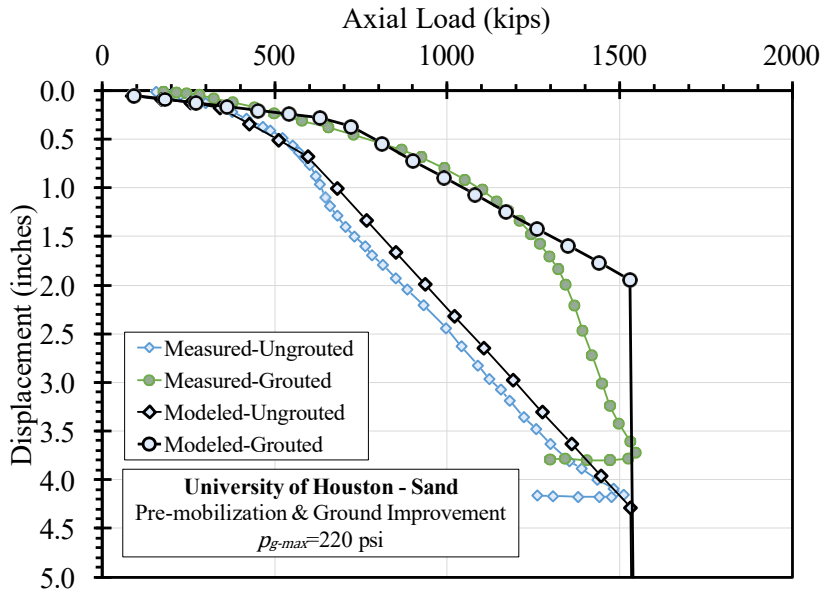


Figure 8.14: Predicted and measured load-displacement response for ungrouted and post-grouted test shafts from the University of Houston Sand site. Predicted response for grouted shaft includes both pre-mobilization and ground improvement.

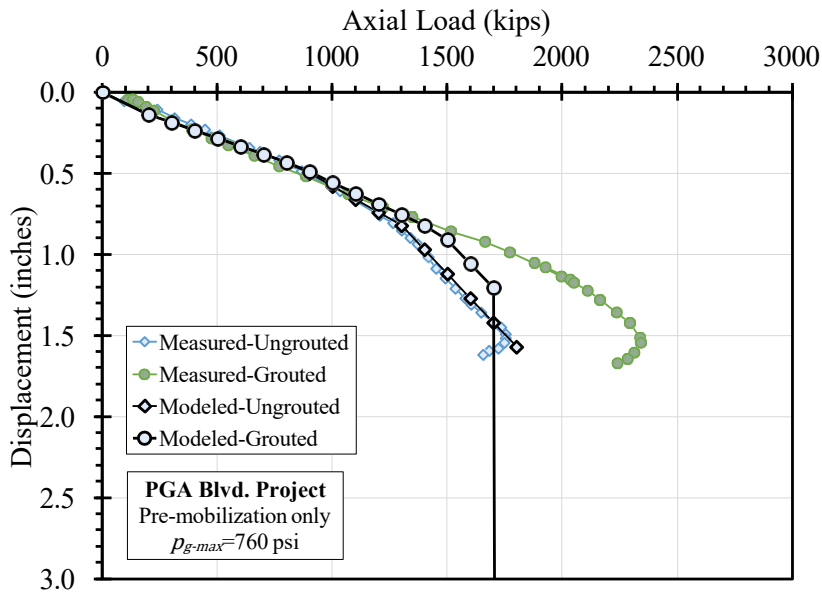


Figure 8.15: Predicted and measured load-displacement response for ungrouted and post-grouted test shafts from the PGA Blvd. site. Predicted response for grouted shaft considers pre-mobilization only with no ground improvement.

Figures 8.13 and 8.15 illustrate the improvement produced from post-grouting based on consideration of pre-mobilization alone, without ground improvement at the shaft tip. In both cases, the simulated response considering pre-mobilization alone falls above the response for the

ungROUTED shaft, particularly at intermediate loads, as was observed for the simple example presented previously. Similarly, the ultimate shaft resistance from the simulations considering pre-mobilization alone is consistent with the measured ultimate resistance for the ungrouted test shafts. However, neither of the simulations considering pre-mobilization alone produces a load-displacement response that is similar to the measured response observed for the post-grouted test shafts. Thus, in these cases, improvement due to pre-mobilization accounts for a portion, but not all, of the observed improvement due to post-grouting. Similar results were observed from analyses performed for the remaining cases considered with shafts in sand.

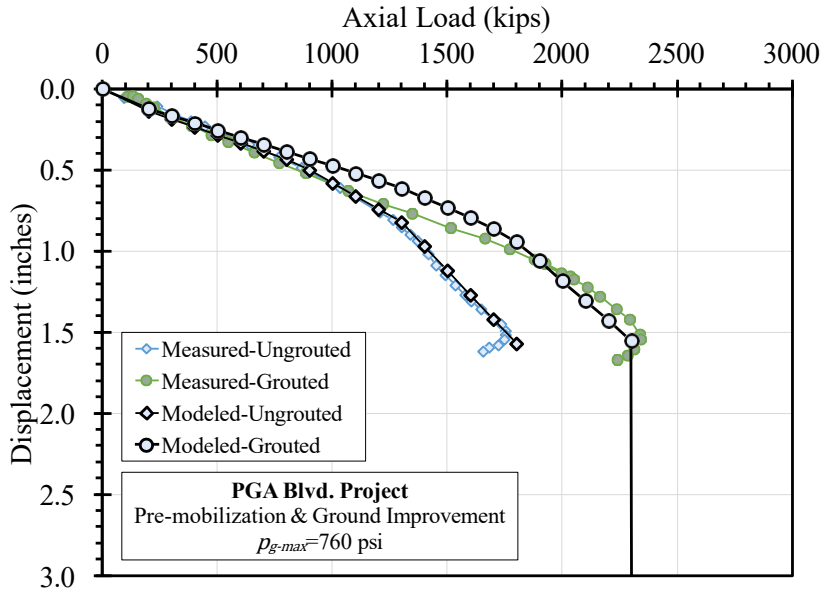


Figure 8.16: Predicted and measured load-displacement response for ungrouted and post-grouted test shafts from the PGA Blvd. site. Predicted response for grouted shaft includes both pre-mobilization and ground improvement.

Figures 8.14 and 8.16 show results from analyses performed considering improvement due to both pre-mobilization and ground improvement at the shaft tip. In both figures, the simulated response considering pre-mobilization and ground improvement reasonably matches the measured response, thus illustrating that the measured response for post-grouted test shafts can be reasonably predicted considering improvement due to some combination of pre-mobilization and ground improvement. Specific values for *GIR* and *TIR* resulting from these analyses, and additional analyses for the other cases considered are presented in the following section.

8.5 Collective Results from Comprehensive Analyses

Figure 8.17 shows the computed *GIR* determined from simulations considering pre-mobilization for the cases where the shafts were tested using top-down loading (conventional static tests and Statnamic tests). *GIR* values are not reported for the cases where bi-directional tests were performed because bi-directional tests do not theoretically capture improvement due to pre-mobilization. Figure 8.17 shows results for four cases where the test shafts were tipped in sand and two cases where the test shafts were tipped in clay. A *GIR* value of 1.0 indicates that the observed improvement in performance can be fully explained by pre-mobilization, while *GIR*

values greater than 1.0 indicate that both pre-mobilization and ground improvement are necessary to explain the observed performance of the post-grouted shaft compared to the conventional shaft. In some cases, the observed performance of the grouted or conventional shafts could be explained using multiple plausible combinations of pre-mobilization and ground improvement. In such cases, bars are shown in the graph to reflect the range of plausible results that could be derived from interpretation of the simulations.

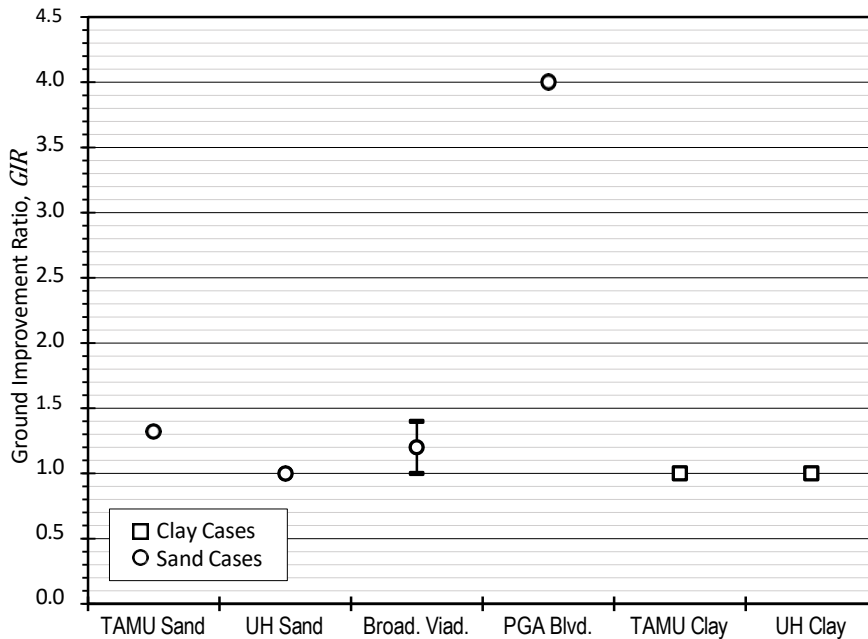


Figure 8.17: *GIR* derived from simulations considering pre-mobilization for all analyzed cases with top-down load tests. Sites with bars indicate the range of *GIR* calculated using different plausible interpretations.

Values of *GIR* derived from test shafts tipped in sand ranged from 1.0 to 4.0, with the calculated *GIR* for the PGA Boulevard case being dramatically greater than for the other cases considered. If the value for the PGA Boulevard case is excluded, the mean value of *GIR* for the remaining three “sand cases” is 1.17, while the computed *GIRs* for the two “clay cases” are both 1.0. Given the relatively small number of cases, this data suggests that post-grouting resulted in nominal “ground improvement” at the shaft tip that increased the ultimate unit tip resistance by approximately 20 percent over that for an ungrouted shaft when the shaft is tipped in sand. For shafts tipped in clay, these analyses show that the improved performance can be fully explained considering pre-mobilization alone, which suggests no ground improvement occurs.

Figure 8.18 shows values of the *TIR* computed by considering improvement due to pre-mobilization and ground improvement at the tip of the shaft collectively in a manner similar to that described for the *TCM* design method in Chapter 7. Several additional cases are included in this figure because results from sites where shafts were tested using bi-directional load tests can be included. As shown in Figure 8.18, values for *TIR* are substantially greater than values for *GIR*. This is expected because the *TIR* reflects the combined improvement due to pre-mobilization and ground improvement at the shaft tip, whereas *GIR* reflects improvement due to

ground improvement alone. The mean value of TIR derived from shafts tipped in sand is 1.64, while the mean value of TIR for shafts tipped in clay is 1.60. Note that computed TIR values derived from bi-directional load tests (tests from Broadway Viaduct in Iowa and the Zoo Interchange project in Wisconsin) are lower than values derived from top-down tests. This result is potentially due to bi-directional load test results not capturing the mechanism of pre-mobilization of tip resistance during post-grouting as top-down tests do, as discussed earlier. If values derived from bi-directional tests are neglected, the mean value of TIR is 1.92 for shafts tipped in sands and 1.75 for shafts tipped in clays.

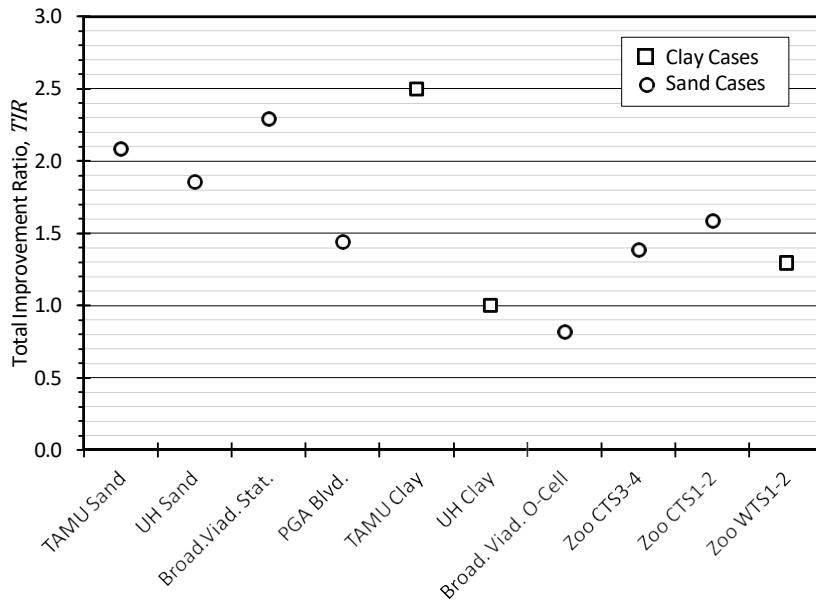


Figure 8.18: TIR derived from simulations considering pre-mobilization and ground improvement collectively for all analyzed cases.

Figures 8.19 and 8.20, respectively, show the values of GIR and TIR plotted as a function of shaft diameter and the maximum sustained grout pressure for the test shafts. Neither of these figures exhibits a clear trend in values with shaft diameter or grout pressure, although it is notable that the TIR values for the smallest diameter shafts are as great or greater than values for larger shafts (something that is also observed in Chapter 9). It is also important to note that the effect of grout pressure should be best evaluated by using a “normalized grout pressure” based on the depth of the tip of the shaft or the effective overburden pressure. However, in the cases evaluated, the range of most of the normalized pressure values was relatively narrow with only a few extreme values, which does not allow development of firm conclusions on the effect of grout pressure on GIR or TIR values.

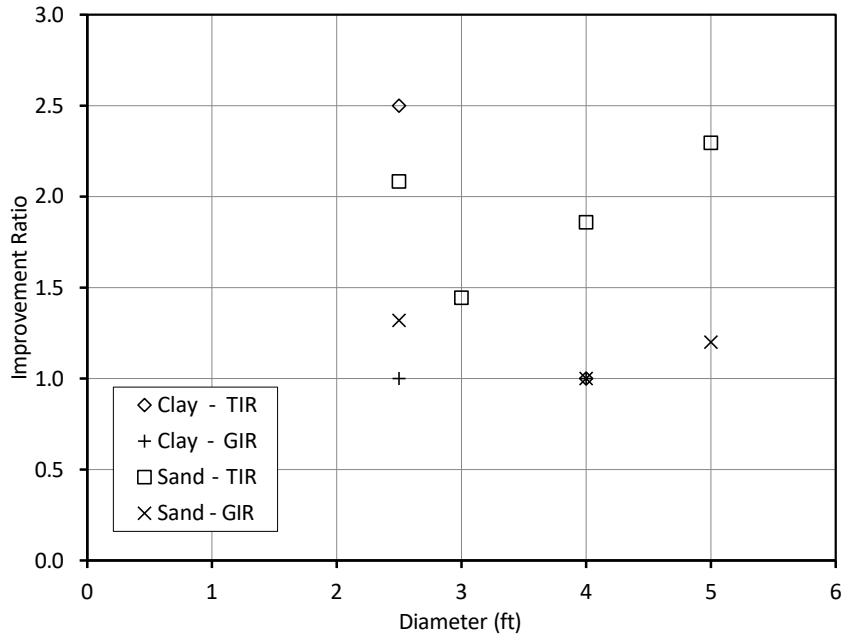


Figure 8.19: Calculated *GIR* and *TIR* for the respective cases plotted as a function of shaft diameter.

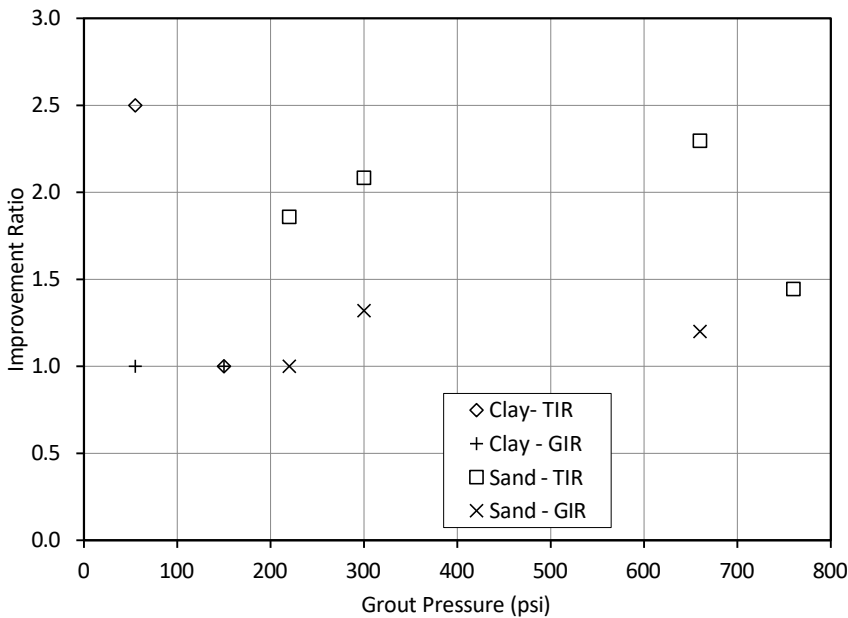


Figure 8.20: Calculated *GIR* and *TIR* for the respective cases plotted as a function of the maximum sustained grout pressure for the respective shafts.

The collective results presented suggest that the improved performance observed from post-grouting for the selected test shafts considered in this chapter can, on average, be predicted by considering pre-mobilization along with a nominal ground improvement ratio of approximately

1.2 applied to the tip resistance estimated for an ungrouted shaft. Similarly, the improved ultimate axial resistance can be predicted, on average, by neglecting pre-mobilization and applying a total improvement ratio of approximately 1.8 to the tip resistance estimated for an ungrouted shaft. The primary advantage of explicitly considering pre-mobilization is that it permits evaluation of the effect of shaft displacement (i.e., serviceability) and the effect of different grout pressures on the expected performance of post-grouted shafts.

8.6 Summary

Results of comprehensive analyses for select cases where similar conventional and post-grouted drilled shafts were load tested were presented in this chapter. The objective of these analyses was to try to separate effects of pre-mobilization from effects of ground improvement at the tip of the shafts. Results of analyses presented in this chapter demonstrate that both pre-mobilization and ground improvement are important components of the improved performance of drilled shafts from post-grouting.

When simulating the performance of PGDS using load-transfer analyses that consider pre-mobilization, the degree of ground improvement can be represented using a “ground improvement ratio,” *GIR*, that reflects improvement in the ultimate unit tip resistance for the soil at the shaft tip. Modeling of pre-mobilization, as described in this chapter, essentially accounts for changes in the stiffness of the load-displacement response of a PGDS and the effect of different grout pressures; simultaneous use of *GIR* accounts for an increase in the ultimate unit tip resistance of a post-grouted shaft. Analyses for the limited number of cases presented in this chapter suggest a mean *GIR* of approximately 1.2 for the cases evaluated for shafts tipped in sands and *GIR* equal to 1.0 for shafts tipped in clays.

The analyses presented also show that the improved performance of drilled shafts from post-grouting can be represented using a “total improvement ratio,” *TIR*, that collectively accounts for improvement from all mechanisms (i.e., from pre-mobilization and ground improvement). Results of analyses presented in this chapter for a limited number of cases suggest a mean *TIR* of approximately 1.8 for shafts tipped in both sands and clays. Values of *TIR* and *GIR* derived from the analyses presented in this chapter were found to be practically independent of shaft size and it was not possible to determine a correlation with grout pressure achieved, because in most cases the ratio of grout pressure to effective overburden stress was similar.

CHAPTER 9: EVALUATION OF PGDS RESISTANCE FROM LOAD TESTS

9.1 Introduction & Methodology

This chapter presents results from evaluation and analysis of an extensive collection of load tests performed on PGDS and comparable ungrouted drilled shafts. The load tests were collected from projects in the U.S., Asia, and Europe. The objectives of the analyses presented in this chapter include: (1) quantifying the total improvement in tip resistance from post-grouting at the shaft tip; (2) identifying how the improvement in tip resistance may vary with different shaft, grouting, and soil characteristics; and (3) comparing predictions of the ultimate resistance for PGDS from several prediction methods to measured resistances from the load tests. The data set considered for the analyses presented in this chapter is substantially larger than that used for the analyses of selected case histories presented in Chapter 8. The analyses therefore focused on the total improvement in tip resistance without differentiating among pre-mobilization, ground improvement and other mechanisms.

The magnitude of improvement due to post-grouting from the individual load tests is quantified using the total improvement ratio (*TIR*) defined in Equation 8.2, where the ultimate unit tip resistances for grouted and ungrouted shafts were established from the load test measurements. Values of *TIR* were sorted by soil type, broadly categorizing each shaft as being tipped in either sand (including gravel), clay (including silt), or rock. For each soil type, several plots of *TIR* were developed to evaluate potential trends with different shaft and grouting parameters.

The ultimate unit tip resistances reported for individual tests were compared to nominal resistances calculated using several available prediction methods presented in Chapter 7. Only selected prediction methods were considered since several require more input parameters than were commonly reported in the literature. Output from the selected prediction methods (e.g., *TCM*, λ_p) generally represents some variation of *TIR*. These parameters are therefore compared to *TIR* as a means to quantify the accuracy and variability of the alternative prediction methods. It is important to note, however, that both *TCM* and λ_p are defined relative to a specific nominal resistance, as described in Chapter 7, rather than relative to the ultimate measured resistance as is the case for the *TIR* values reported in this chapter. *TCM* also varies with the magnitude of shaft displacement, whereas *TIR* is established from the ultimate tip resistance.

9.2 Improvement in Sand from Load Test Results

Fourteen technical papers were identified as having sufficient data to quantify the *TIR* for PGDS tipped in sand. These papers included load test data from post-grouted shafts and comparable ungrouted shafts located some distance away at the same site or located next to the post-grouted shaft. In some cases, the ungrouted shaft was tested, then grouted and retested. The latter category of tests introduces additional uncertainty into interpretation of improvement because reloading may provide benefits separate from the effects of grouting. Analysis of the 14 papers resulted in 40 calculated values of *TIR* for shafts tipped in sand, eight of which are from analyses presented in Chapter 8. Only three of the *TIR* values were for shafts that were tested, grouted, and then re-tested.

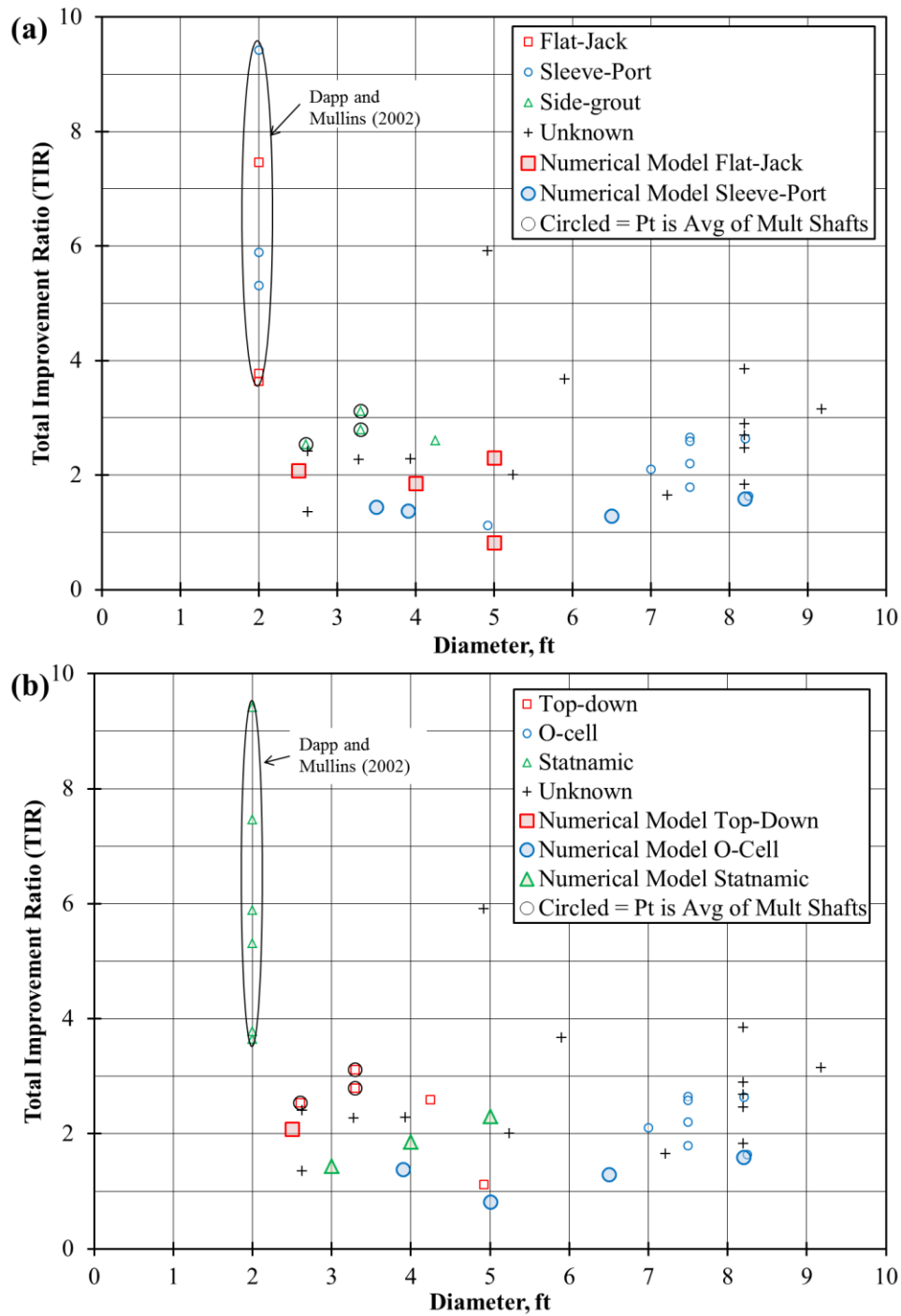
Results of the analysis to evaluate total improvement in sand are summarized with the statistics presented in Table 9.1. The results indicate the ultimate tip resistance is improved by a factor between 2 and 3 on average, but this factor is rather variable with a coefficient of variation around 0.5. A second set of statistics, also shown in the table, excludes the results from Dapp and Mullins (2002). Measurements for those six shafts are not in question, but site conditions (four shafts in a shelly sand, with relatively low blow counts at the tip) and the small diameter of the shafts resulted in low ungrouted tip capacities. Any of these factors might qualify those shafts as a “special case.” The third set of statistics in Table 9.1 also excludes results provided in Dai et al. (2011). Dai et al. (2011) includes a table of tip resistances for a collection of ungrouted and post-grouted shafts installed for various projects completed in Asia. However, the reference does not specifically discuss any of the projects individually, and it is not clear if the tip resistances for ungrouted shafts are from load tests or predictions. Excluding these results and those of Dapp and Mullins (2002) results in a smaller average value of *TIR*, 2.0, and a smaller coefficient of variation, 0.3.

Table 9.1: Summary of *TIR* for drilled shafts tipped and post-grouted in sand.

	All References	Excluding Dapp and Mullins (2002)	Excluding Dapp et al. (2002) and Dai et al. (2011)
Number of Data Points	40	34	20
Range of <i>TIR</i>	0.82 to 9.42	0.82 to 5.91	0.82 to 3.11
Average Value of <i>TIR</i>	2.86	2.32	2.03
Standard Deviation of <i>TIR</i>	1.75	0.94	0.63
Coefficient of Variation of <i>TIR</i>	0.61	0.41	0.31

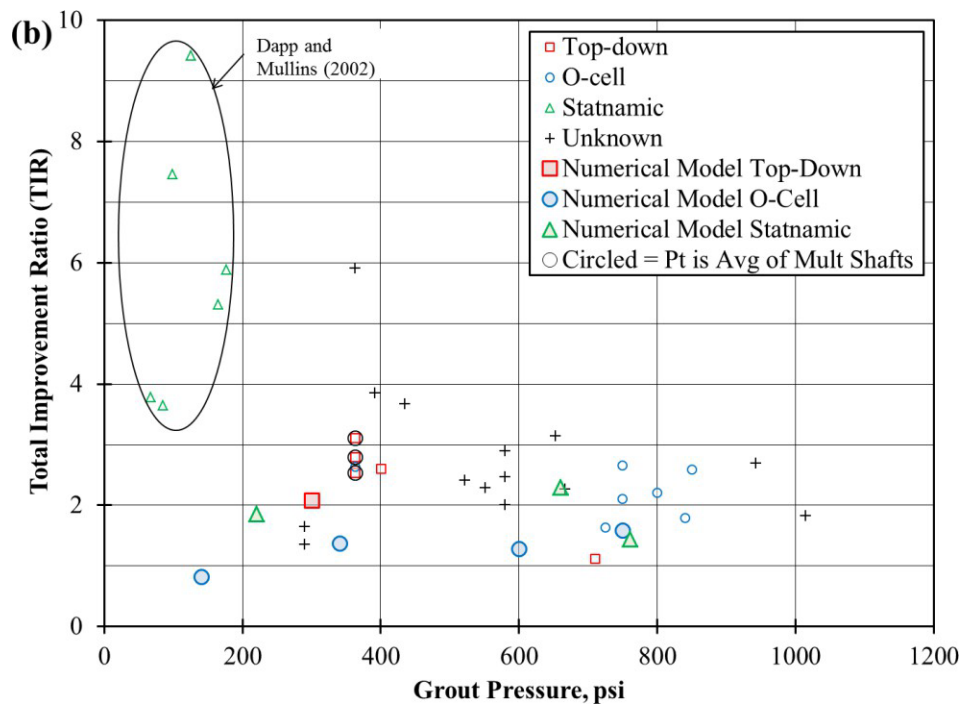
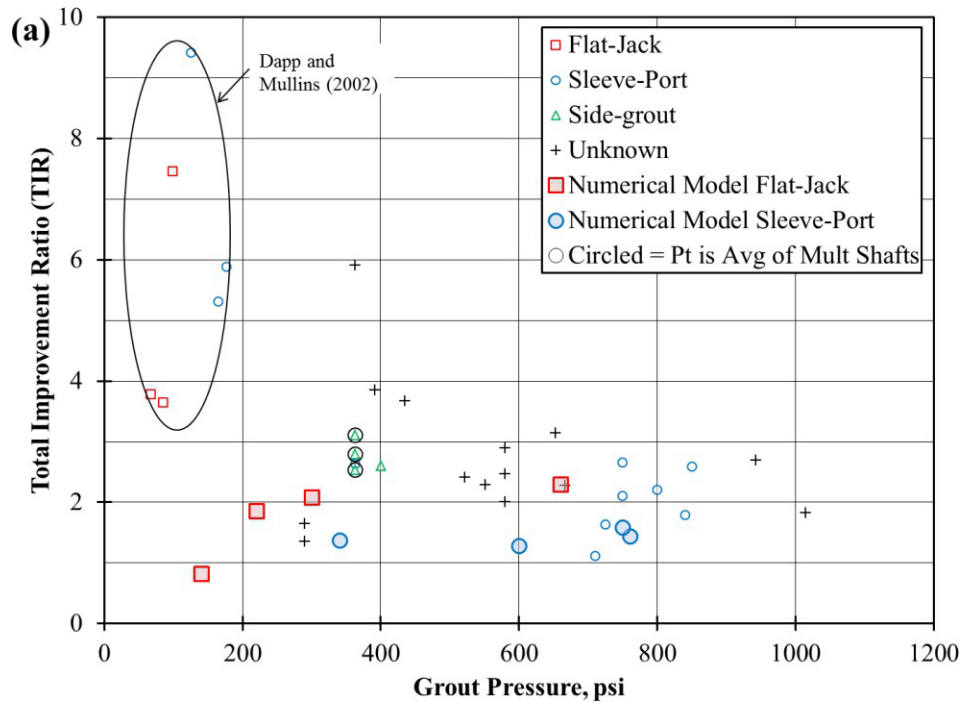
Several graphs of *TIR* in sand were created to identify potential trends with shaft, grouting, or load testing variables. The resulting plots are presented in Figures 9.1 and 9.2. Figure 9.1 plots *TIR* against shaft diameter, and Figure 9.2 plots *TIR* against the reported maximum grout pressure. Two plots are included in each figure. The data points are the same within each of the graphs, but the data point symbols have different meanings in each plot (as shown in respective legends) to identify different categorical variables: (a) grouting apparatus, and (b) type of load test. The publications discussed above and excluded in Table 9.1 are included in Figures 9.1 and 9.2, but are readily identified. The group of points from Dapp et al. (2002) is circled and identified, and the vast majority of the points in the “unknown” category (indicated with “+” symbols) are taken from Dai et al. (2011).

There does not appear to be any trend in *TIR* in sand with diameter, as shown by the plots in Figure 9.1. The *TIR* values derived from the load test measurements mostly fall between values of 1 and 3, consistent with Table 9.1. Figure 9.2 similarly suggests there is no clear trend in *TIR* with grout pressure. Figures 9.1 and 9.2 also suggest the data from Dapp and Mullins (2002) might qualify as a special case (as explained above) since the data points are far removed from the other points.



Note: Larger symbols used for cases considered in Chapter 8.

Figure 9.1: TIR vs. diameter for shafts tipped in sand, plotted according to: (a) grouting apparatus, and (b) load test type.



Note: Larger symbols used for cases considered in Chapter 8.

Figure 9.2: TIR vs. grout pressure for shafts tipped in sand, plotted according to: (a) grouting apparatus, and (b) load test type.

It is important to note that direct comparison of TIR values to grout pressure is not likely a suitable indicator of the improvement of performance due to post-grouting. The magnitude of grout pressure required to exert any type of influence on the ground structure is likely larger at

greater depth or greater overburden pressure. In the tests examined, a significant portion of the tests showed a narrow range of the ratio between grout pressure and depth or between grout pressure and effective overburden pressure. Only a few tests had significantly larger or smaller ratios. Therefore, it is not possible at this time to conclude on the effect of grout pressure on improved shaft performance.

No significant conclusions can be drawn regarding grouting apparatus for shafts tipped in sand (Figures 9.1a and 9.2a), since relatively few of the shafts were grouted using flat-jack devices, and the grouting apparatus used is unknown for many of the tests. The six shafts with side grouting had slightly higher values of *TIR* than average; four of the six were tip-grouted using drill-and-grout techniques. Like the flat-jack, both the side grout and drill-and-grout samples are too small to develop any strong conclusions. It is also difficult to draw any conclusions regarding the influence of the load test type in sand (Figures 9.1b and 9.2b) because of the relatively significant number of shafts for which the test type was unknown, and because of the prevalence of O-Cell testing, particularly for large diameter (high capacity) shafts. There does appear to be some tendency for measurements from O-Cell tests to fall at the lower end of the range of *TIR*; however, the scatter in the measurements is substantial enough to make it difficult to establish whether this is a true trend or simply a result of scatter in the measurements.

9.3 Improvement in Clay from Load Test Results

Six technical papers were identified as having sufficient data to quantify the total improvement ratio for drilled shafts tipped and post-grouted in clay. Results from these papers included load test data from post-grouted shafts and from ungrouted shafts located some distance away at the same site, located next to the post-grouted shaft, or from tests on the same shaft performed prior to post-grouting. Analysis of the six papers resulted in 27 values of *TIR* for shafts tipped in clay, two of which were considered in Chapter 8. Only two of the *TIR* values are from shafts that were tested, grouted, and then re-tested.

Two shafts had *TIR* values that far exceeded the other observations (*TIR* values of 27 and 11 vs. an average of 2.7 for all other shafts), as shown in Figure 9.3. The two shafts with large values of *TIR* were documented in a summary table in Dai et al. (2011) with few grouting or testing details, but both shafts correspond to cases with exceptionally high values of *GPI* (18 and 11) compared with an average *GPI* of 2 for all other shafts. Achieving a grout pressure equal to 18 times the ungrouted tip capacity is at least unusual, so results for these two shafts are omitted from the remaining interpretations in this section.

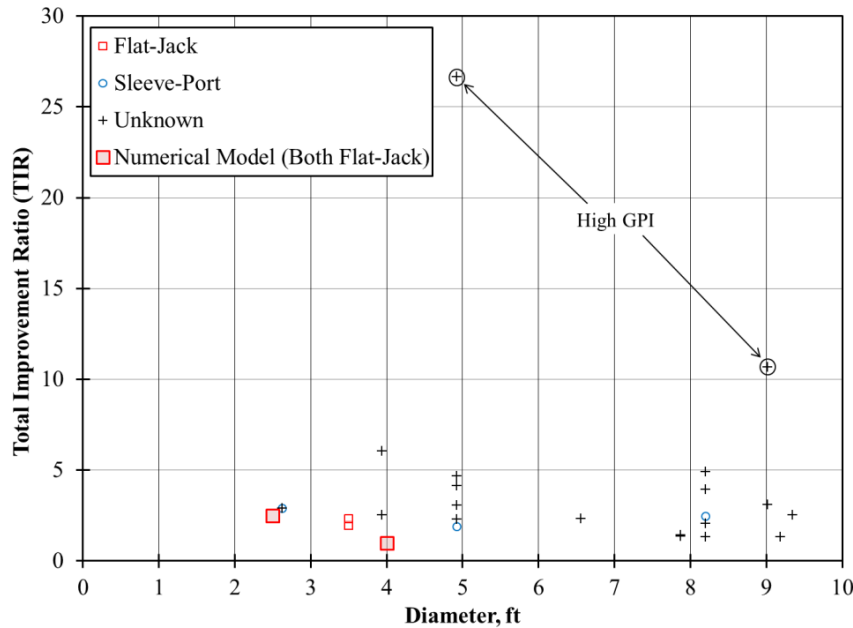


Figure 9.3: *TIR* vs. diameter for shaft tipped in clay, including two points with exceptionally high values for the grout pressure index (*GPI*).

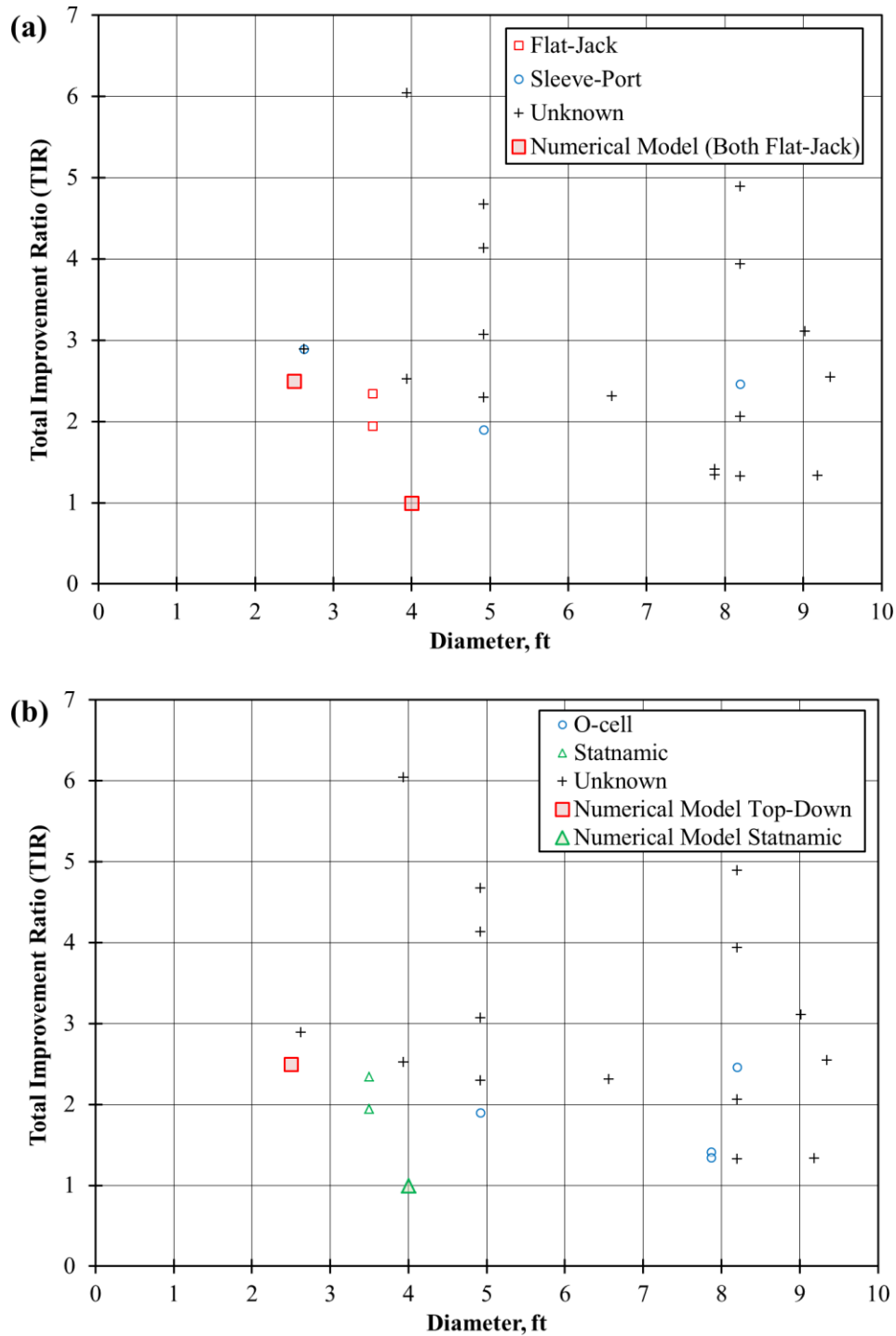
Results of the analysis to evaluate the total improvement for shafts tipped in clay are summarized with the statistics presented in Table 9.2. The results, excluding the two outlying points, indicate that post-grouting improves the ultimate tip resistance in clay by a factor near 2.7, but that this factor is rather variable, with a coefficient of variation near 0.5. The third set of statistics in Table 9.2 also excludes all results from Dai et al. (2011) for the same reasons discussed in the previous section. Excluding the results from Dai et al. (2011) produces a smaller average value of *TIR*, 2.0, and also a smaller coefficient of variation, 0.3. The statistics from Table 9.1 for shafts tipped in sand are repeated in Table 9.2 for comparison, which reveals that *TIR* values for shafts tipped in clay and sand are quite similar if results from Dai et al. (2011) are excluded.

Table 9.2: Summary of *TIR* analysis of drilled shafts tipped and post-grouted in clay and sand.

	Clay			Sand
	All Data Points	Excluding Shafts with High <i>GPI</i>	Excluding High <i>GPI</i> and Dai et al. (2011)	Excl. Dapp et al. (2002) and Dai et al. (2011)
Number of Data Points	27	25	10	20
Range of <i>TIR</i>	1.00 to 26.7	1.00 to 6.04	1.00 to 2.89	0.82 to 3.11
Average Value of <i>TIR</i>	3.86	2.67	1.97	2.03
Standard Deviation of <i>TIR</i>	4.96	1.24	0.59	0.63
Coefficient of Variation of <i>TIR</i>	1.28	0.46	0.30	0.31

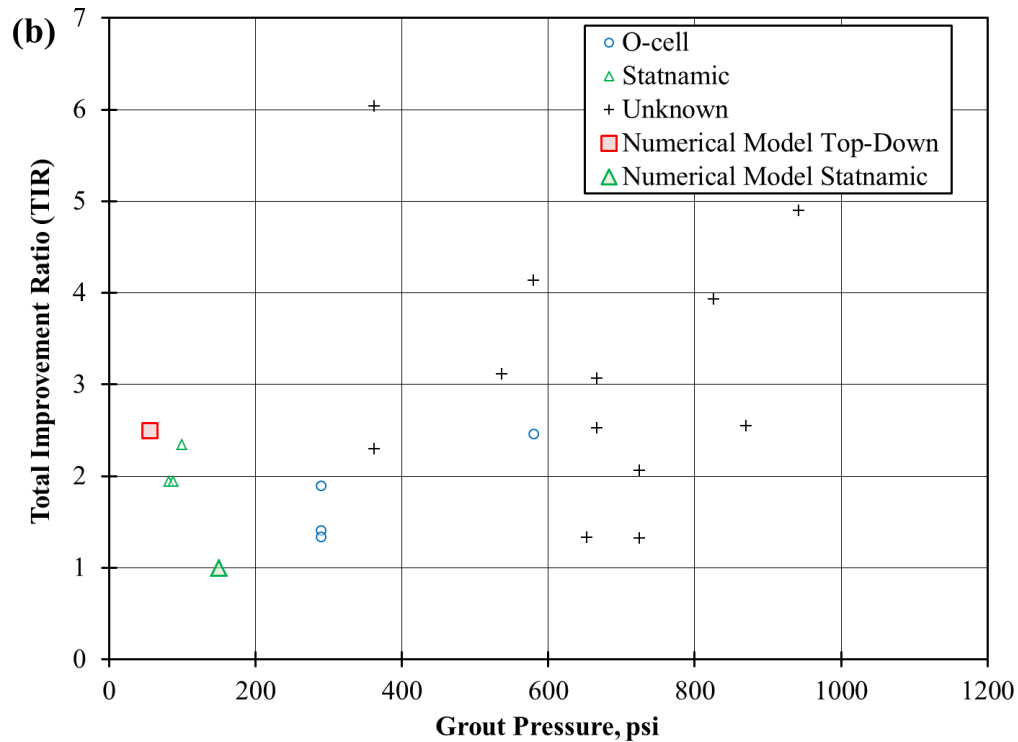
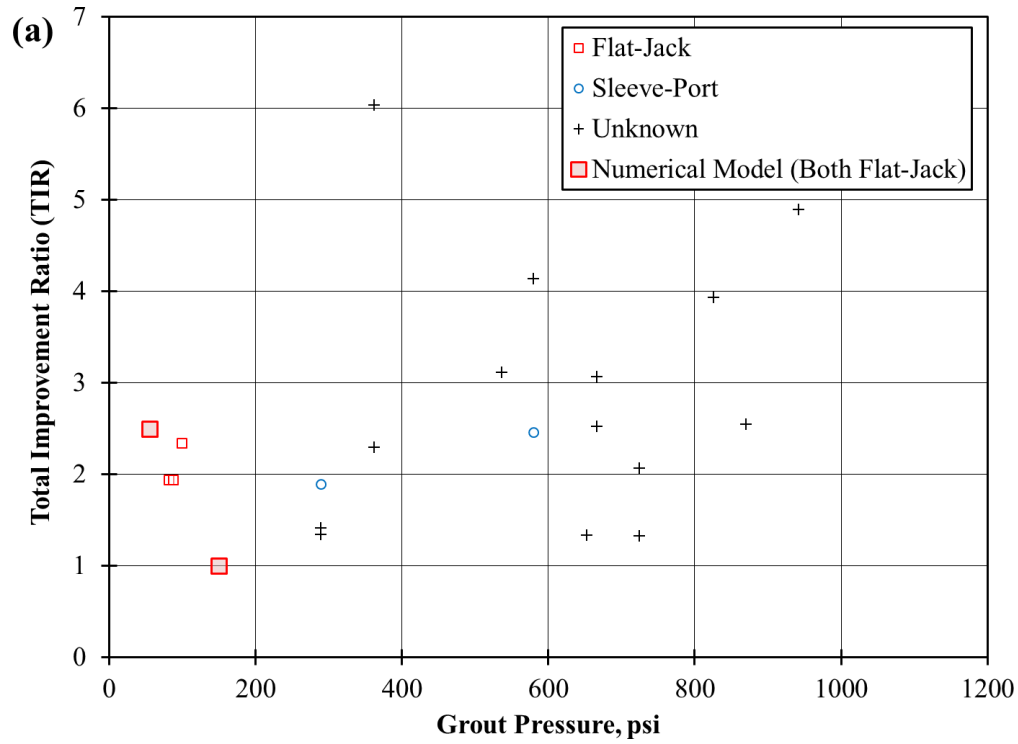
Figures 9.4 and 9.5, respectively, show graphs of *TIR* as a function of shaft diameter and maximum reported grout pressure. Two plots are provided using the same data in each figure,

but the data point symbols reflecting different categorical variables. Results from Dai et al. (2011) are included in Figures 9.4 and 9.5, and are readily identified as being the vast majority of points in the “unknown” category (indicated with “+” symbols).



Note: Larger symbols used for cases considered in Chapter 8.

Figure 9.4: TIR vs. diameter for shafts tipped in clay, plotted according to: (a) grouting apparatus, and (b) load test type.



Note: Larger symbols used for cases considered in Chapter 8.

Figure 9.5: *TIR* vs. grout pressure for shafts tipped in clay, plotted according to: (a) grouting apparatus, and (b) load test type.

As was observed for shafts tipped in sand, there is no evidence of any trend in *TIR* with shaft diameter for shafts tipped in clay, as shown by the graphs in Figure 9.4. *TIR* values mostly fall between 1 and 3.5, which are consistent with what is reported in Table 9.2. Figure 9.5 suggests a potential relationship between *TIR* and grout pressure, but the scatter present is relatively large. As discussed in the previous section, direct comparison of *TIR* values to grout pressure without consideration to overburden pressure is not likely a reliable indicator of the influence of grout pressure on improved shaft performance. No significant conclusions can be drawn regarding the effect of grouting apparatus or load test method from Figures 9.4 and 9.5.

9.4 Improvement in Rock from Load Test Results

Few cases with sufficient data were identified for PGDS tipped in rock. For the cases identified with shafts tipped in rock, none of the load tests reached an ultimate limit state. For instance, Ho (2003) describes a shaft in weak granite that reached a final load of 3,000 kip without reaching failure, corresponding to a *TIR* value of at least 1.44. Nevertheless, four technical papers that were reviewed (Ho, 2003; Kim et al., 2011; Lin et al., 2000; and Kwon et al., 2011) offer evidence of similar improvements in performance, as observed for post-grouting in sands and clays, with each calling attention to increased stiffness observed in load-settlement behavior.

9.5 Comparison of Measured and Predicted Tip Resistance

Values of *TIR* presented in Sections 9.2 and 9.3 were also compared to predictions of similar parameters established using several design methods described in Chapter 7 as well as predictions using the mean *TIR* values provided in Sections 9.2 and 9.3. The design methods considered include the *TCM* methods by Mullins et al. (2006) and Dapp and Brown (2010), and the component multiplier method with coefficients proposed by Dai et al. (2011). Each of these methods involves computing or selecting a multiplier (*TCM* or λ_p) that is applied to a nominal unit tip resistance for an ungrouted shaft. These predicted multipliers are compared to values of *TIR* determined from the load test measurements using a “*TCM/TIR* ratio,” which serves as a simple quantity for comparing the predictions and measurements. Values of *TCM/TIR* less than 1.0 indicate that a particular prediction is conservative, while values greater than 1.0 indicate that a prediction is unconservative. Note that the term *TCM/TIR* ratio is used regardless of whether it is calculated using an actual value of *TCM* or using λ_p for the component multiplier method.

The *TCM* methods produce different values of *TCM* depending on the magnitude of the shaft displacement considered. In order to provide consistency among predictions for the different load tests, predictions presented in this chapter were calculated for shaft displacements equal to 5 percent of the shaft diameter. Such displacements are consistent with the definition of failure used in the Reese and O’Neill (1988) methods that serve as the basis for the *TCM* methods, and generally reflect displacements that are often considered to represent “failure” for drilled shafts. However, it is important to note that the actual displacements observed and reported for the different load tests, and thus displacements that correspond to the computed *TIR* value being used for comparison, may be different than those used to establish *TCM*. Nevertheless, use of *TCM* values established at displacements of 5 percent of the shaft diameter does reflect the intended use of the method, without the benefit of knowing the actual displacement that corresponds to the ultimate resistance (as is the case with *TIR*).

GPI values used for the *TCM* methods were calculated using the measured maximum sustained grout pressures and the nominal unit tip resistance predicted from N_{60} according to Reese and O’Neil (1988) when SPT measurements were available. A separate set of comparisons was also made using the measured ultimate unit tip resistance to compute *GPI* since these data were more widely available. Predictions established using the Dapp and Brown (2010) method were made for all values of *GPI*, despite the fact that the method was developed from measurements on PGDS that were grouted using *GPI* between 2 and 3. Tip capacity improvement coefficients (λ_p) for the component multiplier method were taken to be values falling in the middle of the range recommended by Dai et al. (2011) for the particular soil type reported. Since the maximum sustained grout pressure was not reported in all the cases considered, the number of data points presented in subsequent sections is less than was presented in Sections 9.2 and 9.3.

9.6 Comparison of Predictions for Shafts in Sand

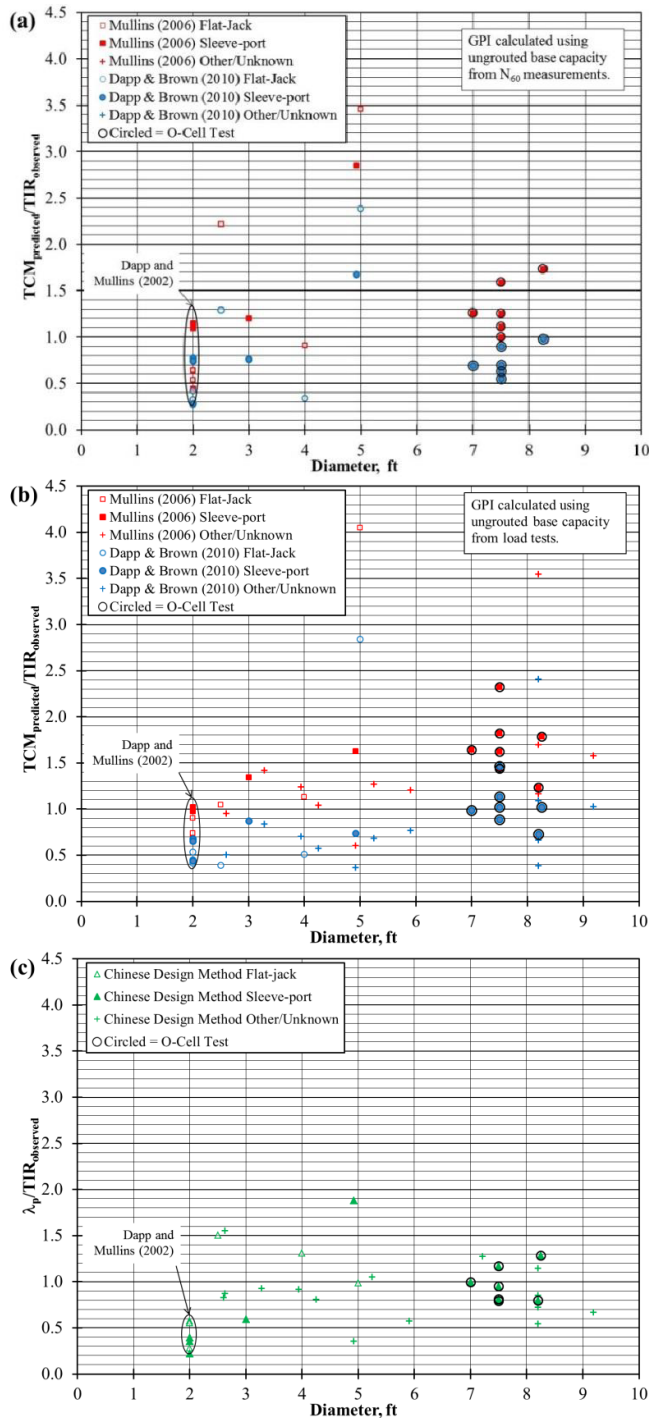
Results of the analysis described above for load tests on shafts tipped in sand are summarized in Table 9.3. The computed ratios of the predicted *TCM* to the observed *TIR* for each method generally span a large range extending from as low as 0.26 to as high as 4.05, which suggests the methods may produce poor predictions for specific shafts. *TCM* estimates from the method by Mullins et al. (2006) are on average unconservative, while the other two published design methods are slightly conservative. This is consistent with Dapp and Brown’s (2010) modification of the *TCM* equation, which produces lower values of *TCM* at large displacements. Use of measured unit tip resistances to calculate *GPI* does not substantially affect the value or variability of *TCM/TIR*. Use of a tip improvement coefficient (λ_p) of 2.1 per Dai et al. (2011) and the average observed *TIR* of 2.03 from Section 9.2 produced similar results, both of which were less variable than either *TCM* method that accounts for displacement and grout pressure.

Table 9.3: Comparison of predictions and measurements for shafts tipped in sand.

	<i>GPI</i> using N_{60}		<i>GPI</i> using Test Data		Dai et al. (2011) $\lambda_p = 2.1$	<i>TIR</i> = 2.03
	Mullins et al. (2006)	Dapp and Brown (2010)	Mullins et al. (2006)	Dapp and Brown (2010)		
Number of Points	17	17	30	30	34	34
Range of <i>TCM/TIR</i>	0.45 – 3.45	0.26 – 2.38	0.60 – 4.05	0.37 – 2.84	0.22 – 1.88	0.22 – 1.82
Average Value of <i>TCM/TIR</i>	1.36	0.81	1.42	0.86	0.86	0.83
Std. Deviation of <i>TCM/TIR</i>	0.82	0.55	0.77	0.55	0.38	0.37
Coeff. of Variation of <i>TCM/TIR</i>	0.60	0.68	0.54	0.64	0.44	0.44

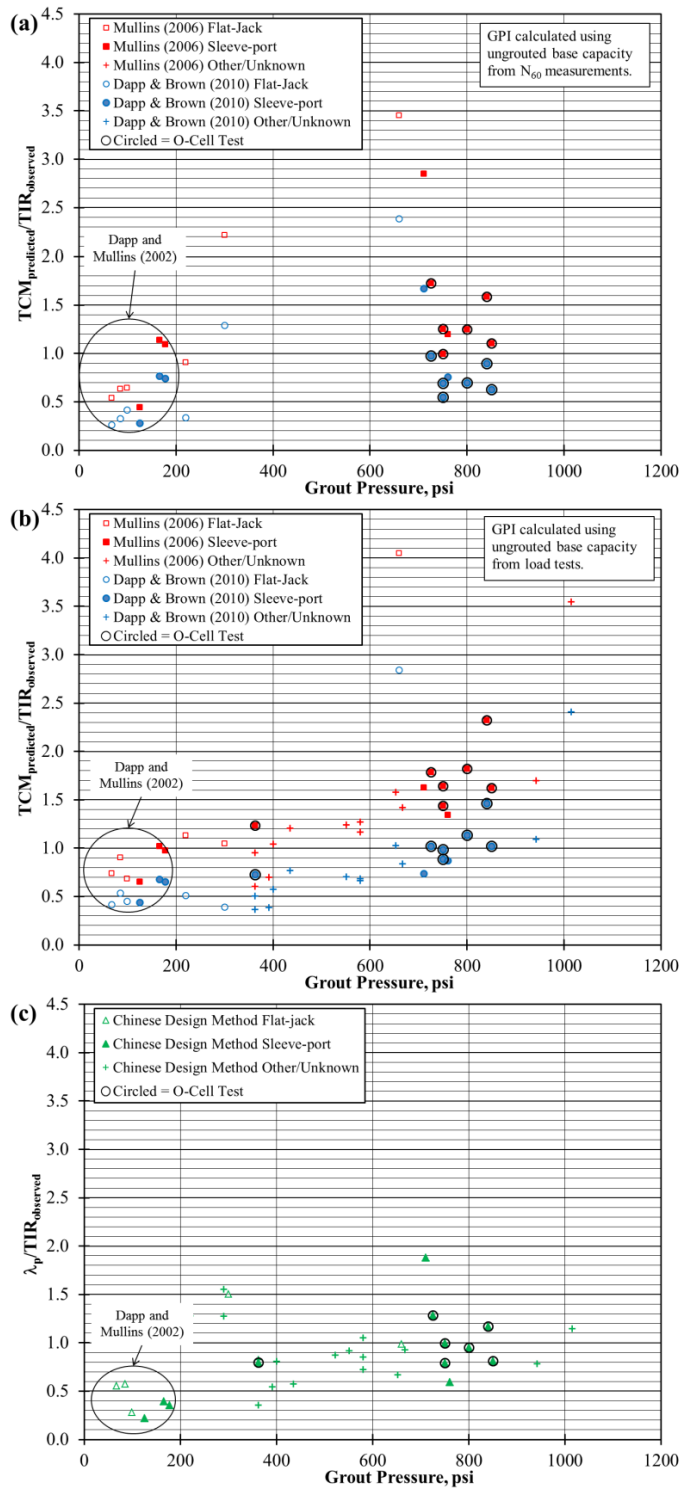
Computed values of *TCM/TIR* are plotted versus shaft diameter in Figure 9.6 and the reported grout pressure in Figure 9.7. Figure 9.6 suggests that the magnitude of *TCM/TIR* increases slightly with increasing shaft diameter, and the variability of *TCM/TIR* clearly increases with

shaft diameter. The value of TCM/TIR also increases with grout pressure, particularly for the TCM methods, perhaps indicating that the methods overstate the effect of grout pressure.



Note: Open symbols reflect use of flat-jack devices; closed symbols reflect use of sleeve-port devices; and cross symbols reflect an unknown grouting apparatus.

Figure 9.6: Ratio of predicted TCM to observed TIR for: (a) TCM using GPI from N_{60} , (b) TCM using GPI from load test measurements, and (c) component multiplier methods vs. diameter for shafts tipped in sand.



Note: Open symbols reflect use of flat-jack devices; closed symbols reflect use of sleeve-port devices; and cross symbols reflect an unknown grouting apparatus.

Figure 9.7: Ratio of predicted TCM to observed TIR for: (a) TCM using GPI from N_{60} , (b) TCM using GPI from load test measurements, and (c) component multiplier methods vs. grout pressure for shafts tipped in sand.

9.7 Comparison of Predictions for Shafts in Clay

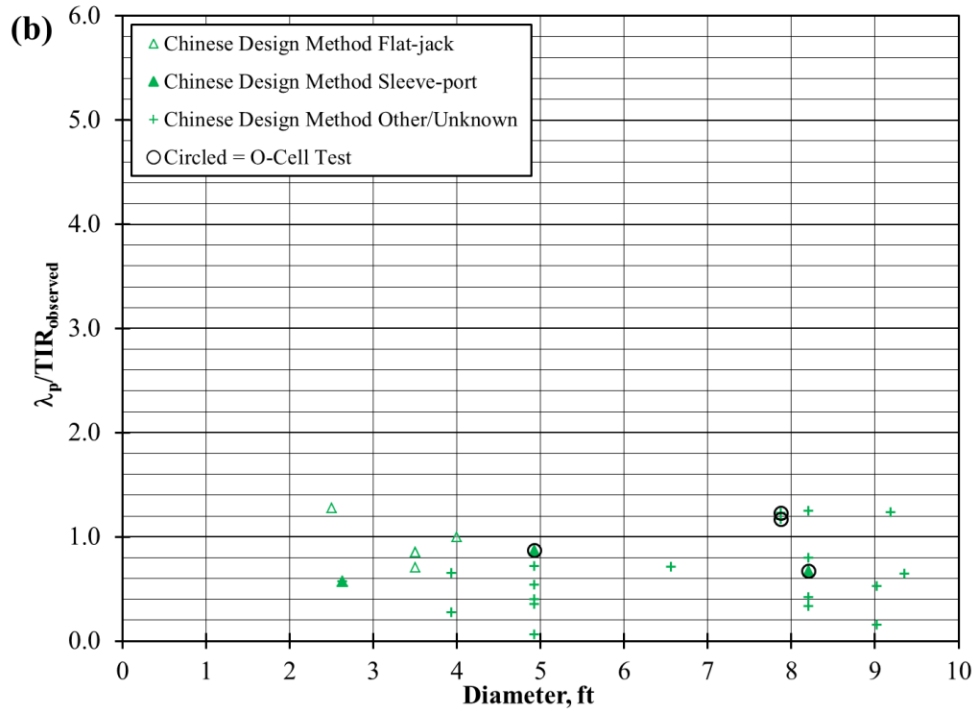
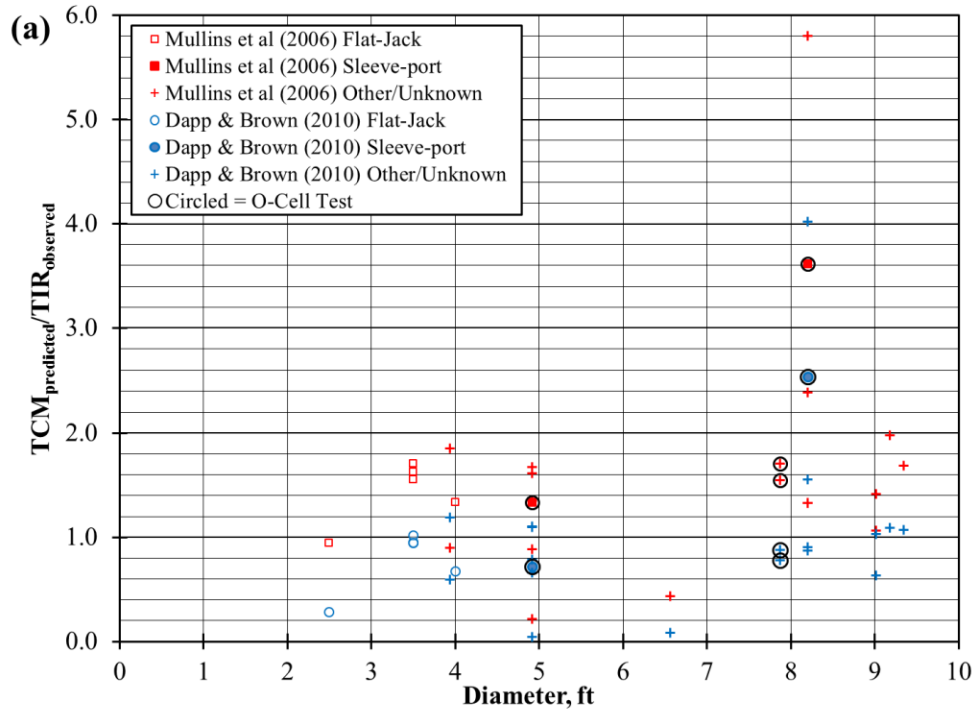
The *TCM* methods were not developed for post-grouted shafts in clay. Nevertheless, similar comparisons were made (using the measured ultimate unit tip resistance to establish the *GPI*) because there are few prediction methods that are appropriate for shafts tipped in clay, and because the *TCM* method has been used for such predictions in practice.

Results of the comparisons for PGDS tipped in clay are summarized in Table 9.4. The ranges of computed *TCM/TIR* ratios in clays are greater than observed for PDGS tipped in sands, extending from as low as 0.04 to as high as 5.80. This observation indicates the poor reliability present when using current design methods that were developed for sands for shafts tipped in clays. The average ratio of predicted *TCM* to observed *TIR* from the method by Mullins et al. (2006) is 1.65, indicating the method overestimates the effect of grouting on average. The average ratio for each of the other methods is nearer to 1 but highly variable, with coefficients of variation of 0.5 and greater. The *TCM* estimate by Dapp and Brown (2010) is on average very near the observed *TIR* but rather variable, with a coefficient of variation near 0.8. Predictions from the component multiplier method using coefficients from Dai et al. (2011) produced the most conservative estimates with the least variability. Predictions based on the average *TIR* value from Section 9.3 (1.97) were also conservative, on average, but less so than for the component multiplier method.

Table 9.4: Comparison of predictions and measurements for shafts tipped in clay.

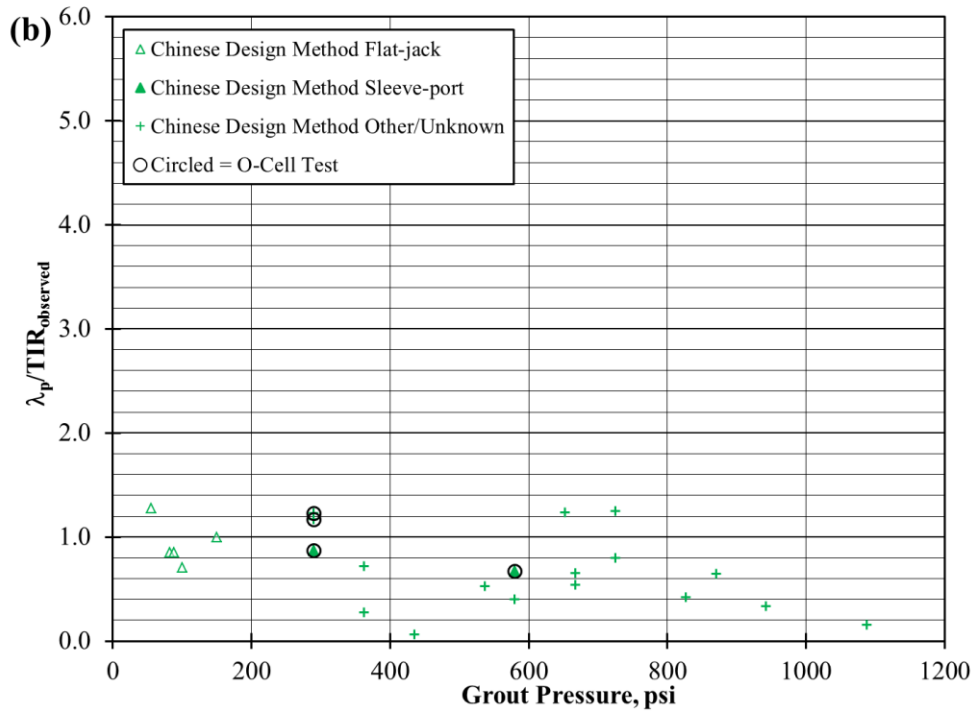
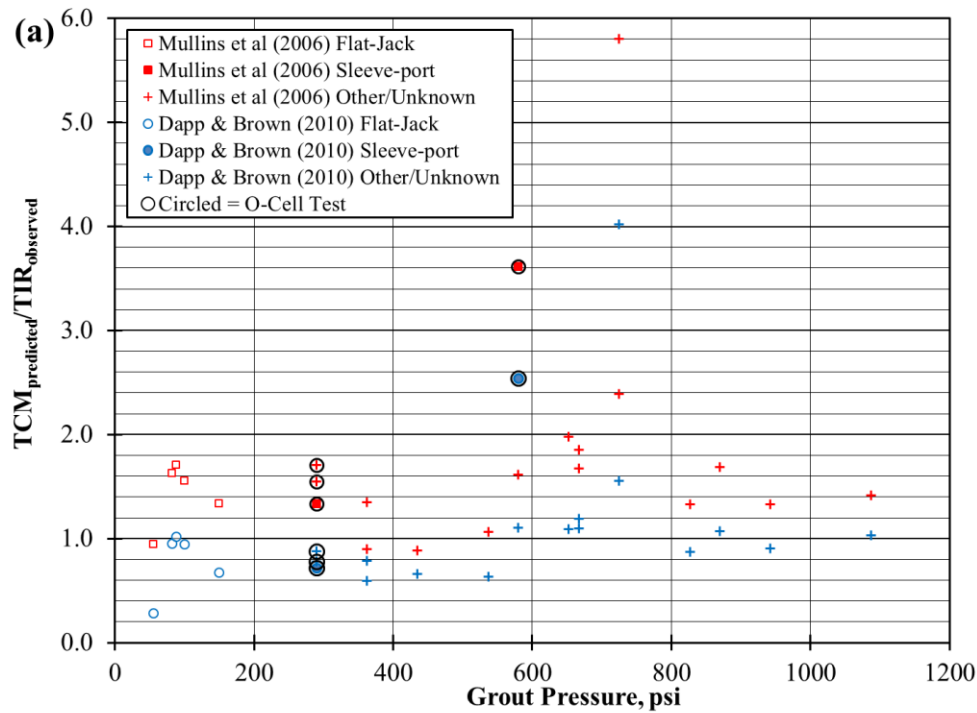
	Mullins et al. (2006)	Dapp and Brown (2010)	Dai et al. (2011) $\lambda_p = 1.65$	<i>TIR</i> = 1.97
Number of Data Points	25	25	27	27
Range of <i>TCM/TIR</i>	0.21 – 5.80	0.04 – 4.02	0.06 – 1.28	0.07 – 1.53
Average Value of <i>TCM/TIR</i>	1.65	1.02	0.70	0.83
Std. Dev. of <i>TCM/TIR</i>	1.08	0.79	0.34	0.41
Coeff. of Var. of <i>TCM/TIR</i>	0.65	0.77	0.49	0.49

Computed values of *TCM/TIR* for shafts tipped in clay are plotted versus shaft diameter in Figure 9.8 and grout pressure in Figure 9.9. As observed for shafts in sand, the figures indicate increasing magnitude and variability of *TCM/TIR* with increasing shaft diameter and increasing grout pressure for the *TCM* methods, whereas the magnitude and variability of *TCM/TIR* for the component multiplier method are largely independent of shaft diameter and grout pressure.



Note: Open symbols reflect use of flat-jack devices; closed symbols reflect use of sleeve-port devices; and cross symbols reflect an unknown grouting apparatus.

Figure 9.8: Ratio of predicted TCM to observed TIR for: (a) TCM using GPI from load test measurements, and (b) component multiplier methods vs. shaft diameter for shafts tipped in clay.



Note: Open symbols reflect use of flat-jack devices; closed symbols reflect use of sleeve-port devices; and cross symbols reflect an unknown grouting apparatus.

Figure 9.9: Ratio of predicted *TCM* to observed *TIR* for: (a) *TCM* using *GPI* from load test measurements, and (b) component multiplier methods vs. maximum reported grout pressure for shafts tipped in clay.

9.8 Summary and Implications

Analysis of *TIR* established from a collection of load test measurements for comparable grouted and ungrouted drilled shafts resulted in several significant observations regarding the magnitude and variability of improvements due to post-grouting, and regarding factors that affect the improvement attributed to post-grouting. These observations supplement the observations regarding both pre-mobilization and ground improvement from Chapter 8.

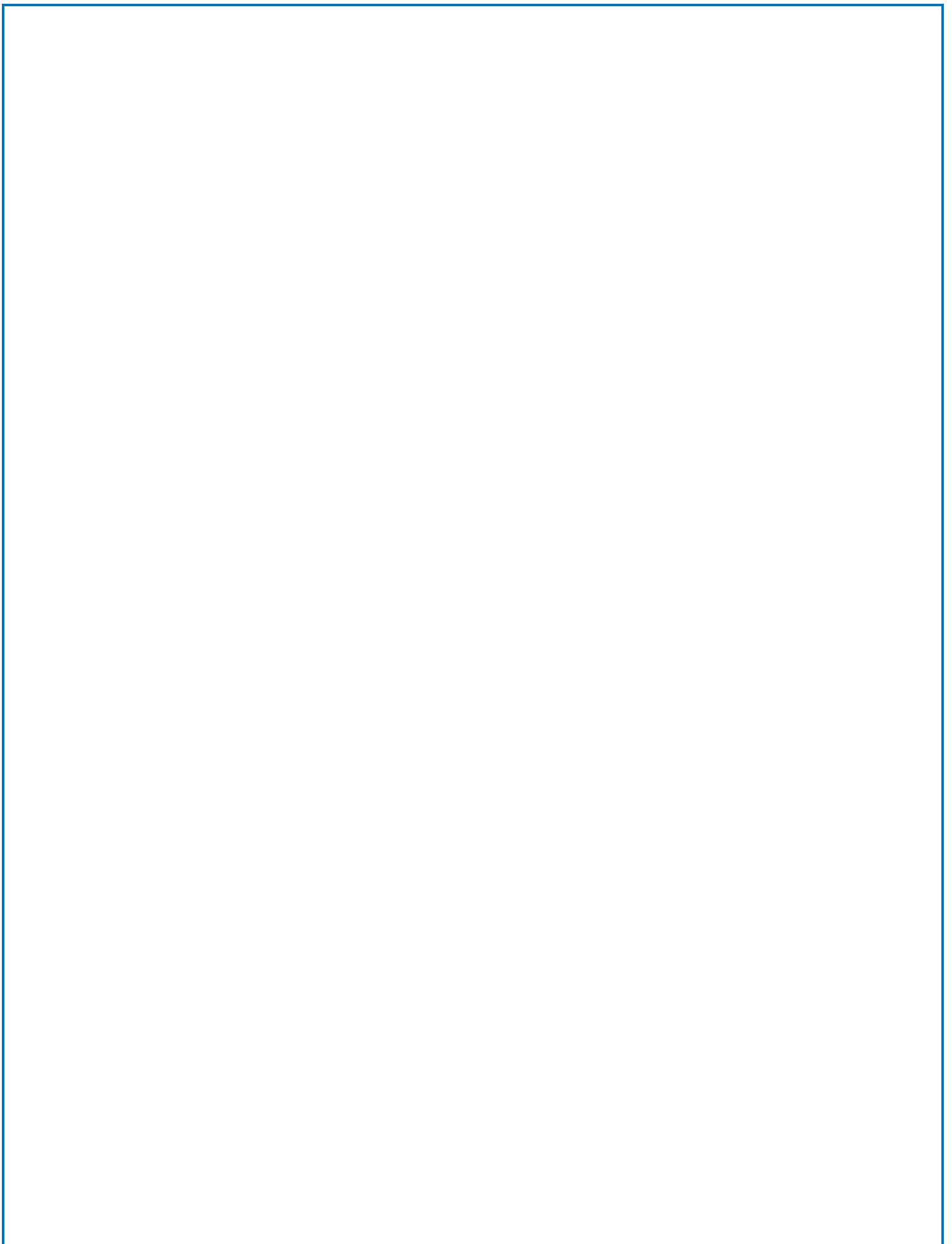
- The observed value of *TIR* appears to be similar for shafts tipped in both sands and clays, typically falling between 1.0 and 3.0 and with an average value slightly less than 2.0.
- The variability of *TIR* is large, with coefficients of variation in sand and clay exceeding 0.3.
- The observed value of *TIR* is largely independent of shaft diameter.
- The relationship between grout pressure and *TIR* for shafts tipped in sand is unclear.
- More load test measurements are needed to quantify the effect of grout pressure for varying depths, grouting apparatus and the effect of load test method on *TIR*.

Methods for predicting the nominal unit tip resistance for PGDS were evaluated by comparing computed values of *TCM* (or equivalent) from each method to values of *TIR* established from the load test measurements. Results of these analyses led to several notable observations:

- The average ratio of predicted ground improvement (*TCM*) to observed ground improvement (*TIR*) was near 1.0 for most methods, indicating the methods produce reasonable predictions for the improvement in unit tip resistance, on average. However, the accuracy of the prediction methods was quite variable, with coefficients of variation of the ratio of predicted to observed improvement exceeding 0.5.
- For shafts tipped in sands, prediction methods that simply factor the nominal unit tip resistance without consideration of grout pressure or displacement (the component multiplier method and using the average *TIR* value from the load test measurements) were as accurate and less variable than *TCM* methods that account for grout pressure and shaft displacement.
- The ratio of *TCM* to *TIR* for shafts tipped in sand appeared to increase with grout pressure for both *TCM* methods (Mullins et al., 2006; and Dapp and Brown, 2010), perhaps indicating the methods overstate the effect of grout pressure.
- For shafts tipped in clay, the *TCM* method by Dapp and Brown (2010) was more accurate than the other methods, on average, but the component multiplier methods and predictions using the average value of *TIR* from the load test measurements considered were less variable and more conservative.
- On average, the ultimate unit tip resistance for PGDS is approximately 2 times greater than the ultimate unit tip resistance for a comparable ungrouted shaft, but this factor varies widely.

Collectively, the findings presented in this chapter clearly demonstrate that post-grouting can be used to improve the resistance for drilled shafts in all kinds of geomaterials. However, currently available design methods do not appear to predict performance with sufficient reliability to permit their use without confirmation from site-specific load tests. Current design methods can

be used to estimate the magnitude of improvement that may be expected, and to develop preliminary shaft designs, but should be accompanied by load testing programs developed to demonstrate that the anticipated capacity can actually be achieved.



CHAPTER 10: LOAD TESTS TO EVALUATE IMPROVEMENT DUE TO PRE-MOBILIZATION

10.1 Introduction

The work presented in previous chapters of this report provides strong evidence that pre-mobilization produces a substantial portion of improvement observed due to post-grouting. However, questions remain regarding whether loads induced during grouting and subsequent top-down loading are consistent with that predicted using load transfer analyses, and whether pre-mobilization loading will produce the improved performance predicted from analyses. To address these questions, a dedicated field load test program was completed to evaluate improvement specifically due to pre-mobilization, as described in this chapter.

10.2 Field Load Test Program

The primary objective of the load test program was to isolate and evaluate improvement due to pre-mobilization. The load test program was therefore designed to minimize improvement that could result from ground improvement beneath the tip of the shafts, from tip enlargement, or from increased side resistance so that pre-mobilization could be accurately isolated. The program also required top-down load tests since improvement due to pre-mobilization arises from reversal of the loading direction between loading from post-grouting and subsequent top-down loading. Details of the load testing program are described in this section.

10.2.1 Site Conditions and Test Shafts

The load tests were conducted at the National Geotechnical Experiment Site (NGES) at Texas A&M University. Tests were conducted at the “clay site” that is predominantly composed of relatively stiff, overconsolidated clay. Figure 10.1 shows the general stratigraphy at the site with a schematic of the test shafts. The undrained shear strength of the clay is relatively uniform and approximately equal to 2300 psf (Briaud, 1997). A 2- to 3-ft thick sand layer is present at a depth of approximately 18 ft. The clay site was selected because the stiff clay is unlikely to be subject to significant ground improvement from grouting so that observed improvement in shaft response to top-down loading is expected to be due to pre-mobilization.

Five test shafts were installed and tested as part of the load test program. All test shafts were practically identical 36-inch diameter shafts extending to a depth of 33 ft below ground surface, as shown in Figure 10.1. All shafts were identically reinforced with eight #8, grade 60 reinforcing bars and identically instrumented with six levels of four vibrating wire strain gages. The only differences among the test shafts were devices placed at the shaft tips for pre-mobilizing bi-directional load prior to top-down load testing. All test shafts were constructed using truck-mounted drilling rigs with conventional auger bits and either bentonite or polymer slurry. The bases of all test shafts were cleaned using a cleanout bucket.

Figure 10.2 shows the layout of the test shafts along with locations for reaction shafts. One test shaft (TS-2) was a conventional shaft with no device at the shaft tip. Two test shafts (TS-1 and TS-3) included conventional Osterberg bi-directional loading cells located at the shaft tips for

mobilizing bi-directional load without the possibility of ground improvement due to grouting (Figure 10.3). One test shaft (TS-4) included a similar RIM Cell device that also allowed bi-directional loading without the possibility of ground improvement from grouting. The final test shaft (TS-5) included a flat jack post-grouting device for post-grouting as shown in Figure 10.3.

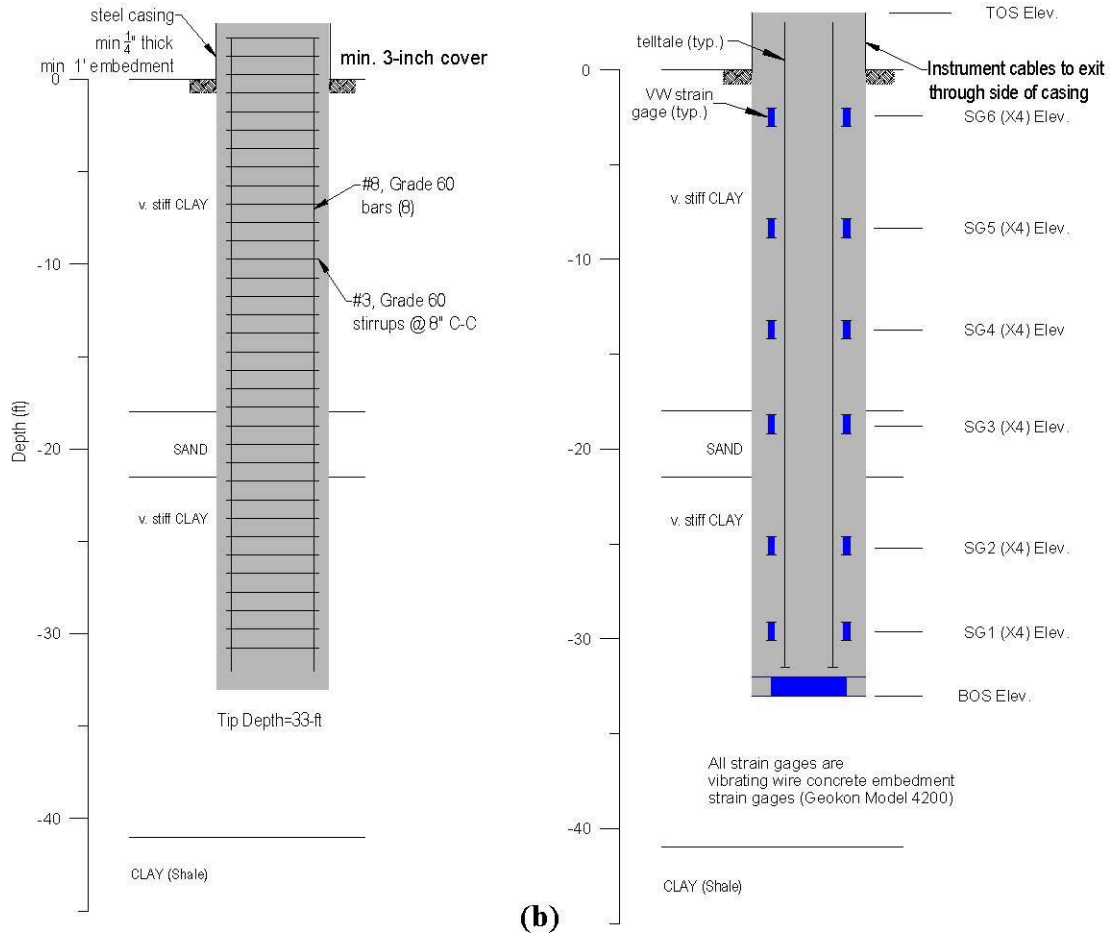


Figure 10.1: Test site stratigraphy: (a) test shafts, and (b) instrumentation.

Top-down static load tests were performed on each shaft using the “Acosta” reaction system provided by the Florida Department of Transportation. The Acosta system uses a set of four reaction girders in a crossed arrangement with four reaction shafts. Reaction shafts were 30-inch diameter shafts reinforced with a single 2.5-inch diameter, high strength steel DWIDAG bar. All shafts were spaced at 18 ft center to center.

10.2.2 Pre-mobilization Loading

All test shafts except for the conventional test shaft (TS-2) were subjected to bi-directional loading at the shaft tip to induce pre-mobilized load in the test shafts prior to subsequent top-down loading. Test Shafts TS-1 and TS-3 were loaded bi-directionally following conventional O-Cell loading procedures prior to being grouted under low pressure for subsequent top-down testing. During loading, both Test Shafts TS-1 and TS-3 experienced substantial displacement of the O-Cell at pressures that were substantially less than anticipated, and substantially less than

bi-directional loads applied for other test shafts. This observation likely resulted from failure to get concrete to adequately flow around the O-Cell and fill the space beneath the O-Cell during construction. As a result, the maximum induced bi-directional load in both shafts was substantially less than expected. The maximum bi-directional load applied for Test Shaft TS-1 was 32 kips, while the maximum applied bi-directional load for Test Shaft TS-3 was 54 kips.

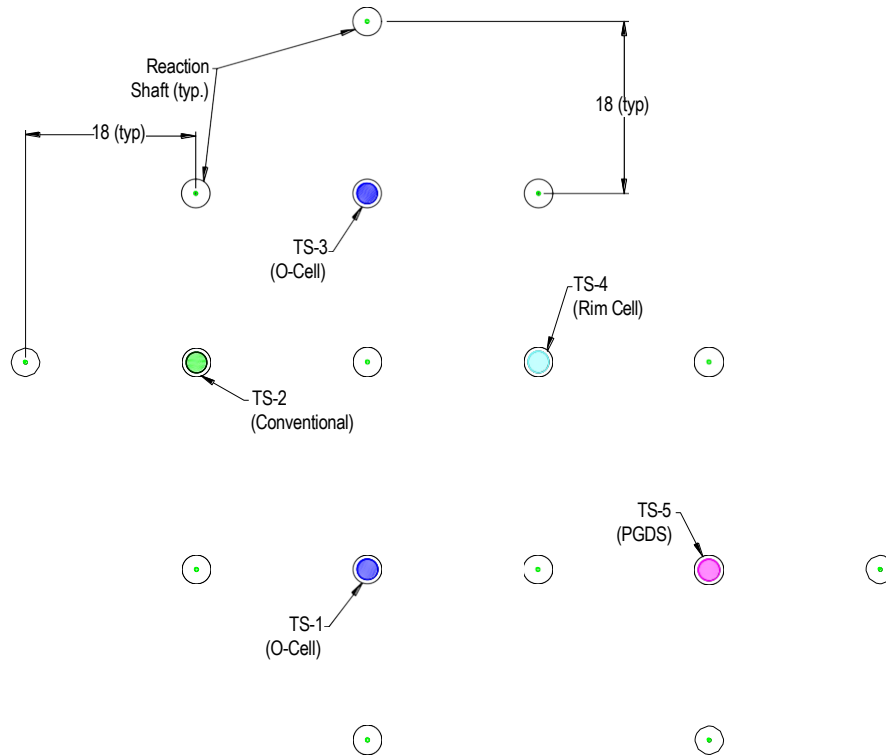


Figure 10.2: Layout of test and reaction shafts.

Test Shaft TS-4 was bi-directionally loaded using neat cement grout as the pressurizing fluid for the RIM Cell device in a manner similar to that commonly adopted for post-grouting. Figure 10.4 shows the applied pressure versus time for TS-4. Figure 10.5 shows the displacement of the top and bottom of the shaft during bi-directional loading. The maximum pressure applied to the RIM Cell device (as measured at the outlet port for the device) was approximately 250 psi, which corresponds to a maximum applied bi-directional load of approximately 120 kips. As shown in Figure 10.5, very little upward movement was observed at the top of the shaft during pre-mobilization loading.

Test Shaft TS-5 was post grouted using neat cement grout with a water to cement ratio of approximately 0.5. Figure 10.6 shows graphs of grout pressure, shaft uplift, and grout volume as suggested by Mullins (2015) during post-grouting of Test Shaft TS-5, as described in Chapter 6. Grouting generally proceeded as desired with gradually and proportionally increasing grout pressure, grout volume, and shaft uplift. The maximum applied grout pressure during post-grouting was approximately 220 psi, which corresponds to a maximum applied bi-directional load of approximately 230 kips. The greater load applied for Test Shaft TS-5 compared to Test Shaft TS-4 occurs because of the greater area of the flat jack device compared to the RIM Cell device. The grouting records shown in Figure 10.6 also indicate that the confining membrane was maintained intact throughout grouting and did not rupture.



Figure 10.3: Bi-directional loading devices: (a) flat jack, (b) RIM Cell, and (c) O-Cell.

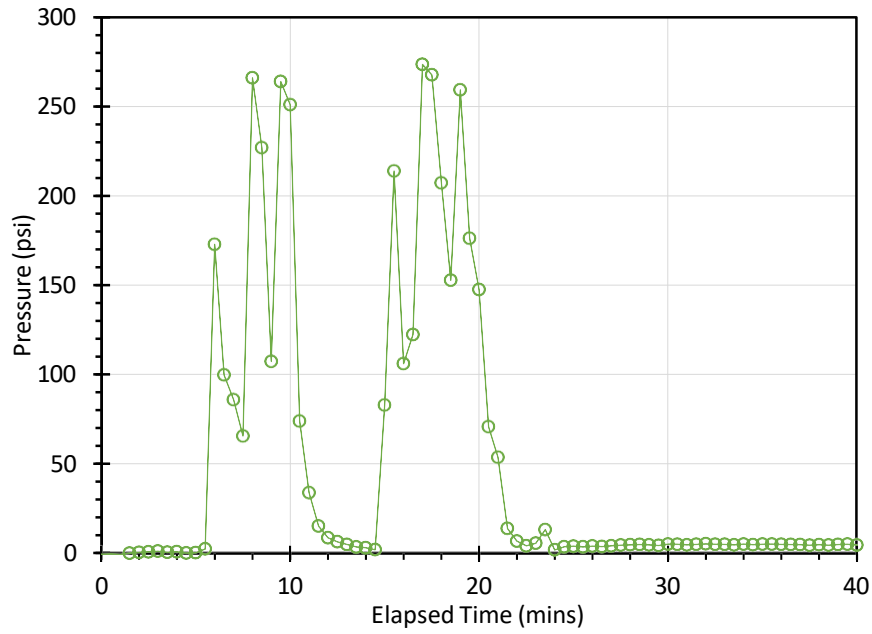


Figure 10.4: Bi-directional loading for TS-4.

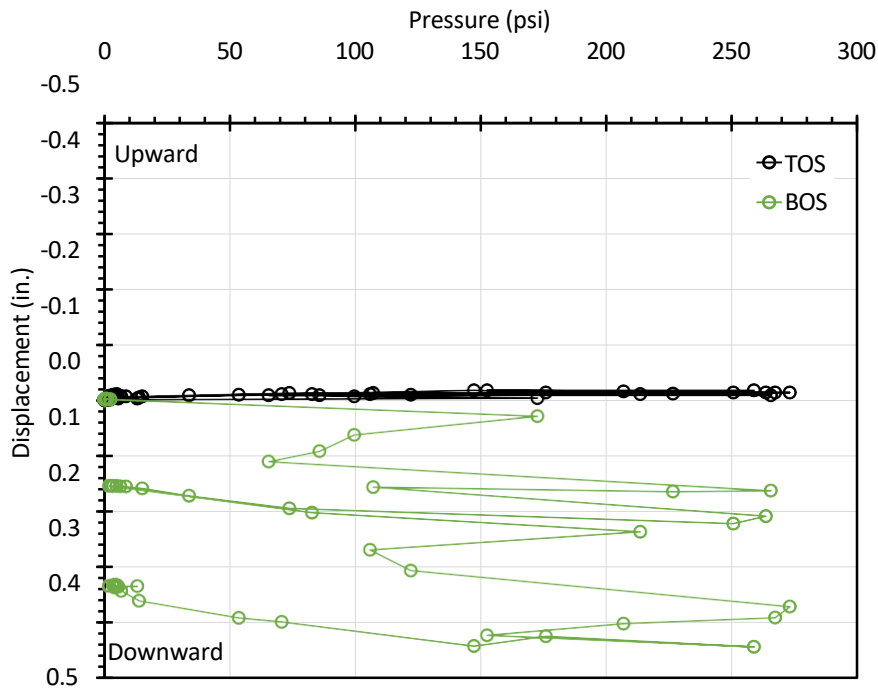


Figure 10.5: RIM Cell pressure versus displacement for TS-4.

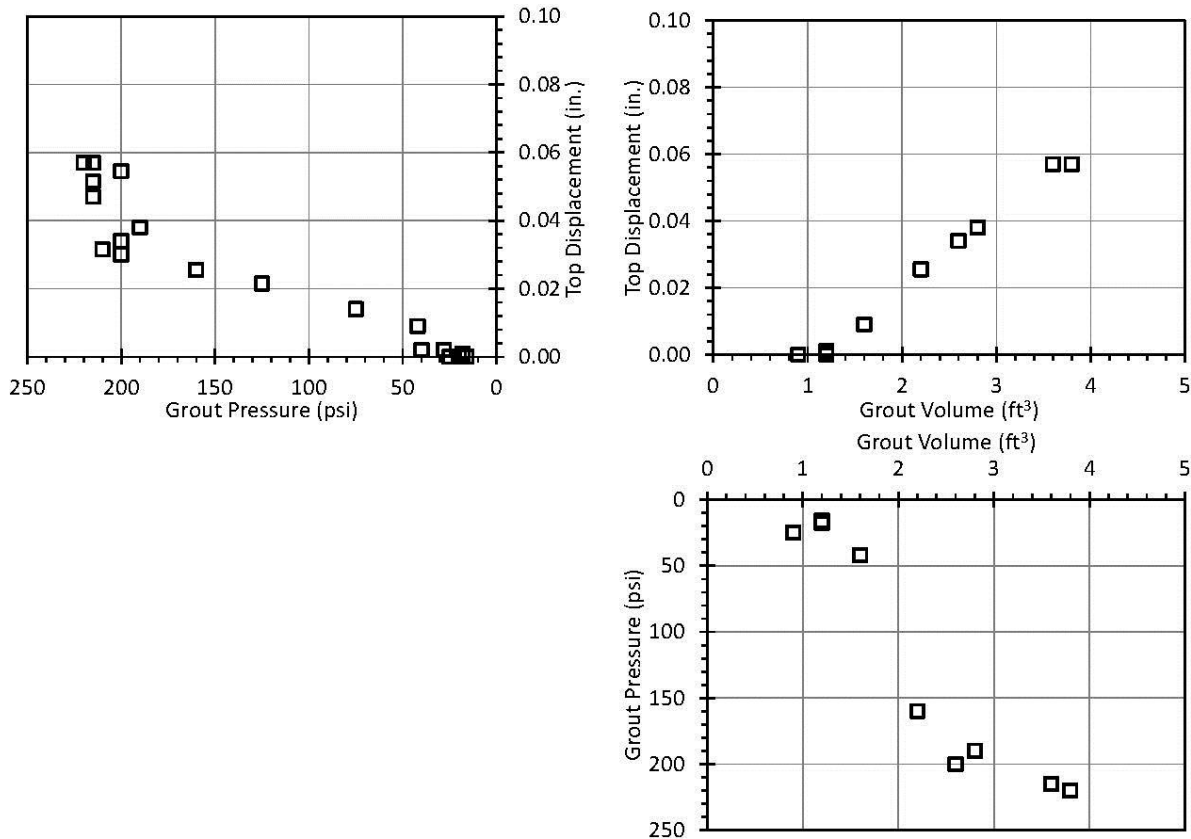


Figure 10.6: QA/QC graphs for post-grouting of Test Shaft TS-5.

10.2.3 Top-Down Loading

All five test shafts were loaded in a top-down manner as shown in Figure 10.7. Top-down loading was generally conducted according to the ASTM “quick test” procedure (ASTM D1143) with 15-minute load increments, with the exception that several load increments for the test performed for Test Shaft TS-2 (the conventional shaft) were maintained for up to 45 minutes. Axial loads were applied in nominal increments of approximately 50 kips (~ 200 psi of hydraulic pressure). The applied axial load was measured using both the hydraulic pressure in the jack and an electronic load cell placed between the jack and reaction frame. Load measurements from the jack hydraulic pressure and the load cell generally differed by less than 2 percent throughout testing. Displacement of the top of the shafts was measured using two Leica optical levels that were recorded at 30-second intervals. Readings from all strain gages were also recorded at 30-second intervals. Shaft compression was also measured for Test Shafts TS-2 and TS-5 using two telltales anchored near the shaft tip.



Figure 10.7: Load test setup for top-down loading.

The measured load-settlement response for all tests is shown in Figure 10.8. The loads shown in the legend for Figure 10.8 reflect the magnitude of the maximum bi-directional load applied during pre-mobilization. The load-settlement responses observed for Test Shafts TS-1 and TS-3, both of which included O-Cells and both of which failed at top-down loads just greater than 600 kips, are similar to one another but clearly different from the response observed for the other test shafts. This behavior is attributed to the belief that concrete did not adequately flow beneath the O-Cells in these two shafts, which resulted in the shafts having less tip resistance than predicted for the shafts, or observed for other test shafts. Because of these issues, further interpretation of the load test results was restricted to Test Shafts TS-2 (the conventional shaft), TS-4 (the shaft with the RIM Cell), and TS-5 (the post-grouted shaft). Figure 10.9 shows the load-settlement response for these three test shafts, excluding the two test shafts that are believed to be unrepresentative.

The response shown for the collection of test shafts in Figure 10.9 is consistent with the improvement expected from pre-mobilization as described in Chapters 2 and 8. All three test shafts exhibit similar response for loads up to approximately 400 kips, where side resistance tends to dominate load-settlement response. The load-settlement response for all three shafts also tends to approach a resistance of approximately 800 kips at large displacements suggesting that the ultimate resistance for the three shafts is practically similar. At intermediate loads, however, the load-settlement response for the three shafts is distinctly different, with Test Shafts TS-4 and TS-5 exhibiting notably stiffer response at intermediate loads. Additionally, the “stiffness” of the load-settlement response at intermediate loads is observed to increase with the

magnitude of the pre-mobilized load (shown in the figure legend) as analyses presented in Chapters 2 and 8 would suggest. Collectively, these observations support the hypothesis that pre-mobilization alone can produce significant improvement in the performance of PGDS, and suggest that predictions presented in Chapters 2 and 8 are at least qualitatively appropriate. Additional comparison of predictions considering pre-mobilization and the observed response is provided subsequently in this chapter.

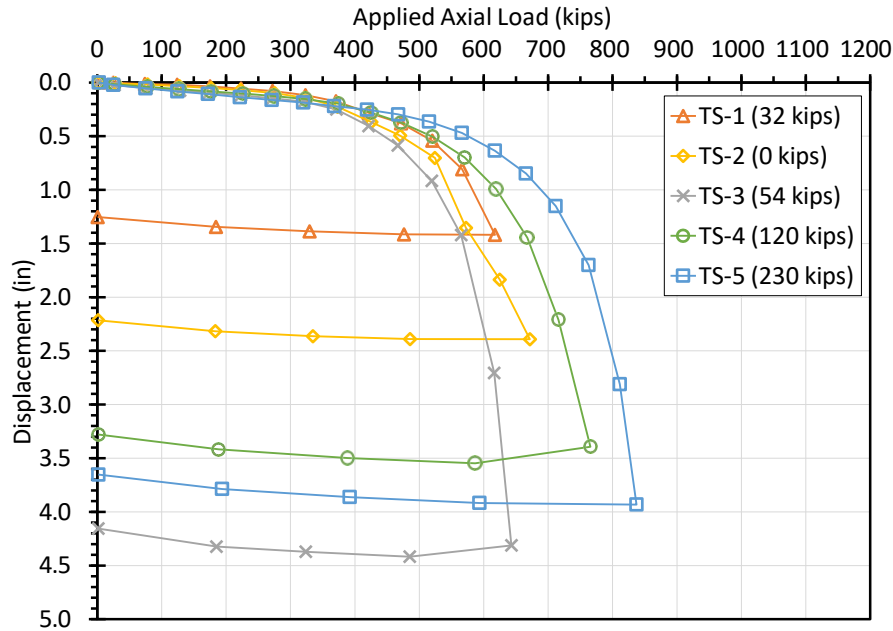


Figure 10.8: Load-settlement response for all test shafts.

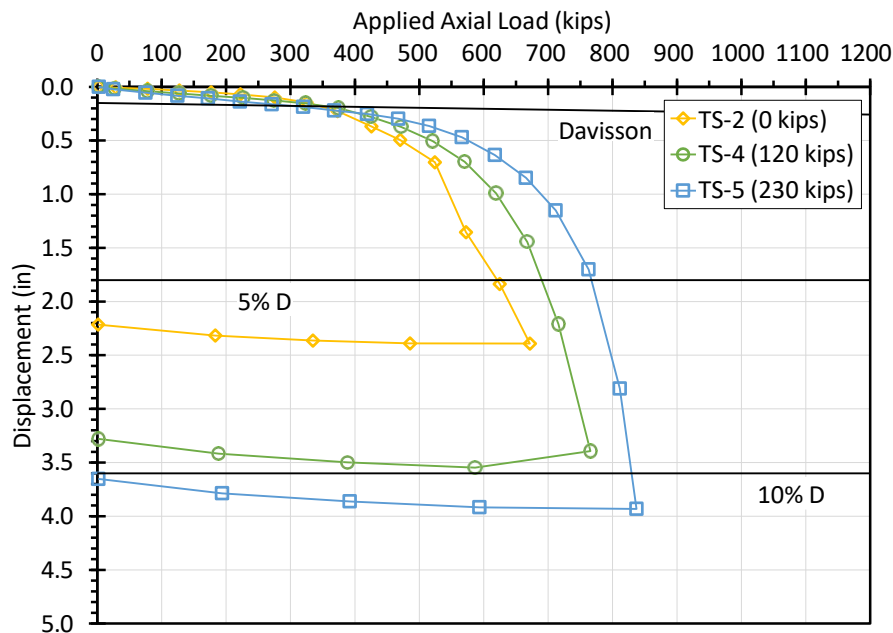


Figure 10.9: Representative load-settlement response.

While few would argue that the load-settlement response observed for Test Shafts TS-4 and TS-5 is not preferable to that observed for the conventional test shaft, the magnitude of quantifiable “improvement” depends on the specific failure criterion adopted for establishing the nominal shaft resistance. Table 10.1 summarizes values for nominal resistance established using three alternative failure criteria: Davisson’s criterion, 5 percent of shaft tip diameter, and 10 percent of shaft tip diameter. The three failure criteria are also shown in Figure 10.9. Also shown in Table 10.1 are percentages that represent the relative improvement in resistance relative to the measured resistance for the conventional test shaft (TS-2) using the same failure criterion. As shown in the table, differences in nominal resistance observed for Davisson’s failure criterion are small, and can likely be primarily attributed to simple variability among shaft performance for similar shafts. In contrast, differences in performance for the 5% D failure criterion are more significant, with Test Shaft TS-4 exhibiting an 11% improvement in nominal resistance and Test Shaft TS-5 exhibiting a 24% improvement in nominal resistance. Differences in nominal resistance for the 10% D failure criterion are much smaller, which reflect the fact that pre-mobilization produces little improvement in the ultimate resistance observed at large displacements in these clay soils. The improvement shown is entirely attributed to pre-mobilization since ground improvement is unlikely to have occurred for the devices used and site conditions present.

Table 10.1: Nominal resistance according to failure criteria.

Failure Criterion	TS-2 (kips)	TS-2 (%)	TS-4 (kips)	TS-4 (%)	TS-5 (kips)	TS-5 (%)
Davisson	344	0	356	+3	300	-13
5%	621	0	690	+11	767	+24
10%	~725	0	770	+6	827	+14

Percentages shown are relative to conventional shaft (TS-2).

10.3 Interpretation of Load Test Measurements

Comparisons of the load-settlement response for the different test shafts shown in Figure 10.9 provide strong evidence that the observed improvement is due to pre-mobilization. Additional analysis of the load test measurements was performed to interpret load transfer from strain gauge measurements taken throughout each test. Figures 10.10, 10.11, and 10.12 show the interpreted load transfer for select load increments for Test Shafts TS-2, TS-4, and TS-5, respectively. In the figures, the symbols reflect calculated values of axial force from strain gauge measurements, while the dashed lines represent interpretations of the distribution of axial force with depth. Values shown in the legends of each figure reflect the magnitude of the applied top-down force.

As is common when interpreting strain gauge measurements, some strain gages were observed to produce unreasonable measurements at different stages of loading. Such problems generally become worse when loading to higher loads, and it is quite common to “lose” a number of gages as the shaft approaches failure. Figure 10.13 illustrates one such condition observed for Test Shaft TS-2. As shown in the figure, measurements for strain gauge Level 5 were initially consistent with other measurements, generally falling between measurements for strain gauge Level 4 and strain gauge Level 6 as expected. However, beginning with the eighth load step,

measurements from strain gauge Level 5 began to depart from the trend observed for other strain gages and eventually became greater than all strain gages (which suggests increasing load with depth, which is physically impossible as a top-down load test approaching failure). When such cases were observed and judged to represent erroneous measurements, strain gauge readings were ignored for interpreting load transfer. The “missing” data points in Figures 10.10 through 10.12 correspond to conditions where strain gauge measurements were ignored.

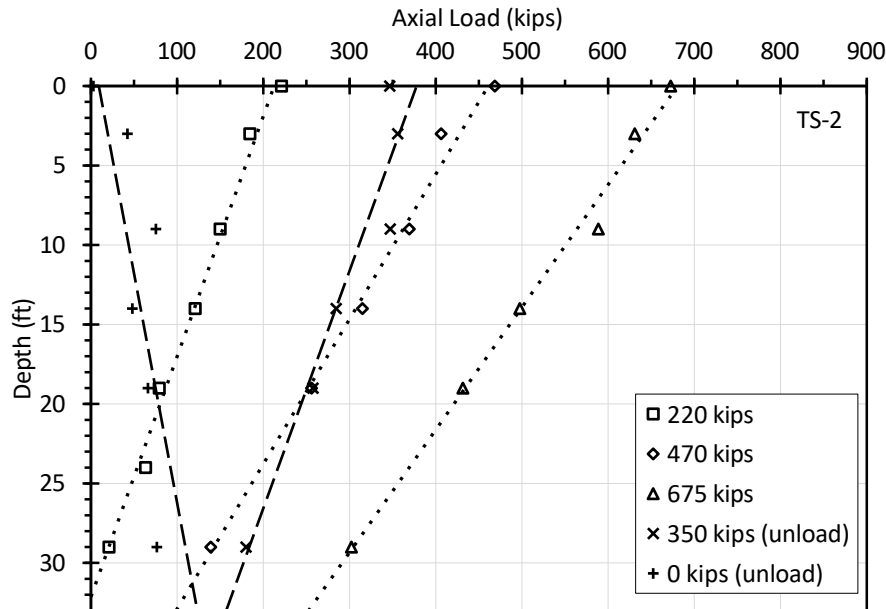


Figure 10.10: Interpreted load transfer for Test Shaft TS-2.

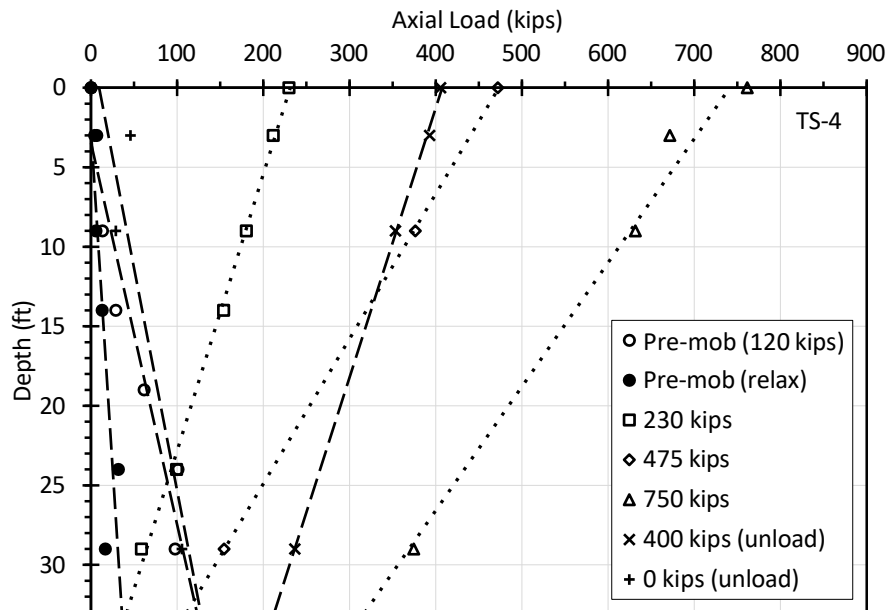


Figure 10.11: Interpreted load transfer for Test Shaft TS-4.

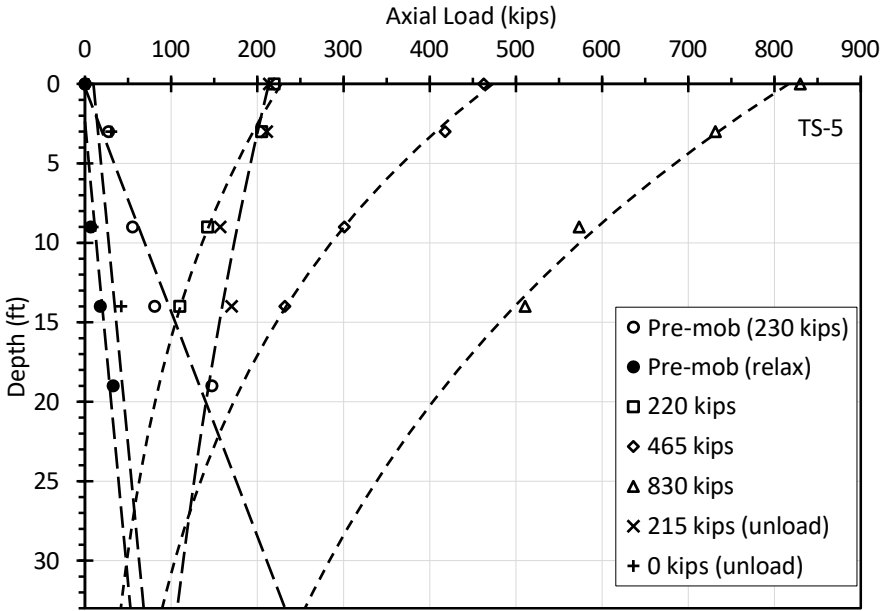


Figure 10.12: Interpreted load transfer for Test Shaft TS-5.

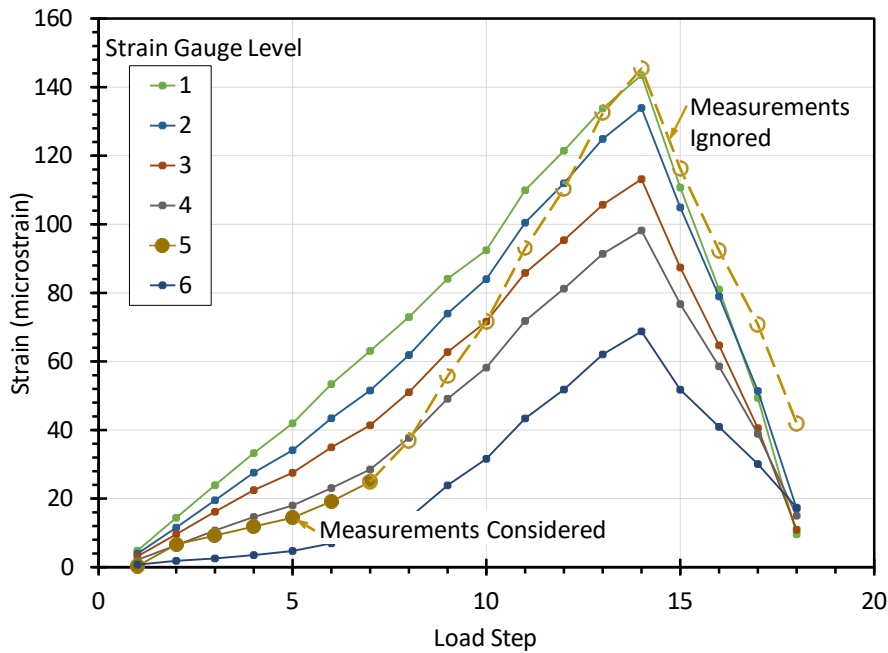


Figure 10.13: Strain gage measurement interpretation.

The load transfer shown in Figure 10.10 for the conventional shaft is typical of axially-loaded deep foundations with axial load decreasing with depth as a result of side resistance along the shaft. Upon removing the applied top-down axial load, the load at the top of the shaft returns to zero, but some load remains in the shaft with depth (in this case equaling approximately 120 kips at the shaft tip).

The load transfer shown for the shafts initially subjected to bi-directional pre-mobilization loads in Figures 10.11 and 10.12 is qualitatively similar to that shown for the conventional shaft in Figure 10.10. However, the load transfer reflects a different “starting point” because of axial load mobilized during bi-directional loading. The load distributions shown for the maximum bi-directional load reflects a maximum load at the tip of the shaft, with approximately linear reduction in load at shallower depths. Both figures also show the distribution of axial load measured following bi-directional loading, just prior to top-down loading. For both TS-4 and TS-5, substantial relaxation of the axial load following bi-directional loading was observed. Subsequent top-down loading increments produce incremental increases in the axial load distribution, starting from the axial load distribution that represents the relaxed pre-mobilization loads.

From the interpretations of load transfer for each loading increment, it is also possible to establish mobilization of side and tip resistance for each test. Mobilized side resistance is determined from the slope of the fitted load transfer curves in Figures 10.10 through 10.12, while the mobilized tip resistance is determined from the magnitude of load at the tip of the shaft. Displacements for each load increment were established from the measured top of shaft displacement, corrected for elastic compression of the shaft determined by integrating the measured strains along the length of the shaft. Figure 10.14 shows the interpreted mobilization of side resistance while Figure 10.15 shows the interpreted mobilization of tip resistance.

For shafts subjected to pre-mobilization prior to top-down loading, Figure 10.14 shows the initial mobilization of negative side resistance to resist the applied bi-directional load at the tip of the shaft. Some of the negative side resistance is recovered as the load in the shaft relaxes prior to top-down loading. The remaining negative side resistance is then overcome during the initial increments of top-down loading after which positive side resistance is mobilized to resist the applied top-down load. The ultimate unit side resistance for the post-grouted test shaft (TS-5) is observed to be slightly greater than that for the conventional test shaft and Test Shaft TS-4. The observed difference is believed to be a result of simple variability in side resistance rather than an artifact of post-grouting, since the flat jack membrane was not ruptured during grouting.

Figure 10.15 also shows the initial mobilization of tip resistance during bi-directional loading, followed by recovery of some tip resistance with relaxation of the pre-mobilization loads. Subsequent top-down loading then mobilizes additional tip resistance beginning from the final stress conditions after relaxation. In general, mobilization of tip resistance among the three test shafts shown is practically similar, with all three test shafts having an ultimate unit tip resistance approaching 50 ksf. This value is approximately double the predicted unit tip resistance from common design methods for stiff clay, but is consistent with the unit tip resistance measured for other load tests performed previously at the site (King et al., 2009). Displacements shown for Test Shaft TS-5 during post-grouting were estimated from the volume of grout injected and are therefore only approximate; the mobilization curves shown for the pre-mobilization phase of loading are therefore presented as dashed lines.

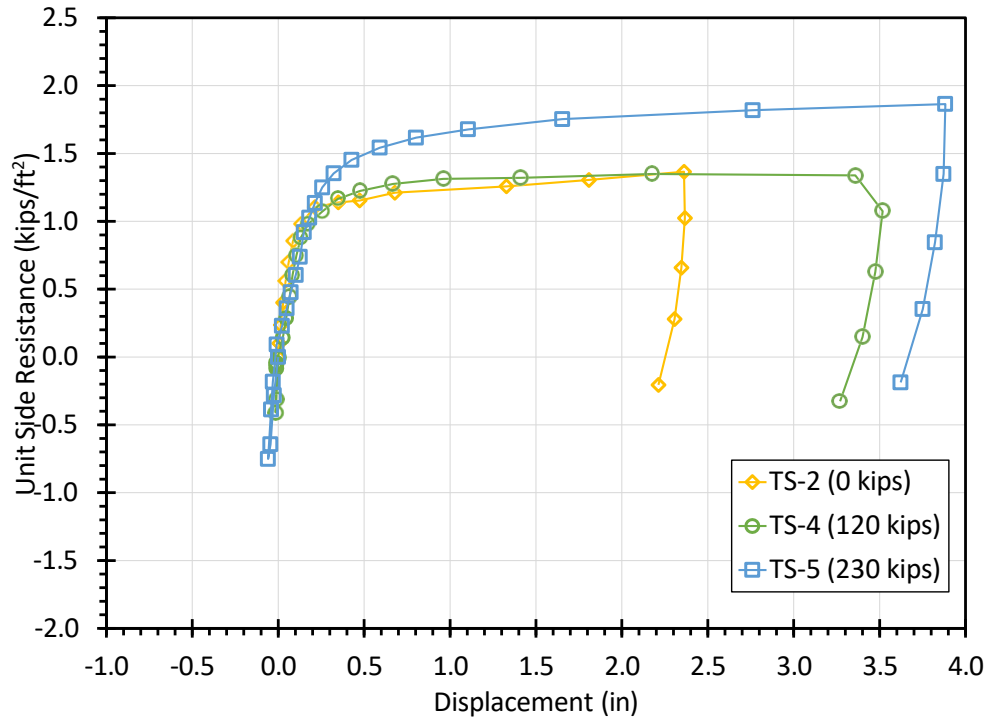


Figure 10.14: Mobilization of unit side resistance.

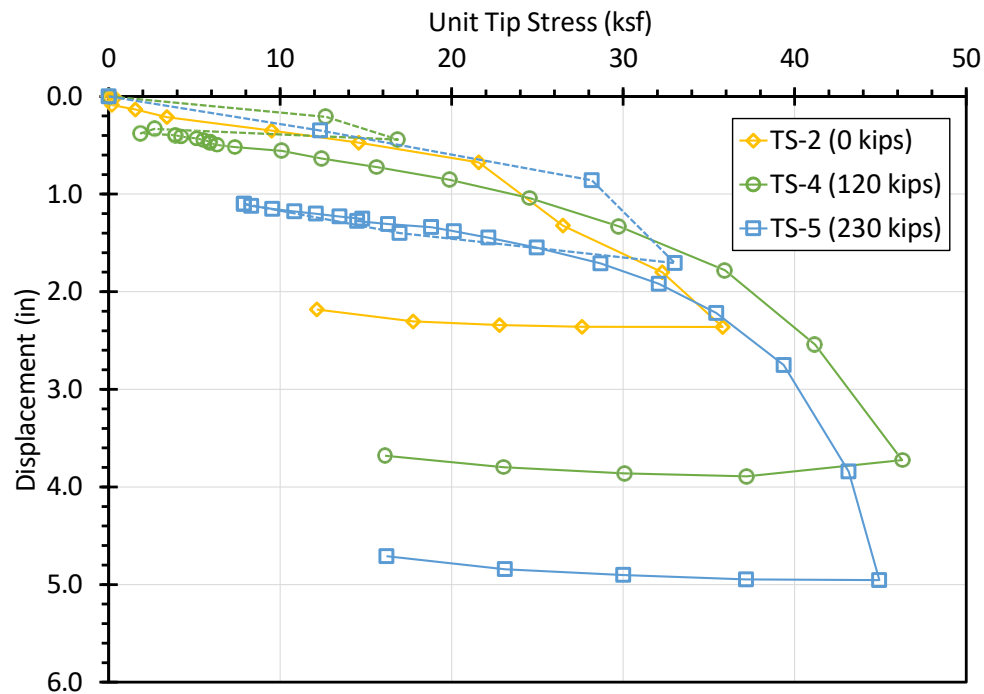


Figure 10.15: Mobilization of tip resistance.

10.4 Comparison of Measured and Predicted Response

The measured response from the load tests presented previously in this chapter is generally consistent with the expected response from pre-mobilization. To further evaluate the observed response, the load tests conducted for Test Shafts TS-2, TS-4, and TS-5 were modeled using the same finite element code used for interpretation of load test measurements described in Chapter 8. Predictions from the numerical model are compared to measurements presented in the previous section to evaluate whether the numerical model can reasonably predict the observed performance. For the load transfer analyses, t - z response was modeled using a scaled-exponential model that was fitted to the measured t - z response for the conventional test shaft (TS-2). The q - w response for tip resistance was similarly modeled and fitted to the observed response for the conventional test shaft. The predicted response for Test Shafts TS-4 and TS-5 was determined by first modeling application of the maximum bi-directional load at the tip of the shaft. The bi-directional load at the shaft tip was then reduced to be consistent with the measured load at the shaft tip following relaxation. Finally, top-down loading was applied to the model to predict the response to top-down loading.

10.4.1 Test Shaft TS-2

Figures 10.16, 10.17, and 10.18 show comparisons of the measured and predicted response for the conventional test shaft (TS-2). Figure 10.16 shows the conventional load-settlement response, while Figures 10.17 and 10.18 show the t - z and q - w response, respectively. For the numerical model, the ultimate unit side resistance (t_{ult}) was taken to be 1.4 ksf, which is consistent with the measured resistance and with theoretical estimates for t_{ult} from the α -method using $\alpha = 0.6$. The ultimate unit tip resistance (q_{ult}) was taken to be 45 ksf. Since these parameters produce predictions that are generally consistent with the observed performance for the conventional test shaft, they were used for modeling pre-mobilization alone for comparison with the observed responses for Test Shafts TS-4 and TS-5.

10.4.2 Test Shaft TS-4

Figures 10.19, 10.20, and 10.21 show comparisons of the load-settlement response, t - z response, and q - w response, respectively, for Test Shaft TS-4. For this test, the predictions considering pre-mobilization alone practically match with the observed performance when using the same parameters (i.e., $t_{ult} = 1.4$ ksf and $q_{ult} = 45$ ksf). The predicted response closely matches the observed load-settlement response except at very large loads. The predicted t - z response also closely matches the observed t - z response. The predicted q - w response is slightly different from the observed response. However, the differences between the measured and predicted q - w response are largely a result of differences in rebound of the shaft tip following application of pre-mobilization loads.

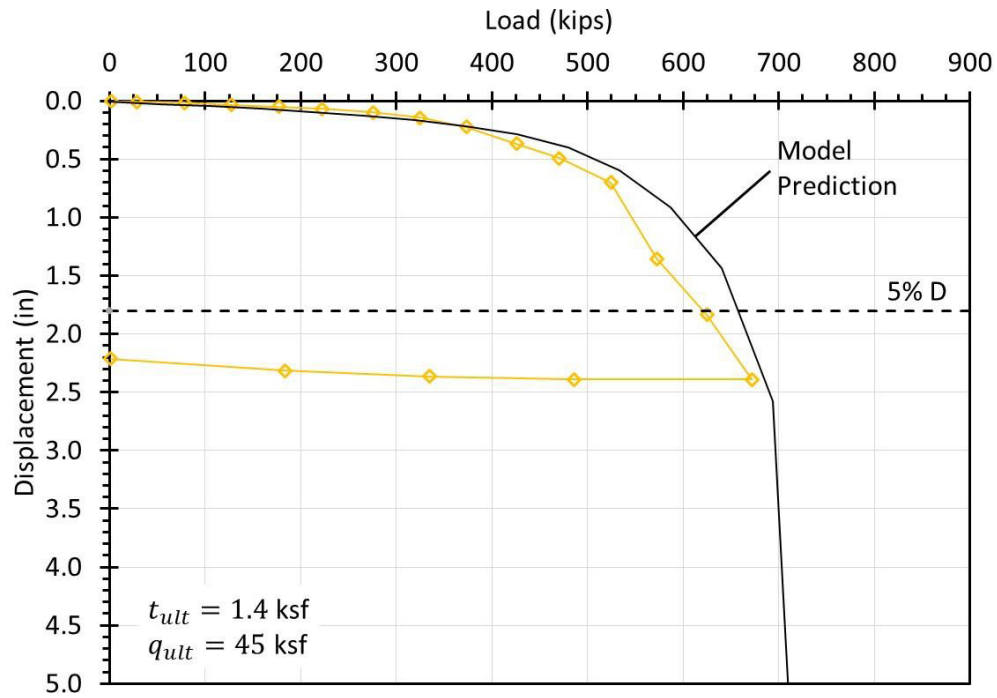


Figure 10.16: Load-settlement response for Test Shaft TS-2.

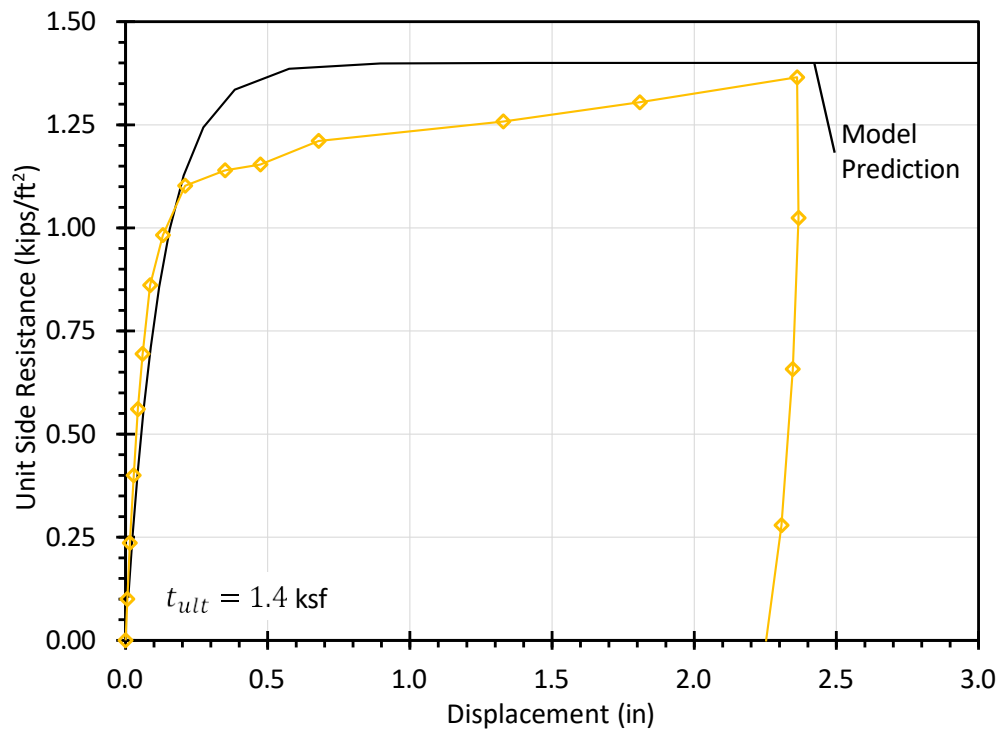


Figure 10.17: t - z response for Test Shaft TS-2.

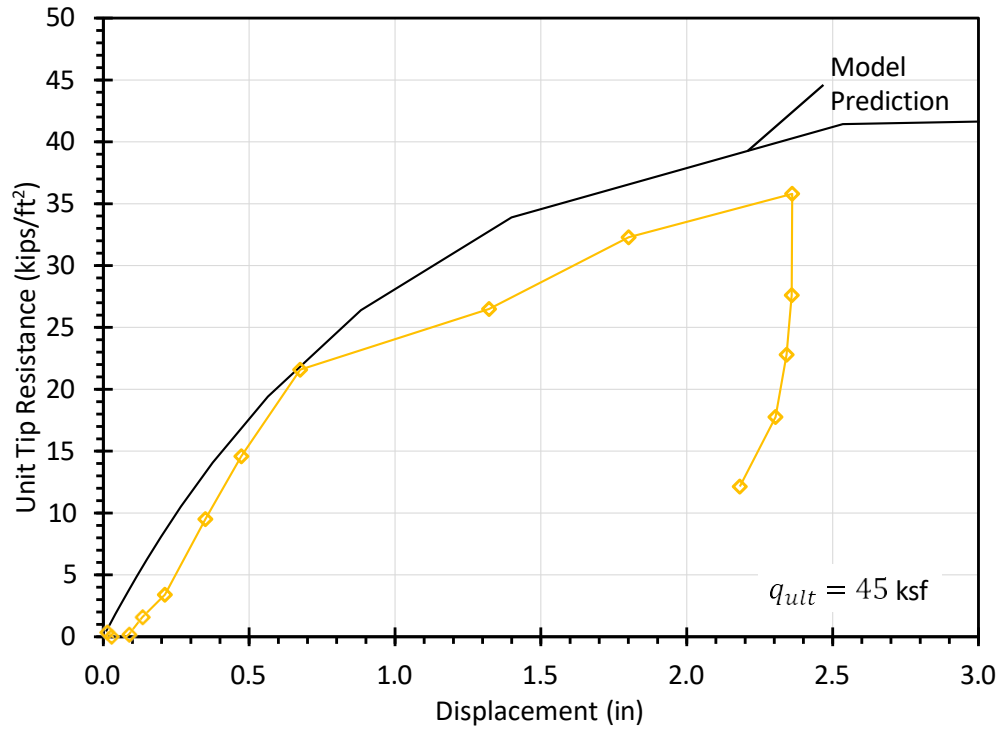


Figure 10.18: $q-w$ response for Test Shaft TS-2.

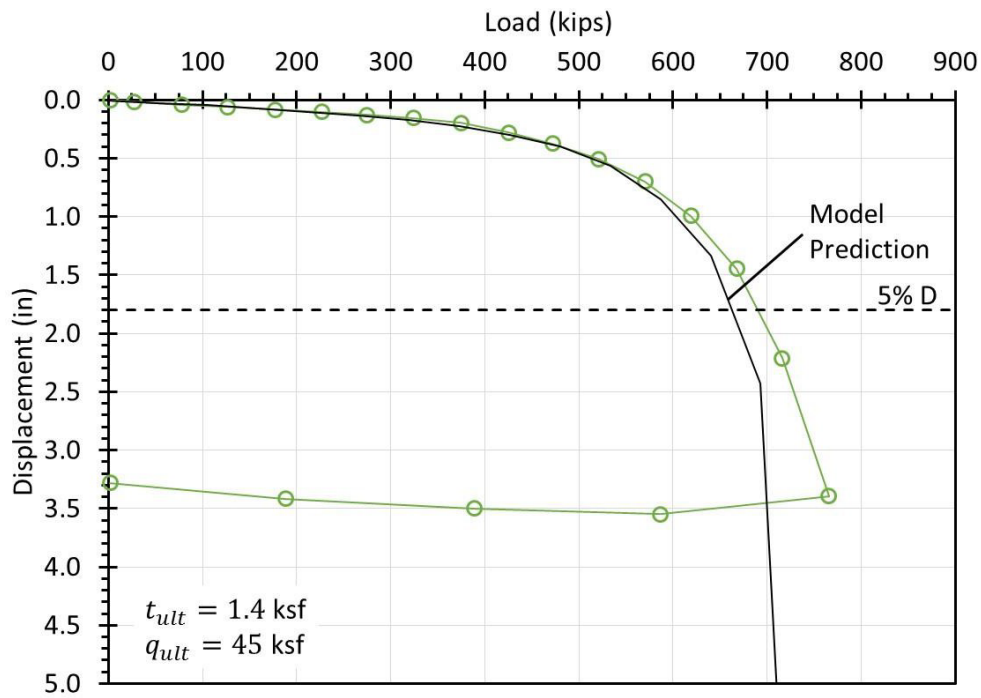


Figure 10.19: Load-settlement response for Test Shaft TS-4.

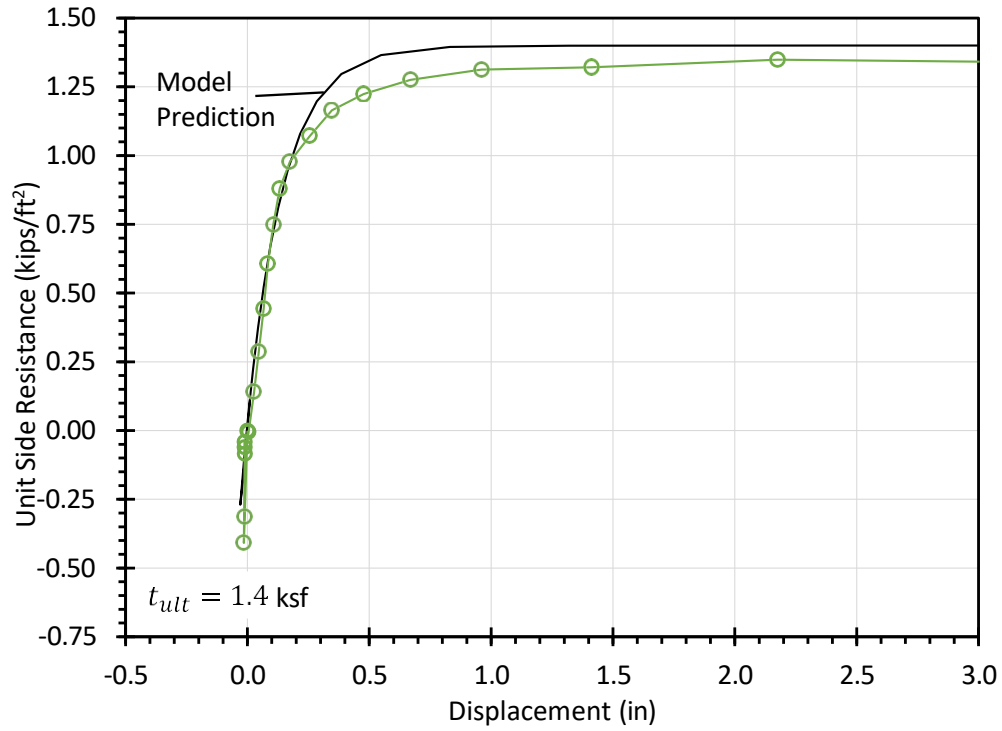


Figure 10.20: t - z response for Test Shaft TS-4.

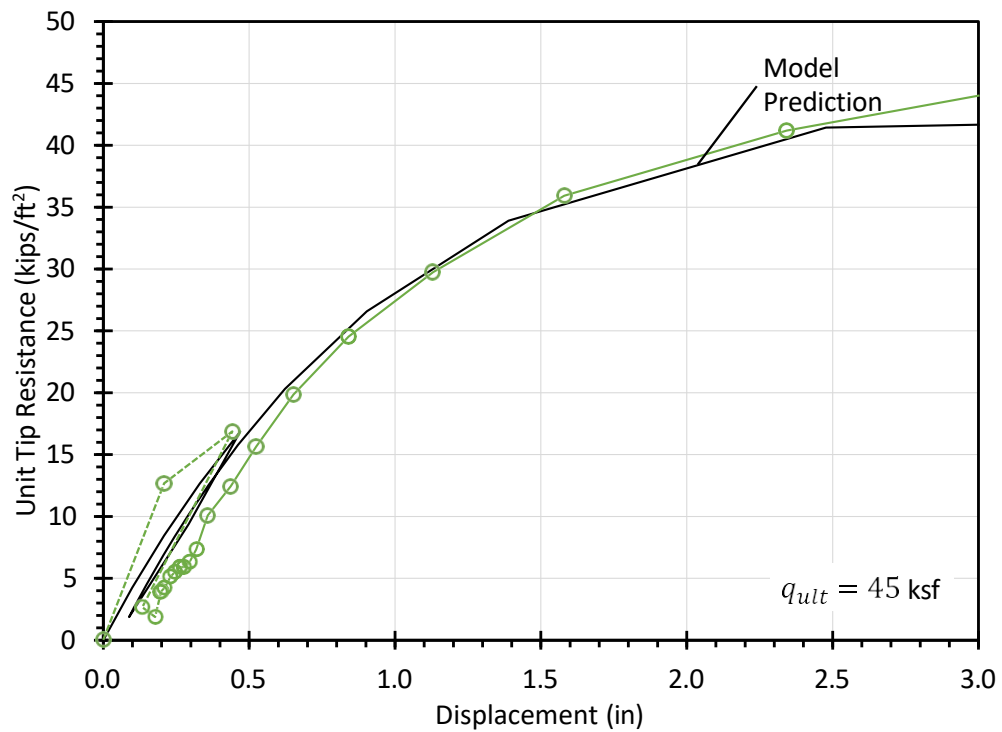


Figure 10.21: q - w response for Test Shaft TS-4.

10.4.3 Test Shaft TS-5

Figures 10.22 through 10.24, respectively, compare the measured and predicted load-settlement response, t - z response, and q - w response for Test Shaft TS-5. Two alternative predictions are presented for this case. The first prediction is based on use of $t_{ult} = 1.4$ ksf and $q_{ult} = 45$ ksf as was used for previously presented predictions for TS-2 and TS-4. As shown in Figures 10.22 through 10.24, these predictions are reasonably consistent with the measured response for applied loads that are less than approximately 500 kips. However, the predictions developed using $t_{ult} = 1.4$ ksf and $q_{ult} = 45$ ksf tend to underestimate the ultimate capacity of the shaft at large displacements. Figures 10.23 and 10.24 show that this result largely arises because the parameters underestimate the observed side resistance. An alternative prediction was therefore considered using $t_{ult} = 1.7$ ksf and $q_{ult} = 45$ ksf. The alternative prediction produces much closer matches with the measured load-settlement and t - z responses shown in Figures 10.22 and 10.23.

As shown in Figure 10.24, both predictions compare reasonably well with the measured q - w response at the shaft tip. The observed difference primarily occurs within the pre-mobilization loading cycle. This result is not surprising since the displacement estimates for the shaft tip during the pre-mobilization loading were estimated from grout volume measurements, with considerable judgment. Such differences are of little consequence, since it is the comparison of the response due to top-down loading that is of primary importance for PGDS. Thus, the fact that the measured and predicted q - w responses for the top-down load sequence are practically similar supports the conclusion that the predicted and observed performance are both qualitatively and quantitatively consistent.

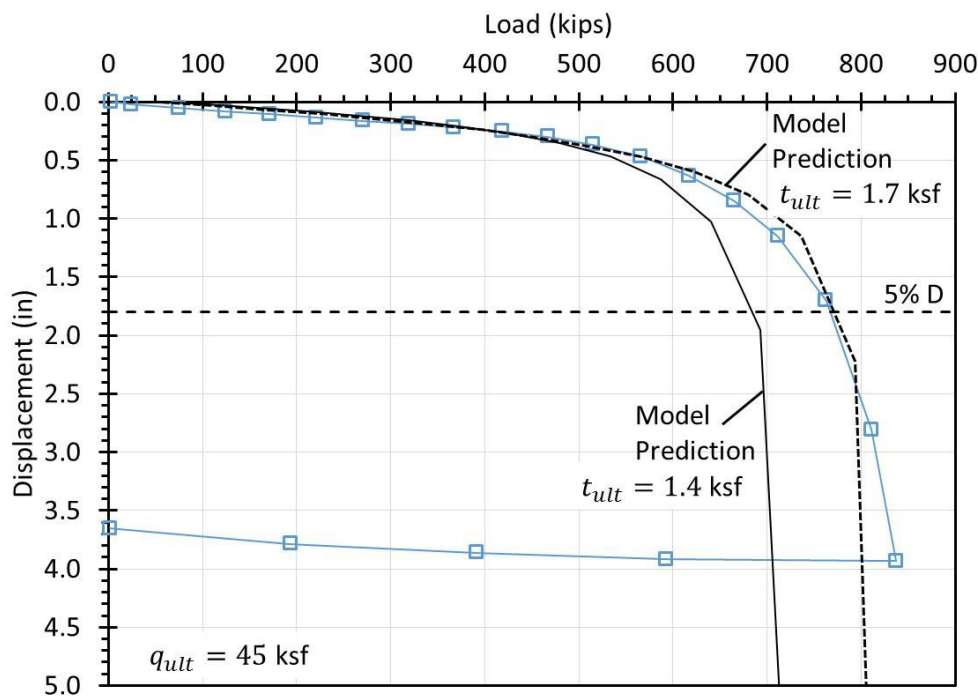


Figure 10.22: Load-settlement response for Test Shaft TS-5.

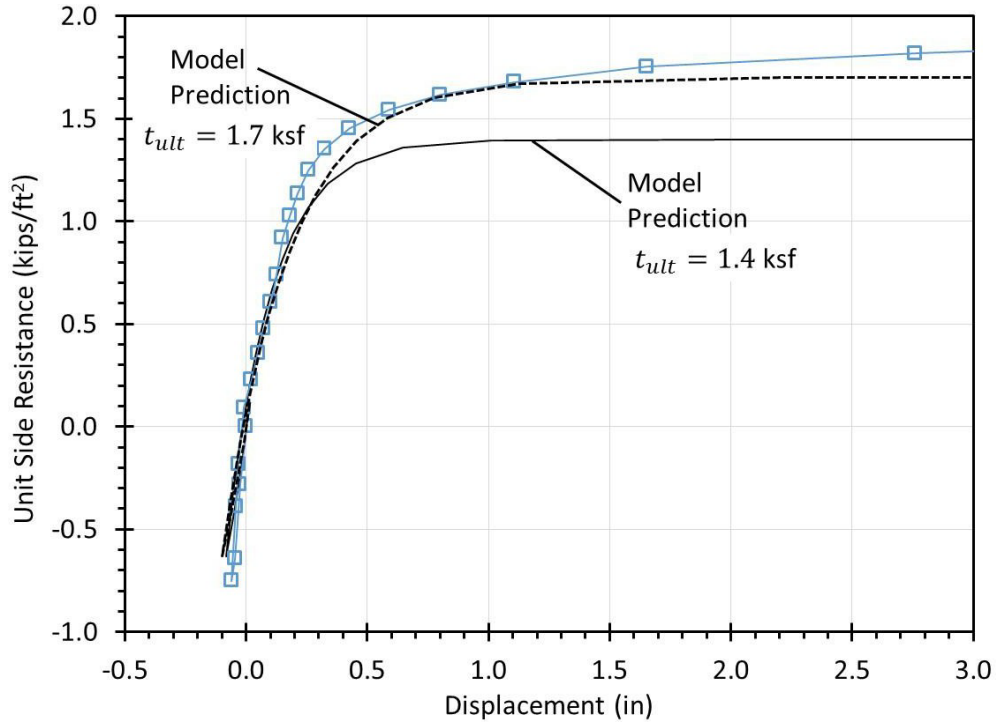


Figure 10.23: t - z response for Test Shaft TS-5.

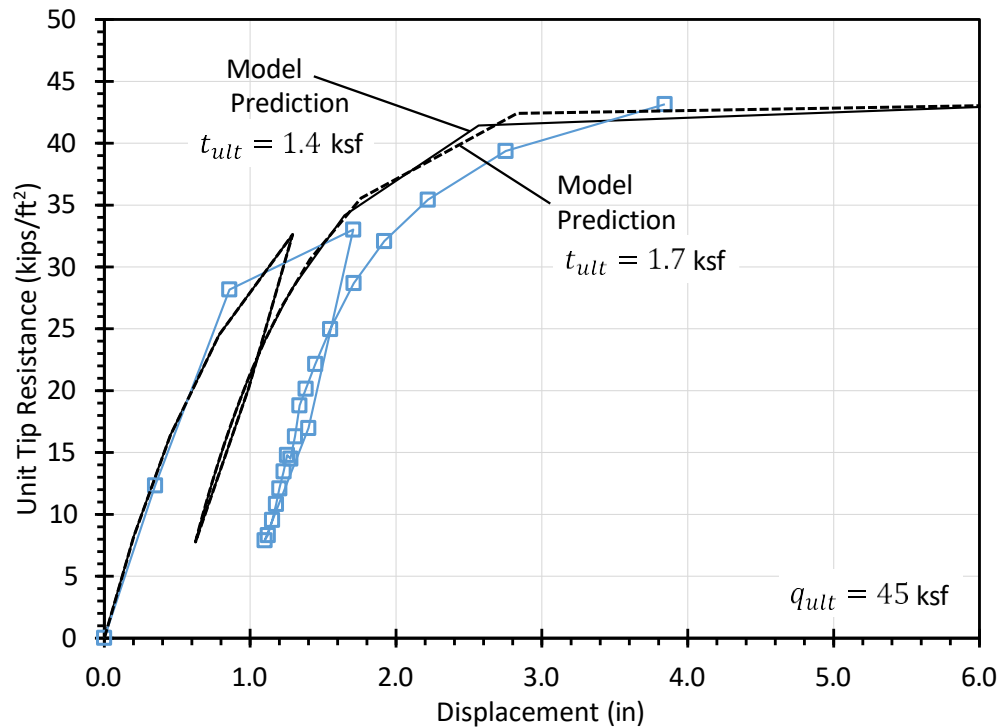


Figure 10.24: q - w response for Test Shaft TS-5.

10.5 Summary and Implications

A load test program was designed and completed specifically to evaluate improvement due to pre-mobilization. The program included five test shafts that were installed and load tested at the NGES clay site at Texas A&M University. All five shafts were practically identical except for the type of device installed at the tip of the shaft to apply bi-directional load for pre-mobilization. One test shaft was a conventional shaft without any device for bi-directional loading at the shaft tip. Two test shafts were installed with O-Cells at the shaft tip. One test shaft was installed with a similar RIM Cell device at the shaft tip. The final test shaft was installed with a flat jack post-grouting apparatus at the shaft tip. All test shafts except for the conventional shaft were subjected to bi-directional loads of varying magnitude prior to top-down load testing. The fact that the shafts were installed in stiff clay, and bi-directionally loaded using sealed devices that are unlikely to produce ground improvement, suggests that the observed response can be strictly attributed to pre-mobilization.

The measured response to both bi-directional and top-down loading was interpreted from the load test measurements and compared to the response predicted using a numerical load transfer model. The measured response shows improvement in the load-settlement behavior of PGDS, with the degree of improvement increasing with the magnitude of the bi-directional load applied prior to top-down loading. The measured response also indicates little improvement in the ultimate shaft resistance at large displacements due to pre-mobilization, but with improvement in nominal resistance of up to 25 percent depending on the failure criterion considered. Comparisons of the measured and predicted response suggests that the observed improvement in shaft performance is both qualitatively and quantitatively consistent with that predicted using the numerical model and, further, that the observed improvement was strictly due to pre-mobilization. These findings suggest that improvement in shaft performance due to pre-mobilization can be reliably predicted using relatively straightforward numerical models and, in turn, that such predictions can form the basis for reliable design of PGDS. For PGDS tipped in clay or rock where little ground improvement can be expected, the load transfer model should be used along with nominal estimates for unit side and unit tip resistance appropriate for conventional drilled shafts. For PGDS tipped in sands that may be improved through densification and/or permeation, the load transfer model should be used with nominal estimates for unit side resistance appropriate for conventional drilled shafts and estimates for unit tip resistance that reflect the degree of ground improvement that may be observed. Analyses presented in Chapter 8 suggest that unit tip resistance in sands may be improved by approximately 0 to 40 percent, but such estimates should be confirmed using site-specific load tests.

CHAPTER 11: SIGNIFICANT FINDINGS AND RECOMMENDATIONS FOR DESIGN AND CONSTRUCTION

11.1 Introduction

The work described in this report included:

- Review of available literature regarding post-grouting practice in the U.S., Europe, and Southeast Asia
- Investigation of post-grouting and contracting practices in the U.S. through interviews with contractors throughout the U.S.
- Collection of load test results for PGDS across the globe, and results for companion conventional drilled shafts where possible
- Evaluation and analyses to develop a better understanding of the different mechanisms that contribute to improved performance due to post-grouting, specifically trying to separate improvement due to pre-mobilization and ground improvement
- Analyses to evaluate the general magnitude of improvement from post-grouting and to evaluate several existing methods for prediction of PGDS resistance
- Completing a load test program intended to specifically evaluate improvement due to pre-mobilization
- Synthesis of the results and findings to develop recommendations to improve post-grouting practice for U.S. infrastructure projects

This chapter provides a summary of the most significant findings and observations from the collective work, and recommendations for improving contracting, design, construction, and monitoring of PGDS for the U.S. transportation industry.

The findings and recommendations presented in this chapter address many of the concerns and questions that currently exist regarding PGDS. As presented in Chapter 1, these concerns include:

- Lack of consensus about the specific mechanisms that contribute to improved performance
- Lack of consensus regarding the magnitude and variability of improvement expected from post-grouting
- Questions regarding the geotechnical conditions that are suitable for post-grouting
- Lack of well-vetted quality control and quality assurance requirements that are established or endorsed by authoritative organizations such as the Federal Highway Administration (FHWA) or the American Association of State Highway and Transportation Officials (AASHTO)
- Need for better means to predict achievable grout pressures during design, including consideration of the potential for grouting-induced hydrofracture
- Potentially detrimental effects of upward displacement of drilled shafts during post-grouting, and lack of established criteria on the acceptable magnitude of upward displacement

- Post-grouting possibly becoming a routine item in specifications as a substitute for proper quality control, even in projects where it is not needed
- Potential for designers to specify post-grouting as a substitute for proper geotechnical design of non-grouted drilled shafts

A substantial number of observations, findings, and recommendations have been included throughout this report. The most significant of these are summarized in this chapter. The findings and recommendations are generally organized according to the concerns listed above, with several additional groupings to address other issues identified during the work.

11.2 Improvement Mechanisms from Post-Grouting

Improvement in the performance of PGDS relative to comparable ungrouted drilled shafts can arise from at least four different “improvement mechanisms”:

- Pre-mobilization that tends to stiffen the response of PGDS but not increase the ultimate axial resistance
- Ground improvement at the shaft tip that increases the ultimate tip resistance
- Enlargement of the shaft tip that also increases the ultimate tip resistance
- Improvement in the ultimate side resistance due to upward flow of grout around the perimeter of the shaft during grouting

Pre-mobilization refers to mobilization of “negative” side resistance along the length of the shafts in proportion to the magnitude of the bi-directional force induced during grouting, with simultaneous consumption of an equal magnitude of tip resistance. The net effect of pre-mobilization is to improve the “stiffness” of the load-displacement response at intermediate loads without changing the ultimate resistance for the PGDS. In order to maximize pre-mobilization, it is advantageous to maximize the bi-directional force due to the grout pressure by: (1) applying the maximum grout pressure possible, (2) ensuring that this grout pressure is applied across the entire tip of the shaft, and (3) sustaining the grout pressure while the grout cures to reduce the potential for relaxation of the pre-mobilized resistance.

Measurements from load tests collected as part of this work convincingly demonstrate that pre-mobilization represents a substantial component of the improvement observed due to post-grouting, and further that pre-mobilization occurs in all types of ground. Analyses performed also demonstrate that improvement due to pre-mobilization can be reliably predicted with knowledge of the magnitude of bi-directional load that is applied during grouting and maintained following grouting.

Pre-mobilization necessarily requires upward displacement of PGDS during grouting. Furthermore, the magnitude of the improvement due to pre-mobilization will increase with increasing upward shaft displacement up to the point where negative side resistance is fully mobilized. One concern about such displacements is that side resistance could potentially degrade with excessive displacement or with repeated upward-downward loading. While such a concern is legitimate and “displacement softening” can certainly occur in some materials, there is little evidence to suggest that substantial softening will occur during a single loading cycle if rational constraints are placed on the magnitude of upward displacement during grouting.

Current upward displacement constraints that often range from ¼ to ½ inch are generally too restrictive and should be relaxed to allow the maximum benefit from pre-mobilization to be attained.

Additional improvement in performance due to post-grouting can also be attributed to ground improvement for shafts tipped in sandy soils, in addition to improvement produced from pre-mobilization. Ground improvement beneath the shaft tip can result from densification of the ground, from permeation of grout into the ground, or some combination of both. Some debate remains on this topic, but the general consensus is that permeation of common neat cement grouts is unlikely to occur in most soils, with the exception being clean, coarse sand and gravel. Improvement due to an enlargement of the shaft tip is also a subject of some debate depending upon whether one subscribes to the densification mechanism or the permeation mechanism. Unless a shaft is exhumed, it is extremely difficult to isolate improvement due to enlargement of the shaft tip from improvement due to densification or permeation, and it is possible that all three mechanisms may occur simultaneously. While the specific mechanism of ground improvement has implications for grouting practices, the practical truth is that densification, permeation, and tip enlargement will all lead to qualitatively similar improvements in the ultimate tip resistance. The debate may therefore be of little practical significance and it is common for densification, permeation, and tip enlargement to be considered collectively (and empirically) as a result. Ground improvement in cohesive soils does not appear to be significant.

Improvement in the ultimate side resistance is beyond the scope of the present work. Improvement in the side resistance does not appear to substantially contribute to the improved performance that has been observed for PGDS in the U.S. However, it is important to note that improvement in side resistance is routinely considered for PGDS in Chinese practice, even for PGDS that are exclusively grouted at the shaft tip.

It is challenging to attribute the improvement observed for specific PGDS to one or more of the individual improvement mechanisms with certainty. However, separate consideration of the different mechanisms is important for improving current design methods, for extending post-grouting practice to ground conditions beyond those commonly considered, and for enabling future improvements to post-grouting practices. Accurate isolation of the different mechanisms can be facilitated using analyses similar to those described in Chapter 8, in combination with carefully monitored instrumentation and detailed records of grout characteristics and grouting procedures similar to that presented in Chapter 10.

11.3 Magnitude of Improvement due to Post-grouting

A substantial collection of load test results for PGDS is presently available, including a relatively large number of tests performed for comparable PGDS and ungrouted shafts constructed in a wide variety of ground conditions ranging from sands to weak rock. Tests for shafts tipped in sands are by far the most common, with substantially fewer test results being available for shafts tipped in clays. Even fewer test results are available for PGDS tipped in rock, and those that are available have seldom been loaded to failure.

Results of analyses performed to evaluate available load test measurements clearly show that post-grouting can substantially and consistently enhance the load-deformation response of drilled

shafts in a wide variety of ground conditions, including cohesive soils and rock. Analyses presented in Chapters 8 and 9 show that post-grouted shafts in coarse-grained soils generally have greater ultimate tip resistance and stiffer load-displacement response at intermediate loads compared to ungrouted shafts of identical dimensions. Post-grouted shafts in clays generally exhibit stiffer load-displacement response at intermediate loads, but similar ultimate resistance at large displacements compare to identical conventional shafts. The increased “stiffness” of the load-displacement response due to post-grouting is largely attributed to pre-mobilization, while improvement in the ultimate resistance is due to ground improvement.

The improvement observed from available load test measurements due to post-grouting was interpreted in two ways: (1) considering improvement from all mechanisms collectively, and (2) considering improvement due to pre-mobilization and ground improvement separately. The collective gain in performance from all mechanisms is represented using a “total improvement ratio,” *TIR*, calculated as the ratio of the ultimate unit tip resistance for the PGDS to the ultimate unit tip resistance for a comparable ungrouted shaft. For the second approach, the enhanced performance due to ground improvement and pre-mobilization was isolated using load transfer analyses to model pre-mobilization, and attributing the remaining measured response to ground improvement, quantified using a “ground improvement ratio,” *GIR*. Thus, *TIR* reflects the collective improvement attributed to all improvement mechanisms, while *GIR* represents the improvement due to ground improvement at the shaft tip alone.

Based on analyses performed considering all improvement mechanisms collectively, the average improvement in the ultimate unit tip resistance was found to be approximately 80 percent of the ultimate unit tip resistance for a comparable ungrouted shaft (i.e., mean *TIR* = 1.8). The magnitude of the *TIR* commonly varied from approximately 1.0 to greater than 3.0 for the load tests considered in this work. For some load tests, the *TIR* due to post-grouting was found to be extremely large. In other rare cases, *TIR* was determined to be less than 1.0, which suggests that post-grouting had a detrimental effect on the performance of the PGDS. However, such observations are most likely a result of inherent variability in the ultimate resistance for the drilled shafts rather than an indication that post-grouting may degrade shaft resistance. Values of the coefficient of variation of *TIR* were on the order of 30 to 50 percent for shafts tipped in both sand and clay.

Values of *GIR* were computed for a subset of the available load tests. Because *GIR* isolates the contribution of ground improvement, these values were generally much smaller than the corresponding values of *TIR*. The mean value of *GIR* for shafts tipped in sands was approximately 1.2, suggesting that ultimate unit tip resistance for PGDS is approximately 20 percent greater than the ultimate unit tip resistance for a comparable ungrouted shaft. Conversely, the mean value of *GIR* determined for shafts tipped in cohesive soils was equal to 1.0, indicating that improvement is completely attributable to pre-mobilization.

11.4 Design of PGDS

Several methods have been proposed for predicting the nominal resistance for PGDS. These methods are generally empirical in nature, although some have a theoretical basis. All of the existing methods identified in this work utilize “multipliers” of some form that are applied to

estimates of nominal resistance for an ungrouted shaft to establish estimates for nominal resistance for PGDS.

Information from available case histories was used to develop comparisons between predicted nominal values and measured ultimate values of tip resistance for PGDS installed in a variety of soils and using various base grouting devices. The *TCM* method proposed by Mullins et al. (2006) tends to overestimate the measured ultimate tip resistance, while the *TCM* method proposed by Dapp and Brown (2010) and the component multiplier method by Dai et al. (2011) tended to slightly underestimate measured values from the load tests considered. The accuracy of predictions for current design methods presented in Chapter 7 are highly variable, however, with coefficients of variation for the ratio of predicted to measured tip resistances ranging from 45 to 70% for the different methods considered. As such, these methods should only be used to develop preliminary estimates for design that must be confirmed with site-specific load tests to confirm that the estimated capacity can actually be achieved.

Because of the considerable variability and uncertainty associated with current PGDS prediction methods, future predictions of PGDS performance for design should be developed using load transfer methods that allow for separately considering pre-mobilization and ground improvement mechanisms, similar to methods described in Chapter 8. Such predictions can be practically performed using simple hand calculations considering the shafts to be rigid, or using numerical methods that can be implemented in common spreadsheet software. Predictions for PGDS tipped in cohesive soils or rock should consider the unit tip resistance to be identical to that considered for conventional shafts. Predictions for PGDS tipped in sands may consider the unit tip resistance to be approximately 20 percent greater than that considered for conventional shafts, although such improvement should also be confirmed using site-specific load tests.

An important component of design for transportation projects in the U.S. is application of resistance factors within the Load and Resistance Factor Design (LRFD) framework. Resistance factors for drilled shafts in the current AASHTO Bridge Design Specifications (AASHTO, 2012) were not developed specifically for use with PGDS, and no resistance factors for PGDS have been proposed to date. Since there is no evidence to suggest that the reliability of PGDS is substantially different from the reliability of conventional drilled shafts, it seems rational to apply current AASHTO resistance factors to the computed nominal resistance for PGDS until “PGDS-specific” resistance factors can be developed.

One significant risk associated with design and construction of PGDS is not being able to sustain the intended grout pressure during construction, in which case corrective measures (e.g., stage grouting, re-design, etc.) become necessary to provide the required nominal resistance. In general, the magnitude of the grout pressure that can be achieved is constrained by the magnitude of available side resistance and the grout pressure that will cause hydrofracture of the ground at the shaft tip. However, both the nominal side resistance and the hydrofracture pressure are uncertain quantities that vary from shaft to shaft. Target grout pressures should therefore be selected with explicit consideration of the hydrofracture pressure and an appropriate margin of safety to reduce the likelihood of not achieving the target grout pressure in the field.

11.5 Grouting Practices

Grouting practices for post-grouted drilled shafts are generally consistent throughout the U.S. The vast majority of experience with post-grouting within and outside the U.S. is based on the use of relatively fluid, neat cement grout with a water-to-cement ratio between 0.4 and 0.7. Numerous documented case histories illustrate that effective control of the grout is not always maintained. Experience has shown that such grouts can flow upwards along the sides of shafts, or substantial distances laterally (either as a result of hydrofracture or other reasons). There is a need to develop grouting procedures with more effective control of grout flow. Much remains to be learned about how the grouting process and grout characteristics affect the performance of PGDS.

In typical PGDS practice, grouting pressures are maintained for a matter of only a few minutes to ensure that the tip of the shaft is pressurized. Pump lines are then generally disconnected and cleaned immediately to avoid clogging from hardened grout. Most commonly, the grout lines are simply disconnected from the pressure source at the completion of grouting, and there is no attempt to maintain pressures at the base of the drilled shaft. However, systems are available (Beck, 2002) that are capable of locking pressure into the grout lines so that the grout cures under pressure. It is reasonable to assume that curing of grout under pressure may reduce potential relaxation of pre-mobilized resistance, and potentially improve the magnitude of ground improvement at the shaft tip. However, no deliberate study of the effects of locking in grout pressure has been conducted to evaluate potential enhancements to PGDS performance.

Staged grouting has been performed successfully on numerous post-grouting projects, but has most often been used when there are problems achieving the target grout pressure in the initial stage of post-grouting. Staged grouting may also compromise the ability to use the applied grout pressure as an indicator of pre-mobilization since initial grouting stages may unintentionally prevent flow of grout across the entire shaft tip. Further investigation is needed to compare the performance of PGDS subjected to multiple stages of grouting with PGDS grouted in a single stage to allow the potential benefits and consequences of routine staged grouting to be identified.

Gravel bedding systems have been used on some projects to distribute grout across the shaft tip and enable more effective distribution of grout pressure. Gravel bedding also aids in achieving a flat bedding surface. There is anecdotal evidence from one case history indicating that use of gravel bedding may adversely affect performance, but such adverse effects may also be attributed to factors other than the gravel bedding. There are no comprehensive studies available that isolate and quantify the influence of gravel bedding on PGDS performance. Such studies should therefore be undertaken.

11.6 Quality Control/Quality Assurance for Post-Grouting Operations

Practices for quality control and quality assurance (QC/QA) of post-grouting operations have not been standardized and adopted by nationally recognized agencies like FHWA and AASHTO. While QC/QA practices for PGDS in the U.S. often include common elements, their implementation varies substantially from project to project. Common elements used for QC/QA generally include:

- Measurement of grout pressure, grout volume, and upward shaft displacement during grouting
- Consideration of three criteria for termination of grouting that include a target grout pressure with a minimum net volume, a maximum upward shaft displacement, and a maximum net volume
- Measurement of specific gravity, viscosity, and/or compressive strength of the grout

These common elements generally provide a rational basis for QC of post-grouting operations in the field, and likely provide a baseline from which to establish effective QA methods for PGDS. However, several changes to current practices should be considered to improve the consistency of QC/QA practices for PGDS.

Grouting termination criteria and the means for measuring the grouting parameters may vary substantially from project to project, often without clear justification or validation. Standard procedures should be developed to establish effective and appropriate grout volume termination criteria that include consideration of important factors such as the size of the shaft and grouting device, and the condition of the ground beneath the shaft tip. Methods for determining the volume of the grout delivery system (used in computing the net grout volume) should also be standardized. Consideration should be given to improving placement of grout pressure gages, potentially including placement of gages near the shaft being grouted, and placement of gages on the grout return line to facilitate rapid identification of problems during grouting. Specific procedures for evaluation of hydraulic head losses should also be included within a QA/QC program.

Strain gages and/or telltales have sometimes been installed in PGDS and monitored during grouting, but such instruments have not been commonly used as part of QC/QA for PGDS. Strain gages can provide important feedback to help determine the effectiveness of grout distribution across the shaft tip and to estimate the axial load at the strain gauge location(s). Monitoring of strain or displacements near the shaft tip allows the induced loading from post-grouting to be quantified and may help to detect the occurrence of blocked grout lines and hydrofracture. Strain gauge and telltale measurements can also be used in combination with measurements of upward shaft displacement to confirm that a certain level of resistance has been pre-mobilized during grouting, and to evaluate the magnitude of relaxation of the pre-mobilized load as the grout cures. Given the multiple benefits of strain gages installed near the shaft tip, consideration should be given to requiring use of strain gages or telltales and incorporation of strain measurements into standardized QC/QA procedures.

Upward movement of the drilled shaft is an important QA parameter that provides verification that some level of pre-mobilization has been achieved. During grouting, the upward movement of PGDS has typically been limited to $\frac{1}{4}$ to $\frac{1}{2}$ inch during a single grouting stage, with no explicit limit on the cumulative upward movement when multiple grouting stages are undertaken. Current QC/QA procedures should be amended to include such a cumulative displacement limit that could serve as the sole upward displacement criterion, or be used in combination with a limit on upward movement during individual grouting stages. There is also great need to objectively evaluate how much upward movement can be tolerated before side resistance is adversely affected in different ground conditions, and to provide specific guidance regarding tolerable magnitudes of cumulative upward displacement for different soil/rock types.

Consideration should also be given to introducing a minimum upward displacement criterion that could serve as a QA measure to help demonstrate that some minimum degree of pre-mobilization has been achieved during grouting.

While measurements of specific gravity, viscosity, and/or compressive strength of the grout are commonly made for many PGDS projects, the frequency of the tests and specific requirements for the measurements are seldom explicitly included in construction specifications or special provisions for PGDS projects. Given that specific gravity, viscosity, and compressive strength are all directly related for neat cement grouts that are commonly used for PGDS, developed standards should not generally require that all three measurements be performed for all PGDS projects to avoid unnecessary requirements. One potential idea may be to measure specific gravity during grouting for the purpose of QC, and then to measure the grout compressive strength as an independent measure for QA. While the magnitude of the grout compressive strength is not likely a primary concern in terms of the performance of PGDS, achieving some minimum strength provides a good, independent measure of whether the grout has been properly proportioned and mixed.

11.7 Use of Post-grouting as a QC/QA Method

While post-grouting appears to have some potential for quality control and assurance for the construction of a drilled shaft, there may be significant challenges to its use for this purpose. It is clear that post-grouting can provide indications of shaft problems (e.g., unusually low side resistance, and unusually soft tip conditions), but extending the technique more formally for QC/QA presents numerous challenges.

CHAPTER 12: RECOMMENDATIONS FOR FUTURE WORK

12.1 Introduction

The findings and recommendations of this work address many questions and concerns that exist regarding post-grouting practice in the U.S. Nevertheless, several important issues remain that could not be resolved based on the information available for the present work. Additional research and development are necessary to improve design and construction procedures that will improve post-grouting practices in the U.S. The findings and recommendations provided in this report should be revisited periodically as additional experience and data are acquired.

The recommendations for future work discussed in this chapter are intended to provide a basis and framework from which future research efforts should be undertaken. The recommendations are provided in order of priority in view of the anticipated impact that each design or construction activity will have on post-grouting practice. Many of the recommendations provided can be addressed through additional load testing and associated data analysis. Consequently, this chapter closes with a series of recommendations for load testing of PGDS.

12.2 Evaluation of Relaxation Following Grouting

The work presented in this report provides convincing evidence that pre-mobilization produces a substantial portion of the improvement that is observed due to post-grouting, and that improvement due to pre-mobilization can be effectively and practically predicted given knowledge of the load induced during grouting. While the maximum load induced during grouting is relatively easy to evaluate, the degree of relaxation of load is more difficult to assess. Observations from measurements collected for the load tests described in Chapter 10 suggest that relaxation may result in pre-mobilized load at the shaft tip of approximately 25 percent of the maximum applied bi-directional load. However, the amount of relaxation is likely dependent on characteristics of the grout (e.g., water-to-cement ratio), characteristics of the surrounding ground (hydraulic conductivity), and whether the grout pressure is locked off following grouting, among other factors. Additional study is therefore needed to evaluate how these factors affect relaxation, and how best to limit relaxation.

12.3 Evaluation and Development of Improved Design Methods

The ultimate goal of future investigations of PGDS should be to improve procedures for estimating the ultimate resistance and load-deflection response of PGDS for design. The load transfer analysis method described in Chapter 8 provides a reasonable and practical approach for separating the effects of pre-mobilization and ground improvement, and providing for estimation of PGDS performance with improved reliability. However, additional evaluation is needed, especially regarding the degree of ground improvement that should be considered for such analyses as described in the following section.

12.4 Evaluation of Ground Improvement

To further refine current understanding of ground improvement at the tip of PGDS, load testing of PGDS should be performed in soils and under circumstances that are conducive to ground

improvement alone (i.e., without pre-mobilization). This could be accomplished by installing test shafts in soils that are prone to densification or consolidation under the grout pressure. Pre-mobilization could be reduced or eliminated by preventing shaft movement during post-grouting, and by sizing or reinforcing the shaft to significantly reduce its compressibility, if needed. Restraint of the shaft movement can be accomplished using a stiff reaction frame that can also be used as reaction for subsequent load testing.

Another important element that requires further study is the effect of grouting pressure on the magnitude of improvement of the performance of PGDS. The evaluation should be based on the value of grout pressure normalized with respect to overburden stress, rather than on the magnitude of grout pressure alone. It is also important to study the range of grout pressures that can be achieved in practice. It is possible that the range of achievable grout pressure values may be sufficiently narrow to prevent adjustment of the pressure to achieve a desired outcome even though grout pressure may have a significant influence on the performance.

12.5 Evaluation of Reliability

A critical issue that remains unresolved is to establish the reliability of PGDS, and more importantly from a design perspective, the reliability of alternative methods for predicting the performance of PGDS. Important questions that remain include:

- What is the reliability of the performance of PGDS?
- Is the performance of PGDS more reliable than that of conventional shafts?
- How is reliability affected by ground conditions, grout characteristics, and grouting procedures?
- Do current QC/QA methods contribute to improved reliability?
- What are the respective reliability values for pre-mobilization and ground improvement effects? Is pre-mobilization more reliable than ground improvement, or vice-versa?

The predominant means for evaluating reliability is to analyze results from full-scale field tests on comparable grouted and ungrouted shafts. A critical part of such evaluations should also include development of resistance factors for LRFD that are specific to different design methods and construction practices, and that accurately reflect the uncertainty associated with PGDS performance, and with the respective design methods.

12.6 Shaft Performance: Stiffness vs. Nominal Resistance vs. Ultimate Resistance

Additional consideration of the relative importance of increased shaft stiffness versus increased ultimate resistance is needed. While increased ultimate resistance and increased stiffness are both beneficial outcomes in terms of the performance of PGDS, they pose different challenges for design. Current U.S. design methodologies, which tend to be dominated by considerations of ultimate resistance (strength limit states), can make it difficult to take advantage of increases in the stiffness of the load-displacement response for PGDS. This issue should be considered in development of improved design methods for PGDS. One possible approach could be to incorporate generation of load-displacement curves for PGDS that reasonably account for contributions from pre-mobilization, ground improvement, and the anticipated soil behavior (e.g., strain hardening behavior during shearing, or a true plunging strength limit state). Such

curves could then be integrated into design in much the same way an idealized load-displacement curve can be incorporated into the current LRFD evaluations for conventional drilled shafts at service, strength, and extreme event limit states.

12.7 Evaluation of Potential for Degradation in Side Resistance

There is a potential for reduction of the side resistance with repeated application of shear stress, or more specifically shear displacements, due to degradation of the shaft-soil interface. Existing QC/QA procedures generally place limits on upward displacements to address this concern. However, such constraints may also limit the magnitude of improvement from pre-mobilization. Additional investigations should therefore be undertaken to investigate the potential for degradation of side resistance when subjected to displacements of varying magnitude. While there are materials that degrade with repeated displacement (e.g., fissured clay, etc.), not all concrete-soil interfaces are susceptible to significant degradation by stress reversals and loading-unloading.

There is a significant amount of published research on the response and degradation of soil-structure interfaces subjected to repeated loading (Gómez et al., 2000, 2003). A thorough review of relevant published research should be performed to gain further information on the potential for interface degradation. This would also aid in developing more accurate shear stress-displacement models that are essential for predicting pre-mobilization effects. Because most of the published research on interfaces is based on shearing of planar interfaces, and because development of side resistance along drilled shafts is a three-dimensional or axisymmetric problem, pilot-scale tests should be performed that include relatively simple compression-tension loading cycles. The tests would be aimed at measuring the displacement-shear stress response of the interface, and may include several unload-reload cycles to investigate the potential for displacement softening. This would greatly help in developing sensible models of interface performance, which are fundamental to evaluating and predicting pre-mobilization in PGDS, and to development of rational and practical methods and procedures for post-grouting.

12.8 Evaluation of Post-Grouting as a QC/QA Tool

A common consideration among many professionals when considering PGDS is whether post-grouting is itself a QC/QA tool. As described previously, post-grouting generally induces bi-directional loading at the tip of the shaft (that is responsible for pre-mobilization). This load has the potential for being used as a QC/QA tool along with other considerations like grout pressure, grout volume, and shaft displacement since upward loading of the shaft can be considered as demonstration of some minimum total resistance. However, current post-grouting practices in the U.S. do not necessarily contribute to effective use of post-grouting as a QC/QA tool. Post-grouting devices are often uncontained (or become uncontained during grouting) and, thus, it is often not possible to ascertain the relationship between grout pressure and induced load.

Use of relatively low viscosity grouts may also lead to some lack of control on grout flow, which may decrease the reliability of using grout pressure as a QC/QA tool. Installation of strain gages near the tip of the shaft may partially alleviate this concern, but little study has been performed to evaluate practical issues associated with use of strain gages, or to develop rational and practical recommendations for their use in a QC/QA program. Finally, even if the induced load is known

precisely, the ultimate resistance of the shaft is generally not achieved during grouting (in fact grouting is controlled to prevent this), and the maximum resistance achieved during grouting is expected to reflect the performance of an ungrouted shaft. Thus, loading from post-grouting will only provide a “censored” measurement of the resistance of an ungrouted shaft (similar in concept to a proof test). All of these issues warrant focused attention and evaluation so that practical and reliable guidance can be provided regarding use of post-grouting for QC/QA.

12.9 Recommendations for Load Testing of PGDS

Many of the recommendations provided in this chapter can be addressed through additional load testing. Such testing may be performed on a project-specific basis, or as part of a more comprehensive research program to systematically address these issues. Regardless of the source of the load test data, it is desirable (from the perspective of improving post-grouting practice) to have results from “side-by-side” grouted and ungrouted shafts of similar size. It is also desirable for the tests to subject the shafts to top-down loading, at least until the issues described previously for bi-directional tests can be reliably addressed. Such tests should be accompanied by thorough site characterization programs to establish relevant soil/rock parameters as well as laboratory testing to reliably establish the shaft stiffness at the time of testing.

Accurate documentation of the “as-built” shaft dimensions is also critical for establishing shaft stiffness. These tests should include a reasonable number of strain gages in the test shafts to evaluate axial load distribution with depth. Such gages should be monitored throughout grouting operations and load testing to help develop a better understanding of load transfer mechanisms for PGDS. Reported test results should include the load-displacement response of both grouted and ungrouted shafts, careful grouting records that document the characteristics of the grout (strength, viscosity, particle size, water-to-cement ratio, etc.), the sequence of grout pressures applied, and records of shaft displacement during grouting and of axial force during grouting and load testing.

REFERENCES

AASHTO (2012), *AASHTO LRFD Bridge Design Specifications, Customary U.S. Units*, 6th Edition, with 2013 Interim Revisions, Publication LRFDUS-6, American Association of State Highway and Transportation Officials, Washington, DC, 1938 pp.

API Recommended Practice 13B-1 (2009), "Recommended Practice for Field Testing Water-based Drilling Fluids," American Petroleum Institute, Section 1, Fourth Edition, 91 pp.

ASTM Standard C150 (2012), "Standard Specification for Portland Cement," ASTM International, West Conshohocken, PA, DOI: 10.1520/C0150_C0150M-12. <www.astm.org>

ASTM Standard C204 (2011), "Standard Test Methods for Fineness of Hydraulic Cement by Air-Permeability Apparatus," ASTM International, West Conshohocken, PA, DOI: 10.1520/C0204-11. <www.astm.org>

ASTM Standard D1143 (2013), "Standard Test Methods for Deep Foundations Under Static Axial Compressive Load," ASTM International, West Conshohocken, PA, DOI: 10.1520/D1143_D1143M. <www.astm.org>

ASTM Standard D4380 (2012), "Standard Test Method for Density of Bentonitic Slurries," ASTM International, West Conshohocken, PA, DOI: 10.1520/D4380-12. <www.astm.org>

ASTM Standard D6910 (2009), "Standard Test Method for Marsh Funnel Viscosity of Clay Construction Slurries," ASTM International, West Conshohocken, PA, DOI: 10.1520/D6910_D6910M-09. <www.astm.org>

ASTM Standard C109 (2013), "Standard Test Method for Compressive Strength of Hydraulic Cement Mortars (Using 2-in. or [50-mm] Cube Specimens)," ASTM International, West Conshohocken, PA, DOI: 10.1520/C0109_C0109M. <www.astm.org>

ASTM Standard C476 (2010), "Standard Specification for Grout for Masonry," ASTM International, West Conshohocken, PA, DOI: 10.1520/C0476-10. <www.astm.org>

Beck, A.H., (2002), "Post Stressed Pier," United States Patent No.: 6,371,698 B1.

Bittner, R., Safaqah, O., Zhang, X., and Jensen, O. (2007). "Design and Construction of the Sutong Bridge Foundations," DFI Journal, The Journal of the Deep Foundations Institute, Volume 1, No. 1, pp. 2-18.

Bo, Z., Weijie, N., Huabin, W. and Zhifeng, L. (2011), "Research on Bearing Capacity of Post-Grouting Pile Groups as Bridge Foundations in Karst Areas," Proceedings of Electric Technology and Civil Engineering (ICETCE), International Conference, 2011. April, 2011: 6115- 6120.

Bolognesi, A.J.L. and Moretto, O. (1973). "Stage grouting preloading of large piles on sand." Proceedings of the 8th Int'l Conference on Soil Mechanics and Foundation Engineering, Moscow, pp. 19-25.

Bourgoyne, A.T., Millheim, K.K., Chenevert, M.E., and Young, F.S. (1986). Applied Drilling Engineering. SPE Textbook Series, Volume 2. Society of Petroleum Engineers. Richardson, TX.

Briaud, J.-L. (2000). "The National Geotechnical Experimentation Sites at Texas A&M University: Clay and Sand," Geotechnical Special Publication No. 93, pp. 26-51, American Society of Civil Engineers, Reston, Virginia.

Brown, D.A., Turner, J.P, and Castelli, R.J. (2010). *Drilled Shafts: Construction Procedures and LRFD Design Methods*, National Highway Institute, Federal Highway Administration, FHWA GEC 010, FHWA-NHI-10-016, 970 pp.

Bruce, D.A. (1986a). "Enhancing the performance of large diameter piles by grouting," Part 1, Ground Engineering, May, pp. 9-16.

Bruce, D.A. (1986b). "Enhancing the performance of large diameter piles by grouting," Part 2, Ground Engineering, July, pp. 11-18.

Bruce, D.A. and Traylor, R.P. (2000). "The Repair and Enhancement of Large Diameter Caissons by Grouting," Geotechnical Special Publication No. 100, New Technological and Design Developments in Deep Foundations, N. Dennis, R. Castelli, and M.W. O'Neill, eds, American Society of Civil Engineers, pp. 59-71.

Bruce, D.A. and Cadden, A.W., (2002). "Challenges In Karstic Limestone: Three Major Case Histories," Ohio River Valley Soil Seminar XXXIII, October 2002.

Brusey, W.G. (2000). "Post-Grouted Test Shafts at JFK International Airport," Geotechnical Special Publication No. 100, New Technological and Design Developments in Deep Foundations, N. Dennis, R. Castelli, and M.W. O'Neill, eds, American Society of Civil Engineers, pp. 18-32.

Byle, M. and Border, R. (1995). "Verification of Geotechnical Grouting," ASCE Geotechnical Special Publication No. 57, October 1995.

Cadden, A.W. and Traylor, R. (1998). "Small Project, Big Karst Problem, Solved with Compaction Grouting," ASCE, Boston, Massachusetts, October 1998.

Cadden, A.W., Bruce, D.A., and Traylor, R. (2000). "The Value of Limited Mobility Grouts in Dam Remediation," ASDSO, September 2000.

Castelli, R.J. and Wilkins, E., (2004). "Osterberg Load Cell Test Results on Base Grouted Bored Piles in Bangladesh," Geotechnical Special Publication 124, GeoSupport 2004 Drilled Shafts, Micropiling, Deep Mixing, Remedial Methods, and Specialty Foundation Systems.

Castelli, R.J., (2012), “Guidelines for the Application of Base Grouting for Drilled Shafts”; *Proceedings of GeoCongress 2012*, ASCE, Recent Advances in Foundation Engineering, pp. 225-234.

China Academy of Building Research (2008). *Technical Code for Building Pile Foundations*, JGJ 94-2008, Architecture and Building Press, Beijing.

Cheng, Y., Gong, W., Zhang, X., and Dai, G. (2010). “Experimental Research on Post Grouting Under Super-Long and Large-Diameter Bored Pile Tip,” *Chinese Journal of Rock Mechanics and Engineering*, Vol. 29, Supp. 2. pp: 3885-3892

Cheng, Y., Gong, W., Zhang, X., and Dai, G. (2010). “Experimental study on size effect of large-diameter bored cast-in-situ piles with post-grouting in soft soil,” *Chinese Journal of Geotechnical Engineering*, Vol. 33, Supp. 2. pp: 32-37

Dai, G., Gong, W., Zhao, X., and Zhou, X. (2011). “Static Testing of Pile-Base Post-Grouting Piles of the Suramadu Bridge”; *Geotechnical Testing Journal*, Vol. 34, No. 1. January, 2011.

Dapp, S.D. and Mullins, G. (2002). “Pressure Grouting Drilled Shafts Tips: Full-Scale Research Investigation for Silty and Shelly Sands”; *Proceedings, Deep Foundations 2002: An International Perspective on Theory, Design, Construction, and Performance*, ASCE – GSP 116. International Deep Foundation Congress, 2002, Orlando, Florida, USA.

Dapp, S.D., Muchard, M., and Brown, D.A. (2006). “Experience with Base Grouted Drilled Shafts in the Southeastern United States,” *Deep Foundations Institute, 10th International Conference on Piling and Deep Foundations*, Amsterdam.

Dapp, S.D. and Brown, D.A. (2010). “Evaluation of Base Grouted Drilled Shafts at the Audubon Bridge,” *Geo-Florida 2010, Advances in Analysis, Modeling and Design*, Geotechnical Special Publication No. 199, ASCE, pp. 1553-1562.

Davisson, M.T. (1972). “High Capacity Piles,” *Proceedings of Innovations in Foundation Construction Lecture Series*, ASCE, Illinois Section, 52 pp.

Diao, Y., Dai, G., and Gong, W. (2011). “Experimental Research on the pile-base post-grouting Effects of Piles of Liao River Bridge”; *Advanced Materials Research Vols. 243-249 (2011)*, pp. 2389-2394.

Doornbos, S. (1989). “Vibration-free driven tubular-piles,” *Proceedings of the International Conference on Piling and Deep Foundations*, London, J.B. Burland and J.M. Mitchell, eds, Vol. 1, pp. 437-444.

Duan, X. and Kulhawy, F.H. (2009). “Tip Post-Grouting of Slurry-Drilled Shafts in Soil: Chinese Experiences,” *Contemporary Topics in Deep Foundations*, Proceedings of the 2009 International Foundation Congress and Equipment Expo, ASCE, GSP 185, pp. 47-54.

Dunnicliff, J. (1988). *Geotechnical Instrumentation for Monitoring Field Performance*. John Wiley & Sons, New York, NY.

Englert, C., Traylor, R., and Cadden, A.W. (2005). "Enhancing the Capacity of Belled Caissons with LMG: A Case History," ADSC GeoFrontiers 2005, Austin, TX, January 2005.

Farouz, E., Muchard, M. and Yang, K. (2010). "Evaluation of Axial Capacity of Post Grouted Drilled Shafts"; Proceedings, GeoShanghai, 2010 International Conference of Deep Foundations and Geotechnical In-Situ Testing, ASCE – GSP 205. pp. 216-223.

Fernandez, A. L., Pando M.A., and King, P.G. (2007). "Load Test Program to Validate Model for Post Grouted Drilled Shafts"; *Contemporary Issues in Deep Foundations*, Proceedings, GeoDenver 2007: New Peaks in Geotechnics, Denver, Colorado, ASCE, GSP 158.

Fleming, W.G.K. (1993). "The Improvement of Pile Performance by Base Grouting"; Proceedings of Institution of Civil Engineers, London, 1993, 97, May, 88-93, paper 3078.

Fu, X. and Zhou, Z. (2003). "Study on Bearing Capacity of Bored Cast-in-Situ Piles by Post Pressure Grouting." Proceedings of Grouting and Ground Treatment. New Orleans (LA, United States), ASCE; 2003; 1:707-715.

Gómez, J.E., Filz, G.M., Ebeling, R.M. (2000). "Extended Load/Unload/Reload Hyperbolic Model for Interfaces: Parameter Values and Model Performance for the Contact Between Concrete and Sand," ERDC/ITL TR-00-7, U.S. Army Engineer and Research and Development Center, Vicksburg, MS.

Gómez, J.E., Filz, G.M., and Ebeling, R.M. (2003). "Extended Hyperbolic Model for Sand-to-Concrete Interfaces," ASCE Journal of Geotechnical and Geoenvironmental Engineering, Vol. 129, No. 11, November 1, 2003.

Gómez, J.E. and Cadden, A.W. (2003). "Shallow Foundations in Karst: Limited Mobility Grout or Not Limited Mobility Grout," Grout 2003, New Orleans, LA, February 2003.

Gómez, J.E. and Cadden, A.W., (2006). "Connection Capacity between Micropiles and Existing Footings- Bond Strength to Concrete." Research Report.

Gómez, J.E., Robinson, H.D., and Cadden, A.W. (2006). "Use of Limited Mobility Grout for Shallow Foundations in Karst", *Geotechnical News*, Volume 24, No 2, pp. 51-56.

Gong, W., Dai, G. and Zhang, H. (2009). "Experimental study on pile-end post-grouting piles for super-large bridge pile foundations"; Proceedings, Frontiers of Architecture and Civil Engineering in China, Volume 3, Number 2 (2009), 228-233.

Ho, C.E. (2003). "Base Grouted Bored Pile on Weak Granite"; *Proceedings of Grouting and Ground Treatment*, New Orleans, LA, ASCE, Vol. 1, pp. 716-727.

Hu, C.-L., Li, X.-D. & Wu, Z.-H. (2001). "Study of bearing capacity for post-grouting bored pile." *Chinese J. Rock Mech. & Eng.*, 20 (4), 546-550 (Chinese).

Jia, J., Zhou, M., and Zheng, J. (2011). "Experimental Study on Bearing Behavior of Large-diameter Over-length Cast-in-place Bored Pile Post-Grouting"; *Advanced Materials Research* Vols. 243-249 (2011), pp. 3251-3258.

Karol, R.H. (2003). *Chemical Grouting and Soil Stabilization*, 3rd Edition, Marcel Dekker, 558 pp.

Kim, S-J., Kwon, O-S., Lee, S-H., Kim, M-M. (2011). "Evaluation of bearing capacity of precast piles with dissimilar post-grouting pressures"; Pan-Am, 14th Pan-American Conference on Soil Mechanics and Geotechnical Engineering, CGS, 64th Canadian Geotechnical Conference.

King, P., Fernandez, A., and Pando M. A. (2009). "Post Grouted Drilled Shafts – A Comprehensive Case History from Texas," *Contemporary Topics in Deep Foundations*, Proceedings, 2009 International Foundation Congress and Equipment Expo, ASCE, GSP 185, pp. 31-38.

Kitchens, Lance, personal communication, 2013.

Kwon, O.S., Jung, S.M. and Choi, Y.K. (2011). "A Case Study of Post-Grouted Drilled Shaft in Weathered Rock"; *Korea Geotechnical Society* Volume 27, Issue No. 6.

Li, Z-x., and Chen, Y-z. (2010). "Bearing Capacity of Cast-in-place Bored Pile with Post Grouting Technique"; *Proceedings of Mechanic Automation and Control Engineering (MACE)*, 2010 International Conference, June 2010: 4178- 4181.

Lin, S., Lin, T., and Chang, L. (2000). "A Case Study for Drilled Shafts Base Mud Treatment," *Geotechnical Special Publication No. 100*, New Technological and Design Developments in Deep Foundations, N. Dennis, R. Castelli, and M.W. O'Neill, eds, American Society of Civil Engineers, pp. 46-58.

Littlejohn, G.S. (1982). *Design of Cement Based Grouts*, Proceedings of the Conference on Grouting in Geotechnical Engineering, ASCE, New Orleans, Louisiana.

Littlejohn, G.S. and Bruce, D.A. (1977). "Rock Anchors - State of the Art." *Foundation Publications*, Essex, England, 50 pp. (Previously published in *Ground Engineering* in 5 parts, 1975-1976.)

Littlejohn, G.S., Ingle, J., and Dadasbilge, K. (1983). "Improvement in Base Resistance of Large Diameter Piles Founded in Silty Sand" *Proceedings, Eighth European Conference on Soil Mechanics and Foundation Engineering*, Helsinki, May 1983.

Liu, J-f., and Cui, X-q. (2011). "Pile Bearing Capacity Improvement by Post-grouting on Tip and Side"; *Advanced Materials Research* Vols. 261-263 (2011), pp. 1313-1318.

Liu, J. and Zhang, Y. (2011). "A Calculation Method Discussion of Vertical Bearing Capacity on End Post-Grouted Drilled Piles," *Advanced Materials Research*, Vols. 243-249, pp. 1033-1037.

Lizzi, F. (1981). "The design of large diameter cast-in-situ bored piles using a 'pilot' pile and congruence equations," *Ground Engineering*, Vol. 14, No. 3, pp. 24-33.

Lizzi, F., Viggiani, C., and Vinale, F. (1983). "Some Experience with Pre-Loading Cells at the Base of Large Diameter Bored Piles," Proceedings of the 7th Asian Regional Conference on Soil Mechanics and Foundation Engineering, Haifa, Israel.

Lyons, W.C. (2010). *Working Guide to Drilling Equipment and Operations*. Elsevier Science. Oxford, UK.

Manai, R. (2010). "Enhancement of Pile Capacity by Shaft Grouting Technique in Rupsa Bridge Project"; *Geotechnical Engineering Journal of the SEAGS & AGSSEA* Vol. 41 No. 3 September 2010 ISSN 0046-5828.

Marchi, M., Gottardi, G., and Soga, K. (2013). "Fracturing Pressure in Clay," *Journal of Geotechnical and Geoenvironmental Engineering*, DOI: 10.1061/(ASCE)GT.1943-5606.0001019, 04013008.

Masing, G. (1926). "Eigenspannungen und Verfürgung beim Messing," Proceedings of the 2nd International Congress on Applied Mechanics, Zurich.

McVay, M., Bloomquist, D., Forbes, H., and Johnson, J. (2009). *Precasted Concrete Pile Installation – Utilized Jetting and Pressure Grouting*, FDOT Contract No. BD545, RPWO#31.

McVay, M., Thiyyakkandi, S., Jiner, J., and Adams, V. (2010). "Group Efficiencies of Grout-Tipped Drilled Shafts and Jet-Grouted Piles"; Department of Civil and Coastal Engineering, University of Florida, FDOT final report, August, 2010.

Muchard, M.K., Mullins, G., and Khouri, B. (2003). "Post-grouted Drilled Shafts: A Case History of the PGA Boulevard Bridge Project," DFI Conference, Miami, Florida.

Muchard, M.K. (2004). "Report of Post Grouted Drilled Shafts," Carolina Bays Parkway Bridge over SC 544, Myrtle Beach, South Carolina.

Muchard, M.K. (2004). "Final Report of Post Grouted Drilled Shafts," Security Checkpoint Building Concourse "C," Palm Beach International Airport, Palm Beach County, Florida.

Muchard, M.K. (2004). "Pier Pressure in Natchez Mississippi," *ADSC Foundation Drilling Magazine*, May.

Muchard, M.K. (2005). "Post-grouting of Drilled Shaft Tips Heightens Quality Assurance," ADSC Geo-Cubed (GEO3) Conference, Dallas, Texas.

Muchard, M.K. (2005). "Report of Post Grouted Drilled Shaft," Bridge over Catherine Creek and Melvin Bayou, Natchez Trace Parkway, Natchez, Mississippi.

Muchard, M.K. (2005). "Report of Drilled Shaft Post Grouting and Statnamic Load Testing," SR 35 over Brazos River, Brazoria County, Texas.

Muchard, M.K., Robertson, D.T., and Santee, T.G. (2007 to 2009). "Project Reports on Drilled Shaft Base Grouting," John James Audubon Bridge, New Roads, Louisiana.

Muchard, M.K. and Robertson, D.T. (2009). "Project Reports on Drilled Shaft Base Grouting," Huey P. Long Bridge Widening, New Orleans, Louisiana.

Muchard, M.K. and Farouz, E. (2009). "Broadway Viaduct Design Phase Load Test Program for Post-grouted Shafts," 34th Annual Conference on Deep Foundations, DFI, Kansas City, Missouri.

Muchard, M.K. (2011). "Project Reports on Drilled Shaft Base Grouting," Honolulu High Capacity Transit Corridor Farrington Guideway, Oahu, Hawaii.

Mullins, G., Dapp, S., and Lai, P. (2000). "Pressure-Grouting Drilled Shaft Tips in Sand," Geotechnical Special Publication No. 100, New Technological and Design Developments in Deep Foundations, N. Dennis, R. Castelli, and M.W. O'Neill, eds, American Society of Civil Engineers, pp. 1-17.

Mullins, G., Dapp, S., Frederick, E., and Wagner, V. (2001). *Post Grouting Drilled Shaft Tips – Phase I*, Final Report to the Florida Department of Transportation.

Mullins, G. (2002). "New Design Method Gives Drilled Shafts a Boost"; <http://www.eng.usf.edu/~gmullins/downloads/Jack%20Harrington/Post%20Grout%20Publications/DEEP%20FOUNDATIONS%20Magazine%202004.pdf>.

Mullins, G. and Winters, D. (2004). "Post Grouting Drilled Shaft Tips – Phase II." Final Report to the Florida Department of Transportation.

Mullins, A.G., Winters, D., and Dapp, S.D. (2006). "Predicting End Bearing Capacity of Post-Grouted Drilled Shaft in Cohesionless Soils," *Journal of Geotechnical and Geoenvironmental Engineering*, Vol. 132, No. 4, pp. 478-487.

O'Neill, M.W. and Reese, L.C. (1999). "Drilled Shafts: Construction Procedures and Design Methods." Publication No. FHWA-IF-99-025.

Pando, M.A., Fernandez, A.L., and Filz, G.M. (2004). "Pile Settlement Predictions Using Theoretical Load Transfer Curves and Seismic CPT Data," *Geotechnical and Geophysical Site Characterization*, Proceedings of the Second International Conference on Site Characterization, ISC-2, Porto, Portugal, Millpress, Vol. II, pp. 1525-1531.

Pando, M.A. and Ruiz, M.E. (2005). *Study of axially loaded post grouted drilled shafts using CPT based load transfer curves*, Geotechnical Engineering Research Report No. CIRC/GT/05-02, Civil Infrastructure Research Center, University of Puerto Rico, Mayaguez, PR, June 2005, 287 p.

Piccione, M., Carletti, G., and Diamanti, L. (1984). "The Piled Foundations of the Al Gazira Hotel in Cairo," Proceedings of the International Conference on Advances in Piling and Ground Treatment for Foundations, Institution of Civil Engineers, London, UK.

Pooranampillai, J., Elfass, S., Vanderpool, W., and Norriss, G. (2009). "Large-Scale Laboratory Study on the Innovative Use of Compaction Grout for Drilled Shaft Tip Post Grouting," *Contemporary Topics in Deep Foundations*, Proceedings, 2009 International Foundation Congress and Equipment Expo, Orlando, FL, ASCE, GSP 185, pp. 39-46.

Pooranampillai, J.D. (2010). *The Development and Assessment of a Post Grouting Method to Increase the Load Carrying Capacity of Deep Foundations*; Dissertation submitted in partial fulfillment of the requirements for Ph.D. degree, University of Nevada, Reno, 292 pp.

Pooranampillai, J., Elfass, S., Vanderpool, W., and Norris, G. (2010). "The Effects of Compaction Post Grouting of Model Shaft Tips in Fine Sand at Differing Relative Densities – Experimental Results," *The Art of Foundation Engineering Practice*, Proceedings of special sessions held in honor of Clyde Baker at Geo-Congress 2010, ASCE, GSP 198, pp. 486-500.

Portland Cement Association. "Chemical Admixtures." web reference accessed in July 2005 <<http://www.cement.org/index.asp>>.

Reese, L.C. and O'Neill, M.W. (1988). "Drilled Shafts: Construction and Design." FHWA, Publication No. HI-88-042.

Reese, L.C., Isenhower, W.M., and Wang, S-T. (2006). *Analysis and Design of Shallow and Deep Foundations*, John Wiley and Sons, Hoboken, New Jersey, 574 pp.

Richards, Thomas, personal communication, 2013.

Ruiz, M.E., Fernandez, A.L., and Pando, M.A. (2005). "Bearing Capacity of Post Grouted Drilled Shafts Using a Load Transfer Approach," *Proceedings of the 30th Annual Conference on Deep Foundations*, Deep Foundations Institute, Chicago, Illinois, pp. 139-149.

Ruiz, M.E. and Pando, M.A. (2009). "Load Transfer Mechanisms of Tip Post-Grouted Drilled Shafts in Sand", *Contemporary Topics in Deep Foundations*, Proceedings, 2009 International Foundation Congress and Equipment Expo, Orlando, Florida, ASCE, GSP 185, pp. 23-30.

Schaefer, V.R., Abramson, L.W., Drumheller, J.C., Hussin, J.D., and Sharp, K.D., Eds. (1997). *Ground Improvement, Ground Reinforcement, and Ground Treatment: Developments 1987-1997*. Proceedings of sessions sponsored by the Committee on Soil Improvement and Geosynthetics of the Geo-Institute of the American Society of Civil Engineers. ASCE, Reston, VA.

Scherer, S. and Gray, R. (2000). "Compaction Grouting: Three Midwest Case Histories," ASCE Special Publication No. 104, August 2000, pp. 65-82.

Sherwood, D.E. and Mitchell, J.M. (1989). "Base grouted piles in Thanet Sands, London," *Proceedings of the International Conference on Piling and Deep Foundations*, London, J.B. Burland and J.M. Mitchell, eds, Vol. 1, pp. 463-472.

Siegel, T. and Belgeri, J. (1999). "Grouting to Reinforce Limestone Residual Soil in East Tennessee," ASCE Geotechnical Special Publication No. 92, October 1999, pp. 134-147.

Sliwinski, Z.J. and Fleming, W.G.K. (1984): “The integrity and performance of bored piles.” Proceedings, ICE Conference on Piling and Ground Treatment, London, March, pp. 211-224.

Taylor, R.M., and Choquet, P. (2012). “Automatic Monitoring of Grouting Performance Parameters,” *Grouting and Deep Mixing*, Proceedings of the 4th International Conference, New Orleans, LA, ASCE, pp. 1494-1505.

Thasnanipan, N., Aye, Z.Z. and Submanee Wong, C. (2004). “Effectiveness of Toe-Grouting for Deep-Seated Bored Piles in Bangkok Subsoil”; *Geo-Support 2004: Drilled Shafts, Micropiling, Deep Mixing, Remedial Methods, and Specialty Foundation Systems*, Geotechnical Special Publication No. 124, ASCE.

Troughton, V.M. and Platis, A. (1989). “The effects of changes in effective stress on a base grouted pile in sand,” Proceedings of the International Conference on Piling and Deep Foundations, London, J.B. Burland and J.M. Mitchell, eds, Vol. 1, pp. 445-453.

Troughton, V.M. and Thompson, P.A., (1996). “Base and shaft grouted piles (Informal Discussion)”; Proceedings of Institution of Civil Engineers, London, 1996, 119, July, 186-192.

Tse, F.S. and Morse, I.E. (1989). *Measurement and Instrumentation in Engineering – Principles and Basic Laboratory Experiments*. Marcel Dekker, Inc. New York, NY.

US Army Corps of Engineers (2009). *Grouting Technology*, Draft EM 1110-2-3506, U.S. Army Corps of Engineers.

Weaver, K.D. and Bruce, D.A. (2007). *Dam Foundation Grouting*, ASCE, Reston, VA

Wilder, D.S., Smith, G.C., and Gómez, J.E. (2005). “Issues in Design and Evaluation of Compaction Grouting for Foundation Repair,” ADSC GeoFrontiers 2005, Austin, TX, January 2005.

Xiao, D., Wu, C., and Wu, C. (2009). “Bored Pile Post-grouting Technology and Its Engineering Application,” *Advances in Ground Improvement*, Proceedings of the US-China Workshop on Ground Improvement Technologies, ASCE, pp. 198-206.

Xu, J., Cheng, G., Li, B., and He, J. (2011). “The application and analysis of pressure grouting technique on filling pile bottom in coastal areas”; *Applied Mechanics and Materials* Vols. 90-93 (2011), pp. 2053-2056.

Yaonian, Z. and Wenqiao, H. (2000). “Large Bored Piles with Grouted Ends in Fuzhou.” Proceedings of GeoEng, International Conference of Geotechnical & Geological Engineering, Melbourne, Australia.

Yates, J.A. and O’Riordan, N.J. (1989). “The design and construction of large diameter base grouted piles in Thanet Sand at Blackwall Yard, London,” Proceedings of the International Conference on Piling and Deep Foundations, London, J.B. Burland and J.M. Mitchell, eds, Vol. 1, pp. 455-461.

Zhang, Z., Lu, T., Zhao, Y., Wang, J. and Li, Y. (2004). "Pile-Bottom Grouting Technology for Bored Cast-In-Situ Pile Foundation"; *Geo-Support 2004: Drilled Shafts, Micropiling, Deep Mixing, Remedial Methods, and Specialty Foundation Systems*, Geotechnical Special Publication No. 124, ASCE.

Zhongmiao, Z. and Qianqing, Z. (2009). "Experimental Study on Mechanical Properties of Post-Grouting Compressive Pile"; *Chinese Journal of Rock Mechanics and Engineering*, Vol. 28 No. 3, March, 2009, pp. 475-482.